

Simplified Techniques for Evaluation and Interpretation of Pavement Deflections for Network-Level Analysis

PUBLICATION NO. FHWA-HRT-12-023

DECEMBER 2012



U.S. Department of Transportation
Federal Highway Administration

Research, Development, and Technology
Turner-Fairbank Highway Research Center
6300 Georgetown Pike
McLean, VA 22101-2296



FOREWORD

Effectively managing pavement infrastructure assets requires not only knowledge of the pavement condition indicators that can be seen (e.g., cracking or rutting) or felt (e.g., roughness), but also knowledge of the pavement's structural capacity. Increased use of structural capacity information with agency-wide coverage has the potential to enhance decision making and enable a more efficient and effective preservation and rehabilitation program. The falling weight deflectometer (FWD) has long been used to determine the structural characteristics of the pavement structure. While there are many viable techniques for evaluating the structural capacity of pavements using FWD data for project-level analysis, many of these techniques are time consuming and require an experienced analyst. As a result, using pavement deflection testing for network-level analysis has been limited to date. In order to solve this problem, the Long Term Pavement Performance (LTPP) program conducted a study to develop techniques that could be used to interpret and evaluate deflection data for network-level pavement management system (PMS) applications. Information and data from the LTPP program provide a consistent, high quality data set that covers the entire United States, has been collected in a consistent manner over a long time period, and includes a variety of pavement structures. The first part of this research focused on identifying and evaluating existing techniques for interpreting pavement deflections with an emphasis on those that are simple, reliable, and easy to incorporate into current PMS practices. The second part of the research detailed the development of guidelines for the application of recommended techniques, along with procedures for determining optimum FWD test spacing and data collection frequency. The findings presented in this report suggest that it is possible and advantageous to define simplified techniques for the evaluation and interpretation of pavement deflections for network-level analysis. This report is intended for pavement managers and pavement investment decision makers across the United States.

Jorge E. Pagán-Ortiz
Director, Office of Infrastructure
Research and Development

Notice

This document is disseminated under the sponsorship of the U.S. Department of Transportation in the interest of information exchange. The U.S. Government assumes no liability for the use of the information contained in this document. This report does not constitute a standard, specification, or regulation.

The U.S. Government does not endorse products or manufacturers. Trademarks or manufacturers' names appear in this report only because they are considered essential to the objective of the document.

Quality Assurance Statement

The Federal Highway Administration (FHWA) provides high-quality information to serve Government, industry, and the public in a manner that promotes public understanding. Standards and policies are used to ensure and maximize the quality, objectivity, utility, and integrity of its information. FHWA periodically reviews quality issues and adjusts its programs and processes to ensure continuous quality improvement.

TECHNICAL REPORT DOCUMENTATION PAGE

1. Report No. FHWA-HRT-12-023	2. Government Accession No.	3. Recipient's Catalog No.	
4. Title and Subtitle Simplified Techniques for Evaluation and Interpretation of Pavement Deflections for Network-Level Analysis		5. Report Date December 2012	
		6. Performing Organization Code	
7. Author(s) R. Carvalho, R. Stubstad, R. Briggs, O. Selezneva, E. Mustafa, and A. Ramachandran		8. Performing Organization Report No.	
9. Performing Organization Name and Address Applied Research Associates, Inc. 7184 Troy Hill Drive, Suite N Elkridge, MD 21075-7056		10. Work Unit No. (TRAIS)	
		11. Contract or Grant No. DTFH61-02-C-00138	
12. Sponsoring Agency Name and Address Office of Infrastructure Research and Development Federal Highway Administration 6300 Georgetown Pike McLean, VA 22101-2296		13. Type of Report and Period Covered Final Report	
		14. Sponsoring Agency Code	
15. Supplementary Notes The Contracting Officer's Technical Representative (COTR) was Larry Wiser, HRDI-30.			
16. Abstract The objective of this study was to develop an approach for incorporating techniques used to interpret and evaluate deflection data for network-level pavement management system (PMS) applications. The first part of this research focused on identifying and evaluating existing techniques by seeking out those that were simple, reliable, and easy to incorporate into current PMS practices, as well as those that produced consistent results. The second part of the research detailed the development of guidelines for the application of recommended techniques, along with procedures for determining optimum falling weight deflectometer (FWD) test spacing and data collection frequency. While there are many viable techniques available for evaluating the structural capacity of pavements that use FWD for project-level analysis, many of these techniques are time consuming and require an experienced analyst. As a result, using pavement deflection testing for network-level analysis has been limited to date. The findings presented in this report suggest that it is possible and, in fact, advantageous to define simplified techniques for the evaluation and interpretation of pavement deflections for network-level analysis.			
17. Key Words Pavement performance, Rehabilitation, Maintenance, Pavement design, Long-term performance, Flexible pavements, Rigid pavements		18. Distribution Statement No restrictions. This document is available to the public through the National Technical Information Service, Springfield, VA 22161.	
19. Security Classification (of this report) Unclassified	20. Security Classification (of this page) Unclassified	21. No. of Pages 198	22. Price

Form DOT F 1700.7 (8-72)

Reproduction of completed page authorized

SI* (MODERN METRIC) CONVERSION FACTORS				
APPROXIMATE CONVERSIONS TO SI UNITS				
Symbol	When You Know	Multiply By	To Find	Symbol
LENGTH				
in	inches	25.4	millimeters	mm
ft	feet	0.305	meters	m
yd	yards	0.914	meters	m
mi	miles	1.61	kilometers	km
AREA				
in ²	square inches	645.2	square millimeters	mm ²
ft ²	square feet	0.093	square meters	m ²
yd ²	square yard	0.836	square meters	m ²
ac	acres	0.405	hectares	ha
mi ²	square miles	2.59	square kilometers	km ²
VOLUME				
fl oz	fluid ounces	29.57	milliliters	mL
gal	gallons	3.785	liters	L
ft ³	cubic feet	0.028	cubic meters	m ³
yd ³	cubic yards	0.765	cubic meters	m ³
NOTE: volumes greater than 1000 L shall be shown in m ³				
MASS				
oz	ounces	28.35	grams	g
lb	pounds	0.454	kilograms	kg
T	short tons (2000 lb)	0.907	megagrams (or "metric ton")	Mg (or "t")
TEMPERATURE (exact degrees)				
°F	Fahrenheit	5 (F-32)/9 or (F-32)/1.8	Celsius	°C
ILLUMINATION				
fc	foot-candles	10.76	lux	lx
fl	foot-Lamberts	3.426	candela/m ²	cd/m ²
FORCE and PRESSURE or STRESS				
lbf	poundforce	4.45	newtons	N
lbf/in ²	poundforce per square inch	6.89	kilopascals	kPa
APPROXIMATE CONVERSIONS FROM SI UNITS				
Symbol	When You Know	Multiply By	To Find	Symbol
LENGTH				
mm	millimeters	0.039	inches	in
m	meters	3.28	feet	ft
m	meters	1.09	yards	yd
km	kilometers	0.621	miles	mi
AREA				
mm ²	square millimeters	0.0016	square inches	in ²
m ²	square meters	10.764	square feet	ft ²
m ²	square meters	1.195	square yards	yd ²
ha	hectares	2.47	acres	ac
km ²	square kilometers	0.386	square miles	mi ²
VOLUME				
mL	milliliters	0.034	fluid ounces	fl oz
L	liters	0.264	gallons	gal
m ³	cubic meters	35.314	cubic feet	ft ³
m ³	cubic meters	1.307	cubic yards	yd ³
MASS				
g	grams	0.035	ounces	oz
kg	kilograms	2.202	pounds	lb
Mg (or "t")	megagrams (or "metric ton")	1.103	short tons (2000 lb)	T
TEMPERATURE (exact degrees)				
°C	Celsius	1.8C+32	Fahrenheit	°F
ILLUMINATION				
lx	lux	0.0929	foot-candles	fc
cd/m ²	candela/m ²	0.2919	foot-Lamberts	fl
FORCE and PRESSURE or STRESS				
N	newtons	0.225	poundforce	lbf
kPa	kilopascals	0.145	poundforce per square inch	lbf/in ²

TABLE OF CONTENTS

CHAPTER 1—INTRODUCTION	1
BACKGROUND	1
PROJECT OBJECTIVES.....	1
DESIRED OUTCOMES AND PROJECT DELIVERABLES.....	2
REPORT ORGANIZATION.....	3
CHAPTER 2—LITERATURE REVIEW	5
INTRODUCTION.....	5
LITERATURE REVIEW APPROACH.....	5
SUMMARY OF FINDINGS FROM PREVIOUS STUDIES	6
Agencies Currently Utilizing Deflection Data for Network-Level Applications	11
Agencies Utilizing Deflection Data in a Manner Potentially Useful to Enhance Network-Level PMS Applications.....	15
Identified Techniques for Simplified Evaluation and Analysis	16
CONCLUSIONS FROM THE LITERATURE REVIEW	19
CHAPTER 3—ASSESSMENT OF DATA.....	21
REVIEW AND ASSESSMENT OF DATA FROM LTPP STUDIES	21
Data Selection Criteria.....	21
Data Elements Needed for Analyses.....	21
Analysis Database Development	23
Data Review Process.....	23
ASSESSMENT OF DATA TO SUPPORT EVALUATION OF IDENTIFIED TECHNIQUES.....	24
Impact of M&R on Pavement Performance Data	24
Analysis of Deflection Data.....	27
ASSESSMENT OF DATA TO SUPPORT OPTIMUM TEST SPACING AND FREQUENCY	27
LTPP Data to Support Optimum Test Spacing Analysis.....	27
Supplemental Data to Support Optimum Test Spacing Analysis	27
LTPP Data to Support Optimum Test Frequency Analysis.....	27
LTPP Data to Support Time of Day and Day of Year Analysis.....	28
CHAPTER 4—EVALUATION OF APPLICABLE LOAD DEFLECTION TECHNIQUES.....	29
ANALYSIS APPROACH.....	30
Binary Logistic Model	30
Stochastic Approach to Evaluate Load Deflection Techniques to Network-Level Applications	33
ANALYSIS STEPS	35
Data Preparation.....	36
Evaluation of Selected Techniques Based on Observed Performance	40
Sensitivity of Model to Deflection Parameter	42
Validation Analysis.....	44
Selection of Deflection Technique.....	45

THEORETICAL VALIDATION.....	45
Mechanistic-Empirical Analysis	46
Comparison with MEPDG Predicted Performance	48
IMPORTANCE OF LOCAL CALIBRATION	50
SUMMARY OF FINDINGS	51
Flexible Pavements	52
Rigid Pavements	54
GUIDELINES FOR SELECTING BEST-FITTING TECHNIQUES	57
1. Data Preparation.....	57
2. Logistic Model Calibration	58
3. Verification of Accuracy.....	58
4. Sensitivity Analysis	59
CHAPTER 5—PROCEDURES FOR OPTIMUM DEFLECTION TEST	
SPACINGS AND FREQUENCY FOR PMS APPLICATIONS	61
ANALYSIS OF TEST SPACINGS FOR FWD DATA COLLECTION	62
Modeling the Error Using a Monte Carlo Simulation	62
Comparison to Available Data.....	72
ANALYSIS OF FREQUENCY FOR FWD DATA COLLECTION	75
Flexible Pavements	75
Rigid Pavements	81
CHAPTER 6—GUIDELINES FOR CONSIDERATION OF TIME OF DAY AND	
SEASON OF YEAR FOR OPTIMAL FWD DATA COLLECTION FOR PMS	
APPLICATIONS	83
SUMMARY OF APPROACHES FROM LITERATURE REVIEW.....	83
RESULTS OF LTPP DATA ANALYSIS.....	84
DEFLECTION ADJUSTMENT PROCEDURES.....	84
RECOMMENDATIONS FOR TIME OF DAY FOR DEFLECTION	
MEASUREMENTS AT NETWORK LEVEL.....	86
RECOMMENDATIONS FOR SEASON OF YEAR FOR MEASUREMENTS AT	
NETWORK LEVEL.....	87
APPLICATIONS AND LIMITATIONS	87
CHAPTER 7—PRACTICAL EXAMPLE	89
INTRODUCTION.....	89
REVIEW OF RECOMMENDED APPLICATION	89
MDSHA EXAMPLE.....	90
Overview on MDSHA PMS	90
Sample of MDSHA Network.....	92
Incorporation of Structural Analysis on MDSHA PMS	93
CONCLUSIONS	99
CHAPTER 8—CONCLUSIONS AND RECOMMENDATIONS	101
SIMPLIFIED TECHNIQUES FOR EVALUATION AND INTERPRETATION	
OF PAVEMENT DEFLECTIONS FOR NETWORK-LEVEL ANALYSIS.....	101
OPTIMUM DEFLECTION TEST SPACINGS AND FREQUENCY FOR PMS	
APPLICATIONS	103
Test Spacing.....	103

Frequency.....	103
Time of Day and Season of Year.....	104
EXAMPLE OF INCORPORATING STRUCTURAL ANALYSIS ON PMS.....	104
APPENDIX A.....	107
APPENDIX B.....	115
PRE-SCREENING OF DEFLECTION PARAMETERS FOR FLEXIBLE PAVEMENTS	115
PRE-SCREENING OF DEFLECTION PARAMETERS FOR RIGID PAVEMENTS	121
FLEXIBLE PAVEMENT STRUCTURAL ANALYSIS.....	132
Models Based on Roughness Performance.....	132
Models Based on Rutting Performance	133
Models Based on Fatigue Cracking Performance.....	134
RIGID PAVEMENT STRUCTURAL ANALYSIS FOR 9,000 LB (4,086 KG)	
FWD LOAD.....	135
Models Based on Roughness Performance (9,000 lb (4,086 kg))	135
Models Based on Faulting at Joints Performance (9,000 lb (4,086 kg))	137
Models Based on Transverse Cracking Performance (9,000 lb (4,086 kg)).....	139
RIGID PAVEMENT STRUCTURAL ANALYSIS FOR 12,000-LB (5,448-KG)	
FWD LOAD.....	141
Models Based on Roughness Performance (12,000 lb (5,448 kg))	141
Models Based on Faulting at Joints Performance (12,000 lb (5,448 kg))	143
Models Based on Transverse Cracking Performance (12,000 lb (5,448 kg)).....	145
APPENDIX C.....	147
FLEXIBLE PAVEMENT STRUCTURAL ANALYSIS.....	147
Models Based on Rutting Performance for Flexible Pavements	147
Models Based on Fatigue Cracking Performance for Flexible Pavements.....	149
RIGID PAVEMENT STRUCTURAL ANALYSIS FOR 9,000-LB (4,086-KG)	
FWD LOAD.....	150
Models Based on Roughness Performance for Rigid Pavements (9,000 lb (4,086 kg)).....	150
Models Based on Faulting at Joints Performance for Rigid Pavements (9,000 lb (4,086 kg)).....	151
Models Based on Transverse Cracking Performance for Rigid Pavements (9,000 lb (4,086 kg))	152
RIGID PAVEMENT STRUCTURAL ANALYSIS FOR 12,000-LB (5,488-KG)	
FWD LOAD.....	154
Models Based on Roughness Performance for Rigid Pavements (12,000 lb (5,445 kg)).....	154
Models Based on Faulting at Joints Performance for Rigid Pavements (12,000 lb (5,445 kg))	155
Models Based on Transverse Cracking Performance for Rigid Pavements (12,000 lb (5,445 kg))	156

APPENDIX D	159
MECHANISTIC-EMPIRICAL ANALYSIS OF FLEXIBLE PAVEMENTS.....	159
Comparison with MEPDG Predicted Performance	161
MECHANISTIC-EMPIRICAL ANALYSIS OF RIGID PAVEMENTS.....	163
Comparison with MEPDG Predicted Performance	165
APPENDIX E	167
APPENDIX F	175
REFERENCES.....	181

LIST OF FIGURES

Figure 1. Equation. Calculation of RoC.....	14
Figure 2. Equation. Calculation of BLI	14
Figure 3. Equation. Calculation of MLI.....	14
Figure 4. Equation. Calculation of LLI.....	14
Figure 5. Equation. Calculation of CI_i	16
Figure 6. Equation. Calculation of F_i	16
Figure 7. Equation. Calculation of S_i	17
Figure 8. Equation. Calculation of I_i	17
Figure 9. Equation. Calculation of RA	17
Figure 10. Equation. Calculation of TA.....	17
Figure 11. Equation. Calculation of SN_{eff}	17
Figure 12. Equation. Calculation of d_0	17
Figure 13. Equation. Calculation of M_r	18
Figure 14. Equation. Calculation of E_0	18
Figure 15. Equation. Calculation of E_{sg}	18
Figure 16. Equation. Calculation of n	18
Figure 17. Equation. Calculation of C	18
Figure 18. Equation. Calculation of $E_{0(r)}$	19
Figure 19. Equation. Calculation of $\sigma_{(r)}$	19
Figure 20. Graph. Variation of roughness in section 06-0509.....	26
Figure 21. Equation. General formulation of the logistic model	30
Figure 22. Equation. General linear formulation for the exponent term of the logistic model	30
Figure 23. Graph. Typical logistic model probability function of a predictor variable X.....	31
Figure 24. Graph. Example of an ROC curve.....	32
Figure 25. Graph. Example of logistic model probability function of a predictor variable X used to create a structural decision matrix	34
Figure 26. Graph. Example of performance extrapolation based on historical data.....	39
Figure 27. Graph. Sensitivity of roughness acceptable probability to deflection parameter I_2 for flexible pavements.....	43
Figure 28. Graph. Sensitivity of roughness acceptable probability to deflection parameter Hogg for flexible pavements.....	44
Figure 29. Equation. Calculation of I_2	45
Figure 30. Graph. Deflection parameter I_2 as a function of SN for a flexible pavement with HMA modulus of 500,000 psi (3,445,000 kPa).....	47
Figure 31. Graph. Sensitivity of deflection parameter I_1 to slab thickness.....	48
Figure 32. Graph. Sensitivity of I_1 structural logistic model probability based on fatigue cracking performance to MEPDG predicted fatigue cracking for flexible pavements.....	49
Figure 33. Graph. Sensitivity of I_1 structural logistic model probability based on roughness performance to MEPDG predicted roughness for rigid pavements.....	50
Figure 34. Equation. Calculation of CI_3	52
Figure 35. Equation. Calculation of I_1	53
Figure 36. Equation. Calculation of CI_5	54
Figure 37. Equation. Calculation of CI_4	55
Figure 38. Illustration. Monte Carlo simulation	63

Figure 39. Illustration. Deflection measurement pairings based on 0.1-, 0.2-, and 0.3-mi (0.161-, 0.322-, and 0.483-km) spacings	64
Figure 40. Graph. Expected average error as function of spacing for 10-mi-(16.1-km)-long sections.....	65
Figure 41. Graph. Expected average errors for 10-mi- (16.1-km)-long section at different spacings and probability levels	66
Figure 42. Graph. Normal distribution	66
Figure 43. Graph. Average error curves for different section lengths	67
Figure 44. Graph. Values of a and b from the seven average error curves	67
Figure 45. Equation. Average expected error due to sampling.....	68
Figure 46. Graph. Standard deviation of average error curves for different section lengths.....	68
Figure 47. Graph. Values of c and d from the seven standard deviation curves	69
Figure 48. Equation. Standard deviation of the expected error due to sampling.....	69
Figure 49. Graph. Observed average error (data points) plotted with the computed average error (lines).....	70
Figure 50. Graph. Observed standard deviation (data points) plotted with the computed average error (lines)	70
Figure 51. Graph. Calculated errors for a 10-mi- (16.1-km)-long section with different means and standard deviations of errors	71
Figure 52. Equation. Calculation of COV shift factor	71
Figure 53. Graph. Maximum and minimum section means and weighted mean deflection for all sections in each State.....	73
Figure 54. Graph. Average error for each spacing.....	73
Figure 55. Graph. Comparison between measured error and predicted error for all New Mexico sections at 0.2-mi (0.322-km) spacing	74
Figure 56. Graph. Comparison between measured error and predicted error for all New Mexico sections at 0.5-mi (0.805-km) spacing	74
Figure 57. Graph. Comparison between measured error and predicted error for all New Mexico sections at 1-mi (1.61-km) spacing	75
Figure 58. Graph. Plot of $\log(D_I)$ versus temperature for SHRP section 501002	76
Figure 59. Equation. Deflection adjustment by temperature	77
Figure 60. Graph. Center deflection measurements versus test date—adjusted and unadjusted	77
Figure 61. Graph. Temperature-adjusted center deflections versus test date for SHRP section 501002	78
Figure 62. Graph. Specificity of fatigue cracking models for flexible pavements	84
Figure 63. Graph. Specificity of rutting models for flexible pavements	85
Figure 64. Graph. Distribution of prescribed treatment for the first intervention	95
Figure 65. Graph. Cost distribution over the analysis period	98
Figure 66. Equation. Calculation of LTEA.....	136
Figure 67. Graph. Sensitivity of rutting acceptable probability to deflection parameter CI_3 for flexible pavements	147
Figure 68. Graph. Sensitivity of rutting acceptable probability to deflection parameter D_I for flexible pavements	148
Figure 69. Graph. Sensitivity of rutting acceptable probability to deflection parameter Hogg for flexible pavements.....	148

Figure 70. Graph. Sensitivity of fatigue cracking acceptable probability to deflection parameter I_f for flexible pavements	149
Figure 71. Graph. Sensitivity of fatigue cracking acceptable probability to deflection parameter Hogg for flexible pavements	149
Figure 72. Graph. Sensitivity of roughness acceptable probability to deflection parameter CI_5 for rigid pavements (9,000 lb (4,086 kg))	150
Figure 73. Graph. Sensitivity of roughness acceptable probability to deflection parameter I_f for rigid pavements (9,000 lb (4,086 kg))	150
Figure 74. Graph. Sensitivity of roughness acceptable probability to deflection parameter LTEA for rigid pavements (9,000 lb (4,086 kg))	151
Figure 75. Graph. Sensitivity of faulting at joints acceptable probability to deflection parameter D_6 for rigid pavements (9,000 lb (4,086 kg))	151
Figure 76. Graph. Sensitivity of faulting at joints acceptable probability to deflection parameter LTEA for rigid pavements (9,000 lb (4,086 kg))	152
Figure 77. Graph. Sensitivity of transverse cracking acceptable probability to deflection parameter CI_4 for rigid pavements (9,000 lb (4,086 kg))	152
Figure 78. Graph. Sensitivity of transverse cracking acceptable probability to deflection parameter D_1 for rigid pavements (9,000 lb (4,086 kg))	153
Figure 79. Graph. Sensitivity of transverse cracking acceptable probability to deflection parameter LTEA for rigid pavements (9,000 lb (4,086 kg))	153
Figure 80. Graph. Sensitivity of roughness acceptable probability to deflection parameter CI_4 for rigid pavements (12,000 lb (5,445 kg))	154
Figure 81. Graph. Sensitivity of roughness acceptable probability to deflection parameter I_f for rigid pavements (12,000 lb (5,445 kg))	154
Figure 82. Graph. Sensitivity of roughness acceptable probability to deflection parameter LTEA for rigid pavements (12,000 lb (5,445 kg))	155
Figure 83. Graph. Sensitivity of faulting at joints acceptable probability to deflection parameter D_6 for rigid pavements (12,000 lb (5,445 kg))	155
Figure 84. Graph. Sensitivity of faulting at joints acceptable probability to deflection parameter LTEA for rigid pavements (12,000 lb (5,445 kg))	156
Figure 85. Graph. Sensitivity of transverse cracking acceptable probability to deflection parameter CI_4 for rigid pavements (12,000 lb (5,445 kg))	156
Figure 86. Graph. Sensitivity of transverse cracking acceptable probability to deflection parameter D_1 for rigid pavements (12,000 lb (5,445 kg))	157
Figure 87. Graph. Sensitivity of transverse cracking acceptable probability to deflection parameter LTEA for rigid pavements (12,000 lb (5,445 kg))	157
Figure 88. Equation. Computation of SN	159
Figure 89. Equation. Computation of the layer coefficient a_2 for base course	159
Figure 90. Graph. Deflection parameter I_2 as a function of SN for a flexible pavement with HMA modulus of 500,000 psi (3,445,000 kPa)	160
Figure 91. Graph. Deflection parameter CI_3 as a function of SN for a flexible pavement with HMA modulus of 500,000 psi (3,445,000 kPa)	160
Figure 92. Graph. Deflection parameter I_f as a function of SN for a flexible pavement with HMA modulus of 500,000 psi (3,445,000 kPa)	161
Figure 93. Equation. Calculation of number of load repetitions to fatigue failure	161
Figure 94. Equation. Calculation of correction for different asphalt layer thickness effects	162

Figure 95. Equation. Calculation of laboratory to field adjustment factor	162
Figure 96. Equation. Calculation of parameter M	162
Figure 97. Equation. Fatigue cracking prediction.....	162
Figure 98. Equation. Calculation of permanent deformation	162
Figure 99. Equation. Calculation of k_1	162
Figure 100. Equation. Calculation of C_1 and C_2	162
Figure 101. Graph. Sensitivity of CI_3 structural logistic model probability based on rutting performance to MEPDG predicted rutting for flexible pavements	163
Figure 102. Graph. Sensitivity of deflection parameter D_6 to slab thickness	164
Figure 103. Graph. Sensitivity of deflection parameter CI_4 to slab thickness.....	164
Figure 104. Graph. Sensitivity of D_6 structural logistic model probability based on faulting performance to MEPDG predicted faulting for rigid pavements.....	165
Figure 105. Graph. Sensitivity of CI_4 structural logistic model probability based on slab cracking performance to MEPDG predicted slab cracking for rigid pavements	166
Figure 106. Graph. Comparison between measured error and predicted error for all Kansas sections at 0.2-mi (0.322-km) spacing	172
Figure 107. Graph. Comparison between measured error and predicted error for all Kansas sections at 0.5-mi (0.805-km) spacing	172
Figure 108. Graph. Comparison between measured error and predicted error for all Kansas sections at 1-mi (1.61-km) spacing	173
Figure 109. Graph. Comparison between measured error and predicted error for all Oregon sections at 0.2-mi (0.322-km) spacing	173
Figure 110. Graph. Comparison between measured error and predicted error for all Oregon sections at 0.5-mi (0.805-km) spacing.....	174
Figure 111. Graph. Comparison between measured error and predicted error for all Oregon sections at 1-mi (1.61-km) spacing.....	174

LIST OF TABLES

Table 1. Summary of useful practices for FWD use in network-level analyses	7
Table 2. Structural condition associated with deflection bowl parameters	15
Table 3. LTPP database tables used to support data collection	23
Table 4. LTPP data availability to support evaluation of identified techniques	24
Table 5. Data assessment summary after multiple section analysis	27
Table 6. FWD data availability for SMP sites	28
Table 7. Example of structural decision matrix	34
Table 8. Input continuous data summary for flexible pavement sections	37
Table 9. Input discrete data summary for flexible pavement sections	37
Table 10. Input continuous data summary for rigid pavement sections	38
Table 11. Input discrete data summary for rigid pavement sections	38
Table 12. Structural distresses in flexible and rigid pavements	38
Table 13. Distress threshold for flexible and rigid pavements	39
Table 14. Traffic characteristics used for sampling	40
Table 15. Statistics of calibrated models based on roughness performance of flexible pavements	42
Table 16. Example of validation results for the structural logistic model based on roughness for flexible pavements	45
Table 17. Variables in the I_2 final model (based on roughness)	45
Table 18. Summary of the mechanistic analysis inputs for flexible pavements	46
Table 19. Summary of the mechanistic analysis inputs for rigid pavements	47
Table 20. Benefits of local calibration	51
Table 21. Variables in the I_2 final model for flexible pavements based on roughness performance	52
Table 22. Variables in the CI_3 final model for flexible pavements based on rutting performance	52
Table 23. Variables in the I_1 final model for flexible pavements based on fatigue cracking performance	53
Table 24. Variables in the CI_5 final model for rigid pavements based on roughness performance (9,000 lb (4,086 kg))	54
Table 25. Variables in the CI_4 final model for rigid pavements based on roughness performance (12,000 lb (5,448 kg))	55
Table 26. Variables in the D_6 final model for rigid pavements based on faulting at joints performance (9,000 lb (4,086 kg))	55
Table 27. Variables in the D_6 final model for rigid pavements based on faulting at joints performance (12,000 lb (5,448 kg))	56
Table 28. Variables in the CI_4 final model for rigid pavements based on transverse slab cracking performance (9,000 lb (4,086 kg))	56
Table 29. Variables in the CI_4 final model for rigid pavements based on transverse slab cracking performance (12,000 lb (5,448 kg))	57
Table 30. Errors in percentage for 90 percent reliability based on various section lengths, sample spacings, and COV of 33 percent	72
Table 31. Deflection data for New Mexico, Oregon, and Kansas	72
Table 32. Annual change in D_1 by SHRP test section	79

Table 33. Rate of deflection change by traffic level	80
Table 34. Rate of deflection change by subgrade type	80
Table 35. Rate of deflection change by AC thickness	80
Table 36. Rate of deflection change by climate classification.....	81
Table 37. Statistics for flexible pavement fatigue cracking models: D_I versus D_I adjusted	85
Table 38. Statistics for flexible pavement rutting models: D_I versus D_I adjusted	85
Table 39. Statistics for flexible pavement IRI as a function of season.....	87
Table 40. MDSHA pavement classification based on IRI values.....	91
Table 41. MDSHA PMS treatment decision matrix	92
Table 42. Summary statistics of MDSHA sections used in the example.....	93
Table 43. Summary statistics of MDSHA sections used in the example (percent distribution of sections)	93
Table 44. Structural decision matrix based on roughness and rutting performance	94
Table 45. Adjustment of MDSHA treatment option based on structural analysis.....	95
Table 46. Results from the PMS optimization considering the structural analysis	97
Table 47. Impact on costs from the PMS optimization considering the structural analysis	98
Table 48. Useful practices for FWD use in network-level analyses.....	107
Table 49. Pre-screening of deflection variables for roughness-based logistic model for flexible pavements	115
Table 50. Pre-screening of deflection variables for rutting-based logistic model for flexible pavements	117
Table 51. Pre-screening of deflection variables for fatigue cracking-based logistic model for flexible pavements.....	119
Table 52. Pre-screening of deflection variables for drop 2 roughness-based logistic model for rigid pavements	121
Table 53. Pre-screening of deflection variables for drop 2 faulting at joints-based logistic model for rigid pavements	123
Table 54. Pre-screening of deflection variables for drop 2 transverse cracking-based logistic model for rigid pavements	125
Table 55. Pre-screening of deflection variables for drop 3 roughness-based logistic model for rigid pavements	127
Table 56. Pre-screening of deflection variables for drop 3 faulting at joints-based logistic model for rigid pavements	129
Table 57. Pre-screening of deflection variables for drop 3 transverse cracking-based logistic model for rigid pavements	131
Table 58. Statistics of calibrated models based on roughness performance of flexible pavements—all models.....	132
Table 59. Statistics of calibrated models based on rutting performance of flexible pavements—all models	133
Table 60. Variables in the CI_3 final model (based on rutting)	133
Table 61. Variables in the Hogg final model (based on rutting)	133
Table 62. Variables in the D_I final model (based on rutting)	134
Table 63. Statistics of calibrated models based on fatigue cracking performance of flexible pavements	134
Table 64. Variables in the I_I final model (based on fatigue cracking)	134
Table 65. Variables in the Hogg final model (based on fatigue cracking)	134

Table 66. Statistics of calibrated models based on roughness performance of rigid pavements (9,000 lb (4,086 kg))	135
Table 67. Variables in the CI_5 final model (based on roughness) (9,000 lb (4,086 kg))	135
Table 68. Variables in the I_I final model (based on roughness) (9,000 lb (4,086 kg))	135
Table 69. Variables in the LTEA final model (based on roughness) (9,000 lb (4,086 kg))	135
Table 70. Statistics of calibrated models based on roughness performance of rigid pavements for alternative FWD test locations (9,000 lb (4,086 kg))	136
Table 71. Variables in the D_I final model for FWD testing at edge corner slab (based on roughness) (9,000 lb (4,086 kg))	136
Table 72. Variables in the D_I final model for FWD testing at edge midslab (based on roughness) (9,000 lb (4,086 kg))	136
Table 73. Statistics of calibrated models based on faulting at joints of rigid pavements (9,000 lb (4,086 kg))	137
Table 74. Variables in the D_6 final model (based on faulting at joints) (9,000 lb (4,086 kg)) ...	137
Table 75. Variables in the LTEA final model (based on faulting at joints) (9,000 lb (4,086 kg))	137
Table 76. Statistics of calibrated models based on faulting at joints of rigid pavements (9,000 lb (4,086 kg))	138
Table 77. Variables in the D_I final model for FWD testing at edge corner slab (based on faulting at joints) (9,000 lb (4,086 kg))	138
Table 78. Variables in the D_I final model for FWD testing at edge midslab (based on faulting at joints) (9,000 lb (4,086 kg))	138
Table 79. Statistics of calibrated models based on transverse cracking of rigid pavements (9,000 lb (4,086 kg))	139
Table 80. Variables in the CI_4 final model (based on transverse cracking) (9,000 lb (4,086 kg))	139
Table 81. Variables in the D_I final model (based on transverse cracking) (9,000 lb (4,086 kg))	139
Table 82. Variables in the LTEA final model (based on transverse cracking) (9,000 lb (4,086 kg))	140
Table 83. Statistics of calibrated models based on transverse cracking of rigid pavements (9,000 lb (4,086 kg))	140
Table 84. Variables in the D_I final model for FWD testing at edge corner slab (based on transverse cracking) (9,000 lb (4,086 kg))	140
Table 85. Variables in the D_I final model for FWD testing at edge midslab (based on transverse cracking) (9,000 lb (4,086 kg))	140
Table 86. Statistics of calibrated models based on roughness of rigid pavements (12,000 lb (5,448 kg))	141
Table 87. Variables in the CI_4 final model (based on roughness) (12,000 lb (5,448 kg))	141
Table 88. Variables in the I_I final model (based on roughness) (12,000 lb (5,448 kg))	141
Table 89. Variables in the LTEA final model (based on roughness) (12,000 lb (5,448 kg))	141
Table 90. Statistics of calibrated models based on roughness of rigid pavements (12,000 lb (5,448 kg))	142
Table 91. Variables in the D_I final model for FWD testing at edge corner slab (based on roughness) (12,000 lb (5,448 kg))	142

Table 92. Variables in the D_I final model for FWD testing at edge midslab (based on roughness) (12,000 lb (5,448 kg))	142
Table 93. Statistics of calibrated models based on faulting at joints of rigid pavements (12,000 lb (5,448 kg))	143
Table 94. Variables in the D_6 final model (based on faulting at joints) (12,000 lb (5,448 kg)).....	143
Table 95. Variables in the LTEA final model (based on faulting at joints) (12,000 lb (5,448 kg)).....	143
Table 96. Statistics of calibrated models based on faulting at joints of rigid pavements (12,000 lb (5,448 kg))	144
Table 97. Variables in the D_I final model for FWD testing at edge corner slab (based on faulting at joints) (12,000 lb (5,448 kg))	144
Table 98. Variables in the D_I final model for FWD testing at edge midslab (based on faulting at joints) (12,000 lb (5,448 kg))	144
Table 99. Statistics of calibrated models based on transverse cracking of rigid pavements (12,000 lb (5,448 kg))	145
Table 100. Variables in the CI_4 final model (based on transverse cracking) (12,000 lb (5,448 kg))	145
Table 101. Variables in the D_I final model (based on transverse cracking) (12,000 lb (5,448 kg))	145
Table 102. Variables in the LTEA final model (based on transverse cracking) (12,000 lb (5,448 kg))	146
Table 103. Statistics of calibrated models based on transverse cracking of rigid pavements (12,000 lb (5,448 kg))	146
Table 104. Variables in the D_I final model for FWD testing at edge corner slab (based on transverse cracking) (12,000 lb (5,448 kg))	146
Table 105. Variables in the D_I final model for FWD testing at edge midslab (based on transverse cracking) (12,000 lb (5,448 kg))	146
Table 106. Information about the different States used in the analysis	167
Table 107. Errors in percentage for 50, 70, and 80 percent reliability for section lengths up to 10 mi (16.1 km)	170
Table 108. Errors in percentage for 90, 95, and 99.5 percent reliability for section lengths up to 10 mi (16.1 km)	171
Table 109. Description of the Maryland sections used in the example	175
Table 110. FWD test data for all of the Maryland sites.....	178

CHAPTER 1—INTRODUCTION

BACKGROUND

The concept of a pavement management system (PMS) was developed following the American Association of State Highway Officials (AASHO) successful Road Test in the 1950s. Pavement performance was first characterized at the AASHO Road Test, providing the necessary information to compare design alternatives and expectations over the service life of flexible and rigid pavement structures. A link was established between performance and planning, designing, constructing, and maintaining pavements, and the concept of PMS was defined accordingly.

Surface distress measurements and roughness are the main components in determining a pavement's existing condition. These quantities can be used for predicting future performance and programming maintenance and construction/reconstruction activities, despite the fact that structural capacity has a major effect on how the pavement will perform in the future (i.e., rate of deterioration, types and severity of distresses, etc.). Therefore, it is important to consider the existing structural capacity of pavements and current surface distresses to predict the pavements' future condition with reasonable accuracy.

There are several techniques available to evaluate the structural capacity of pavements, most of which were developed for project-level applications (i.e., provide structural quality assessments for designing pavement rehabilitation or reinforcement). Many of these techniques are time consuming, and some require an experienced analyst. They generally provide more detail than is necessary for decision trees, making them less attractive and less cost effective for network-level applications. As a result, using pavement deflection testing for network-level analysis has been limited, even within agencies that extensively use a falling weight deflectometer (FWD) for project-level analysis.

However, some of these project-level techniques can be adapted to assist with network-level PMS applications. The key is to improve each technique in such a way that a simple parameter (or set of parameters) can be computed to describe the overall structural capacity of a uniform pavement section. Applicable techniques to assess pavement structural condition should improve the accuracy of PMS through enhanced project scoping and timing, potentially saving transportation agencies considerable funds and reducing construction delays (and therefore user costs) from poorly timed or ineffective projects. States including Texas, Kansas, New Jersey, Virginia, and Alaska have successfully incorporated structural indices in network-level applications. Such techniques are also used in countries such as South Africa, Finland, Denmark, France, and Australia.

PROJECT OBJECTIVES

The primary objectives of this study were to identify, develop, verify, and recommend simplified deflection-based analytical techniques suitable for rapid automated screening of pavement structural capacity for inclusion in a network-level PMS. These techniques have been derived from information gathered from the Long-Term Pavement Performance (LTPP) database and from other highway agencies currently using structural information in their PMS.⁽¹⁾ The success

of this study hinges on identifying solutions that can be implemented readily in national, State, and local municipality systems.

Another objective of the study was to develop and recommend data collection procedures that maximize testing productivity and minimize risk while still providing adequate information for use in a typical PMS. Test point spacing and frequency of data collection are the two primary parameters of interest.

It is intended that the results of this study are applicable to agencies that do not use deflection testing in their PMS but still use nondestructive deflection testing as part of their project-level analysis and design activities.

DESIRED OUTCOMES AND PROJECT DELIVERABLES

The following list describes the project's desired outcomes and deliverables:

- The development of a rational approach to evaluate deflection techniques capable of assessing pavement structural capacity for network-level analyses.
- The recommendation of practical and efficient techniques for evaluating deflection data for network-level analyses.
- Statistical procedures for determining the optimum test spacing and frequency of deflection measurements for network-level applications.
- Guidelines for considering the best time of day and/or period of the year for deflection data collection and procedures for incorporating historical data into the network-level deflection analysis.
- A prototype version of software that is capable of computing deflection-based parameters for network-level PMS applications using selected, simplified techniques.
- A final report describing the analysis approach, findings, and recommendations from the study.
- A stand-alone guide with step-by-step instructions for using deflection interpretation techniques for network-level analyses.

REPORT ORGANIZATION

This report documents the findings from phase 1 and phase 2 of the project. The information presented in this report is organized in the following chapters:

- Chapter 1 includes an introduction to the study, as well as background information, project objectives, desired outcomes, and project deliverables.
- Chapter 2 provides a literature review, including a summary of findings from previous studies and a list of the techniques for simplified load deflection data evaluation and analysis.
- Chapter 3 provides an assessment of LTPP data to support this investigation, including an evaluation of the need for supplemental data from other sources.
- Chapter 4 includes the methodology for evaluating and selecting applicable techniques for simplified evaluation and analysis.
- Chapter 5 includes the methodology for determining the optimum test spacing and frequency for network-level analyses.
- Chapter 6 includes guidelines for consideration of time of day and season of year for optimal data collection.
- Chapter 7 provides a practical example of how to apply the outcome of this research in existing PMS.
- Chapter 8 provides the conclusions and recommendations.

CHAPTER 2—LITERATURE REVIEW

INTRODUCTION

An essential part of this project was to conduct an extensive literature search. While FWD load deflection data have long been used to carry out project-level analyses, using these data to conduct network-level surveys is performed less frequently. Nevertheless, the existing literature shows that several agencies are already using FWD data in their network-level pavement analysis procedures.

Some agencies have also developed procedures that may assist in the development of a simplified approach to using deflection data in a network-level analysis that links pavement structural parameters, determined through the use of FWD data to pavement performance.

A review of all available literature was duly conducted, including obtaining information from agencies outside the United States, to ascertain which agencies use deflection data, which approach they employ, and whether these particular approaches may be useful in the present study. All deflection parameters (measured or computed) included in this report refer to the Strategic Highway Research Program (SHRP) seven sensor positions.⁽²⁾

LITERATURE REVIEW APPROACH

Relevant literature references were reviewed on the following subjects to achieve the literature review objectives:

- **Network versus project-level structural analysis:** Searched for differences and similarities in deflection data collection, such as parameters used, spacing, frequency, and loading.
- **Data collection:** Searched and compiled information regarding data collection (sampling or systematic), section length, and spacing between tests.
- **Data sources:** Investigated the source of deflection data and what the data are used for in terms of network-level surveys, project-level surveys, or both.
- **Data interpretation:** Compiled information about how the data were analyzed (deterministic, probabilistic, combination, etc.).
- **Required structural information:** Identified which parameters were required and utilized for network-level structural analysis, such as the following:
 - Center deflection (D_0): The deflection at the center of the applied load.
 - Curvature index ($D_0 - D_i$): The difference between the center deflection and the deflection at a prescribed offset from the load center.
 - Load-normalized and temperature-corrected center deflection (\bar{D}_0).

- Radius of curvature (RoC).
- Various “AREA” values of the deflection basin.
- Closed-form and two-layer solutions.
- **Relationship to performance:** Searched for literature that reports practices and research on incorporating structural evaluation of pavements based on deflections and performance measures.
- **PMS implementation:** Compiled information on studies about implementation of deflection-based parameters on PMS.
- **Report findings on each subject:** Compiled relevant information from references grouped by key topics in tabular form.

It is crucial to establish a reasonable body of knowledge on these topics to address the following:

- Establish the objectives of a structural network-level analysis.
- Determine the necessary structural information.
- Decide which conditions pavement deflections are useful for providing the required information for a network-wide structural evaluation,
- Determine performance indicators are currently used to link structural condition or integrity to the level of pavement distresses observed in the field.

SUMMARY OF FINDINGS FROM PREVIOUS STUDIES

Table 1 provides a summary of potentially relevant agency practices for FWD data collection and use for network-level analyses identified during the literature review study (see the complete table of references in appendix A).

Table 1. Summary of useful practices for FWD use in network-level analyses.

Agency and Publication	Test Point Spacing	FWD Test Frequency	FWD Sensor Positions	Limiting Factors	Basic Details of the PMS Approach
California Department of Transportation (Caltrans); "Test to Determine Overlay and Maintenance Requirements by Pavement Deflection Measurements" ⁽³⁾	N/A	N/A	N/A	None; currently used for flexible and composite pavements only	Uses center deflection only, plus existing asphalt concrete (AC) or AC + portland cement concrete (PCC) layer thickness.
Federal Highway Administration (FHWA); <i>Review of the LTPP Backcalculation Results</i> ⁽⁴⁾	N/A	N/A	N/A	None; may be used for flexible, composite, and rigid pavements alike	Uses Hogg model for subgrade modulus calculation. While it is possible that surface course stiffness can be derived using a related approach reported to FHWA by the authors, this is probably too complex and not worth the effort.
National Cooperative Highway Research Program (NCHRP); Project 10-48: <i>Assessing Pavement Layer Condition Using Deflection Data</i> ⁽⁵⁾	Probably not studied	Probably not studied	SHRP positions, generally	None; all pavement types studied using LTPP database (flexible, rigid, and composite)	Uses easy-to-obtain deflection basin parameters and relates these parameters to observed pavement distresses.
FHWA; <i>Temperature Predictions and Adjustment Factors for Asphalt Pavement</i> (FHWA-RD-98-085) ⁽⁶⁾	N/A	N/A	N/A	N/A	The adjustment for asphalt pavements for temperature-at-depth and center deflection adjustments for pavement temperature may be used to assist in the present study.

Agency and Publication	Test Point Spacing	FWD Test Frequency	FWD Sensor Positions	Limiting Factors	Basic Details of the PMS Approach
Kansas Department of Transportation (KDOT); “Network-Level Pavement Deflection Testing and Structural Evaluation” ⁽⁷⁾	A minimum of three tests per mile; five is preferred	One-third of network per year; however, one-fifth of network may be adequate	Unknown; probably unimportant	Flexible pavements only	Used data from one Kansas district on AC surfaces only (non-interstate), which is a similar approach to the current study. Based on the 1993 American Association of State Highway and Transportation Officials (AASHTO) <i>Guide for Design of Pavement Structures</i> . ⁽⁸⁾ The FWD, especially the center deflection value, added considerably to predictive capability of method used. Based on the concept of pavement structural evaluation (PSE). PSE was found to be twice as important to predict pavement performance as any other observable parameter. Recommended the use of Bayesian statistical models.
Alaska Department of Transportation (AkDOT); <i>Modeling Flexible Pavement Response and Performance</i> ⁽⁹⁾	0.1 mi	After repaving	SHRP positions	No limits	Deflections are converted to layer moduli, which are then used to obtain stress/strain values under a standard equivalent single-axle load (ESAL). Transfer functions relate stress/strain to cracking in bound layers and permanent deformation in unbound layers.
Texas Department of Transportation (TxDOT); <i>Incorporating a Structural Strength Index into the Texas Pavement Evaluation System</i> (FHWA/TX-88/409-3F) ⁽¹⁰⁾	0.5 mi	One recommended per year	1 ft	Flexible pavements less than 5.5 inches AC thickness	Structural strength index (SSI) varies from zero to 100 (weak to strong). Based on normalized basin parameters, such as outer deflections, surface curvature index (SCI), and center deflection under a 9,000-lb load. Can characterize subgrades and pavement structure independently in terms of relative stiffness. System based on statistical evaluation of deflections statewide.

Agency and Publication	Test Point Spacing	FWD Test Frequency	FWD Sensor Positions	Limiting Factors	Basic Details of the PMS Approach
TxDOT; <i>Network-Level Deflection Data Collection for Rigid Pavement</i> ⁽¹¹⁾	0.5 mi	N/A	1 ft	Rigid pavements	Not very useful from an analytical standpoint; mostly gives recommendations regarding field test procedures, estimated costs for testing and analysis, and reference to maximum allowable deflections for rigid pavements for network testing.
Virginia Department of Transportation (VDOT); <i>Network-Level Pavement Evaluation of Virginia's Interstate System Using the Falling Weight Deflectometer</i> (Report VTRC 08-R18) ⁽¹²⁾	0.2 mi	4–5-year cycle	SHRP positions	None	Flexible pavements were analyzed by calculating the subgrade resilient modulus, the effective pavement modulus, and the effective structural number (SN). Rigid and composite pavements were analyzed by calculating the area under the deflection basin and the static modulus of subgrade reaction (<i>k</i> -value).
National Laboratory for Civil Engineering; <i>Use of Deflections at Network Level in England for Programming and Other Purposes</i> ⁽¹³⁾	N/A; Used deflectograph, complemented by FWD	3–5 years	N/A	Flexible pavements only	Used Transport and Road Research Laboratory (TRRL) equations to calculate residual life and strengthening requirements based on deflection. The conclusion was that deflection does not increase with time and in some cases actually decreases due to an increase in pavement materials stiffness due to aging, etc. This approach was used until 2000.

Agency and Publication	Test Point Spacing	FWD Test Frequency	FWD Sensor Positions	Limiting Factors	Basic Details of the PMS Approach
South Africa; “Benchmarking the Structural Condition of Flexible Pavements with Deflection Bowl Parameters” ⁽¹⁴⁾	0.2 km	N/A	300 mm typical	Flexible pavements only	Pavement is divided into three zones based on depth. Uses basin parameters to characterize base, middepth, and subgrade structural condition such as “sound,” “warning,” or “severe.”
Association of Australian and New Zealand Road Transport and Traffic Authorities; <i>Use of FWD in the Network Level Pavement Condition Survey</i> ⁽¹⁵⁾	N/A	N/A	0, 900, and 1,500 mm	Flexible and semi-rigid pavements	Uses adjusted SN as indicator for pavement bearing capacity. SN is calculated based on d_0 , d_{900} , and d_{1500} , in which d represents deflection and i is the distance from the center of the plate (0, 900 and 1,500 mm).

N/A = Not available.

1 mi = 1.61 km

1 inch = 25.4 mm

1 ft = 0.305 m

1 lb = 0.454 kg

Agencies Currently Utilizing Deflection Data for Network-Level Applications

Findings from the literature indicate that only five agencies use, or are planning to use, load deflection data directly within their PMS.

United Kingdom

The United Kingdom uses traveling deflectograph data, not FWD or dynamic load deflection data; therefore, these data are not applicable to the present study.^(13,16) The traveling deflectograph does not correlate well with the FWD (or even the rolling wheel deflectometer (RWD)) due to the large differences in loading time and the Benkelman beam style apparatus involved, among other salient factors. While researchers in the United Kingdom have tried to supplement their traveling deflectograph data with FWD data, they discovered that the two do not correlate well, as expected; therefore, the FWD was dropped in favor of the traveling deflectograph. Interestingly, the old Caltrans traveling deflectograph, which was similar to the UK device, was dropped at least 30 years ago, first in favor of the Dynaflect[®] and later the FWD.

Alaska

AkDOT uses a multiyear cycle for deflection readings based on ongoing pre-and post-rehabilitation projects. Their PMS approach using FWD data was only recently initiated.⁽⁹⁾ It cannot be considered a simple process since back-calculation of sorts is currently used to determine remaining life. How well AkDOT's FWD evaluation procedure actually translates to pavement distresses, and therefore to pavement life expectancy, remains to be seen. Alaska's application of load deflection data within their PMS is relatively new. Accordingly, a few more years' worth of data will be needed to evaluate structural versus performance correlations. At the time this report was written, AkDOT gathered over 300 mi (483 km) of FWD data on the Parks Highway. These data were subsequently used as an example of how to incorporate the simplified methodology developed herein and will be shown later in this report.

Conversely, the methodology used to calculate the subgrade "seed" modulus using the AkDOT procedure is straightforward and immediately useable as a stand-alone parameter. Therefore, it can be used to correlate the subgrade modulus from the LTPP FWD database to see how well that particular approach (i.e., a nonlinear subgrade modulus model) relates to the various performance indicators in the mature LTPP database. The AkDOT procedure currently applies to flexible pavements only; however, rigid pavements may be investigated using the same subgrade modulus closed-form back-calculation process.

Texas

TxDOT currently uses deflection data in their PMS for flexible pavements only (district optional). (See references 10, 11, 17, and 18.) The publication *Incorporating a Structural Strength Index into the Texas Pavement Evaluation System* has been in use since its publication in 1988 in some of Texas's districts.⁽¹⁰⁾ It is currently used for relatively thin asphalt-surfaced pavements in 4 of 13 districts in Texas—Fort Worth, Houston, San Antonio, and Pharr. It is expected that the entire State will soon use the newer process shown in table 1.⁽¹⁰⁾

In an older TxDOT method, network-level deflection basins were collected at selected locations in the State to determine averages and ranges for a variety of pavement thicknesses and subgrade types. Basin parameters were developed and used in lieu of a back-calculation approach due to the lack of pavement structural data (i.e., number of layers, layer thicknesses, and material types). The greatest drawback to this approach is that it does not provide an indication of remaining structural life or bearing capacity. This approach essentially uses two basin parameters: SCI and W7, which is the deflection measured 6 ft (1.83 m) from the FWD load center. SCI is the difference between the deflections measured at the center of the load plate and the deflection measured 12 inches (304.8 mm) from the load plate. From these two parameters, an SSI is determined from one of three tables: one for surface treated pavements, one for thin asphalt pavements, and one for intermediate and thick asphalt pavements. SSI is further adjusted for traffic and rainfall levels to arrive at a final SSI. SSI ranges from 100 for a 100 percent structurally adequate pavement to zero for a 100 percent structurally inadequate pavement (meaning zero percent adequacy). This approach allows the user to determine where the inadequacies lie, whether within the subgrade or somewhere within the pavement structural section itself, above the subgrade.

Virginia

VDOT recently began using deflection data in their PMS, covering the entire network on a 4- to 5-year cycle for both flexible and rigid pavements.⁽¹²⁾ The procedure is simple and straightforward. However, since it is relatively new, the current study will have to evaluate the relationship of Virginia's structural determination procedures to pavement performance data in the LTPP database.

In developing the VDOT method, a two-phase evaluation of a proposed network-level structural evaluation technique was carried out in 2007 and 2008. Both phases were restricted to interstate pavements. In phase I, only I-64 and I-77 were included in the study. The results looked promising, so phase II was initiated on the remainder of Virginia's interstate system. A final report was published in 2008, which concluded that network-level deflection testing could be used to address network needs in terms of rehabilitation strategies and funding management decisions.⁽¹²⁾ The author further suggested that the network-level structural analysis should be expanded to include Virginia's primary network.

Pavement types in the study included flexible, rigid, and composite pavement structures. For flexible pavements, the analysis was conducted according to the 1993 *AASHTO Guide for Design of Pavement Structures*.⁽⁸⁾ For rigid and composite pavements, the analysis was conducted according to the 1998 *Supplement to the AASHTO Guide for Design of Pavement Structures: Part II—Rigid Pavement Design and Rigid Pavement Joint Design*.⁽¹⁹⁾

For flexible pavements, the resilient modulus (M_r) is first calculated according to the 1993 *AASHTO Guide for Design of Pavement Structures*.⁽⁸⁾ The effective pavement modulus (E_p) is calculated from the center deflection and subgrade modulus, also according to AASHTO procedures. Finally, an effective structural number (SN_{eff}) is determined from E_p and the total pavement thickness above the subgrade.⁽⁸⁾

For rigid and composite pavements, the deflection basin AREA and the static modulus of subgrade reaction, k , are used to quantify overall structural condition.

A cumulative distribution curve of SN_{eff} and M_r was developed for all flexible pavements in the study. Similar curves were developed for center deflections and deflection basin AREA for rigid pavements. These distribution curves are used to identify structurally weak areas of the network for further project-level investigation.

One factor that contributed to the overall success of this approach is the availability of pavement layer data (thicknesses, material types, etc.) in VDOT's Highway Traffic Record Information System database.⁽²⁰⁾ Also noted were rather high subgrade M_r in the cumulative distribution curves. The 50th percentile value of the subgrade stiffness was around 12,500 psi (86,125 kPa). This may have been due in part to the presence of rigid or semi-rigid layers in the subgrade, which the AASHTO method does not address, and in part due to the typical non-linear behavior of cohesive subgrades (with a lower effective modulus under the load than at increasing distances from the load). The 1993 AASHTO *Guide for Design of Pavement Structures* equations utilize the outer deflection sensors to characterize the subgrade modulus, not the true effective modulus of the subgrade under the load.⁽⁸⁾

South Africa

The Republic of South Africa uses FWD testing at 656-ft (200-m) intervals to ascertain the bearing capacity of three roadway “zones” or layers (surface, base, and subgrade). The methodology relies on direct deflection basin parameters, not back-calculation.⁽¹⁴⁾ A benchmarking technique was developed to relate direct deflection values and basin parameters to the structural condition of the pavement at both the project and network levels. This benchmarking technique can be used in the absence of detailed information regarding pavement composition.

The South African method correlates FWD deflections to structural layers or zones within the pavement structure. These zones are numbered 1 through 3, where zone 1 corresponds to the materials closest to the load plate within the pavement structure, extending out to 11.7 inches (300 mm) in terms of the deflection basin (and probably somewhat less in terms of depth within the structure). In zone 2, the inflection point in the deflection basin occurs and generally lies from < 1 to 2 ft (< 0.305 to 0.61 m) in depth below the pavement surface. Zone 3 extends from approximately 2 to 6.5 ft (0.61 to 1.98 m) from the center of the load plate and thus represents the deepest layers in the pavement structure—primarily the subgrade.

In the South African method, the following deflection parameters and associated pavement structural zones are represented:

- D_0 , or the maximum deflection as measured at the center of loading (also known as center deflection) is correlated to all three zones, since it represents the response of the entire pavement structure.
- RoC is correlated to zone 1 (the upper pavement layers) and is derived using the equation in figure 1.

- The base layer index (BLI) is correlated to zone 1 and is calculated using the equation in figure 2.
- The middle layer index (MLI) is correlated to zone 2 and is calculated using the equation in figure 3.
- The lower layer index (LLI) is correlated to zone 3 and is calculated using the equation in figure 4.

$$RoC = \left(\frac{(L^2)}{2D_0(1 - D_{200} / D_0)} \right)$$

Figure 1. Equation. Calculation of RoC.

$$BLI = D_0 - D_{300}$$

Figure 2. Equation. Calculation of BLI.

$$MLI = D_{300} - D_{600}$$

Figure 3. Equation. Calculation of MLI.

$$LLI = D_{600} - D_{900}$$

Figure 4. Equation. Calculation of LLI.

Where:

L = Diameter of the load plate of the FWD (mm).

D_0 = Deflection at center of load plate (mm).

D_{200} = Deflection at 8 inches (200 mm) from the center of the load plate (mm).

D_{300} = Deflection at 12 inches (300 mm) from the center of the load plate (mm).

D_{600} = Deflection at 24 inches (600 mm) from the center of the load plate (mm).

D_{900} = Deflection at 36 inches (900 mm) from the center of the load plate (mm).

These deflection bowl parameters are related to a structural condition rating according to the structural condition and the type of base layer, as described in table 2, extracted from Horak's "Benchmarking the Structural Condition of Flexible Pavements with Deflection Bowl Parameters."⁽¹⁴⁾

The basin parameters LLI, MLI, and BLI are plotted against stationing for a particular roadway to facilitate the structural assessment procedure. This plot of structural condition is often used in conjunction with visual assessments to determine the type of rehabilitation required to restore the pavement to a good condition.

Table 2. Structural condition associated with deflection bowl parameters.⁽¹⁴⁾

Base Type	Structural Condition Rating	Deflection Bowl Parameters				
		D_0 (μm)	RoC (m)	BLI (μm)	MLI (μm)	LLI (μm)
Granular base	Sound	< 500	> 100	< 200	< 100	< 50
	Warning	500–750	50–100	200–400	100–200	50–100
	Severe	> 750	< 50	> 400	> 200	> 100
Cementitious base	Sound	< 200	> 150	< 100	< 50	< 40
	Warning	200–400	80–150	100–300	50–100	40–80
	Severe	> 400	< 80	> 300	> 100	> 80
Bituminous base	Sound	< 400	> 250	< 200	< 100	< 50
	Warning	400–600	10–250	200–400	100–150	50–80
	Severe	> 600	< 100	> 400	> 150	> 80

Note: These criteria can be adjusted to improve sensitivity of benchmarking.

1 mil = 25.4 μm

1 ft = 0.305 m

The surface modulus is calculated at the various sensors and plotted against distance from the load plate to assess nonlinearity. The standard Boussinesq equations are used for this purpose. Points where the surface modulus increases with increasing distance from the load center are regarded as “stress softening.” If the surface modulus is similar for all measured deflections, the subgrade is regarded as linear-elastic. Decreasing surface modulus with increasing distance from the load center indicates a “stress stiffening” subgrade.

Agencies Utilizing Deflection Data in a Manner Potentially Useful to Enhance Network-Level PMS Applications

In addition to the previously listed agencies that already utilize load deflection data within their PMS, the following agencies use deflection data with potential network-level PMS applications:

- **Caltrans:** Currently uses deflection data for project-level pavement analysis and design only; however, the design method is simple and straightforward and was therefore tried during phase 2 of this study as a potential network-level PMS tool.⁽³⁾
- **KDOT:** This approach is simple and straightforward. If the equations can be used to regress against LTPP performance measures, this could have been tried; however, since KDOT used this approach for flexible pavements only and only in one district for a trial project, the methodology was not further investigated.⁽⁷⁾

The following publications do not describe deflection data applications of specific agencies, but they are relevant to the scope of this project:

- **NCHRP Project 10-48:** This study was similar to the current study, and it utilized the LTPP database.⁽¹⁾ Equations cover flexible, composite, and rigid pavements as deflections relate to performance.⁽⁵⁾

- **Temperature Predictions and Adjustment Factors for Asphalt Pavement (FHWA-RD-98-085):** This study applies to asphalt temperature corrections and mid-depth temperature determinations for asphalt pavements only (not needed for concrete but likely applicable if needed).⁽⁶⁾ The equations found in this publication are potentially useful for performance measures that relate FWD center deflection to pavement performance. However, after regressing against both temperature-corrected and temperature-uncorrected values of center deflection (D_I) (or their inverse), it was determined that no improvement in any of the logistic models resulted.⁽⁶⁾
- **Use of FWD in the Network Level Pavement Condition Survey:** This study utilizes center deflection and measures of curvature, along with roughness, rutting, and skid resistance.⁽¹⁵⁾ Center deflection (or its inverse) was utilized during this research, with some (but not universal) success. The results are presented later in this report.

Identified Techniques for Simplified Evaluation and Analysis

Based on the literature review and summary of useful practices presented in table 1, a list of deflection techniques was created. Several techniques were considered to be applicable to the scope of this project and were selected for further analysis. The following techniques and equations were selected when applicable:

1. D_I , measured at the center of the load plate in millimeters. (See references 14, 3, 7, 15, and 21.)
2. Direct deflection basin, D_I through D_7 , where D_i is the deflection measured at sensor $i = 1$ through 7 according to SHRP's seven sensor positions.^(2,21)
3. Curvature index (CI) (see figure 5).^(14,15,21)

$$CI_i = D_i - D_{i+1}$$

Figure 5. Equation. Calculation of CI_i .

Where D_i is the deflection measured at sensor $i = 1$ through 7.

4. Shape indicator (F) (see figure 6).⁽²¹⁾

$$F_i = \left(\frac{D_{i-1} - D_{i+1}}{D_i} \right)$$

Figure 6. Equation. Calculation of F_i .

Where i is the sensor 1 through 7.

5. Slope variance (S) (see figure 7).⁽²¹⁾

$$S_i = D_1 - D_i$$

Figure 7. Equation. Calculation of S_i .

Where i is the sensor 1 through 7.

6. Reciprocal indicator (I) (see figure 8).⁽²¹⁾

$$I_i = \frac{1}{D_i}$$

Figure 8. Equation. Calculation of I_i .

Where i is the sensor 1 through 7.

7. Rectangular area indicator (RA) (see figure 9).⁽²¹⁾

$$RA = \frac{\sum_{i=1}^{i=7} D_i}{D_i}$$

Figure 9. Equation. Calculation of RA.

Where i is the sensor 1 through 7.

8. Trapezoidal area indicator (TA) (see figure 10).⁽²¹⁾

$$TA = \frac{D_1 + D_7 + \sum_{i=2}^{i=6} 2D_i}{D_i}$$

Figure 10. Equation. Calculation of TA.

Where i is the sensor 1 through 7.

9. SN_{eff} (see figure 11).^(17,18,7)

$$SN_{eff} = 0.0045 \cdot D \cdot (E_p)^{1/3}$$

Figure 11. Equation. Calculation of SN_{eff} .

Where D is the total pavement layer thickness above the subgrade (mm) and E_p is the effective pavement modulus, computed using the equation in figure 12.

$$d_0 = 1.5 \cdot p \cdot a \left(\frac{1}{M_r \sqrt{1 + \left(\frac{D}{a} \sqrt{\frac{E_p}{M_r}} \right)^2}} + \frac{1 - \left(1 + \left(\frac{D}{a} \right)^2 \right)^{-\frac{1}{2}}}{E_p} \right)$$

Figure 12. Equation. Calculation of d_0 .

Where d_0 is deflection at the center of the load plate (mm), P is load plate pressure (MPa), a is load plate radius (mm), D is pavement layers thickness above subgrade (mm), and M_r is the resilient modulus, given by the following expression:

$$M_r = \frac{2.4P}{d_r r}$$

Figure 13. Equation. Calculation of M_r .

Where M_r is resilient modulus (MPa), P is applied load (kN), d_r is deflection at a distance r from the center of the load (mm). r is chosen as the distance to the seventh sensor.

10. Deterministic-empirical back-calculation model (closed form solution) for effective subgrade modulus (Hogg model).⁽⁴⁾

$$E_0 = I \frac{(1 + \mu_0)(3 - 4\mu_0)}{2(1 - \mu_0)} \left(\frac{S_0}{S} \right) \left(\frac{P}{\Delta_0 I} \right)$$

Figure 14. Equation. Calculation of E_0 .

Where E_0 is subgrade modulus (effective) (MPa), μ_0 is Poisson's ratio for subgrade, S_0 is the theoretical point load stiffness (MPa), S is the pavement stiffness (MPa), P is applied load (kPa), Δ_0 is the deflection at center of load plate (mm), L is the characteristic length (mm), and I is the influence factor.⁽⁴⁾

11. Radius of curvature, shown in figure 1 (page 14) for completeness.⁽¹⁴⁾
12. Elmod, nonlinear subgrade parameters.⁽²²⁾

$$E_{sg} = C \left(\frac{\sigma}{\sigma'} \right)^n$$

Figure 15. Equation. Calculation of E_{sg} .

$$n = \frac{\log \left(\frac{E_{0(r1)}}{E_{0(r2)}} \right)}{2 \log \left(\frac{r2}{r1} \right)}$$

Figure 16. Equation. Calculation of n .

$$C = \frac{E_{0(r1)} - E_{0(r2)}}{\left(\frac{\sigma_{(r1)}}{\sigma'} \right)^n - \left(\frac{\sigma_{(r2)}}{\sigma'} \right)^n}$$

Figure 17. Equation. Calculation of C .

$$E_{0(r)} = \frac{(1 - u^2)P}{\pi r(d_r)}$$

Figure 18. Equation. Calculation of $E_{0(r)}$.

$$\sigma_{(r)} = \frac{3P}{2\pi R^2} \cos^3 \theta$$

Figure 19. Equation. Calculation of $\sigma_{(r)}$.

Where:

E_{sg} = Subgrade modulus (kPa).

C = A layer constant, n is a layer constant representing the nonlinearity of the subgrade.

σ = Principle stress (MPa).

σ' = Reference stress (14.5 psi (0.1 MPa)).

$E_{0(r)}$ = Surface modulus at distance r from load center (MPa).

r = Horizontal distance from load center (mm).

z = Vertical depth with respect to the pavement surface (mm).

$\sigma_{(r)}$ = Principle stress at depth z (assuming $z = r$).

μ = Poisson's Ratio, $d_{(r)}$ is deflection at distance r from load center (mm).

P = Applied load on pavement surface (MPa).

R = Distance to evaluation point ($R^2 = r^2 + z^2$).

θ = Angle with respect to vertical axis through load center.

In addition to the parameters mentioned, the load transfer efficiency (LTE) value was calculated for rigid pavements. There are two ways of calculating LTE—in one method, the FWD test is performed at the slab before the joint (joint approach), and in the second method, the FWD test is performed at the slab after the joint (joint leave). An analysis of both was conducted, and the values were close to each other. Therefore, for simplification, only one LTE value was chosen. The option was for the first method with LTE at the joint approach because it does not require any modification on the configuration of the FWD. The LTE at joint approach is referred to as “LTEA” in this report and was calculated as the ratio of the deflection at the third sensor (12 inches (304.8 mm) from the center of the load) and the deflection at the center of the load.

CONCLUSIONS FROM THE LITERATURE REVIEW

Several successful techniques for use in network-level PMS applications were identified through the literature search. A few highway agencies have been using deflections as part of their network condition assessment. Among those, Texas, Virginia, and South African approaches were selected for further investigation in succeeding tasks with little or no modification. In addition, there were several techniques that could be utilized in the present study even though these techniques were not used in a network-level PMS. Combining all sources available, a list of potential applicable techniques that are relevant to the scope of this project was created as a result of the literature review and is shown in table 1. These deflection techniques formed the basis for the analyses carried out in this project.

CHAPTER 3—ASSESSMENT OF DATA

REVIEW AND ASSESSMENT OF DATA FROM LTPP STUDIES

Data Selection Criteria

The goal of this task was to review data from LTPP studies that are relevant to the scope of this study. Of particular interest was the assessment of LTPP sites that had sufficient deflection information, site characteristics (structure, climate conditions, traffic, and age), and historical performance data consisting of load-related distresses and roughness levels. Data from both General Pavement Studies (GPS) and Specific Pavement Studies (SPS) were considered. SPS sites are particularly valuable due to the extensive material testing and performance data concurrently available. In addition, sites from the Seasonal Monitoring Program (SMP) provided useful information for studying environmental effects, as well as the timing and frequency of deflection testing for network-level coverage.

One objective of a PMS is to establish long-term maintenance and rehabilitation (M&R) strategies for the network. Therefore, only those pavement sections for which the database included at least 5 years' worth of data were included in the analysis database.

Data Elements Needed for Analyses

The following data elements were identified as necessary for the analysis:

- Performance data:
 - AC surfaces.
 - Rutting.
 - International Roughness Index (IRI).
 - Fatigue cracking.
 - Transverse cracking.
 - Longitudinal cracking.
 - Alligator cracking.
 - PCC surfaces.
 - IRI.
 - PCC faulting at joints.
 - PCC faulting at cracks.

- Transverse cracking.
 - Longitudinal cracking.
 - Durability cracking.
 - Number of corner breaks.
- Pavement structure:
 - Pavement layer type.
 - Representative thickness for a layer in a section.
 - Type of material (AC, PCC, etc.).
- Pavement deflection data:
 - Peak deflection values.
 - Drop height.
 - Peak load (peak load equals peak plate pressure).
 - Lane number.
 - Lane location.
 - Measured pavement surface temperature.
 - Time of day.
- Climatic data:
 - Average temperature.
 - Average precipitation.

Table 3 provides a summary of data types that were assessed in this investigation, along with the corresponding LTPP data tables containing the required data elements.

Table 3. LTPP database tables used to support data collection.

Type of Data	Data Element Chosen	Relevant LTPP Tables
Traffic	<ul style="list-style-type: none"> • Average annual daily truck traffic (AADTT) • Vehicle classifications 	TRF_MONITOR_VEHICLE_DISTRIB
Climate	Temperature	CLM_VWS_TEMP_MONTH
	Precipitation	CLM_VWS_PRECIP_MONTH
FWD deflection surveys	Deflection data	MON_DEFL_DROP_DATA
	Test location	MON_DEFL_LOC_INFO
	Test temperature	MON_DEFL_TEMP_VALUE MON_DEFL_TEMP_DEPTHS
	FWD sensors	MON_DEFL_DEV_SENSORS
Performance	Rutting	MON_T_PRF_INDEX_SECTION
	Longitudinal profile	MON_PROFILE_MASTER
	Hot mix asphalt (HMA) surface distresses	MON_DIS_AC_REV
	PCC faulting	MON_DIS_JPCC_FAULT_SECT
	PCC surface distresses	MON_DIS_JPCC_REV
Structure	<ul style="list-style-type: none"> • Layer type (material) • Layer thickness 	TST_L05B
General information	<ul style="list-style-type: none"> • Construction history • LTPP assignment date • Experiment type 	EXPERIMENT_SECTION

Analysis Database Development

The LTPP Standard Data Release (SDR) 23 database (the most up-to-date version at the time this study was conducted) was examined for the identified data elements to determine the extent of data availability.⁽¹⁾ Data were extracted from the LTPP database, imported into a Microsoft Access[®] analysis database, and stored in various data tables. These tables were set up according to the principles of the relational databases so that they could be manipulated and linked together for various analysis purposes.

Data Review Process

Data for the sites that satisfied the data selection criteria were reviewed for quality, reasonableness, and availability in light of supporting the evaluation of identified deflection techniques.

The first step in the data review process was to eliminate test sections that had less than 5 years of performance and/or deflection data from the beginning of the monitoring period. In the sequence, quality and reasonableness were evaluated for all sections selected. The performance plots and deflections versus time were then visually inspected. Outliers and unreasonable trends

were identified for a more detailed evaluation. A summary of the data assessment results is presented in the following sections.

Outliers identified in performance trends were marked for possible exclusion from the datasets. Ultimately, whether an outlier was excluded depended on its influence on the performance trend over the years that data were collected and its impact on predicting future performance. Details of this approach are provided in chapter 4 of this report.

ASSESSMENT OF DATA TO SUPPORT EVALUATION OF IDENTIFIED TECHNIQUES

All deflection data collected during the experiment were obtained from the LTPP SDR 23 database and assessed.⁽¹⁾ In total, there were 1,027 sections in the SPS and GPS experiments with 5 or more years of performance and deflection data available. These sections include all pavement types—flexible, rigid, and composite. These sections may or may not have been rehabilitated during the course of data collection. Table 4 lists the experiments, number of sections available with deflection and performance data, and average period of time of data coverage.

Table 4. LTPP data availability to support evaluation of identified techniques.

Pavement Type	Experiment Type	Number of Sections with FWD Data	Distress Data Availability (average years)
Flexible	GPS-1	233	12.8
	GPS-2	146	13.4
	GPS-6A	62	11.6
	SPS-5	152	12.7
	Total	593	
Rigid	SPS-6	51	11.0
	GPS-3	133	14.5
	GPS-4	69	13.1
	GPS-9	21	13.3
	Total	274	
Composite	GPS-7A	35	10.9
	SPS-6	125	12.7
	Total	160	

Impact of M&R on Pavement Performance Data

In addition to verifying performance requirements and deflection availability, it was also important to consider any M&R work on the LTPP lane of the analysis sections. When one section is rehabilitated, performance invariably improves, and this affects the outcome of the analysis. Of the 1,027 sections selected, 47 of the flexible sections, 105 of the rigid sections, and 97 of the composite sections had been rehabilitated (almost 25 percent of all sections). An approach to identify these sections and split them based on the rehabilitation work performed (i.e., change in structure and reduction of distress level) was developed. The main reason for performing this type of analysis was the possibility of increasing the number of available

representative pavement sections, especially for the more sparsely populated rigid and composite pavement types.

The multiple section analysis was designed to enhance the chances of using sections with rehabilitation work performed during the monitoring period. Usually, any rehabilitation work done on the pavement is indicated in the LTPP database by a change in construction number. This is an event number used to relate changes in pavement structure with other time-dependent data elements. This field is set to “1” when a test section is accepted into the LTPP program and is incremented with each M&R activity.

The first step was to plot the performance data as a function of time for all sections. A simple macro-based code was written to expedite this process. The analysis of performance change is required because sometimes the M&R work is done outside the LTPP lane (e.g., at the shoulder) with no implication on LTPP lane performance.

For this analysis, the IRI was the performance measure used to determine the cutoff date to split the section based on recorded M&R activities. IRI is sensitive to M&R work performed on the pavement, and IRI measurements are more frequent in the LTPP distress survey campaign, which enhances the chances of finding sections that can be successfully split and still provide enough data for analysis.

Figure 20 shows section 06-0509, which illustrates how the section split was done based on rehabilitation work executed on the pavement. This example is a flexible pavement section located on I-40 in California, and the figure shows the variation of roughness over time. There were two rehabilitation interventions executed during the time the section was monitored. Three distinct pavement structures are identified. The first subsection (A) corresponds to the pavement from the original construction. The first split creates another subsection (B) with a new structure due to partial milling of the existing pavement and placing a hot mix recycled asphalt concrete overlay. The second split creates the third pavement subsection (C) due to a single layer of surface treatment applied to the existing surface. These two splits yield the following subsections and pavement structures:

- Structure A has a construction number index of 1, corresponding to the following original pavement structure:
 - Untreated subgrade.
 - Unbound (granular) subbase.
 - Bound (treated) base.
 - HMA concrete.

- Structure B has a construction number index of 2, corresponding to partial milling of the existing surface layer in A, followed by filling and overlay using a hot recycled asphalt concrete mix.
- Structure C has a construction number index of 3, which corresponds to another HMA concrete overlay placed on top of B.

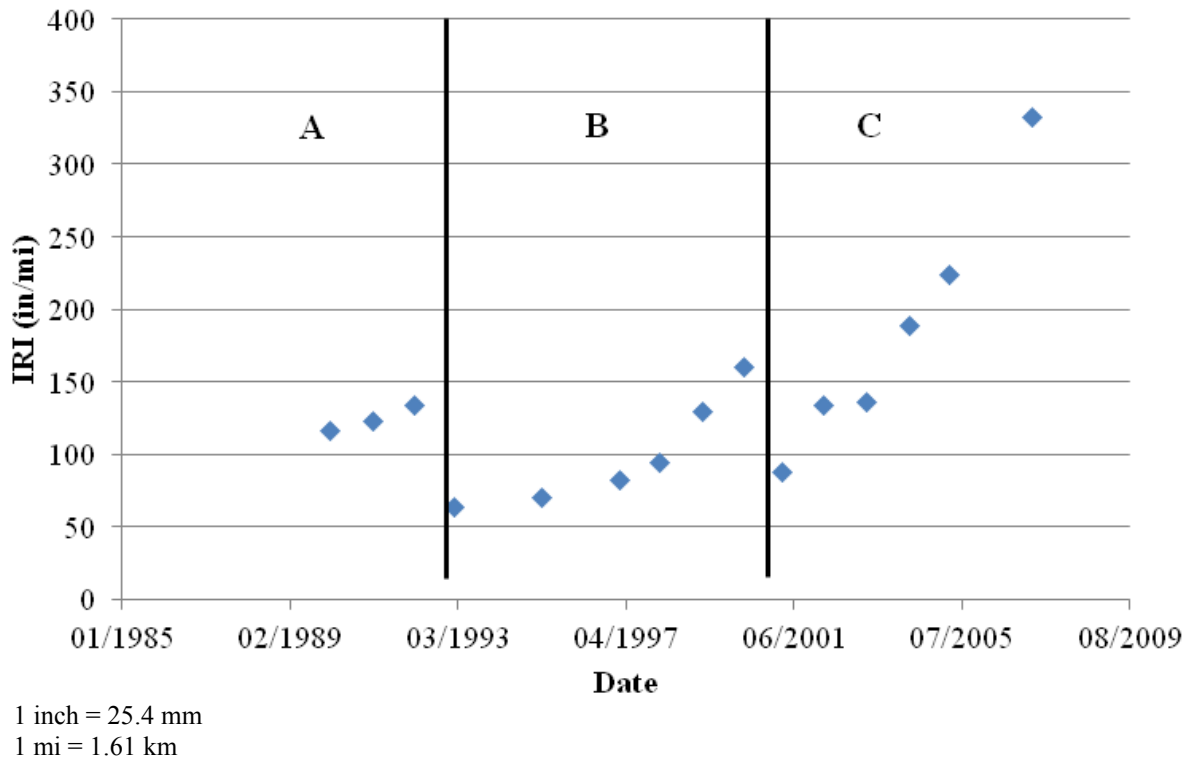


Figure 20. Graph. Variation of roughness in section 06-0509.

After the multiple section analysis was concluded, each of the three new subsections was reevaluated based on the 5-year performance criterion. The first subsection (A) was excluded from the analysis because it had less than 5 years of performance data. Subsections B and C both had more than 5 years of performance data and were therefore included in the project's dataset.

This process was carried out on all LTPP sections selected to support the evaluation of simplified deflection-based analysis techniques. Table 5 shows the final data assessment summary after performing the multiple section analysis. Notice that if the sections that received one or more M&R procedures after being assigned to the LTPP database were excluded altogether from the dataset, the total number of available sections would have been 827. After splitting the sections and including the subsections with 5 years or more of performance data, the total number of available sections increased to 1,033. Accordingly, the multisection analysis minimized the loss of LTPP data points available for the study.

Table 5. Data assessment summary after multiple section analysis.

Pavement Type	Total Sections	Selected Sections After Multiple Section Analysis
Flexible	573	623
Rigid joint plain concrete pavement (JPCP)	127	175
Rigid joint reinforced concrete pavement	64	79
Composite	63	156
Total	827	1,033

Note: Total sections include sections before multiple section split and excluded rehabilitated sections.

Analysis of Deflection Data

Deflection data were analyzed for quality and reasonableness. Prior LTPP studies investigated the quality of deflection data, and the recommendations and final tables originating from these studies were used as the source of data mining for this project.⁽²³⁾ After the data were extracted into spreadsheets, each deflection-based technique or parameter was computed. Table 1 lists the deflection techniques investigated in this project.

ASSESSMENT OF DATA TO SUPPORT OPTIMUM TEST SPACING AND FREQUENCY

LTPP Data to Support Optimum Test Spacing Analysis

As part of phase I, the applicability of LTPP data for this type of analysis was verified. One of the concerns with LTPP data was the limited length of the LTPP sections (generally 500 ft (152.5 m)), which is not ideal for a statistical analysis of optimum test point spacing on the network level. A theoretical statistical study was conducted to evaluate the implications of different sampling strategies (i.e., different test spacings) on the expected error of average deflections of homogenous road segments, when compared with comprehensive test spacings. The comprehensive test spacings were defined as the typical 0.1-mi (0.016-km) spacing commonly used by transportation departments for project-level FWD testing. The theoretical statistical study was then compared to field data obtained from State transportation departments.

Supplemental Data to Support Optimum Test Spacing Analysis

Supplemental data were required to investigate optimum FWD test spacings for network-level deflection data collection. FWD data from three State transportation departments were obtained and used to test results obtained from the theoretical statistical study.

LTPP Data to Support Optimum Test Frequency Analysis

Selected sections from the GPS and SPS studies were monitored for temperature and moisture at higher-than-normal intervals for distress, deflection, and longitudinal profile (IRI). These sections were part of the SMP database and were classified as either flexible or rigid pavements.

Table 6 shows the classification of these SMP sections and the availability of FWD data from these sections.

Table 6. FWD data availability for SMP sites.

Pavement Type	Experiment Type	Number of SMP Sections with FWD Data	Number of Years (Average)
Flexible	SPS-1	10	13.7
	SPS-5	1	16.6
	SPS-8	2	14.1
	SPS-9N	1	14.0
	SPS-9O	1	9.3
	GPS-1	26	8.8
	GPS-2	5	8.9
	Total	46	
Rigid	SPS-2	4	13.6
	GPS-3	8	17.7
	GPS-4	6	21.0
	Total	18	

The SMP data sections were scrutinized in the same manner as was used for the GPS and SPS sections for data quality and reasonableness. The objective of incorporating the SMP sections was to provide data elements for the analysis of frequency of deflection measurements for network-level applications. Moreover, the data were used to evaluate and develop guidelines for the optimum time of day and season of year for FWD (or equivalent deflection testing device) data collection.

After initial inspection of data availability, it was found that monthly collection of data in most SMP sections occurred for about 2 years (or a maximum of 3 years). This volume of data reduced the chances for a robust assessment of the optimum frequency of FWD data collection for network-level applications. Therefore, it was decided to complement the dataset with additional LTPP sections from the dataset defined for the study of deflection-based techniques. The approach for using both datasets is further described in chapter 5 of this report.

LTPP Data to Support Time of Day and Day of Year Analysis

Different agency practices and provisions related to time-of-day and time-of-year data collection and analysis were reviewed. For example, the UK highway agency has a requirement for network-level deflectograph data collection from March 15 to June 15 and from September 15 to November 30. This requirement is primarily based on the climate in the United Kingdom. For the United States, different climate zones will most likely have different periods during which data collection will be most favorable to capture useful network-level deflection data. The subset of the LTPP database used to evaluate the deflection techniques was also used to analyze FWD data for different climatic zones that were taken during different months to determine favorable data collection periods for different regions.

CHAPTER 4—EVALUATION OF APPLICABLE LOAD DEFLECTION TECHNIQUES

Deflection data analysis provides qualitative and quantitative assessment of the structural integrity and bearing capacity of a pavement. Pavements with poor structural quality are more likely to develop distresses prematurely. It is commonly expected that the rate of deterioration increases as the structural condition worsens. Identifying pavements in poor structural condition is important to prevent early and rapid development of load-related distresses. This is the main motivation for the approach presented in this chapter.

Based on these premises, a probabilistic approach was developed to determine the likelihood of premature failure using load deflection techniques. Premature failure is defined by the presence of excessive distress (i.e., levels of distress higher than design threshold) occurring prior to the end of the design life of the pavement section.

Deflection data are commonly used at project-level analysis, mostly through back-calculation of layer moduli for overlay design purposes. Limited use has been observed at network-level analysis, in part due to difficulties in establishing thresholds to guide the structural evaluation. On such occasions, deflection data are used to create a rating system which yields a qualitative assessment of the structural condition. This assessment is used to determine prospective M&R treatments or remaining service life of the pavement. The rating criteria are often based on experience and common trends observed in the network.

The probabilistic approach proposed in this research can be used to establish thresholds for deflection data based on performance measures and assist with the creation of the network-level structural decision matrix. The following list includes benefits of using a deflection-based probabilistic model sensitive to structural pavement performance:

- It provides a direct link to pavement performance by estimating the likelihood of the development of load-related distresses in early stages of the pavement's service life. The intent is not to have a regression predictive model based on deflection data, but rather a simplified procedure to identify critical sections with a high likelihood of developing structural distresses prematurely.
- Rating criteria can be created in the same manner equivalent to the functional decision matrix. Different tiers of structural quality can be defined based on deflection thresholds and the likelihood of acceptable performance. The structural decision matrix can then follow rating criteria similar to the functional decision matrix which facilitates the implementation in existing PMS algorithms.
- The probabilistic models can be locally calibrated to meet the network characteristics (e.g., typical surface distresses observed, interval between M&R projects, and the threshold of acceptable limits for distresses).
- The probabilistic models can be recalibrated as new survey data are collected.

ANALYSIS APPROACH

Binary Logistic Model

Logistic regression is useful to predict the outcome of an event based on a set of predictor variables. Logistic models are best used when the dependent variable is dichotomous (i.e., variables that assume binary values, such as acceptable and not acceptable). It is a powerful analysis tool to model complex problems where the number of variables affecting the outcome is large.⁽²⁴⁾

Formulation and Calibration

The logistic regression model general equation is provided in figure 21. In this case, P is the probability that an event will occur, and b is the exponent parameter in logistic distribution, which is a linear function of the predictor variables, as given in general form by the equation in figure 22. The event is defined as the performance of the pavement section, “acceptable” for sections outlasting the design life and “not acceptable” for sections exhibiting premature failure. The predictor variables, also known as explanatory variables, are selected to best explain the behavior of the event. In this research, the predictor variables were load deflections and site characteristics, such as climate, traffic, and pavement structure. A typical logistic model probability function of a predictor variable X is shown in figure 23.

$$P(event) = \frac{1}{1 + e^{-b}}$$

Figure 21. Equation. General formulation of the logistic model.

$$b = a_0 + a_1b_1 + a_2b_2 + \cdots + a_nb_n$$

Figure 22. Equation. General linear formulation for the exponent term of the logistic model.

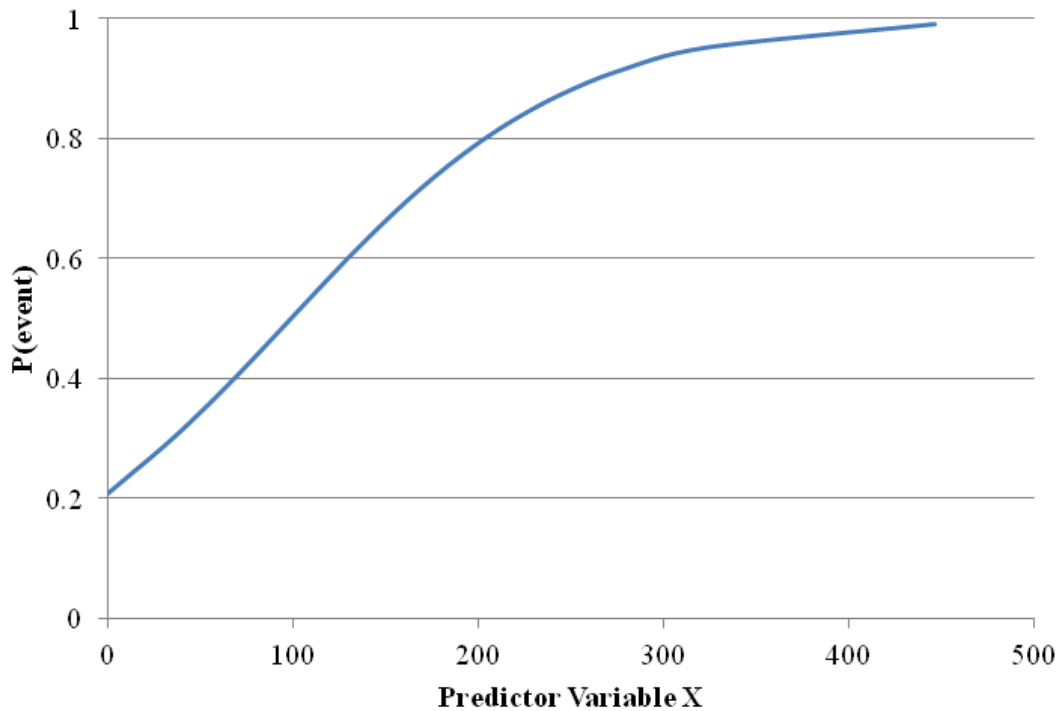


Figure 23. Graph. Typical logistic model probability function of a predictor variable X.

Predictor variables can be continuous (e.g., traffic volume) or discrete (e.g., pavement subgrade type assigned to coarse- or fine-grained soil). The dichotomous event is modeled as binary numbers—1 for acceptable and 0 for not acceptable. The model coefficients are computed using optimization algorithms. The most widely used is the maximum likelihood estimate. In this algorithm, the coefficients of the predictor variables are obtained to maximize the probability of the event occurring. The maximum likelihood estimate is well suited for problems in which the event occurs in the majority of the cases. This is the case in pavement performance where the majority of the pavements are expected to perform well.

There is no limitation to the number of predictor variables used. In fact, it is part of the process to eliminate variables with no significant relevance to the probabilistic function. This characteristic greatly helps the analysis—there is no need to refine the selection of variables, and all possible candidates can be considered. The selection of significant variables is achieved through a stepwise regression. At first, all predictor variable candidates are used in the calibration process. The predictor coefficients are calculated using the optimization algorithm, and the significance of each predictor to the probability function is computed. One by one according to step, the predictors with the least significance to the problem are eliminated.⁽²⁵⁾ The process is concluded when all remaining variables have significance levels higher than 95 percent or the maximum number of iterations is reached. This approach is called “backward elimination.”

Conventional statistics cannot be used to measure the goodness-of-fit of binary logistic models. Instead, the receiver operating characteristics (ROC) curve is used to evaluate the accuracy of the model. ROC curves have been used in signal detection theory to depict the tradeoff between hit rates and false alarm rates of classifiers, and they are also used in medical decisionmaking.⁽²⁶⁾

Recently, ROC curves have also been used in data mining research. One important characteristic is that ROC analysis allows the selection of possibly optimal models and allows researchers to discard suboptimal ones independently from the class distribution of the predictor.

ROC curves are useful for organizing predictors and visualizing their performance. The ROC curve is drawn using the true positive rate (TPR) and false positive rate (FPR). TPR is determined by the number of true positive predictions normalized by total number of positive observed values. Conversely, FPR defines how many incorrect positive results occur among all negative samples available during the test.

The ROC space is defined by FPR and TPR as the x- and y-axes, respectively, which depict the relative trade-offs between true positive and false positive. TPR is often described as the sensitivity of the model, while $(1 - \text{FPR})$ is often seen as the true negative rate (TNR) or specificity. Therefore, the ROC curve is also referred to as the sensitivity versus $(1 - \text{specificity})$ curve.

Each case consisting of a prediction and observed values represents one point in the ROC space. Given the discrete nature of the problem (i.e., the predicted probability is associated with a discrete definition of pavement performance, acceptable or not), algorithms are used to create the ROC curve.⁽²⁶⁾

An example of an ROC curve is shown in figure 24. Several points in the ROC curve are important to note. The best possible prediction would yield a point in the upper left corner or coordinate (0,1) of the ROC space, representing 100 percent sensitivity (no false negatives) and 100 percent specificity (no false positives). The (0,1) point is also called a perfect classification. A completely random guess would give a point along a diagonal line, also referred to as line of no discrimination, which consists of points (0,0) and (1,1). Points above the diagonal line indicate good classification results. In comparative terms, one point in ROC space is better than another if it is to the northwest (TPR is higher, FPR is lower, or both) of the first.

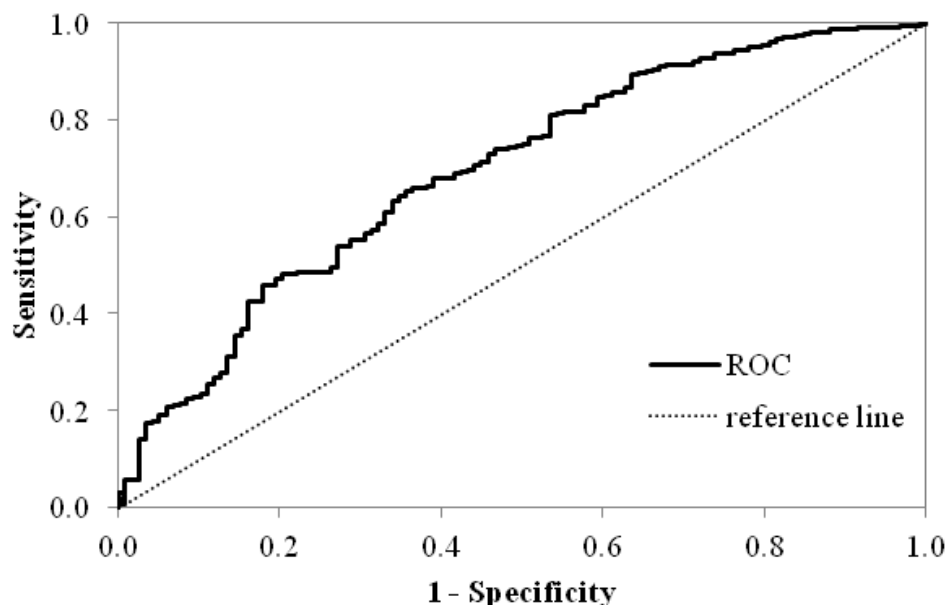


Figure 24. Graph. Example of an ROC curve.

The area under the ROC curve defines the goodness-of-fit of the predictions. In an analogy with measures of linear optimization techniques, the area under the ROC curve can be viewed as the R^2 value. By definition, the area under the ROC curve cannot be lower than 0.5, which corresponds to the reference line in figure 24. The highest value is determined by the boundary of the graph, which represents the perfect classification when the area under the ROC curve equals 1.

In addition to the goodness-of-fit, the ROC curve is used to define the cutoff value of the model. This is an important parameter that defines how the results from the probability density function can be interpreted in a binary system (i.e., the threshold used to separate probabilities that are referred to as acceptable and not acceptable). The *cutoff* is defined as the probability value that corresponds to the point in the ROC curve closest to the perfect classification point (0,1). When the cutoff is used to convert the predicted probabilities into binary outcomes, the model yields the highest level of accuracy (i.e., highest TPR and TNR).

Stochastic Approach to Evaluate Load Deflection Techniques to Network-Level Applications

The objective of a pavement design is to provide a structure that will exhibit adequate performance throughout its design life. In this case, *performance* is defined as the level of distresses that can affect the ride quality of the pavement or its structural adequacy. Therefore, a pavement has acceptable performance if distress levels do not exceed the threshold during a period of time (e.g., fatigue cracking does not exceed 25 percent of the total area in 15 years of service). Since the logistic model describes the likelihood of an event being acceptable or not as a function of a predictor variable, it can be used to model probability of acceptable performance with measurements of deflections or parameters (techniques) computed from them.

The goal of the stochastic approach proposed is to use the probability density function to obtain information about the pavement structural condition required to achieve the desired performance during a period of time. This new knowledge can then be used to define strategic treatments (maintenance or rehabilitation) to be used in the PMS optimization process.

A typical logistic model probability function is shown in figure 25. It describes the likelihood of the pavement section to exhibit acceptable performance in a particular distress as a function of a given deflection parameter, named “predictor variable X.” In this example, the cutoff value was determined from the ROC curve and plotted in the figure.

In the proposed stochastic approach, the probability density function is used to determine the thresholds that define the structural condition. By definition, the cutoff value in a logistic model determines how to convert the continuous probability prediction as a dichotomous outcome (i.e., predicted probabilities above the threshold are defined as acceptable while others are defined as not acceptable). In addition to the cutoff threshold, other values can be used to further detail the structural condition. As an example, figure 25 describes a second threshold created at the 0.4 probability level and used to define sections with fair structural condition from poor ones. (Note that this definition is arbitrary and can be adjusted to better fit an agency’s rehabilitation practices or network characteristics.)

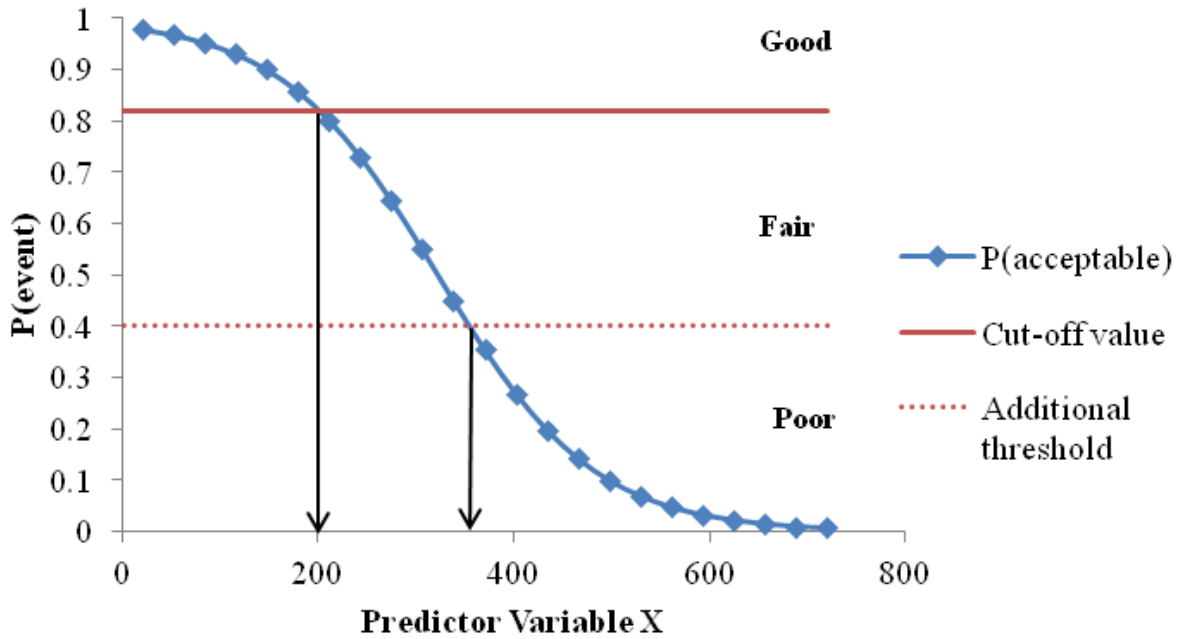


Figure 25. Graph. Example of logistic model probability function of a predictor variable X used to create a structural decision matrix.

Once thresholds and their respective deflection parameters are identified, a structural decision matrix (also referred to as a structural rehabilitation matrix) can be generated. Table 7 shows an example of a structural decision matrix obtained from the probability density function in figure 25.

Table 7. Example of structural decision matrix.

Structural Condition	Deflection Parameter
Good	< 200
Fair	200–350
Poor	> 350

The advantages of the stochastic process to evaluate the structural condition of the pavement for network-level analysis are as follows:

- The structural condition is related to the performance through a probability density function.
- The probability density function is based on qualitative performance measure—acceptable and not acceptable.
- The stochastic model is site-specific (i.e., additional variables may be incorporated that reflect site characteristics, such as traffic and pavement structure).

- Different structural decision matrices can be defined based on different types of distress. Therefore, the final evaluation can be made based on the most critical or the most typical distress.
- The calculations are simple and do not require an interactive process. Therefore, it can be automated and incorporated in virtually any PMS in which deflection data are available.
- The logistic models can be calibrated locally to enhance its goodness-of-fit and accuracy of predictions.
- Deflection data obtained from project level analysis or quality control after construction can be used in this process.

ANALYSIS STEPS

The evaluation of applicable deflection techniques was based on the quality and accuracy of the corresponding logistic model developed. A selection process was established to evaluate each model within each distress group and pavement type (e.g., roughness in flexible pavements). The evaluation criteria considered the accuracy of the logistic model, the consistency with engineering principles, and errors in the predictions (error types I and II). The entire analysis process can be summarized in the following steps:

Data preparation:

1. Compile performance measurements, deflections, pavement structure, climate, and traffic for each eligible site in the LTPP database.
2. Compute deflection techniques as referenced in table 1.
3. Rate the performance over time as acceptable or not acceptable according to load-related distresses.
4. Prepare a subset of the data for model validation.

Evaluation of selected techniques based on observed performance:

1. Conduct a preliminary screen to sort out the best deflection techniques as potential candidates for logistic model development.
2. Develop and calibrate a logistic model using the LTPP analysis database. There should be one model developed for each load-related distress using each screened deflection technique.
3. Compute descriptive statistics of each model.

Verification of deflection techniques:

1. Compare stochastic analyses of performance, inferred by the deflection technique under study, with measured pavement performance.

2. Adjust the logistic model based on previous comparisons.
3. Conduct sensitivity analysis of model parameters.

Validation analysis:

1. Analyze the models using an LTPP set-aside dataset for validation (part of the database not used to develop the models).
2. Perform a theoretical analysis through mechanistic simulations.

Selection of deflection technique:

1. Recommend logistic models based on deflection parameters for different pavement types and critical distresses.

The following sections describe the steps in the analysis process in greater detail. An example is provided in each step to illustrate the process.

Data Preparation

The data selected for this study were prepared following the steps and processes described in chapter 3 of this report. The data type and respective LTPP table sources were described in table 3. Basic statistics on the final data set used are presented in table 8 and table 9 for flexible pavements and table 10 and table 11 for rigid pavements.

Microsoft Excel[®] spreadsheets were used to compute all of the deflection parameters identified in the literature review as potential candidates for evaluating the structural condition of pavements (see table 1). In the case of closed-form mechanistic parameters (i.e., subgrade Hogg and Elmod moduli), macros were used to solve the equations.

The dichotomous performance variable was determined based on expected service life of flexible and rigid pavements—arbitrarily defined as 15 years for flexible pavements and 20 years for rigid pavements. The average year in service when the first deflection measurement was taken was 2 years for both pavement types. The LTPP sections compiled for this study exhibited an average service life of 11.3 years (flexible) and 13.8 years (rigid) at the last performance measurement. As a requirement of the logistic model assumption for acceptable performance, all pavement sections had to be evaluated at the end of the chosen expected service life. Therefore, extrapolations of the performance curves were computed to achieve this requirement—3.7 years for flexible pavements and 6.2 years for rigid pavements. Typical load-related distresses in flexible and rigid pavements are given in table 12.

Table 8. Input continuous data summary for flexible pavement sections.

Input Data	Average	Standard Deviation	Minimum	Maximum	Median
Service life used	1.5	1.4	0.0	10.5	1.0
Annual precipitation (mm)	843.9	442.2	73.2	2,153.3	876.9
Annual minimum temperature (°C)	6.4	5.9	-7.0	20.8	6.7
Annual maximum temperature (°C)	19.6	6.2	3.8	31.3	20.3
Annual mean temperature (°C)	13.0	6.0	-1.6	25.6	13.3
AADTT	723.8	728.7	7.3	3,955.0	454.7
Total thickness (inches)	22.1	9.4	6.3	85.5	20.3
AC thickness (inches)	7.3	3.5	0.9	23.2	7.1
Class 5 (volume)	146.8	141.7	2	1,770.0	106.3
Class 9 (volume)	401.7	554.6	1	2,838.0	175.9

1 inch = 25.4 mm

1 °F = 1.8(°C) + 32

Table 9. Input discrete data summary for flexible pavement sections

Input Data	Possible Attributes and Corresponding Binary Values	Percentage of Sections in the Database
Subgrade type	Fine-grained soil (1)	32.6 percent
	Coarse-grained soil (0)	67.4 percent
Pavement type	Bound base layer (1)	42.3 percent
	Unbound base layer (0)	57.7 percent

Table 10. Input continuous data summary for rigid pavement sections.

Input Data	Average	Standard Deviation	Minimum	Maximum	Median
Service life used	2.2	1.5	0.0	9.7	2.2
Annual precipitation (mm)	848.0	372.1	128.9	1,856.4	894.7
Annual minimum temperature (°C)	5.9	4.8	-2.2	21.0	5.1
Annual maximum temperature (°C)	18.7	5.1	9.9	30.9	17.8
Annual mean temperature (°C)	12.3	4.8	3.8	25.8	10.9
AADTT	1267.2	1039.5	99.3	5,157.0	891.6
Total thickness (inches)	19.6	9.1	9.2	61.3	16.4
AC thickness (inches)	10.0	2.5	6.4	20.4	9.4
Class 5 (volume)	238.0	232.2	14	998	178.3
Class 9 (volume)	705.3	752.6	13	866	415.3

1 inch = 25.4 mm

1 °F = 1.8(°C) + 32

Table 11. Input discrete data summary for rigid pavement sections.

Input Data	Possible Attributes and Corresponding Binary Values	Percentage of Sections in the Database
Subgrade type	Fine grain soil (1)	42.1 percent
	Coarse grain soil (0)	57.9 percent
Pavement type	Bound base layer (1)	55.3 percent
	Unbound base layer (0)	44.7 percent

Table 12. Structural distresses in flexible and rigid pavements.

Flexible Pavements	Rigid Pavements
<ul style="list-style-type: none"> • Fatigue cracking • Rutting • Roughness 	<ul style="list-style-type: none"> • Transverse cracking • Joint faulting • Roughness

Extrapolations were computed on a section-by-section basis by fitting nonlinear regression models to the historical data. Figure 26 provides an example of nonlinear extrapolation used to adjust the performance data.

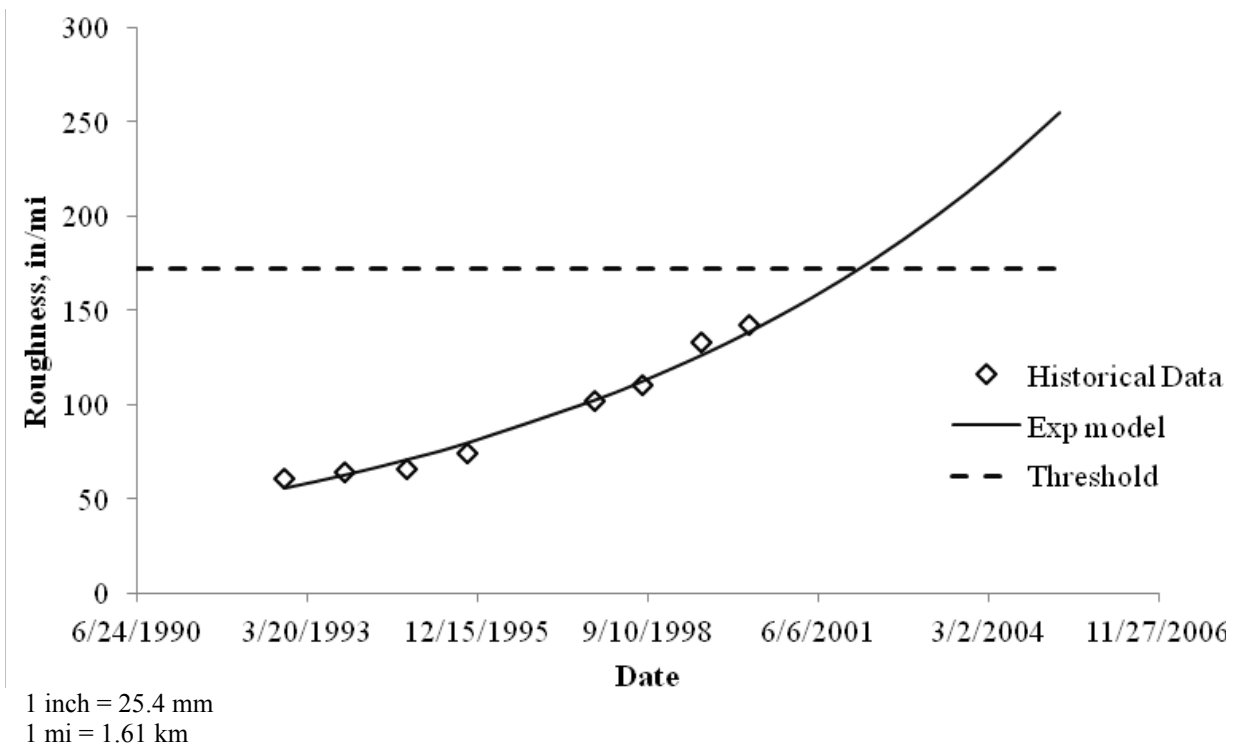


Figure 26. Graph. Example of performance extrapolation based on historical data.

The threshold for an acceptable performance was defined based on the *Mechanistic-Empirical Pavement Design Guide* (MEPDG) limit values for an acceptable design and are described in table 13.⁽²⁷⁾ The acceptable level for each distress could also be defined based on the network characteristics and the agency's practice for defining rehabilitation and maintenance timing, which would provide the agency with greater flexibility to adjust the technique based on its network characteristics and preferred M&R timing.

Table 13. Distress threshold for flexible and rigid pavements.

Flexible Pavements		Rigid Pavements	
Distress	Threshold	Distress	Threshold
Roughness	172	Roughness	172
Rutting (inches)	0.5	Joint faulting (inches)	0.12
Fatigue cracking (percent of total area)	25	Transverse cracking (percent of slabs)	15

One section would be classified as exhibiting acceptable performance for a given distress if the deterioration was lower than or equal to the threshold at 15 years for flexible pavements and 20 years for rigid pavements.

The final step in data preparation was the selection of a subset of data for model validation. The selection was based on a stratified sampling technique. The technique consisted of selecting 12 percent of the original dataset in a random process designed to pick sections distributed in a variety of site characteristics that would result in a representation equivalent to the original

dataset. Climate conditions, traffic volume, pavement type (in terms of base layer type), and subgrade type were used.

The climate condition was defined based on the freeze index and average rainfall for each site. Sites with an average annual rainfall greater than 39 inches (1,000 mm) were classified as wet, otherwise dry. Sites with a freeze index greater than 140 °F (60 °C) were classified as freeze; sites with a freeze index less than 140 °F (60 °C) were classified as no freeze. This classification is part of the LTPP experiment definition. The classification of traffic was defined based on two characteristics: volume and commercial vehicle distribution. These characteristics are easy to evaluate and are most influential on pavement performance predictions estimated with the MEPDG. The combination of criteria generated two groups of sites, one identified as low traffic and the other as high traffic. Table 14 describes the characteristics of both groups used in this study.

Table 14. Traffic characteristics used for sampling.

AADTT	Low Traffic	High Traffic
	340–950	75–2,750
Vehicle class 5 (percent in volume)	25–75	5–20
Vehicle class 9 (percent in volume)	10–50	40–85

In total, 51 deflection parameters were computed based on the literature review findings. The first deflection survey available after construction/rehabilitation was used to compute these parameters. The latest performance measurement available was used. This process was repeated for all load-related distresses in both pavement types evaluated.

Evaluation of Selected Techniques Based on Observed Performance

The evaluation of selected deflection techniques was based on the logistic model approach and the notion that the best deflection techniques yield the most accurate models. Since there were many deflection parameters to be evaluated, a first screening was conducted to eliminate poor correlations. A simple linear Pearson regression was used to test the level of correlation between measured performance and the deflection parameter. Although this correlation is not expected to be good, Pearson's R^2 and the significance level were used to identify good candidates for the full binary logistic analysis. The screenings were conducted for both flexible and rigid pavements and all load-related distress types. Tables with the results from the screening process are presented in appendix B.

As a general rule, the deflection techniques that resulted in high Pearson's R^2 values and a significance level inferior to 0.05 were selected. In this case, the significance level is the probability that the null hypothesis is accepted, meaning that no correlation exists between the deflection parameters and the performance measure. Some deflection techniques were computed based on maximum deflection adjusted for temperature using the process described by Lukanen et al.⁽⁶⁾

After the screening was completed, the selected deflection parameters were used one at a time to develop logistic models for each load-related distress described in table 12. The statistical package IBM SPSS Statistics[®] was used to develop the logistic models. The process of developing the model follows a backward elimination approach. All variables described in table 8 through table 11 for flexible and rigid pavements, respectively, were used in the first step, along with the deflection parameter and the independent performance variable (acceptable or not acceptable).

The model's exponent, b , (see figure 21) was calibrated to minimize the false positives and false negatives in the probability analysis. The significance of each variable was computed, and the less significant variable was removed from the calculation in the next step, eliminating the variable with the least relationship with performance. This process continued until all remaining variables had significance levels higher than 95 percent or the maximum number of iterations was achieved. With each step, the number of variables decreased and the overall level of significance decreased, indicating an improvement in the model's capability of predicting the likelihood of acceptable performance.

The significance terminology may seem confusing, but the significance level represents the probability of the *null hypothesis*, which is defined as the nonexistence of any relationship between the variable in question and the predicted likelihood of acceptable performance. Therefore, high values of significance mean a high probability that the variable has a weak or no relationship as a performance predictor.

This process was repeated for all deflection variables, resulting in one model for each variable. After this first step was completed, each model was evaluated to eliminate confounding variables and unreasonable trends. Confounding variables are dependent variables that are related to each other to some extent. Volume of class 5 and 9 trucks, which according to typical vehicle class distributions are inversely proportional to each other, are a good example of confounding variables. The various site-specific temperature values selected as part of the inputs are also related to each other. During the review of each model, only one variable of each group was allowed to remain in the model. The one with the highest significance level was chosen.

Variables that resulted in unreasonable trends were also eliminated. An example of this situation was a model in which pavement thickness had an inverse trend with performance—thicker pavements would yield lower probability of acceptable performance, which is a contradiction to expected behavior. After confounding variables and variables resulting in unreasonable trends were eliminated, the model with the best accuracy was selected.

Table 15 provides the results for the logistic model based on roughness performance of flexible pavements. The primary model evaluation consists of best deflection models after the first screening was conducted and detailed analysis of each model's variables was completed to remove confounding variables and unreasonable trends.

Table 15. Statistics of calibrated models based on roughness performance of flexible pavements.

Deflection Parameter	Primary Model Evaluation					
	I_2	CI_4	CI_5	D_2	D_3	Hogg
Area ROC	0.733	0.720	0.731	0.720	0.727	0.694
Hosmer-Lemeshow significance test	0.397	0.137	0.339	0.351	0.592	0.198
Calibration—correct cases (percent)	68.4	62.8	67.9	64.6	67.3	63.9
Validation—correct cases (percent)	74.2	61.3	69.4	66.1	71.0	74.2
Error type I (false acceptable) (percent)	6.6	4.7	5.7	5.9	6.5	7.0
Error type II (false not acceptable) (percent)	25.0	32.5	26.4	29.4	26.2	29.1
TPR (acceptable) (percent)	69.3	60.0	67.5	63.8	67.8	64.2
TNR (not acceptable) (percent)	64.4	75.0	69.2	68.3	65.4	62.5

The following observations can be made when analyzing table 15:

- The area under the ROC curve represents the accuracy of the model.
- The removal of confounding variables and unreasonable trends from the preliminary analysis of the I_2 model had a small effect on the model's accuracy. This is often expected because these variables usually exhibit poor significance to the predictability of the performance variable.
- The Hosmer-Lemeshow test is another way to evaluate the significance of the model. This test is commonly used to evaluate binary logistic models when the conventional Pearson's R^2 is not possible.
- The error type I (false acceptable) is the worst error type in the problem at hand. It occurs when the model predicts that the pavement section has a good structural condition when, in fact, the structural condition is the contrary. From an agency's perspective, this would be the worst outcome from the model prediction.
- The TPR (true acceptable) and the TNR (true not acceptable) are good at 64 percent.

Sensitivity of Model to Deflection Parameter

In addition to evaluating basic statistics of each model, it was necessary to evaluate the sensitivity of models' outcome to the deflection parameter. The main objective of this evaluation was to observe if there was any bias in the models' predictions towards acceptable or not acceptable performance.

Figure 27 shows the sensitivity curve of the I_2 model based on roughness performance. In this case, the cutoff is set at 0.812, which corresponds to I_2 equal to 0.1092 1/mil (0.0043 1/ μm) (or D_2 equals to 9.13 mil (232 μm)), which is a reasonable value for a well designed pavement structure. (Recall that the deflection for D_2 measured at 8 inches (203.2 mm) from the center of the load.) Therefore, figure 27 indicates that flexible pavements with D_2 deflections below 9.13 mil (232 μm) have a higher than 80 percent chance of exhibiting acceptable roughness performance for the next 12 years and can therefore be classified as good structural condition.

In contrast, figure 28 shows the sensitivity curve of the Hogg model based on roughness. The cutoff value of 0.802 yields a Hogg value of 65,000 psi (447,850 kPa), which is high and unreasonable for subgrade moduli. In this case, the Hogg model is biased toward probabilities under the cutoff value and, consequently, toward low probabilities of acceptable performance.

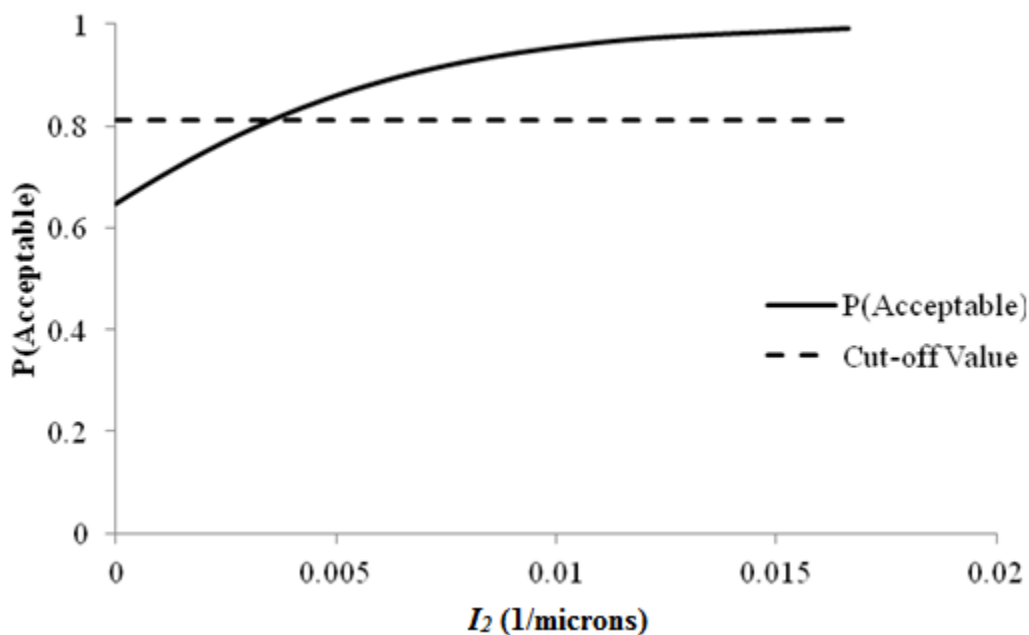


Figure 27. Graph. Sensitivity of roughness acceptable probability to deflection parameter I_2 for flexible pavements.

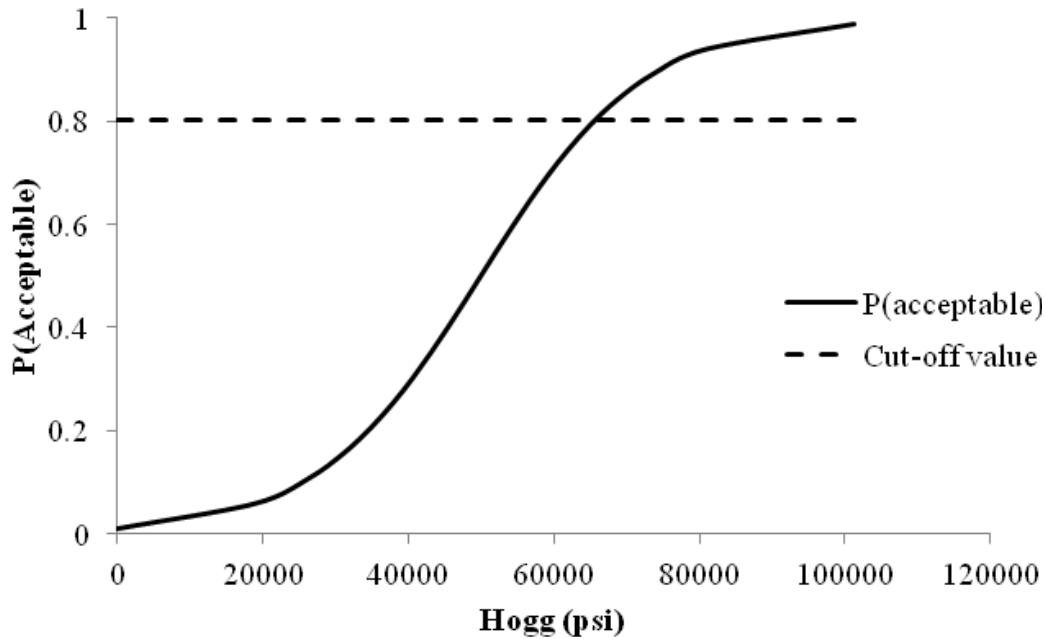


Figure 28. Graph. Sensitivity of roughness acceptable probability to deflection parameter Hogg for flexible pavements.

This type of sensitivity analysis was performed to all models developed and proved to be essential to rule out models that provided very good statistics at first but were biased. The sensitivity analyzes of other logistic models are provide in appendix C.

Validation Analysis

The validation analysis was performed on a subset of the database that was set aside prior to model calibration. In total, 12 percent of the sections available for calibration were removed from the database. Since the LTPP database covers a wide range of pavement sections, traffic levels, and environmental conditions, a stratified random sampling technique was employed to retrieve the sections. The following characteristics were used in the stratified sampling approach:

- **LTPP climate regions:** Wet-freeze (WF), wet-no freeze (WNF), dry-freeze (DF), and dry-no freeze (DNF).
- **Traffic:** Low versus high (as described in table 12).
- **Base layer type:** Unbound versus bound (only for flexible pavement).
- **Subgrade type:** Fine-grained versus coarse-grained soil.

The stratified random sampling technique consists of grouping all sections in all possible combinations of the characteristics defined for the selection. After the groups are formed, the target percentage of samples is randomly selected proportionally to the size of each group and its participation in the entire dataset. For example, if one group consisting of sections with WF, low traffic, unbound base type, and fine subgrade has 43 sections, the sampling of this group would

yield 5 sections randomly selected. There were 32 possible combinations of all characteristics mentioned. An algorithm was written to group the sections with equal characteristics and randomly select the target number of sections.

The validation was performed in all steps of the model evaluation. Table 14 provides the results for the structural logistic model based on roughness for flexible pavements. In this case, the validation dataset consisted of 61 sections, which is a proportional representation of all sections available in the database for model calibration. The results indicate that good accuracy was also observed in the validation dataset, which suggests that the final model is capable of identifying the structural condition of the pavement based on expected roughness performance. The validation results for all models developed in this study are provided in appendix B along with the statistics of the calibrated equation.

Table 16. Example of validation results for the structural logistic model based on roughness for flexible pavements.

Deflection Parameter	Primary Model Evaluation						Final Model
	I_2	CI_4	CI_5	D_2	D_3	Hogg	I_2
Validation— correct cases (percent)	74.2	61.3	69.4	66.1	71.0	74.2	69.4

Selection of Deflection Technique

The logistic model based on deflection parameter I_2 had the best accuracy. Table 17 shows the final model variables with respective p -values (i.e., significance of the variable to the performance variable) and the corresponding cutoff value that resulted in the highest accuracy.

Table 17. Variables in the I_2 final model (based on roughness).

Variables (b_i)	a_i	p -Value
I_2	239.849	0.000005706
Current life	-0.189	0.01174
Class 9 volume	-0.0006781	0.0001037
Constant	0.8375	0.01071
Cutoff	0.812	

Note: Variables b_i and a_i are defined in the equation in figure 22.

Figure 29 provides the equation used to compute the deflection parameter.

$$I_2 = \frac{1}{D_2}$$

Figure 29. Equation. Calculation of I_2 .

THEORETICAL VALIDATION

Deflections are normally used to back-calculate the elastic moduli of the pavement layers. In an inverse process, the mechanistic validation consisted of simulating different pavement structures and material properties using simple multilayer elastic theory. Computed responses (deflections,

stresses, and strains) were used to compute the deflection parameters and estimate damage and performance through mechanistic-empirical models. The structural logistic models were used with the computed deflection parameters as inputs. The probabilities of good structural condition were then compared with the estimated performance.

The software KENPAVE, developed by Huang, was used to model typical flexible and rigid pavement structures.⁽²⁸⁾ The mechanistic responses were then used to predict performance using the MEPDG.⁽²⁷⁾ This section describes the theoretical validation and provides examples of each step in the process. The complete validation for flexible and rigid pavement models is provided in greater detail in appendix D.

Mechanistic-Empirical Analysis

Flexible Pavements

Several pavement structures were simulated using the KENLAYER computer program that is part of the KENPAVE software. The intention was to evaluate different asphalt concrete and base layer thicknesses at different stiffnesses and different subgrade moduli. A factorial study was designed and is presented in table 18.

Table 18. Summary of the mechanistic analysis inputs for flexible pavements.

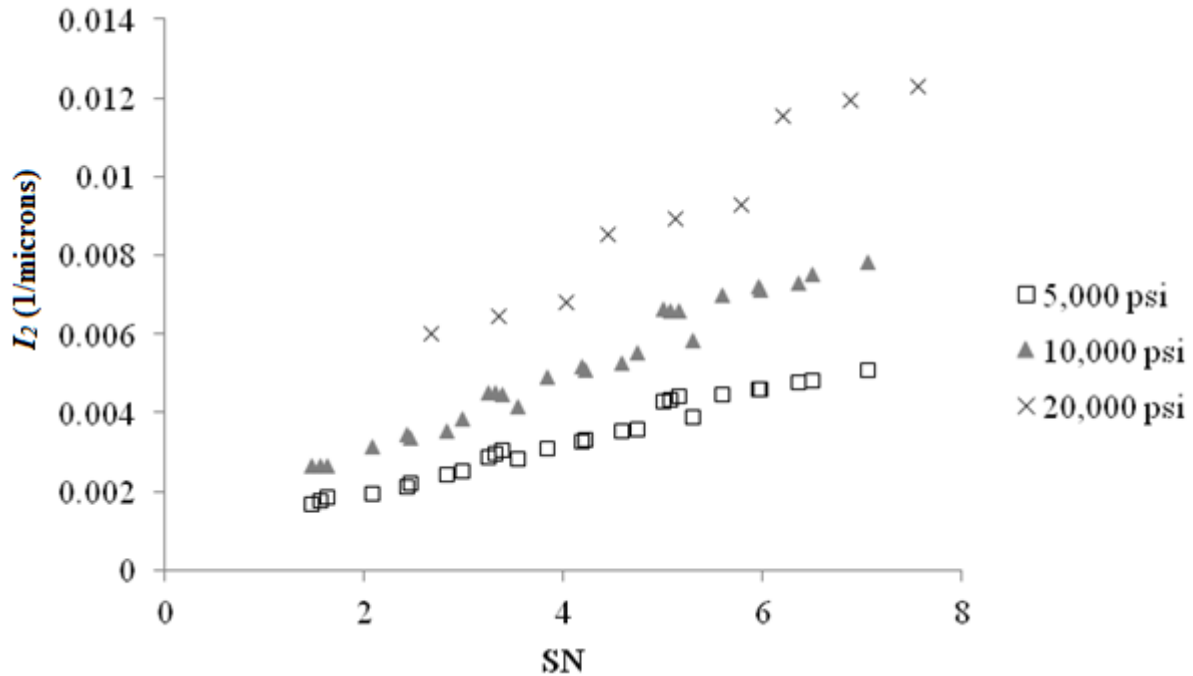
HMA Thickness (inches)	HMA Modulus (psi)	Base Thickness (inches)	Base Modulus (psi)	Subgrade Modulus (psi)
3, 7, 11	250,000, 500,000, 750,000, 1,000,000, 1,250,000, 1,500,000, 1,750,000, 2,000,000, 2,250,000, 2,500,000, 2,750,000, 3,000,000	8, 12, 16	10,000, 20,000, 30,000, 40,000	5,000, 10,000, 20,000

1 inch = 25.4 mm

1 psi = 6.89 kPa

The combination of all parameters in the factorial experiment resulted in 1,296 sections. It was necessary to find a common variable for comparing the mechanistic responses among different combinations of the input parameters. The choice was the SN used in the 1993 AASHTO *Guide for Design of Pavement Structures*.⁽⁸⁾ The equations for computing SN are provided in appendix D.

The deflection parameters of the best logistic models developed were computed for the structures simulated in the factorial experiment. Figure 30 shows the trends between deflection parameter I_2 and SN. For simplicity, the data were grouped by subgrade modulus. I_2 was chosen for the final structural logistic model based on roughness performance. Plots for deflection parameters used in the structural logistic models based on rutting and fatigue cracking are provided in appendix D.



11/ μm = 25.4 1/mil
1 psi = 6.89 kPa

Figure 30. Graph. Deflection parameter I_2 as a function of SN for a flexible pavement with HMA modulus of 500,000 psi (3,445,000 kPa).

Rigid Pavements

Several pavement structures were simulated using KENSLAB, which is part of the KENPAVE software.⁽²⁸⁾ The intention was to evaluate different JPCP slab thicknesses and subgrade moduli and the consequences to the outcome of the structural logistic models. The pavement structure was simulated as an elastic slab on a dense liquid foundation. A factorial study was designed and is presented in table 19.

Table 19. Summary of the mechanistic analysis inputs for rigid pavements.

PCC Thickness (inches)	PCC Modulus (psi)	Subgrade Modulus (psi)
8, 9, 10, 11, 12	4,000,000	5,000, 10,000, 20,000

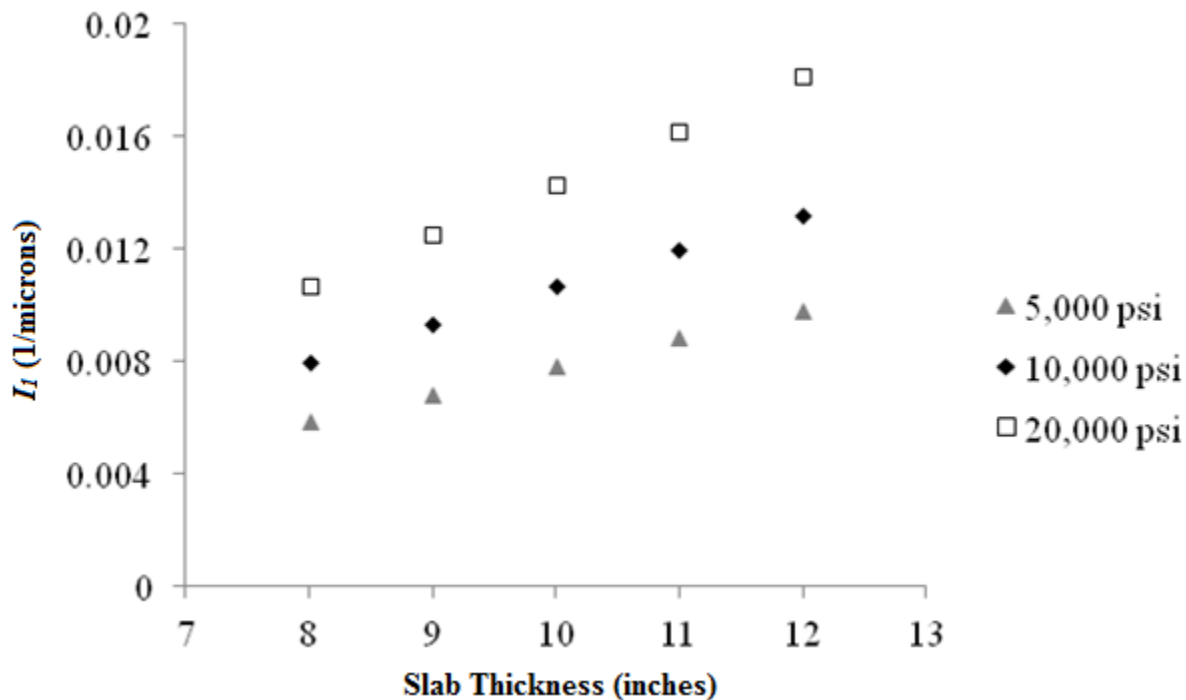
1 inch = 25.4 mm

1 psi = 6.89 kPa

The deflection parameters of the best logistic models developed were computed for the structures simulated in the factorial experiment. Only the FWD test at the center of the slab was evaluated. The objective was to verify if trends would agree with expected outcomes from the models. At first, the deflection parameters were plotted against the slab thickness (i.e., considered as reference for the strength of the pavement section).

Figure 31 shows the trends between deflection parameter I_1 and slab thickness for three subgrade moduli. I_1 was chosen for the final structural logistic model based on roughness performance.

The results indicate that I_l increases as slab thickness increases, as expected. Plots for deflection parameters used in the structural logistic models based on faulting and slab cracking are provided in appendix D.



$11/\mu\text{m} = 25.4 \text{ 1/mil}$
 $1 \text{ inch} = 25.4 \text{ mm}$
 $1 \text{ psi} = 6.89 \text{ kPa}$

Figure 31. Graph. Sensitivity of deflection parameter I_l to slab thickness.

Comparison with MEPDG Predicted Performance

The MEPDG performance prediction models were used to compare predicted distress performance at the end of the design life with the estimated structural condition obtained from the logistic structural model. This task was accomplished by applying the MEPDG models using the mechanistic responses calculated by KENPAVE.

Flexible Pavements

Two models were considered for flexible pavements—rutting and fatigue cracking. At first, the roughness model was also included in the scope. However, this particular model requires additional site factors that often dominate the analysis. Therefore, a comparison between the outcome of the structural logistic model based on roughness and predicted roughness performance was not included in this exercise. The calculations were performed in Microsoft Excel® and not within the MEPDG software due to computational time required to run all scenarios. Since the objective is the comparison and trend evaluation, this assumption had no impact on the outcome or conclusions.

Figure 32 shows an example of the sensitivity of I_f structural logistic model probability based on fatigue cracking to MEPDG predicted fatigue cracking performance for flexible pavements. It can be seen that the trends agree with expectations; high probabilities of good structural condition are associated with low levels of fatigue cracking. As the probability decreases, the predicted area of fatigue cracking increases.

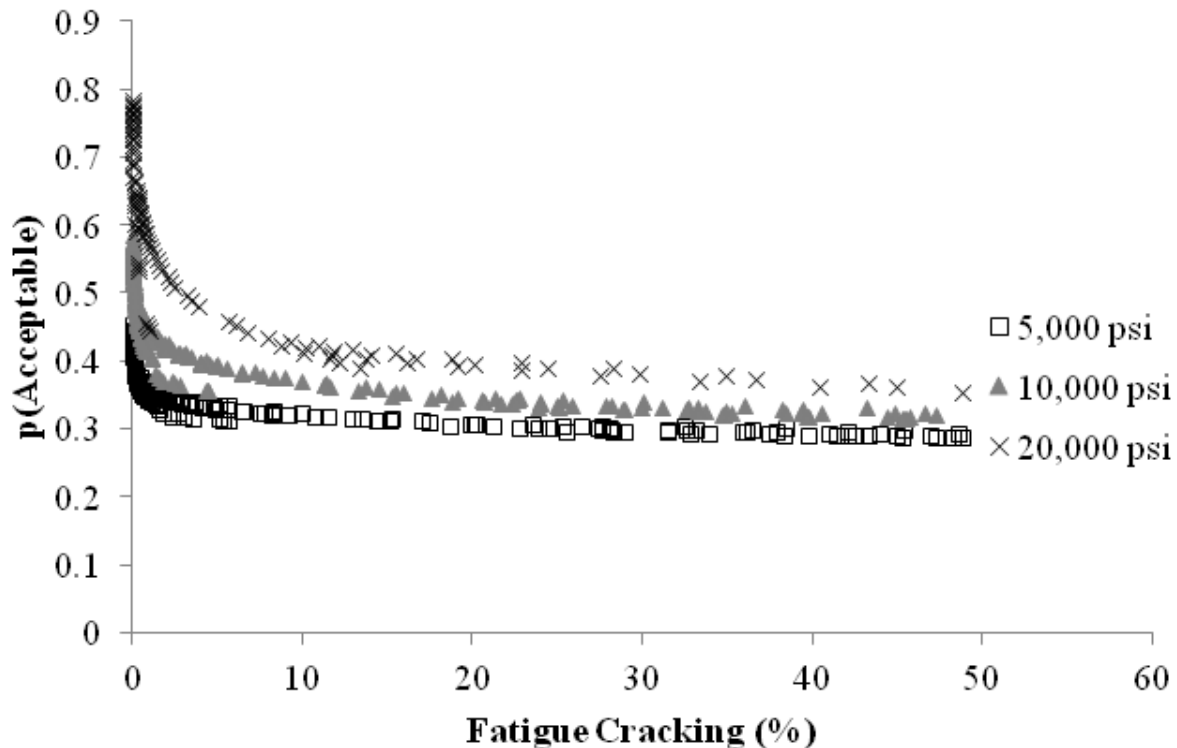


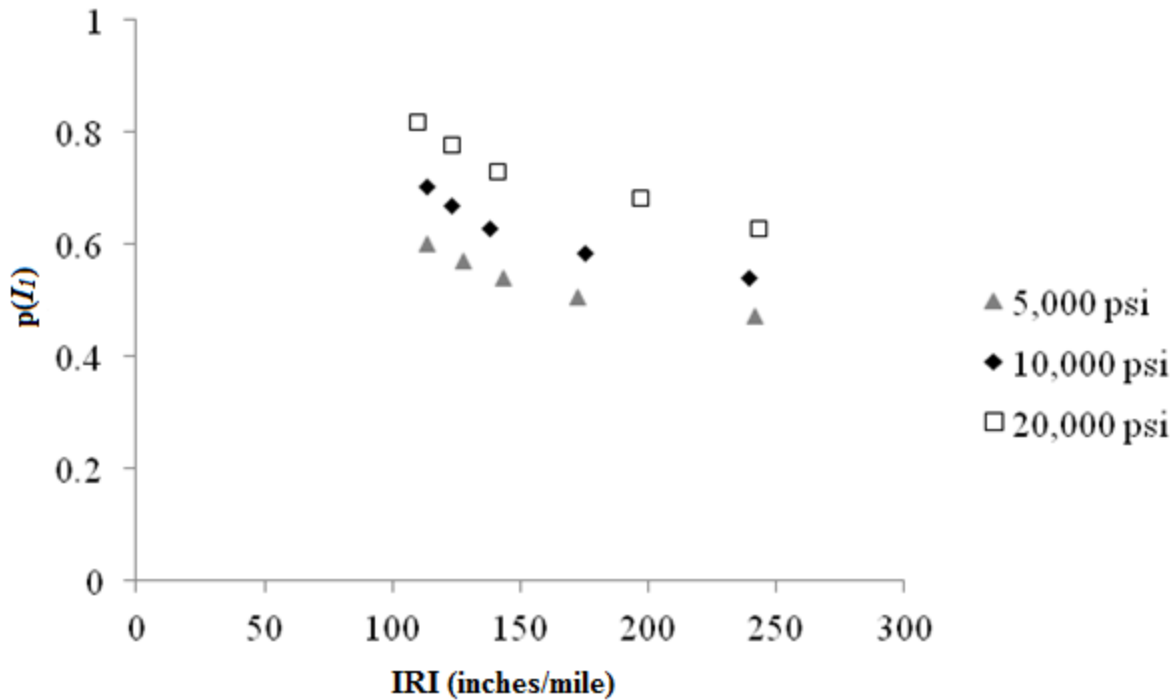
Figure 32. Graph. Sensitivity of I_f structural logistic model probability based on fatigue cracking performance to MEPDG predicted fatigue cracking for flexible pavements.

The complete comparison between the outcome of the structural logistic models and MEPDG predicted performance are described in appendix D, which also includes the predictive model equations for fatigue cracking that were implemented in Microsoft Excel[®].

Rigid Pavements

In the case of rigid pavements, the MEPDG was used to generate the performance predictions. There were 15 scenarios to run, and the rigid pavement analysis was performed much faster in the MEPDG than the flexible pavement analysis.

Figure 33 shows the sensitivity of the I_f structural logistic model probability based on roughness to MEPDG predicted roughness performance for rigid pavements. The trends agree with expectations—high probabilities of good structural condition are associated with low values of IRI. As the probability decreases, the predicted IRI increases. This plot confirms that the structural logistic model is capable of providing an assessment of structural condition that is tied to an expectation of performance. The complete comparison between the outcome of the structural logistic models and MEPDG predicted performance is described in appendix D.



1 inch = 25.4 mm
 1 mi = 1.61 km
 1 psi = 6.89 kPa

Figure 33. Graph. Sensitivity of I_f structural logistic model probability based on roughness performance to MEPDG predicted roughness for rigid pavements.

IMPORTANCE OF LOCAL CALIBRATION

The models developed in this research were calibrated using data from several States and different local conditions. It is expected that the accuracy of the models can be improved by local calibration, which is hypothesized to minimize variability and to reduce sources of errors. Local calibration is achieved by selecting a sample dataset from the local network in which the models are to be applied and perform a local calibration of the logistic model.

Since data from a local network with comprehensive performance data for calibrating the models were not available, the LTPP database was used for this purpose. It was assumed that the models would improve accuracy if calibrated for an individual State (i.e., data from one State would have less variability and could be considered as part of a local network). Four States were used in this exercise—Texas, Minnesota, California, and Alabama. They were chosen based on the availability of data—the more data available, the higher the likelihood of a meaningful calibration.

This exercise was performed only for flexible pavements. States with a large number of rigid pavement sections were searched, but no State was found to have enough sections for this purpose. The structural logistic model based on fatigue cracking was chosen because it was the model with the least accuracy of all three models developed for flexible pavements.

The calibration process followed the same steps described in earlier sections of this chapter. Table 20 shows the statistics of the locally calibrated model for each of the four States. The statistics for the model calibrated with the entire dataset are also provided under the name of national calibration. It can be seen from the results that local calibration can significantly improve the accuracy of the model.

Table 20. Benefits of local calibration.

Statistics	National	Texas	Minnesota	California	Alabama
Number of sections	467	57	21	33	17
Accuracy	0.72	0.73	0.76	0.92	0.90
Correct cases (percent)	63	70	76	85	88
Error type I (percent)	15.5	5.3	4.8	9.1	5.9
TPR (percent)	63	58	78	83	92
TNR (percent)	63	67	67	86	80

The national calibration resulted in a logistic fatigue cracking model with an equivalent R^2 of 0.66. The simulation of local calibration yielded models with R^2 values ranging from 0.73 to 0.92. The improvement in correct predictions increased from 63 to 88 percent, which was a good improvement considering the nature of the problem. Another indication of the benefits of local calibration was the improvement in TPR. As seen in table 18, TPR values increased from 63 to 92 percent. These improvements are most likely attributed to the uniformity of the dataset in terms of site characteristics (materials, traffic, and climate) and similar design procedures.

The four examples of local calibration presented in this section show the potential improvements in accuracy and predictability that can be obtained if local data are used to calibrate the probabilistic models. Although these cases are just simple exercises retrieved from the LTPP database, it is clear that local calibration ultimately enhances the accuracy and quality of predictions, which significantly benefits analyses using PMS, especially for creation and allocation of M&R resources.

SUMMARY OF FINDINGS

The logistic model notation is described in figure 21 and figure 22. The general form of the probabilistic logistic model is given in the equation shown in figure 21, in which the exponent term is given by the general linear equation provided in figure 22. All logistic models developed in this study follow this notation.

During the course of this research, several models were developed and evaluated according to the principles and approach described in earlier sections in this chapter. Different structural logistic models were developed based on different distress performance measures using the national LTPP database. Detailed statistics of all models evaluated are provided in appendix B. The final models are presented in this section.

Flexible Pavements

Model Based on Roughness Performance

The model variables are described in table 21. The deflection parameter used is in figure 29, where D_2 is the deflection 8 inches (203.2 mm) from the center of the load. The accuracy, measured by the area under the ROC curve, is 0.72, and the cutoff value is 0.812. Additional detailed statistics are provided in appendix B.

Table 21. Variables in the I_2 final model for flexible pavements based on roughness performance.

Variables (b_i)	a_i	p -value
I_2	239.849	0.000005706
Current life	-0.189	0.01174
Class 9 volume	-0.0006781	0.0001037
Constant	0.8375	0.01071
Cutoff		0.812

Roughness performance depends on the strength of the entire pavement structure. For example, it is expected that one robust pavement section tends to be smoother for longer periods of time than one weak section, assuming both have the same climate, traffic conditions, and subgrade. Therefore, the predominance of the deflection variable in the model is justified. Current life and traffic play a significant role in estimating the likelihood of premature failure due to roughness performance.

Model Based on Rutting Performance

The model variables are described in table 22, and the deflection parameter is in figure 34. The accuracy, measured by the area under the ROC curve, is 0.66, and the cutoff value is 0.792. Additional detailed statistics are provided in appendix B.

Table 22. Variables in the CI_3 final model for flexible pavements based on rutting performance.

Variables (b_i)	a_i	p -value
CI_3	-0.01146	0.00001594
Precipitation (mm)	-0.0005259	0.04018
Class 9 volume	-0.0007688	0.00005421
Constant	2.6586	1.0136×10^{-13}
Cutoff		0.792

$$CI_3 = D_3 - D_4$$

Figure 34. Equation. Calculation of CI_3 .

Where D_3 is the deflection 12 inches (304.8 mm) from the center of the load and D_4 is the deflection 18 inches (457.2 mm) from the center of the load.

The rutting model is based on deflections located at the middle of the measured deflection basin. The influence of the base and subbase is mostly noted on the deflection measured at this location. The strength of the underlying layers is critical in the development of rutting in the asphalt concrete layer and the sublayers, as well. One important aspect of the rutting phenomenon is the influence of the subgrade. It is understood that the subgrade contributes to the overall magnitude of rutting and the rate of development over time. The influence of the subgrade is not completely captured by the deflections used in this model. During the model development the type of subgrade (fine or coarse) was included as a variable, but it was excluded by the calibration process. However, the influence of precipitation was observed, which directly affects the subgrade strength more than any other granular layer in the pavement structure. Further improvements to this model at local calibration level should include the subgrade type and subgrade modulus if possible.

Model Based on Fatigue Cracking Performance

The model variables are described in table 23, and the deflection parameter is in figure 35. The accuracy, measured by the area under the ROC curve, is 0.72, and the cutoff value is 0.605. Additional detailed statistics are provided in appendix B.

Table 23. Variables in the I_f final model for flexible pavements based on fatigue cracking performance.

Variables (b_i)	a_i	p-value
I_f	154.764	0.0006015
AADTT	-0.0005073	0.0007847
Pavement type	0.3774	0.07598
Constant	-0.2202	0.4422
Cutoff	0.605	

$$I_f = \frac{1}{D_f}$$

Figure 35. Equation. Calculation of I_f .

Where D_f is the deflection at the center of the load.

Fatigue cracking performance is influenced by the stiffness of the asphalt concrete layer, the number of load repetitions, and the type/strength of underlying layers. Stiff asphalt concrete layers are more susceptible to cracking because the binder hardens and becomes brittle, which reduces its flexural strength. The overall stiffness of the pavement can be captured in part by the maximum deflection, represented in this model as I_f . The mechanism for crack initiation and propagation, regardless of the location where it starts (bottom or surface), depends on the growing damage due to load repetitions. The truck volume in the model addresses this issue to some extent. Finally, the type of pavement (unbound or bound base layer) is related to the stiffness of the underlying layers. Pavements with a bound base layer are less likely to develop fatigue cracking than pavements with an unbound base layer.

Rigid Pavements

Two sets of models were developed for rigid pavements: one based on FWD testing at a 9,000-lb (4,086-kg) load and one at a 12,000-lb (5,448-kg) load. These tests are identified in the LTPP database as drops 2 and 3, respectively.

Model Based on Roughness Performance (9,000 lb (4,086 kg))

The model variables are described in table 24. The deflection parameter is shown in figure 36. The accuracy, measured by the area under the ROC curve, is 0.65, and the cutoff value is 0.665. Additional detailed statistics are provided in appendix B.

Table 24. Variables in the CI_5 final model for rigid pavements based on roughness performance (9,000 lb (4,086 kg)).

Variables (b_i)	a_i	p -value
CI_5	-0.078	0.00406
Class 9 volume	-0.0003877	0.115
Constant	2.057	0.00002168
Cutoff		0.665

$$CI_5 = D_5 - D_6$$

Figure 36. Equation. Calculation of CI_5 .

Where D_5 is the deflection 24 inches (609.6 mm) from the center of the load and D_6 is the deflection 36 inches (914.4 mm) from the center of the load. Both deflections are obtained from tests at the center of the slab. Additional models based on FWD tests at different locations in the slab were investigated (i.e., tests at joint approach, corner edge, and mid-edge). Since they are unusual locations for typical FWD surveys conducted by State transportation departments (with the exception of the joint test), they are provided only in appendix B.

Roughness in rigid pavements is mainly related to faulting. Faulting is a distress that is directly related to the stiffness of the support layer and the quality of the dowel bars. The deflection parameter CI_5 captures the influence of the underlying layer stiffness. The traffic load repetition is represented by the volume of class 9 trucks, which are the most damaging commercial vehicles to the pavement performance.

Model Based on Roughness Performance (12,000 lb (5,448 kg))

The model variables are described in table 25. The deflection parameter is shown in figure 37. The accuracy, measured by the area under the ROC curve, is 0.66, and the cutoff value is 0.695. Additional detailed statistics are provided in appendix B.

Table 25. Variables in the CI_4 final model for rigid pavements based on roughness performance (12,000 lb (5,448 kg)).

Variables (b_i)	a_i	p -value
CI_4	-0.117	0.007378
Class 9 volume	-0.0004607	0.06459
Constant	2.148	0.0000447
Cutoff	0.695	

$$CI_4 = D_4 - D_5$$

Figure 37. Equation. Calculation of CI_4 .

Where D_4 is the deflection 18 inches (457.2 mm) from the center of the load and D_5 is the deflection 24 inches (609.6 mm) from the center of the load. Both deflections are obtained from tests at the center of the slab. Additional models based on FWD tests at different locations in the slab were investigated and are provided in appendix B. This model is similar to the one developed based on the 9,000-lb (4,086-kg) FWD load. The deflection parameter is D_5 in this case, which is also related to the stiffness of the underlying layers.

Model Based on Faulting at Joints Performance (9,000 lb (4,086 kg))

The model variables are described in table 26. The accuracy, measured by the area under the ROC curve, is 0.64, and the cutoff value is 0.635. Additional detailed statistics are provided in appendix B.

Table 26. Variables in the D_6 final model for rigid pavements based on faulting at joints performance (9,000 lb (4,086 kg)).

Variables (b_i)	a_i	p -value
D_6	-0.009225	0.138
Subgrade type	-0.495	0.2003
Constant	1.499	0.005818
Cutoff	0.635	

Where D_6 is the deflection 36 inches (914.4 mm) from the center of the load. The deflection is obtained from tests at the center of the slab. Additional models based on FWD tests at different locations in the slab were investigated and are provided in appendix B.

Faulting is a distress that is directly affected by the condition of the subgrade or the underlying base layer. The variables that were selected during the calibration process reflect the importance of the subgrade on the faulting performance of the pavement. The further the measured deflection is from the center of the applied load, the greater the contribution of the underlying layers to its magnitude. The deflection parameter D_6 can be related to the instant stiffness of the supporting layers. In addition, the subgrade type (fine or coarse) was also selected as one of the variables, which confirms the importance of the subgrade on faulting performance.

Model Based on Faulting at Joints Performance (12,000 lb (5,448 kg))

The model variables are described in table 27. The accuracy, measured by the area under the ROC curve, is 0.63, and the cutoff value is 0.651. Additional detailed statistics are provided in appendix B.

Table 27. Variables in the D_6 final model for rigid pavements based on faulting at joints performance (12,000 lb (5,448 kg)).

Variables (b_i)	a_i	p-value
D_6	-0.008789	0.06896
Subgrade type	-0.579	0.139
Constant	1.734	0.002499
Cutoff	0.651	

Where D_6 is the deflection 36 inches (914.4 mm) from the center of the load. The deflection is obtained from tests at the center of the slab. Additional models based on FWD tests at different locations in the slab were investigated and are provided in appendix B.

Model Based on Transverse Slab Cracking Performance (9,000 lb (4,086 kg))

The model variables are described in table 28. The deflection parameter used is shown in figure 37. The accuracy, measured by the area under the ROC curve, is 0.77, and the cutoff value is 0.7. Additional detailed statistics are provided in appendix B.

Table 28. Variables in the CI_4 final model for rigid pavements based on transverse slab cracking performance (9,000 lb (4,086 kg)).

Variables (b_i)	a_i	p-value
CI_4	-0.254	0.0003759
Class 9 volume	-0.001012	0.001084
Constant	3.630	0.0000003134
Cutoff	0.7	

For this model, D_4 is the deflection 18 inches (457.2 mm) from the center of the load, and D_5 is the deflection 24 inches (609.6 mm) from the center of the load. Both deflections are obtained from tests at the center of the slab. Additional models based on FWD tests at different locations in the slab were investigated and are provided in appendix B.

Slab cracking develops when the slab support is no longer adequate or loading is too excessive for the designed concrete slab. As any crack mechanism, it also develops over traffic load repetition. The final model developed based on transverse slab cracking incorporates both characteristics. The deflection parameter is obtained from the midsection of the deflection basin which can be associated with the instant stiffness of the underlying support layers of the concrete slab. The load repetition is characterized by the volume of class 9 trucks.

Model Based on Transverse Slab Cracking Performance (12,000 lb (5,448 kg))

The model variables are described in table 29. The deflection parameter is shown in figure 37. The accuracy, measured by the area under the ROC curve, is 0.66, and the cutoff value is 0.695. Additional detailed statistics are provided in appendix B.

Table 29. Variables in the CI_4 final model for rigid pavements based on transverse slab cracking performance (12,000 lb (5,448 kg)).

Variables (b_i)	a_i	p-value
CI_4	-0.231	0.00007858
Class 9 volume	-0.001029	0.001282
Constant	3.9796	0.0000001201
Cutoff		0.71

In this model, D_4 is the deflection 18 inches (457.2 mm) from the center of the load, and D_5 is the deflection 24 inches (609.6 mm) from the center of the load. Both deflections are obtained from tests at the center of the slab. Additional models based on FWD tests at different locations in the slab were investigated and are provided in appendix B.

GUIDELINES FOR SELECTING BEST-FITTING TECHNIQUES

The process for selecting the best-fitting technique is simple. A complete example is described in the previous sections of this chapter. A summary of the steps is provided as guidelines for selecting the best-fitting deflection techniques.

The process for selecting the best model is as follows:

1. Data Preparation

Data availability is important. Logistic regression models are obtained from the statistical analysis of several independent variables that may potentially have an impact on pavement performance. At first, no variable should be eliminated without it properly being assessed. Typical groups of variables include deflection, structure, traffic, climate, and performance. It is important that any available variable in these categories is used, but dependent variables that are related to each other to some extent should be avoided.

Deflections obtained from FWD testing are used to compute deflection parameters to be used as independent variables in the logistic models. A detailed literature review of most used and more successful applications was done as part of this research.

In this study, thickness and material type were used as structure variables. In addition, two dichotomous variables based on the structure characteristics were used—one related to the subgrade type (coarse- or fine-grained) and other related to the base type (bound or unbound). Traffic was limited to the total volume of trucks and the volume of the two most predominant classes in the FHWA truck classification, classes 5 and 9. Two main variables for climate were used—precipitation and temperature. For simplification, annual averages were used for both.

The main characteristic of a logistic model is the prediction of a probability of an event occurring given a set of independent variables. The assumption is that the rate of deterioration increases as the structural condition worsens, and the probability of a pavement failing prematurely can be calculated based on a combination of a deflection parameter and site characteristics. Therefore, performance must be transformed in a dichotomous variable representing the occurrence of this event (acceptable performance after a number of years in service). The service life can be chosen to reflect the expected performance in the network.

2. Logistic Model Calibration

The calibration and evaluation of selected deflection techniques is based on the logistic model approach and the notion that the best deflection techniques yield the most accurate models. Each deflection parameter available can be used to develop a logistic model for each performance measure in the dataset. A statistical package can be used to expedite the process, although a spreadsheet can be used to program the optimization algorithm. In this study, PASW Statistics™ (formerly known as SPSS) was used to develop the logistic models with an approach called backward elimination. The general formulation of the logistic model is shown in figure 21 and figure 22.

The model's exponent, b , is calibrated to minimize the false positives and false negatives in the probability analysis. The significance of each variable is computed, and the least significant variable is removed from the calculation. This process continues until no improvements in accuracy can be made or the maximum number of iterations is achieved.

3. Verification of Accuracy

Logistic model accuracy is best evaluated through the analysis of the ROC curve. An ROC analysis allows researchers to select possible optimal models and discard suboptimal ones independently from the class distribution of the predictor.

The ROC curve is drawn using only the TPR and FPR. TPR is determined by the number of true positive predictions, normalized by total number of positive observed values. Conversely, FPR defines how many incorrect positive results occur among all negative samples available during the test.

The ROC space is defined by FPR and TPR as x- and y-axes, respectively, which depicts the relative tradeoffs between true positive and false positive. TPR is often described as the sensitivity of the model, while $(1 - \text{FPR})$ is often seen as TNR or specificity. Therefore, the ROC curve is also referred to as the sensitivity versus $(1 - \text{specificity})$ curve. Each case consisting of a prediction and observed values represents one point in the ROC space. Details about the ROC curve were provided earlier in this chapter and are shown in figure 24.

The area under the ROC curve defines the goodness-of-fit of the predictions. In an analogy with measures of linear optimization techniques, the area under the ROC curve can be viewed as the R^2 value. In addition to the goodness-of-fit, the ROC curve is used to define the cutoff value of the model. This is an important parameter that defines how the results from the probability density function can be interpreted in a binary system (i.e., the threshold used to separate probabilities that are referred to acceptable and not acceptable). The *cutoff* is defined as the

probability value that corresponds to the point in the ROC curve closest to the perfect classification point (0,1). When the cutoff is used to convert the predicted probabilities into binary outcomes, the model yields the highest level of accuracy (i.e., highest TPR and TNR).

4. Sensitivity Analysis

The last step in the analysis process is the sensitivity of the logistic models to its variables. It is important that the model produces as accurate results as possible, as well as reasonable probabilities with reasonable values of the deflection parameter. Plots of predicted probability versus the deflection parameter can provide valuable information about the reasonableness of the model for a given set of site characteristic variables (e.g., high truck volume, unbound base, and cold climate). If results from the sensitivity plots are unreasonable, a new model must be calibrated to eliminate unrealistic outcomes.

CHAPTER 5—PROCEDURES FOR OPTIMUM DEFLECTION TEST SPACINGS AND FREQUENCY FOR PMS APPLICATIONS

One important aspect of optimum deflection test spacing and frequency is the measurement accuracy. The accuracy is mainly a function of the combined effects of different sources of variability, such as number of measurements, equipment variability, and spatial variability, which is often associated with the inherent section variability.⁽²⁹⁾ In addition to measurement accuracy, optimum deflection test spacing and frequency for PMS applications is a function of the following considerations:

- Priority and level of sophistication of the structural prediction models in the PMS.
- PMS system inventory mileage.
- Equipment availability.
- Personnel availability and flexibility.
- Traffic levels.
- Available budget to conduct testing.

Structural models in pavement management systems range from the very simple to relatively complex. The simplest models utilize deflections or deflection basin parameters to characterize subgrade and pavement structural properties. For example, the outer deflections can be used to estimate subgrade stiffness, while the inner deflections are indicative of the degree of support provided by the pavement layers above the subgrade. The more complex structural models utilize pavement layer moduli (derived from deflections) and pavement layer thicknesses and material types to calculate pavement response which is then used to predict failure, much like project-level pavement design analysis. Any PMS system using the latter more complex approach would undoubtedly need more deflection information than the former more simplistic approach.

PMS inventory mileage is another consideration in deflection spacing. Texas maintains approximately 89,000 centerline mi (143,290 centerline km) of pavement, while Alaska maintains approximately 5,000 centerline mi (8,050 centerline km). Certainly, it would be easier to collect deflection data on the majority system for a State with fewer miles, and the deflection spacing could be closer.

Most States and local agencies only have a handful of FWDs, and these are mainly used to collect project-level deflection data for scoping M&R work and for research purposes. PMS deflection data collection are, in most cases, prioritized below project-level work, so the equipment availability for network level data collection is often limited.

Data collection for PMS requires equipment operators to be in the field for long periods of time, often weeks at a stretch, as it is not efficient for the operator to mobilize back and forth from the home base to the job site. Multiple operators are required, and the agency must be flexible in its overtime policies as it is more efficient to work a 10- or 12-h day in the summer as opposed to

the traditional 8-h day, 40-h work week. Personnel turnover is an issue as well. Many operators are motivated by the high-tech aspects of operating the FWD. They tend to be highly capable and multitalented and, as such, are often quickly promoted through the agency, leaving a void to fill. FWD operator turnover within the agency is often higher than other positions, so the issue of training new operators must be addressed.

Traffic levels are a significant factor when determining optimum (i.e., “minimum possible”) test spacing. Higher traffic facilities require expensive lane closures. Moderate traffic requires at least a sign truck and a crash attenuator mounted on a large vehicle, typically a flatbed single unit truck. These operations require three personnel, one for each vehicle. Ironically, the lowest traffic facilities are typically ranked lowest in priority in the PMS data collection effort but afford the opportunity to collect the most data.

Given the above, the annual agency budget ultimately controls the quantity of deflection data that can be collected in any given year. Objective recommendations and guidelines are provided in this report to determine optimum test spacings, but in the end, the optimum spacings for any agency, network, or portion of the network will be dictated by data collection priorities (project versus network), total mileage to be tested, equipment and personnel availability, traffic levels, and the portion of the annual budget available for network-level testing.

ANALYSIS OF TEST SPACINGS FOR FWD DATA COLLECTION

The objective of this analysis was to develop an approach to determine the optimum spacing between FWD tests for use in network applications. The approach is based on an evaluation of the probability of introducing errors as a function of different test spacings and pavement section lengths. Different spacings were evaluated in a probabilistic procedure, resulting in a set of expected error curves for various reliability levels that can be used in the future for determining the optimum test spacing. The error represents the expected difference between the sample of the data and the idealized true value of the population, which, in this case, is represented by the average deflection value of a homogeneous road segment. Monte Carlo simulations were used to model the error function. They are particularly useful in this type of problem in which variables are stochastically distributed and analytical solutions are difficult to obtain. The effectiveness of this approach was verified using data from various road segments in five states. The expected outcome of this study is a procedure that can be easily implemented in a pavement management system during the planning stages of the survey campaigns by simply defining an acceptable magnitude of error and a reliability level.

Modeling the Error Using a Monte Carlo Simulation

The main purpose of this task was to evaluate the sources of variability of FWD testing associated with different sampling strategies and their impact on the average deflection values measured in a road segment. This analysis also provides an opportunity to compare a desirable level of accuracy with the costs associated with the associated sampling strategy (i.e., level of expected error versus number of data points in the sample).

An assumption has to be made about the pavement segment for which the sampling strategy is being defined. The segment must be homogenous in the following characteristics:

- Road functional class.
- Pavement structure.
- Traffic (volume, vehicle class, and load distributions).
- Surface condition of pavement.

The characteristics are likely to provide a pavement segment with a deflection profile without significant variations in deflection magnitudes. These conditions are necessary for any sampling strategy to be effective and produce meaningful results.

The basic approach involves the use of a Monte Carlo simulation to assess the effects of each source of variability. The Monte Carlo simulation is an iterative method for evaluating a deterministic model using sets of random numbers as inputs. This method is useful when the model is complex, nonlinear, or involves more than just a few uncertain parameters. By simulating the probability distributions for each source of variability, it is possible to evaluate the overall error of average FWD measurements when different sampling procedures are selected at network-level. Figure 38 represents the process to evaluate different sampling alternatives.

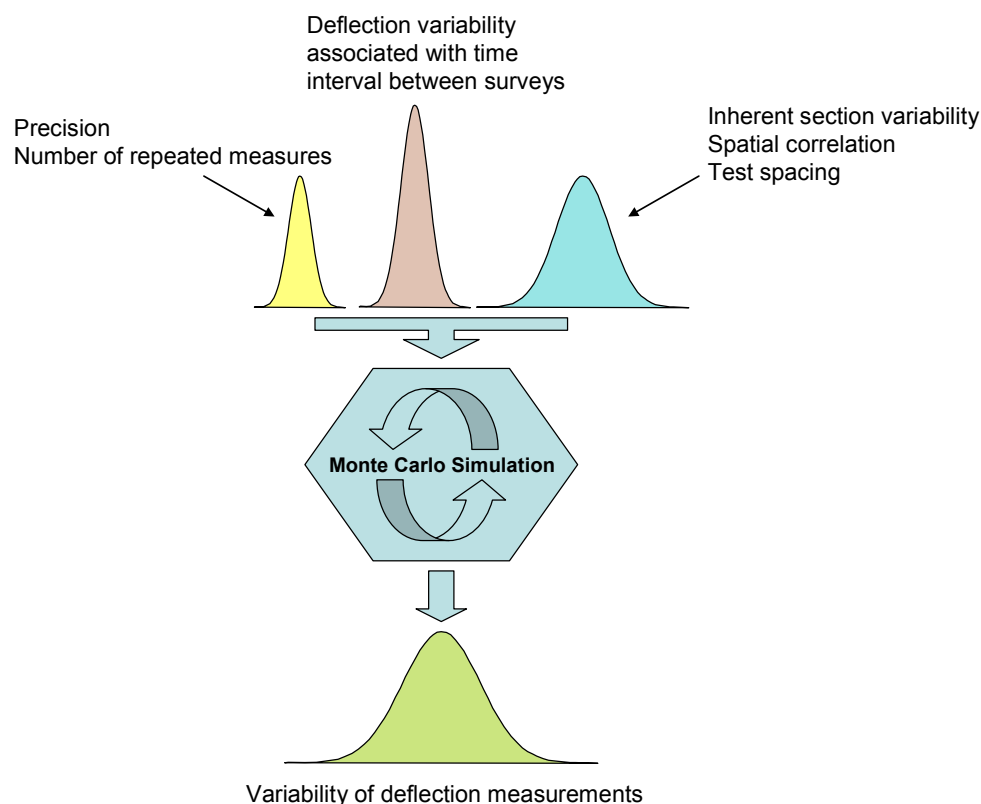


Figure 38. Illustration. Monte Carlo simulation.

To begin a Monte Carlo simulation, operators should select random deflection data that were generated for a 10-mi- (16.1-km)-long section at an assumed 0.1-mi (0.161-km) interval between test points. In each scenario, different means and standard deviations were simulated. The chosen values for means and standard deviations were selected based on observations of data in the LTPP database and State transportation department data available for this research. The interval of 0.1 mi (0.161 km) was chosen because it represents the typical spacing used at FWD surveys for project-level designs. The average deflection of this randomly generated profile was used as the true deflection value for the section (i.e., the errors associated with sampling strategies were determined in relation to this value).

First, the entire data in each randomly generated deflection profile were divided in groups of increasing spacing by skipping up to 19 deflection points, which corresponds to a 0.2- to 2-mi (0.322- to 3.22-km) spacing. These subgroups represented different sampling strategies defined by the spacing between deflection points. All possible combinations of data points that yield the target spacing were generated. For instance, the first spacing was achieved by skipping one deflection point. In this case, two combinations were possible, one starting with the first data point and skipping the second and the other by skipping the first and starting with second one. For each consequent spacing, the number of combinations was increased by one. This is exemplified in figure 39 for spacings of 0.2 and 0.3 mi (0.322 and 0.483 km).

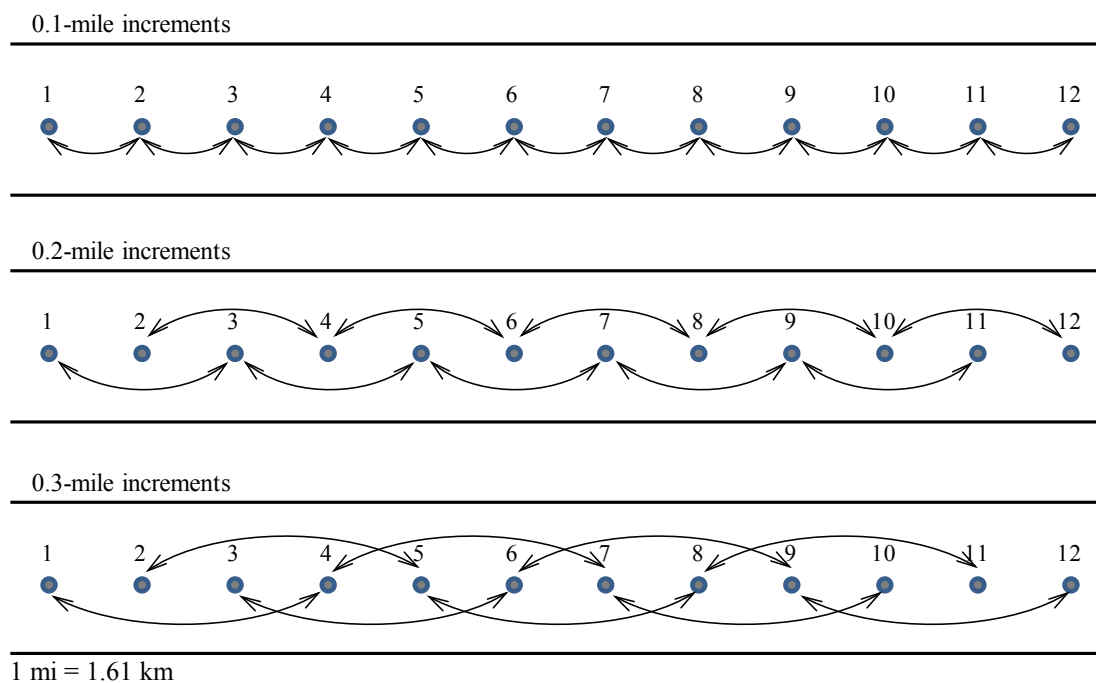


Figure 39. Illustration. Deflection measurement pairings based on 0.1-, 0.2-, and 0.3-mi (0.161-, 0.322-, and 0.483-km) spacings.

After each subgroup was defined, the mean for each spacing combination was calculated and compared to the mean of the entire dataset created at a 0.1-mi (0.161-km) spacing. (Recall that the mean of the 0.1-mi (0.161-km) spacing data was considered to be the true mean.) The errors associated with each spacing were calculated as a percentage of the true mean. This process was repeated for each random simulation in the Monte Carlo process. A total of 5,000 simulations

were run, and the results were used to create a distribution of average errors with spacing. The error distribution as function of test spacing is plotted in figure 40. This graph indicates that as the spacing between test points increases, the error increases in relation to the reference value (i.e., true mean). The error is interpreted as the accuracy of the average deflection of the homogeneous segment associated with a selected sampling strategy (spacing) when compared to the true mean given by a FWD survey at a 0.1-mi (0.161-km) spacing.

In addition to modeling the expected average error, the results from the Monte Carlo simulation can be also used to model a probabilistic component to the calculation of expected error. Therefore, expected levels of reliability can be included in the analysis, which is an important characteristic in pavement design and evaluation today (e.g., the MEPDG).⁽²⁷⁾ The standard deviation of the error was computed for each spacing combination. Normal distribution of the error was assumed, and the expected error at different spacings and different reliability levels could be calculated. The average expected error is shown in figure 41 for various spacings and different probability levels for sections that are 10 mi (16.1 km) long.

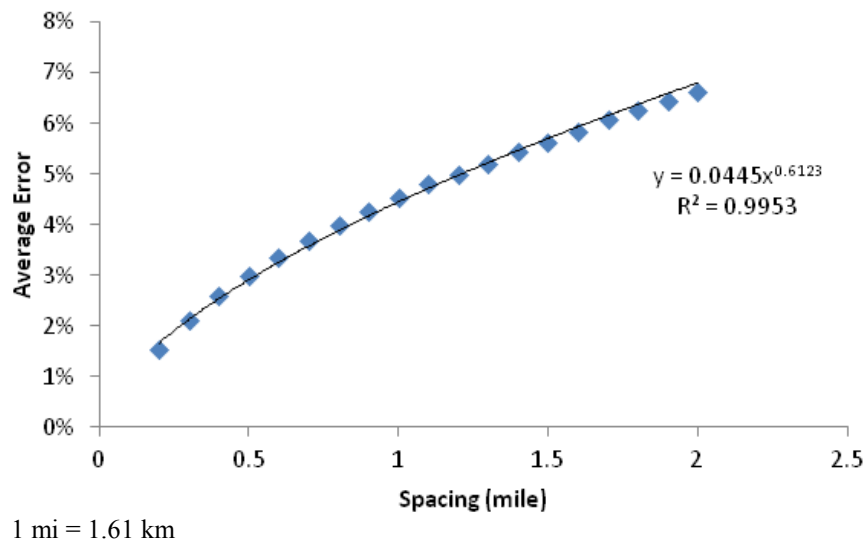


Figure 40. Graph. Expected average error as function of spacing for 10-mi-(16.1-km)-long sections.

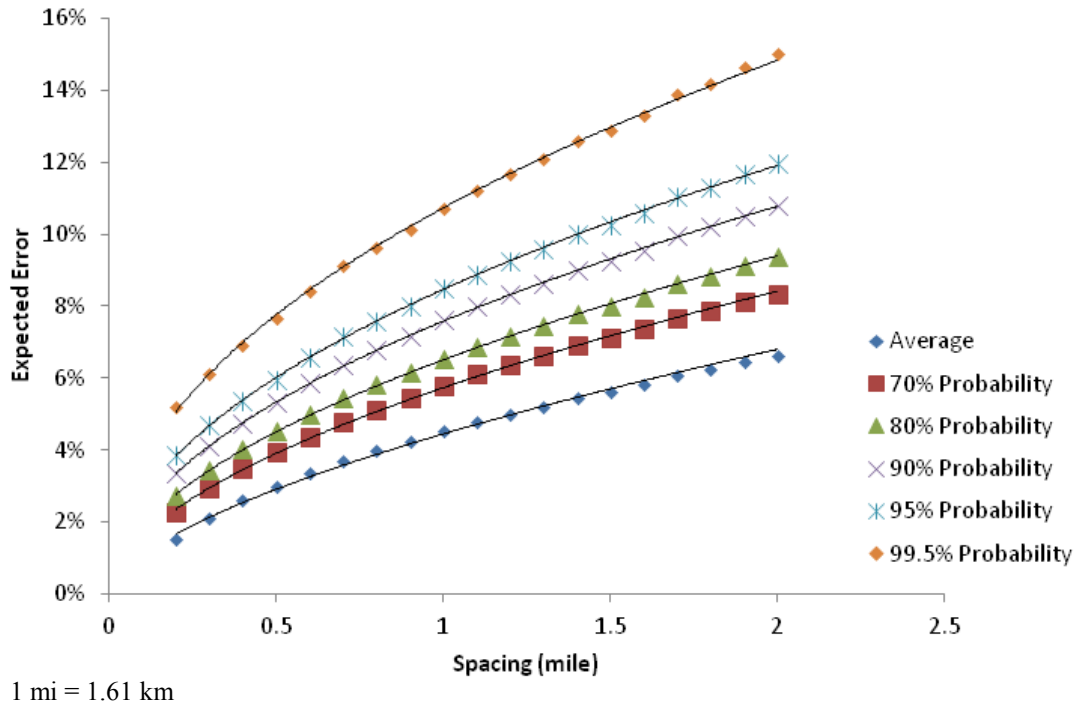


Figure 41. Graph. Expected average errors for 10-mi- (16.1-km)-long section at different spacings and probability levels.

An example of how the process works is illustrated in figure 42. For a given spacing, s , the probability distribution can be computed based on the average error and standard deviation obtained from the Monte Carlo simulation. In the figure, ε_{90} is the error calculated for a 90 percent probability at s . This means that $P(\varepsilon < \varepsilon_{90}) = 0.9$. If ε_{90} is an acceptable error, choosing s implies that there is a 90 percent probability that the error associated with this sampling strategy is less than ε_{90} .

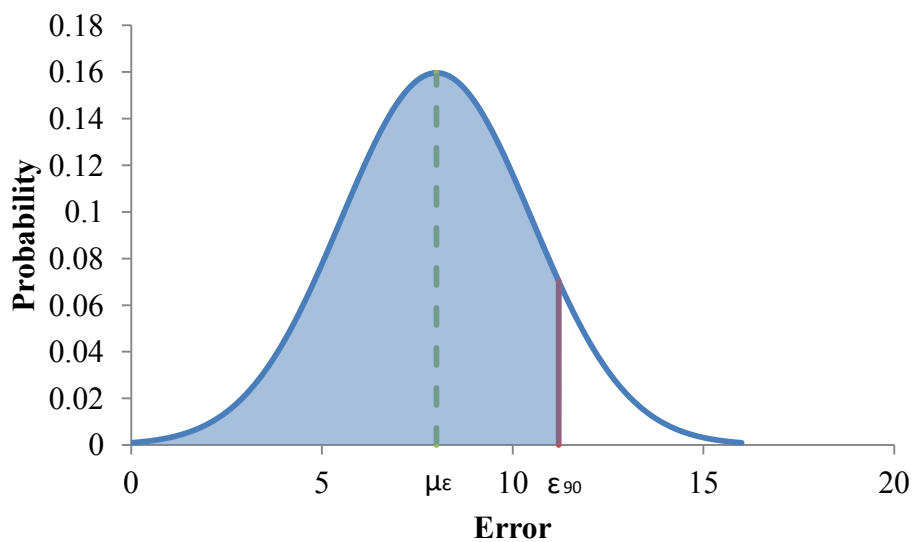


Figure 42. Graph. Normal distribution.

A concern was raised about the influence of the section length on the expected error, since the error in samples is a function of the number of test points in the sample. The hypothesis was that for the same spacing, errors would increase for shorter sections and decrease for longer sections. For this reason, a set of 5,000 simulations were run for sections that were 2, 3, 5, 10, 15, 20, and 25 mi (3.22, 4.83, 8.05, 16.1, 24.15, 32.2, and 40.25 km) long with deflections randomly generated every 0.1 mi (0.161 km). The average error was plotted against spacing for each length (see figure 43). Looking at the graph, it is evident that the length of the section influences the magnitude of the expected error. A power curve of the form $y = a \times x^b$ was fit to all curves. Comparing the intercept, a , and the exponent, b , in each curve suggested that these values could be modeled as power functions of the section length themselves. These two functions are shown in figure 44.

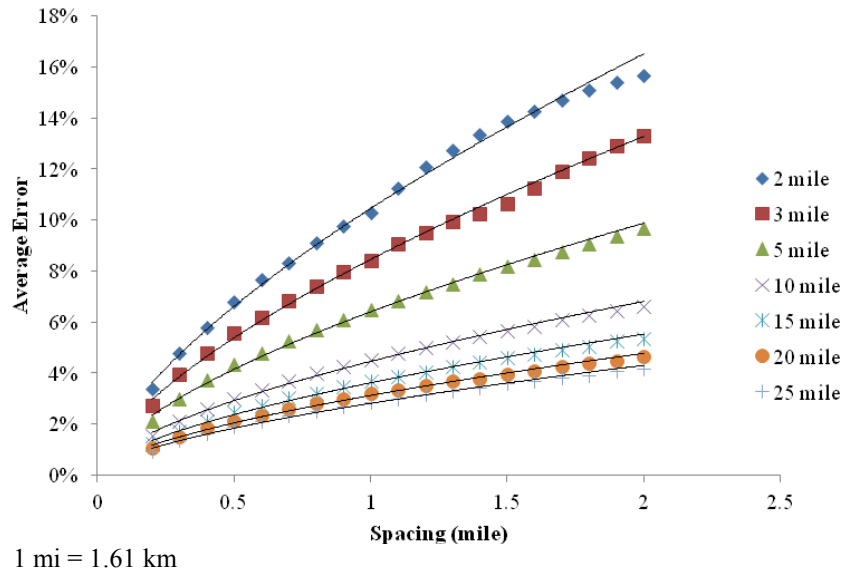


Figure 43. Graph. Average error curves for different section lengths.

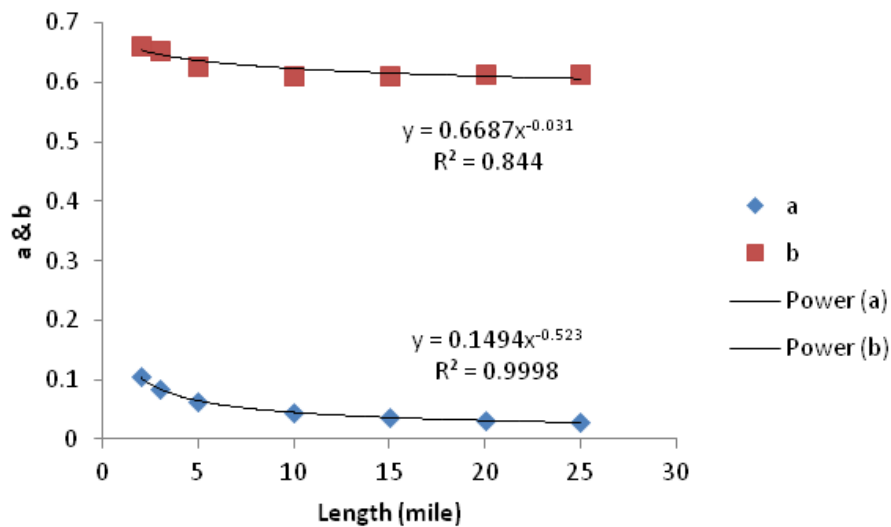


Figure 44. Graph. Values of a and b from the seven average error curves.

The results from figure 43 and figure 44 suggest that the expected error can be calculated for a particular section depending on its length and the chosen sampling strategy (spacing) according to the equation in figure 45.

$$\mu_{\varepsilon} = 0.1494 \cdot L^{-0.523} \cdot s^{0.6687 \cdot L^{-0.031}} \quad (R^2 = 0.998)$$

Figure 45. Equation. Average expected error due to sampling.

Where:

μ_{ε} = Expected average error (percent).

L = Length (miles).

s = Spacing (miles).

The same process was repeated for the standard deviation of the expected error, which is shown in figure 46. The two functions for the intercept, a , and exponent, b , are shown in figure 47. The standard deviation of the expected error can be calculated for a particular section depending on its length and the chosen sampling strategy (spacing) according to figure 48.

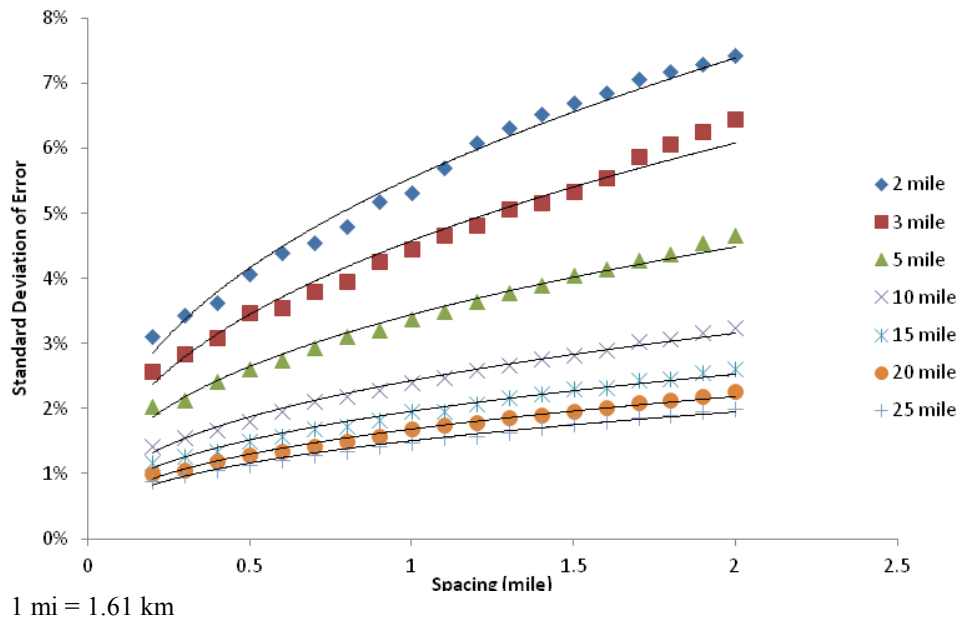


Figure 46. Graph. Standard deviation of average error curves for different section lengths.

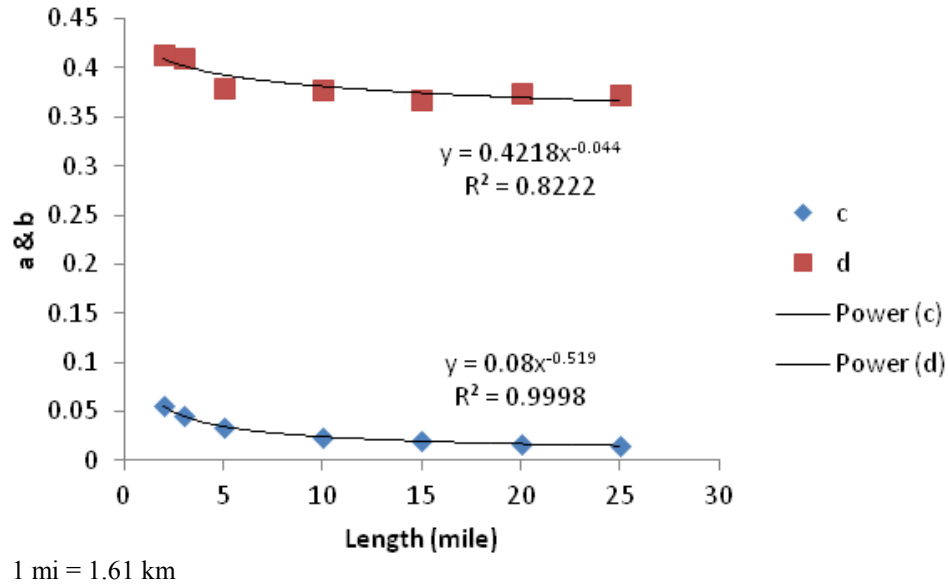


Figure 47. Graph. Values of c and d from the seven standard deviation curves.

$$\sigma_{\varepsilon} = 0.08 \cdot L^{-0.519} \cdot s^{0.4218 \cdot L^{-0.044}} \quad (R^2 = 0.996)$$

Figure 48. Equation. Standard deviation of the expected error due to sampling.

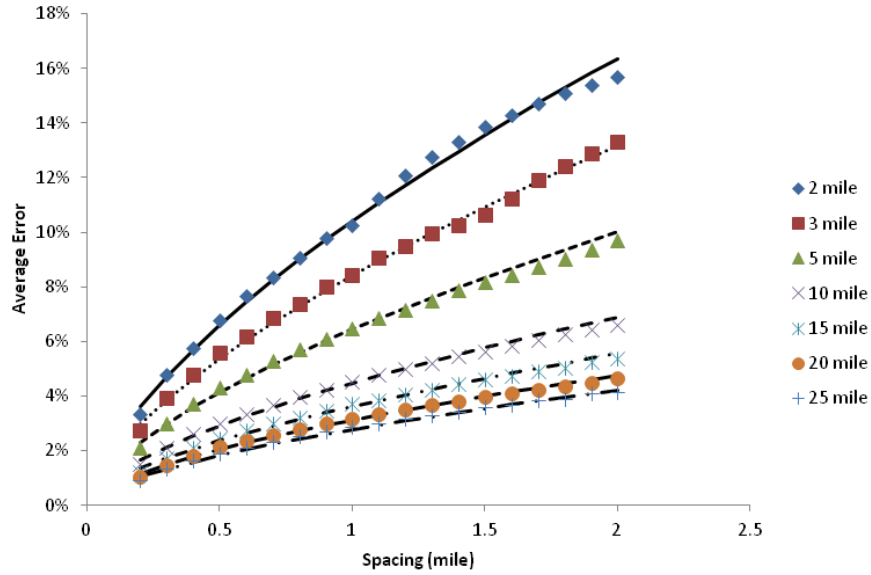
Where:

σ_{ε} = Standard deviation of the expected error (percent).

L = Length (miles).

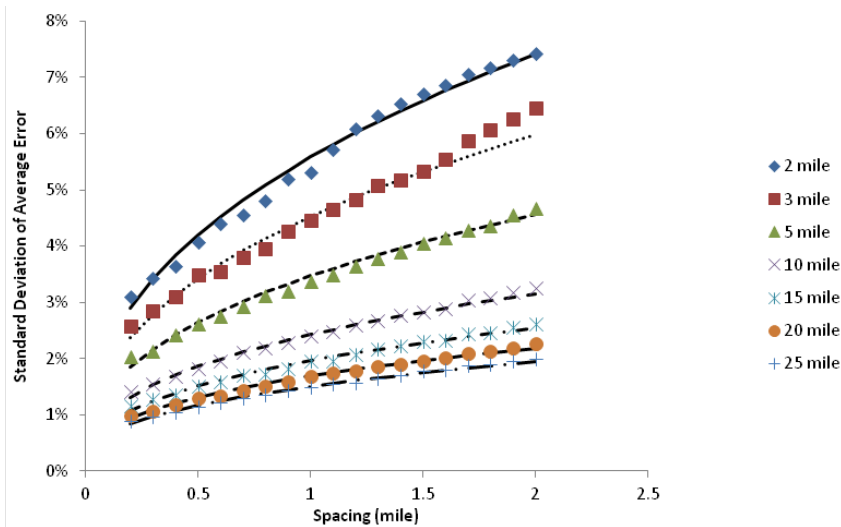
s = Spacing (miles).

The effectiveness of these two equations is demonstrated in figure 49 and figure 50. Both figures show a good fit between the predicted error and standard deviation of error versus computed values from the Monte Carlo simulation.



1 mi = 1.61 km

Figure 49. Graph. Observed average error (data points) plotted with the computed average error (lines).



1 mi = 1.61 km

Figure 50. Graph. Observed standard deviation (data points) plotted with the computed average error (lines).

The final step in the development of these equations involved the influence of the coefficient of variation (COV) on the average error. For this purpose, simulations were run for various means and standard deviations. The results are shown in figure 51. The numbers in the legend correspond to the mean, standard deviation, and COV. For the same COV, the average error remains the same regardless of the mean and standard deviation. Also, it is important to point out that an increase in COV increases the average error significantly.

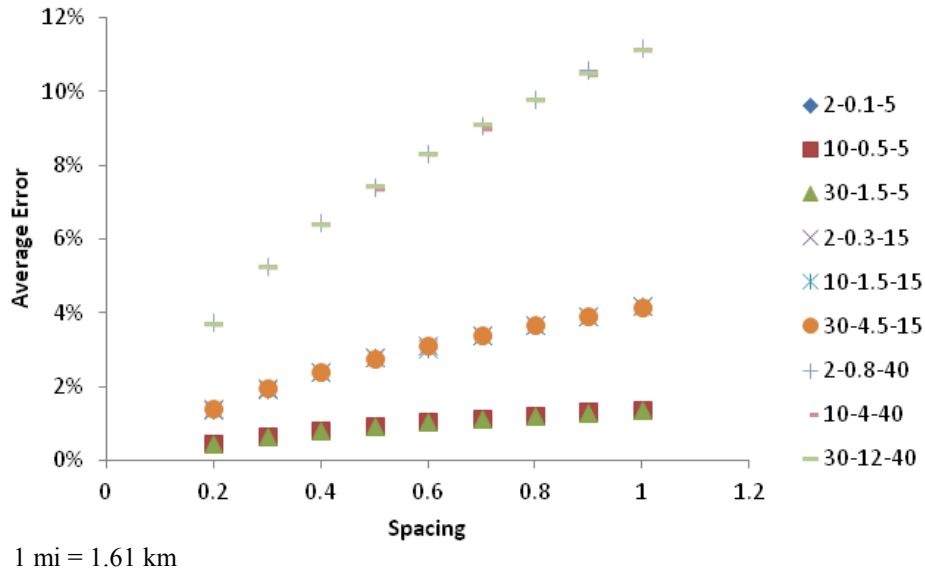


Figure 51. Graph. Calculated errors for a 10-mi- (16.1-km)-long section with different means and standard deviations of errors.

In order to consider the effect of COV, a shift factor was determined to incorporate COV into the average error equation. The equation for the COV shift factor is shown in figure 52.

$$f_{cov} = 5.342 \cdot COV$$

Figure 52. Equation. Calculation of COV shift factor.

Although the shift factor was calculated and is available, COV will not likely be known prior to surveying the road with an FWD. Therefore, for practical applications, it is recommended that the average error should be calculated for a COV of 33 percent. This value was obtained from the FWD measurements used in this study and could be representative of the variability observed in field FWD data. This value was also used in this research for verifying the reliability approach laid out in this section. The verification of this approach is described in the following section.

Being able to predict the expected error and its standard deviation enables the development of error curves for different section lengths and reliability levels without running any more Monte Carlo simulations. Table 30 can be used to calculate the expected error in the average deflection as a result of a selected sampling strategy (spacing) for a given section length and 90 percent reliability. Additional tables were developed using this approach for a variety of section lengths and different reliability levels and are presented in appendix E.

Table 30. Errors in percentage for 90 percent reliability based on various section lengths, sample spacings, and COV of 33 percent.

Probability	Length (mi)	Spacing (mi)								
		0.2	0.3	0.4	0.5	0.6	0.7	0.8	0.9	1
90 percent	1	14.18	17.94	21.24	24.22	26.98	29.57	32.02	34.35	36.59
	2	10.10	12.71	14.98	17.03	18.93	20.70	22.37	23.96	25.48
	3	8.28	10.38	12.21	13.86	15.38	16.80	18.13	19.41	20.62
	4	7.19	9.00	10.56	11.97	13.27	14.48	15.63	16.71	17.75
	5	6.44	8.05	9.44	10.69	11.84	12.91	13.92	14.88	15.80
	6	5.89	7.35	8.61	9.74	10.78	11.75	12.67	13.54	14.36
	7	5.46	6.80	7.97	9.01	9.97	10.86	11.70	12.49	13.25
	8	5.11	6.36	7.45	8.42	9.31	10.14	10.92	11.66	12.36
	9	4.82	6.00	7.02	7.93	8.76	9.54	10.27	10.96	11.62
	10	4.58	5.69	6.65	7.51	8.30	9.03	9.72	10.38	11.00

1 mi = 1.61 km

Comparison to Available Data

Deflection data from various roads in three States (New Mexico, Oregon, and Kansas) were obtained and analyzed. FWD data from New Mexico and Kansas were spaced at 0.1 mi (0.161 km) per test point, while Oregon was spaced at 0.05 mi (0.08 km). Overall statistics are presented in table 31. The roads were further separated into smaller sections based on the asphalt concrete layer thickness and base thickness (not available for every road) for creating homogenous sections. An overview of the deflection data for each state is given in figure 53. More detailed information is presented in appendix E.

Table 31. Deflection data for New Mexico, Oregon, and Kansas.

Statistics	New Mexico	Oregon	Kansas
Maximum (mil)	11.34	22.48	18.20
Minimum (mil)	4.33	4.31	4.27
Average (mil)	7.12	11.30	10.68
Standard deviation (mil)	2.51	3.90	3.09
COV	0.352	0.345	0.289

1 mil = 25.4 μ m

First, similar to the theoretical approach, the entire section data were divided in groups of increasing spacing by skipping up to 19 deflection points when enough data were available. The average error for each spacing was then computed for all sections. Next, the mean was compared to the mean of the entire section, which was assumed to be the true mean. Figure 54 shows the average error of means at different spacings averaged for all the sections in New Mexico. It can be noted that as the spacing increased, the difference to the true mean increased, as well, similar to the randomly generated deflections. The same trend follows for the other States.

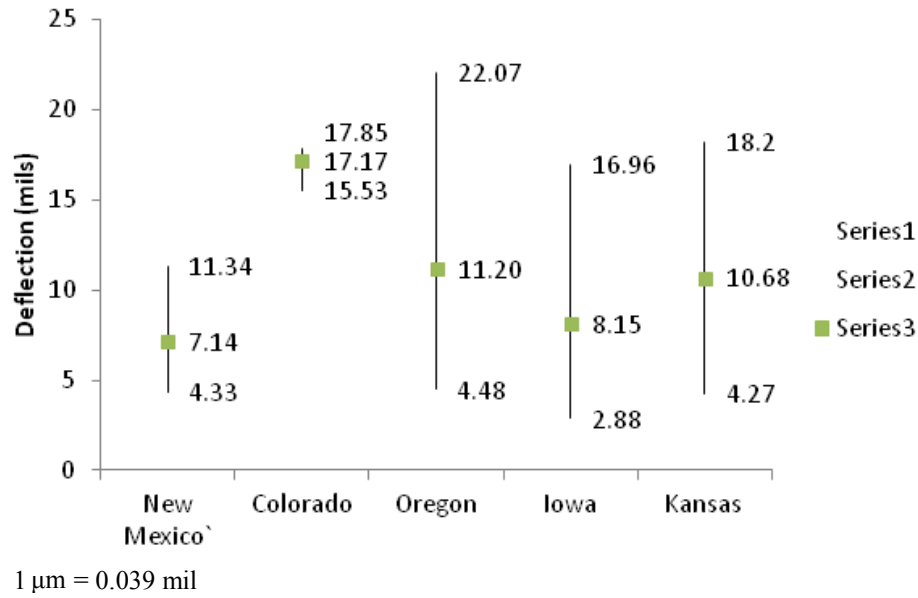


Figure 53. Graph. Maximum and minimum section means and weighted mean deflection for all sections in each State.

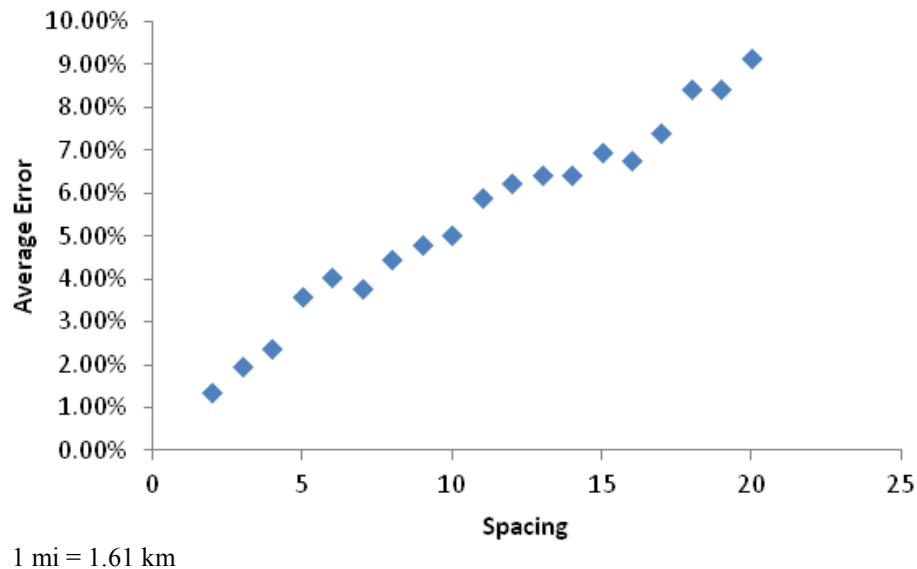


Figure 54. Graph. Average error for each spacing.

The verification of the theoretical approach with field measured data was done by comparing the expected average error, computed using the equation in figure 45 and the COV shift factor equation in figure 52, with calculated values from the field distribution. Figure 55 through figure 57 show the measured error for a specific sampling strategy (spacing) and the expected error computed by the equations developed in the theoretical approach considering a reliability level of 50 percent (i.e., without including the standard deviation). As a consequence, it is expected that at least 50 percent of the sections would have errors less than or equal to the calculated error. It can be seen from all three figures that the theoretical approach provides a reasonable estimate of the error expected when one particular sampling strategy is selected.

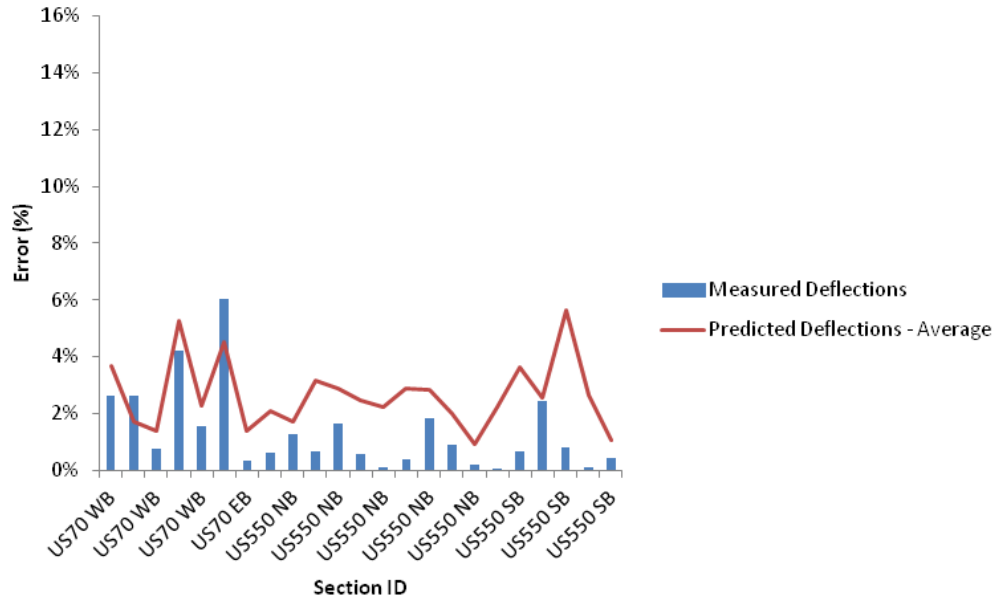


Figure 55. Graph. Comparison between measured error and predicted error for all New Mexico sections at 0.2-mi (0.322-km) spacing.

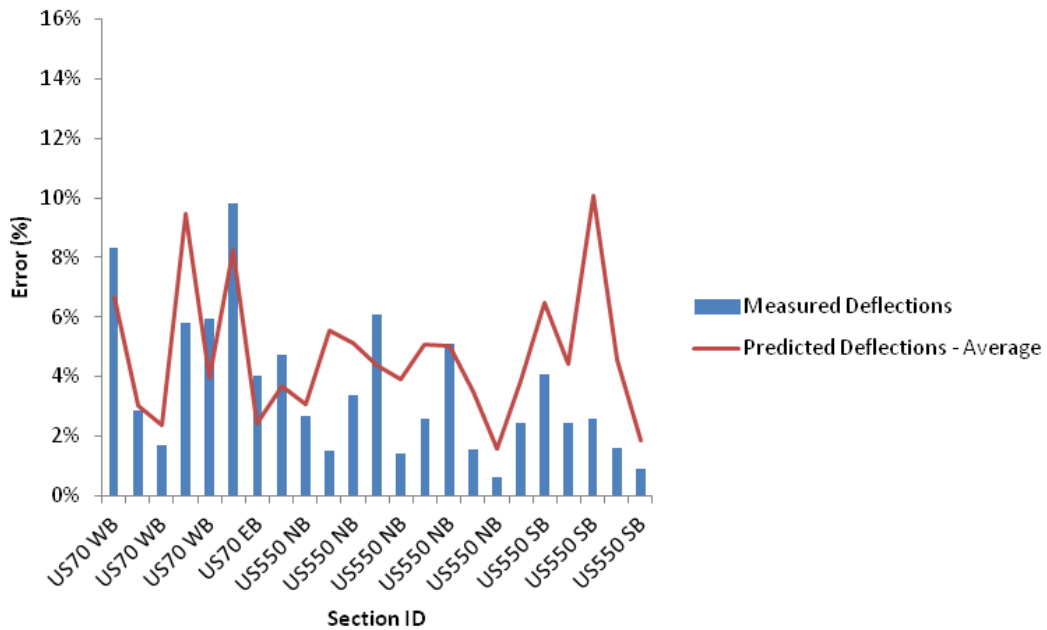


Figure 56. Graph. Comparison between measured error and predicted error for all New Mexico sections at 0.5-mi (0.805-km) spacing.

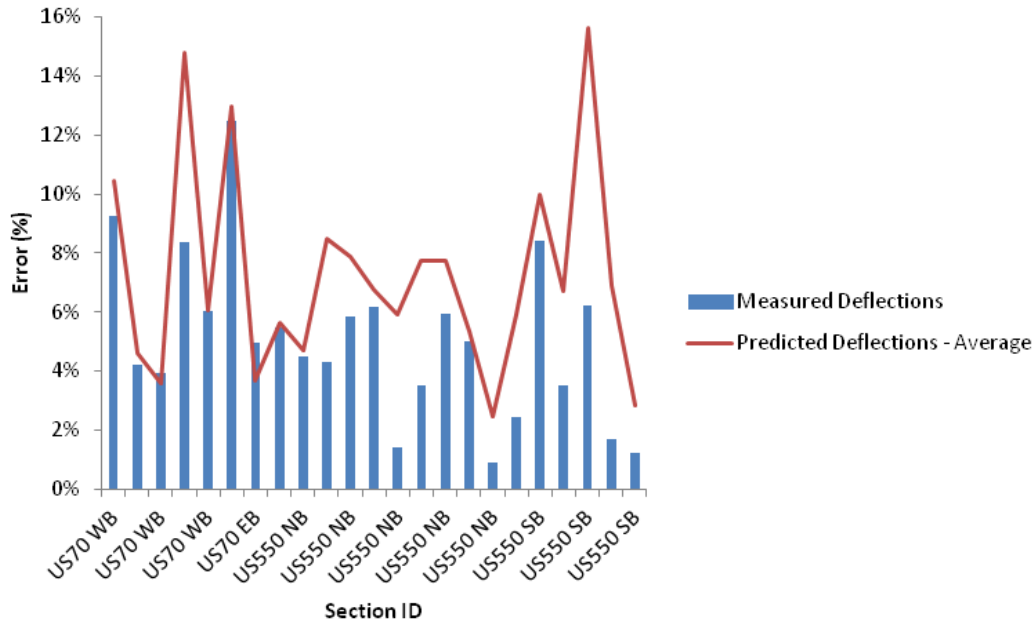


Figure 57. Graph. Comparison between measured error and predicted error for all New Mexico sections at 1-mi (1.61-km) spacing.

ANALYSIS OF FREQUENCY FOR FWD DATA COLLECTION

The recommended frequency of FWD data collection on pavements is dependent on the overall “rate of change” of structural conditions over time. Since pavement deflection measurements, particularly the deflection at the center of the load plate, are a direct measurement of the overall structural condition of a pavement, the LTPP database was evaluated to determine how quickly deflections change over the range of testing dates and pavement thicknesses contained in the database. Flexible pavements were evaluated separately from rigid pavements with recommendations given for each.

Flexible Pavements

The objective of this analysis was to determine the rate of change of the center deflections over time for a variety of asphalt pavement thicknesses, traffic levels, subgrade types, and climatic conditions. The rate of change is used to determine how often deflection measurements should be taken on a network-level basis. Center deflections were used because they represent the total response of all the layers in the pavement structure.

The LTPP database contains 2,873 days of FWD tests taken for 59 State codes, 297 SHRP sites, and 8 construction cycles. Each record in the database contains the average of the deflections collected on a particular day over the entire SHRP test section along the outer wheel path. The records also contain the average air and mid-depth AC temperatures for the day of test. The deflection data were reviewed for statistical outliers, such as deflections measured on frozen pavements which were removed. In addition, those sites with too few or insufficient data collection cycles were omitted from the analysis.

The analytical process consisted of the following steps:

1. Sort the order of the records by the total number of test days on a particular test section, as well as the standard deviations of center deflections (D_I).
2. Normalize the deflections to a 9,000-lbf (40,050 N) load for each SHRP section.
3. Determine the degree of temperature sensitivity due to the AC layer for each SHRP section by regressing D_I versus mid-depth AC temperatures.
4. Remove the influence of temperature from the D_I measurements by adjusting them to a reference temperature of 68 °F (20 °C).
5. Regress D_I versus time to determine the slope (change in D_I over time).
6. Determine relationship between the slope and AC thickness, traffic levels, subgrade type, and climatic conditions (WF, DF, WNF, and DNF).

This process is demonstrated in figure 58 for one particular SHRP section. In this case, the State code is 50 and the SHRP ID number is 501002, which is US-7 near New Haven, VT. This section is composed of 8.5 inches (215.9 mm) of AC over 26 inches (660.4 mm) of unbound base or subbase materials, a fine-grained subgrade, and a WF climatic designation. There were 60 days of FWD data collection available for analysis on this section, starting in September 1989 and ending in October 2003. The traffic classification for this section was high, with an AADTT of 300 and 28 percent trucks of the class 9 variety. The deflection versus temperature characteristics for $\log(D_I)$ are shown in the figure 58.

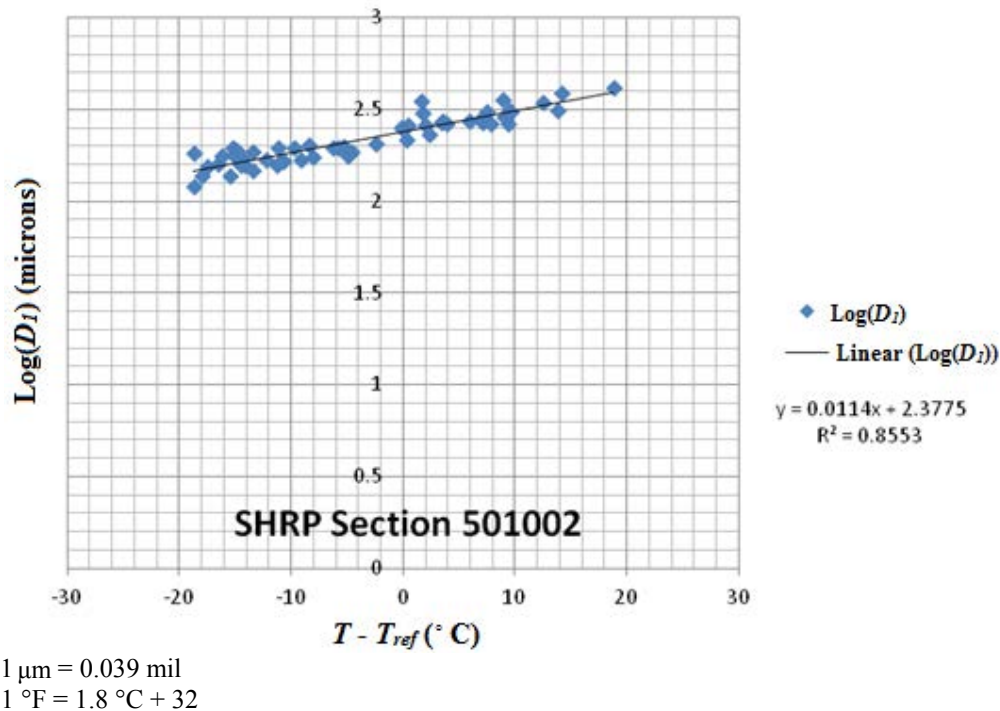


Figure 58. Graph. Plot of $\log(D_I)$ versus temperature for SHRP section 501002.

The slope of the regression line is 0.0114 and is used in the following equation in figure 59 to adjust each deflection to the standard temperature of 68 °F (20 °C):

$$D_{Iadj} = 10^{\log(D_{I meas}) - b(T - T_{ref})}$$

Figure 59. Equation. Deflection adjustment by temperature.

Where D_{Iadj} is the center deflection adjusted to 68 °F (20 °C), $D_{I meas}$ is the center deflection adjusted to 9,000 lb (4,086 kg), load b is the slope of the regression equation, T is the average mid-depth temperature, and T_{ref} is the reference temperature of 68 °F (20 °C).

Figure 60 shows the center deflections plotted against test date for SHRP section 501002 before and after the temperature corrections were applied.

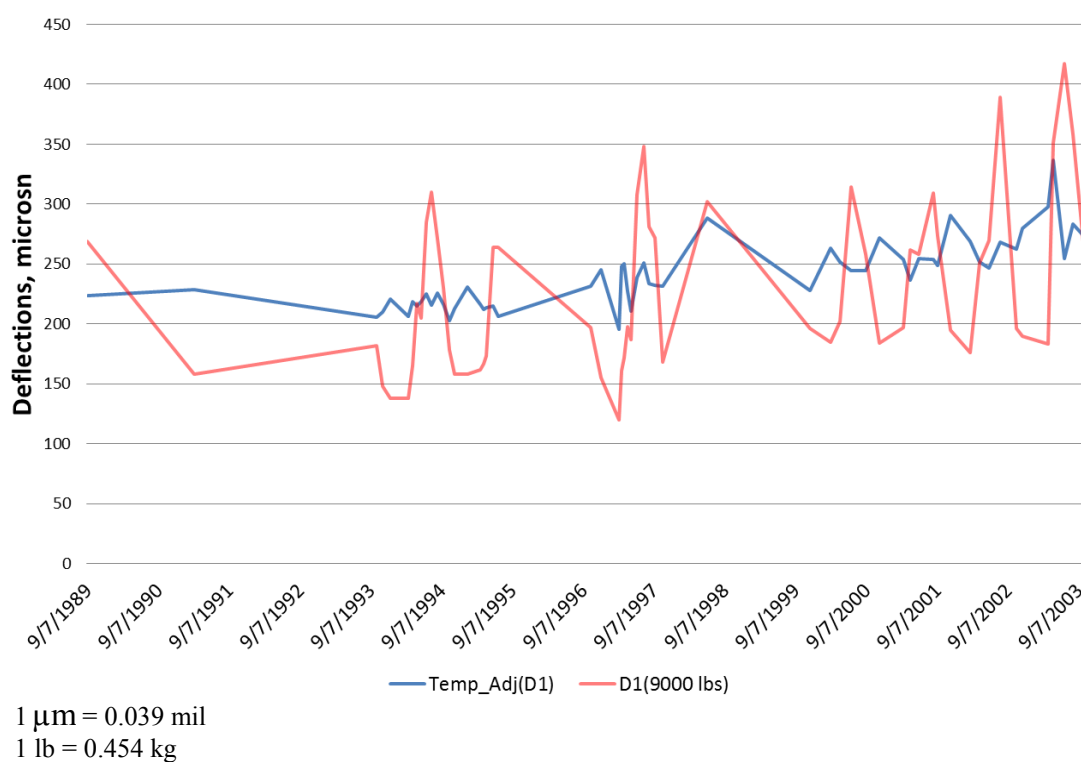


Figure 60. Graph. Center deflection measurements versus test date—adjusted and unadjusted.

Note that in figure 60, a long-term trend of increasing deflections can be detected. There are some seasonal variations, but these are minor in relation to the overall trend.

By fitting a linear regression line to the temperature adjusted data, as seen in figure 61, the rate of change of structural condition on the section can be determined. Note that the change is essentially linear. The slope of the regression line, 0.0164, represents the increase in microns per day for the center deflection. This can be converted to a yearly rate by multiplying it by 365, which equals roughly 0.234 mil (6 μm) per year.

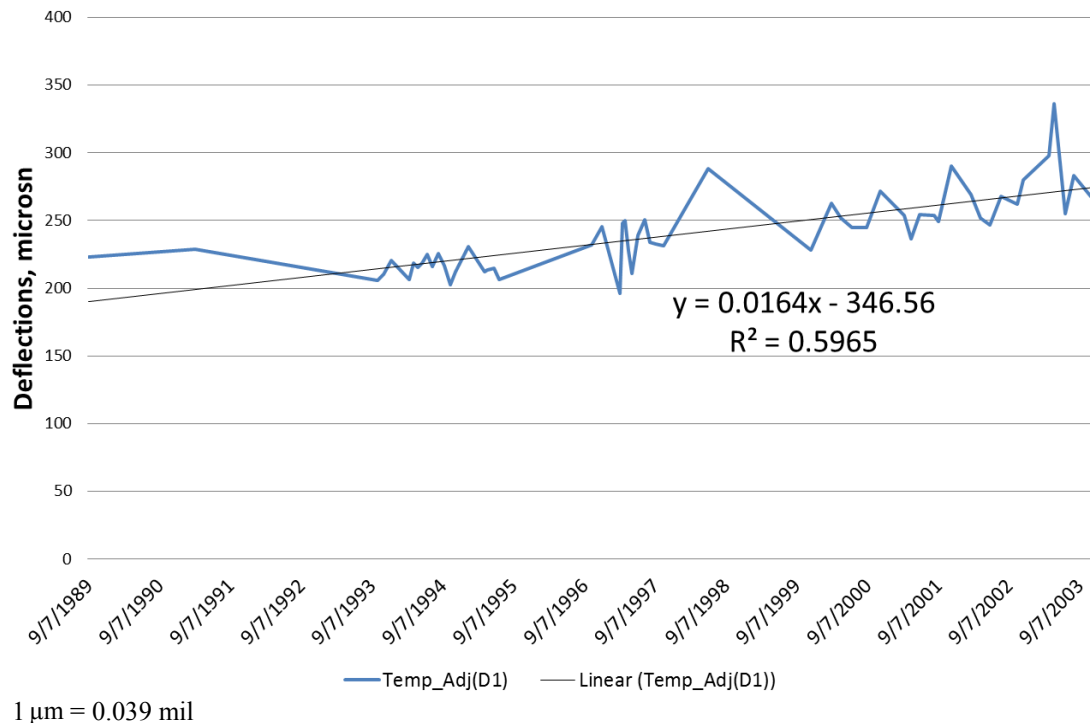


Figure 61. Graph. Temperature-adjusted center deflections versus test date for SHRP section 501002.

A similar analysis was done for the remaining selected sections. Some sections displayed decreasing deflections over time, so the scalar value of the slope was used for the analysis. A summary of slope values is provided in table 32. The average slopes were grouped by traffic level, subgrade type, AC thickness, and climate classification in table 33 through table 36.

Table 32. Annual change in D_I by SHRP test section.

State Code	SHRP_ID	Construction Number	Annual Deflection Change (microns)	Number of Test Dates
48	3739	1	24.68	13
1	1019	1	21.28	4
20	1010	1	20.99	9
31	1030	2	18.50	10
27	6251	2	15.18	9
30	509	2	14.16	4
90	6405	1	12.67	17
49	1001	1	10.94	21
1	4155	1	9.85	4
83	1801	1	8.58	20
4	1024	3	8.15	13
27	1018z	4	8.03	10
20	1005	1	7.72	11
48	1060	1	6.98	32
33	1001	1	6.72	33
16	1010	1	6.32	28
50	1002	1	5.98	57
34	502	2	4.88	11
48	1119	2	4.64	5
56	1007	1	4.56	25
30	8129	1	4.31	33
23	1026	2	4.10	14
28	1802	1	3.76	21
2	1008	1	2.90	4
28	1016	1	2.21	18
2	1004	2	1.95	4
1	6019	3	1.84	4
1	4125	1	1.63	4
23	1026	1	1.51	18
24	507	2	1.44	9
34	507	2	1.43	13
87	1622	1	1.22	24
13	1031	1	1.18	4
13	1031	3	1.18	26
34	509	2	1.18	12
2	6010	1	1.12	4
34	506	2	1.07	12
13	1005	2	1.02	28
8	1053	1	0.96	39
24	1634	1	0.96	28
27	6251	1	0.83	30
37	1028	1	0.79	31

34	505	2	0.78	10
1	509	2	0.71	6
40	4165	1	0.68	29
34	504	2	0.56	12
2	1002	1	0.51	5
1	6012	1	0.50	4
27	1028	1	0.42	25
9	1803	1	0.30	12
35	1112	1	0.29	39
1	4127	2	0.24	4
34	508	2	0.23	12
34	503	2	0.10	14

1 μm = 0.039 mil

Table 33. Rate of deflection change by traffic level.

Traffic Classification	Average Annual Rate of Change in Center Deflection (microns)
High	3.8
Low	4.5

1 μm = 0.039 mil

Table 34. Rate of deflection change by subgrade type.

Subgrade Type	Average Annual Rate of Change in Center Deflection (microns)
Fine	4.2
Coarse	4.4

1 μm = 0.039 mil

Table 35. Rate of deflection change by AC thickness.

AC Thickness (mm)	Average Annual Rate of Change in Center Deflection (microns)
≤ 50	7.8
51–100	4.3
101–250	4.5
> 250	2.8

1 mm = 0.039 inches

1 μm = 0.039 mil

Table 36. Rate of deflection change by climate classification.

Climate	Average Annual Rate of Change in Center Deflection (microns)
DF	5.8
DNF	6.4
WF	2.8
WNF	3.1

1 μm = 0.039 mil

From table 32 through table 36, the following can be concluded:

- The annual rate of change of pavement deflections shows little correlation with traffic levels.
- The annual rate of change of pavement deflections shows little correlation with subgrade type.
- The annual rate of change of pavement deflections does show some correlation to AC thickness—lower thicknesses produce higher rates of change, as expected.
- Dry climates seem to produce larger annual changes in pavement deflections, which is counter-intuitive.
- Once temperature influences are removed, the rate of change of deflection measurements is relatively small for most pavement sections contained in the LTPP database.⁽¹⁾

Based on the analysis of these pavement sections, a test frequency of 5 years between tests is recommended for flexible pavements.

Rigid Pavements

The rigid pavement sections that were evaluated also exhibited temperature dependency and were adjusted to a standard temperature of 68 °F (20 °C). This dependency is most likely due to slab curling under higher temperatures. Subsequent to normalizing the deflections to 9,000 lb (4,086 kg) and then removing the temperature effects, the annual change in D_I was less overall than that observed on the flexible pavement sections. It appears that the frequency of network level testing of rigid pavements can be less than flexible sections, perhaps up to 10 years between tests.

CHAPTER 6—GUIDELINES FOR CONSIDERATION OF TIME OF DAY AND SEASON OF YEAR FOR OPTIMAL FWD DATA COLLECTION FOR PMS APPLICATIONS

SUMMARY OF APPROACHES FROM LITERATURE REVIEW

Since little has been published until recently about including deflection data in PMS applications, it stands to reason that even less has been published on the subjects of time of day and season of year when FWD testing should take place.

However, in July 2009, the Michigan Department of Transportation (MDOT) mentioned the potential of utilizing FWD load deflection testing at the network level.⁽³⁰⁾ According to the report, MDOT intended to prescribe 500-ft (152.5-m) testing intervals, or about 10 test points per mile of pavement. MDOT also mentioned spring and late summer/early fall; however, no particular time of day to conduct deflection tests was mentioned.

Other agencies by and large either do not utilize load deflection tests at the network level, or the few that already use deflection testing generally allow their engineers to fix the proper test point intervals and/or the time of year to test, depending on the application and climatic region. For example, AkDOT also utilizes 500-ft (152.5-m) test intervals; however, it does not yet use deflection testing on their entire roadway network and is currently adding FWD test results as time allows (only the Parks Highway has been completed to date). The viable testing season is vastly shortened in Alaska due many months of frost penetration as well as the occasional year-round permafrost presence.

The vast majority of deflection testing—whether at the network or project level—is generally carried out during normal daytime work hours. Similarly, with seasonal testing, it is generally believed that the gathering of deflection data should occur when these data can be gathered as climatic conditions allow (and the pavement temperature is above freezing). This is to allow agencies to carry out network-level testing as far as possible at their own convenience because what is convenient as far as timing goes will most likely produce good deflection data for use in the stochastic relationships developed for this project.

While there are exceptions to the above statements, particularly when concrete pavements are tested, the general rule from the literature and practice alike is to test whenever possible during the day or year and not restrict when an agency can test for PMS applications. At some point in the future, it is also likely that the RWD will become a feasible and reasonably low-cost alternative to the FWD; but this is not currently the case, so this eventuality is not considered in this report.

It is also important to consider the issue of protection and maintenance of traffic (P&MT). For most medium to high traffic roads, FWD testing must be fit around the periods of high traffic flow, which often happens in the morning (6 to 9 a.m.) and afternoon periods (3 to 5 p.m.).

RESULTS OF LTPP DATA ANALYSIS

The LTPP database was reviewed in detail to ascertain whether limitations should be imposed, or suggested, to either the time of day or season of year when network-level FWD testing should (or should not) take place. At the outset, it was assumed that any significant limitations of this nature would tend to discourage the use of simplified techniques for both gathering and analyzing load deflection data, since roadway networks are, by definition, very extensive compared to individual projects.

DEFLECTION ADJUSTMENT PROCEDURES

The main reasons for adjusting the measured pavement deflections (at a given load level) is pavement temperature for flexible pavements or temperature gradients for PCC pavements.

For flexible pavements, in general, the use of an adjusted deflection level due to pavement temperature was not observed. Figure 62 shows the accuracy of the fatigue cracking model developed in chapter 4 for flexible pavements. The figure shows the ROC curve for two deflections, one adjusted by temperature and the other not adjusted. The fatigue cracking model indicates no improvement whatsoever by adjusting D_I due to pavement surface temperature variation. A similar analysis is provided in figure 63 for rutting. The statistics of these regressions are shown in table 37 and table 38.

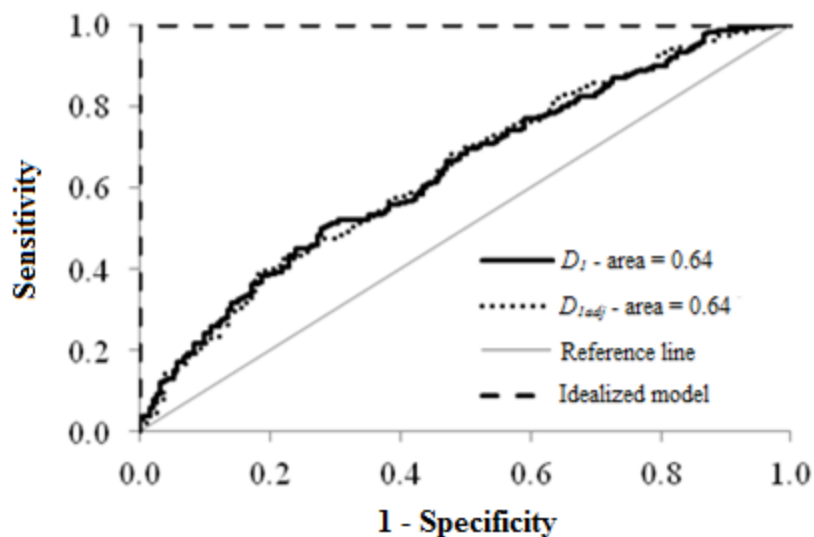


Figure 62. Graph. Specificity of fatigue cracking models for flexible pavements.

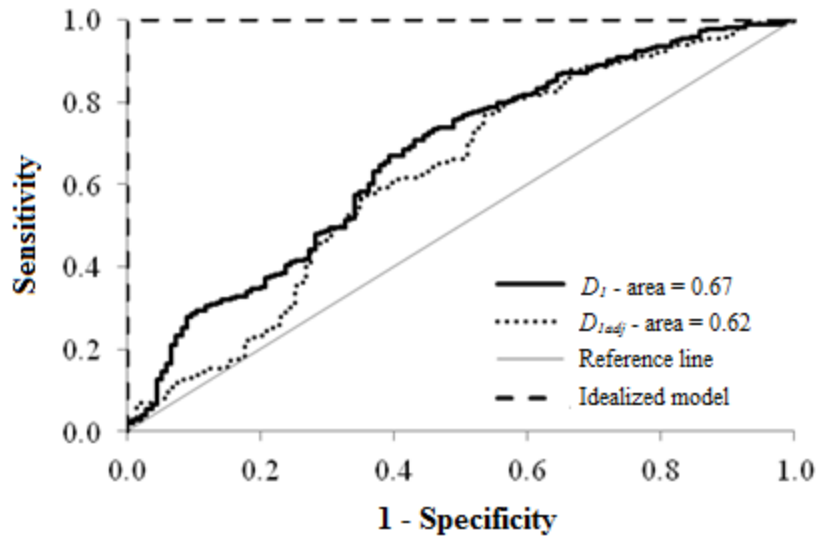


Figure 63. Graph. Specificity of rutting models for flexible pavements.

Table 37. Statistics for flexible pavement fatigue cracking models: D_I versus $D_{I\text{adj}}$ adjusted.

Model	Significance	Area Under ROC Curve	Correct Cases—Modeling (percent)
D_I	0.53	0.64	59.0
$D_{I\text{adj}}$	0.73	0.64	61.7

Table 38. Statistics for flexible pavement rutting models: D_I versus $D_{I\text{adj}}$ adjusted.

Model	Significance	Area Under ROC Curve	Correct Cases—Modeling (percent)
D_I	0.40	0.67	68.3
$D_{I\text{adj}}$	0.12	0.62	59.5

While the fatigue cracking model showed virtually no change in either the area under the ROC curve or the correct cases predicted by the model, no improvement was noted. For the rutting model, on the other hand, adjusting D_I made the model inferior to the unadjusted model.

In the case of the roughness model, deflection parameters involving D_I were not among those that showed the most promise overall. Therefore, the question of adjusting D_I or not is mute.

It was concluded that an adjustment to D_I due to asphalt temperature variations is neither helpful nor worth the time and effort to carry out this extra step for applications at the network level. Such an adjustment would also cause agencies to have to gather even more data—in this case, air and pavement surface temperature plus the previous day's high and low temperatures at a minimum. To keep the network-level PMS application of adding simplified deflection analysis techniques to routine pavement management data would be counterproductive and is ill advised.

Since concrete surfaces are not subject to the same visco-elasticity that asphalt surfaces are, a temperature correction for concrete surfaces was not investigated.

Recommendation: Do not adjust deflection measurements—not even D_I —due to temperature variations in any visco-elastic surface course layer.

RECOMMENDATIONS FOR TIME OF DAY FOR DEFLECTION MEASUREMENTS AT NETWORK LEVEL

As mentioned in the previous section, “Results of LTPP Data Analysis,” no limits for agencies are recommended for the time of day for FWD load deflection testing except normal daytime working hours. The main reason for this is to encourage agencies from doing network-level deflection testing by restricting the time of day when measurements should be conducted. A secondary but equally important reason is that the time of day generally does not appreciably affect the accuracy of the simple models used by the logistic model, as recommended in this report. Networks are very large compared to individual projects, and since at least a statistically significant sampling of each uniform or standard pavement management section should be sampled, it would indeed be discouraging for an agency to also have to further limit their FWD testing window due to the large number of lane miles involved to cover an entire network.

Exceptions to this rule may apply to jointed PCC pavements when large temperature gradients within the slab are present. Another possible exception is very high volume urban freeways when traffic control will be an issue. In such cases, only late evening through early morning testing is feasible and should be carried out in lieu of doing nothing. Finally, running FWD load deflection tests while the underlying unbound layers may be frozen, or during the spring thaw in many of the northerly regions, should also be avoided for network-level FWD testing.

Exactly when concrete pavements have excessive temperature gradients and thus curling or warping due to these gradients is largely a function of local weather patterns, temperature differentials between day and night air temperatures (e.g., in desert regions), and when there is little or no cloud cover during the daytime, in which case, there is probably not a significant temperature gradient. If highly variable daily temperature swings occur on a 24-h basis, it is generally recommended to only test during morning hours before the sun has excessively heated the concrete slabs at the top (thus causing slab warping).

Recommendation: Limit the agency’s time window for testing flexible pavements to normal daytime working hours. Oftentimes, jointed concrete pavements are an exception to this rule, depending on climatic zone and/or temperature gradients in the slab, etc. Urban freeways are also a potential exception for safety reasons. Finally, do not test when the unbound materials are frozen beneath the pavement or during spring thaw.

RECOMMENDATIONS FOR SEASON OF YEAR FOR MEASUREMENTS AT NETWORK LEVEL

An analysis and review of the FWD data in the LTPP database reveals that testing at virtually any (completely) thawed time of year is acceptable for network-level deflection testing. An example of the LTPP data analysis is shown in table 39.

Table 39. Statistics for flexible pavement IRI as a function of season.

Statistics	All Data	Spring	Summer	Fall	Winter
Accuracy of model	0.73	0.65	0.78	0.77	0.80
Correct prediction rate (percent)	68	56	68	69	77
Error type I (false positive) (percent)	6.6	5.3	2.5	5.1	7.5
TPR (percent)	69	54	63	68	81
TNR (percent)	64	68	88	71	67

Note: Error type I predicts acceptable performance incorrectly, TPR predicts correctly acceptable performance, and TNR predicts correctly not acceptable performance.

In this example and almost all other seasonal examples, there is little important difference between the overall goodness-of-fit and the corresponding values where the data are broken down by season. In table 39, the apparent improvement for some statistical categories during winter testing is due to the fact that only two of the four climatic regions are represented—DNF and WNF. Error type I (false positive), the most serious of the two potential error types, is evidently improved by using summer season data only, which is the time of year that is most likely suitable for field testing and scheduling for most agencies.

For network data collection purposes, deflection testing during the spring thaw period for the DF and WF zones should be avoided because these data tend to cause bias results toward rehabilitation of those pavements that were tested during spring thaw.

Recommendation: Do not limit an agency's seasonal time window for network-level deflection testing except during spring thaw conditions.

APPLICATIONS AND LIMITATIONS

The real issues indicted in the foregoing sections are that depending on location and environmental circumstances, the overall recommendations as to when to conduct FWD test surveys at the network-level may differ significantly. Obviously, limitations will inhibit any potential network testing program to the degree these limitations impose testing restrictions not generally encountered otherwise by agencies that manage roadway networks.

In areas such as Florida and coastal California, winter restrictions are more of an oxymoron than a real test scheduling hindrance, so winter testing can and should take place. Conversely, in Alaska, the testing season is greatly shortened for equally obvious reasons.

Finally, the deciding factor for mainline highways, especially urban freeways, may be traffic control. Accordingly, sometimes testing with the FWD will have to take place during nighttime closure hours—if it can take place at all.

Regard the above suggestions and recommendations as being general in nature, not specific for every region of the United States and Canada that was covered by the extensive LTPP monitoring and testing program, which was started by SHRP in the late 1980s.

CHAPTER 7—PRACTICAL EXAMPLE

INTRODUCTION

This chapter provides a practical example of how to apply the methodology resulting from this research to evaluate FWD load deflection data in network-level applications. At first, three large datasets were considered: the Illinois Tollway, the Maryland State Highway Administration (MDSHA), and Parks Highway in Alaska.

The majority of the Illinois Tollway system consists of composite pavements. Since no reliable model was found during this research for composite pavements due to the shortage of data, the analysis of the Illinois Tollway dataset was jeopardized. The effort to retrieve only sections for rigid and flexible pavements was significant and not efficient.

The Parks Highway in Alaska has a simple and straightforward dataset. The pavements were already managed using a statewide PMS. FWD data were available for use with the appropriate flexible pavement models. The State's treatment decision matrix was based on roughness. However, there were significant limitations on the variety of available treatments. The Parks Highway, which is located between Anchorage and Fairbanks, AK, uses few alternative treatments, most of which consist of mill and fill or a thin overlay. The impact of introducing a decision matrix based on structural condition would have been minimal, since no alternative was available for preventive treatment in part due to the light traffic using the facility.

MDSHA has a pavement management system that is based on ride quality (i.e., IRI). It utilizes PMS software for network analysis, budget optimization, and pre- and post-processing. Deflection data are available at the project level. There are a variety of treatment options covering preventive M&R.

This chapter illustrates how to apply simplified deflection techniques for structural analysis in network-level applications. The example uses the available dataset retrieved from MDSHA's PMS.

REVIEW OF RECOMMENDED APPLICATION

The objective of a pavement design is to provide a structure that will exhibit adequate structural performance throughout its design life. It is expected that the structural condition affects the rate the pavement deteriorates over time. By definition, a given pavement structure has acceptable performance if distress levels do not exceed their threshold values during a period of time (e.g., fatigue cracking not to exceed 25 percent of the total area within the first 15 years of service).

Logistic models describe the probability of an event being acceptable or unacceptable as a function of a predictor variable. Therefore, they can be used to establish a link between performance and structural condition by modeling the probability of acceptable performance using measurements of deflections or parameters (techniques) computed from deflection basins.

The goal of the proposed stochastic approach is to use the probability density function from the logistic model to obtain insightful information about the pavement structural condition required to achieve the desired performance during a desirable (design) period of time. This new PMS-based knowledge can then be used to define strategic treatments (maintenance or rehabilitation) to be used in the PMS optimization process.

A typical logistic model probability function is described in chapter 4 of this report (see figure 25). It describes the likelihood of the pavement section exhibiting acceptable performance of a particular distress as a function of a given deflection parameter, named “predictor variable X.” In this example, the cutoff value was determined from the ROC curve and plotted.

In the stochastic approach, the probability density function is used to determine the thresholds that define structural condition. By definition, the cutoff value in a logistic model determines how to convert the continuous probability prediction as a dichotomous outcome (i.e., predicted probabilities above the threshold are defined as acceptable, while others are defined as unacceptable). In addition to the cutoff threshold, other values can be used to define further details about the structural condition. For example, figure 25 describes a second threshold created at the 0.4 probability level, and it is used to separate sections with fair structural condition from poor ones. (Note that this definition is arbitrary and can be adjusted to better fit an agency’s rehabilitation practices or network characteristics.)

Once thresholds and their respective deflection parameters are identified, a structural decision matrix (also referred to as a structural rehabilitation matrix) can be generated. Table 7 shows an example of structural decision matrix obtained from the probability density function in figure 25.

MDSHA EXAMPLE

MDSHA is responsible for managing approximately 17,000 lane-mi (27,370 lane-km) of roadways (about 11,000 directional-mi (17,710 directional-km) or some 22,000 centerline-mi (35,420 centerline-km)). The budget for the Pavement System Preservation Program is between \$150 million and \$190 million per year, and it covers the maintenance and improvement of MDSHA’s pavement network. The network is divided into three regions: Mountain, Central, and Coastal. Among these, there are seven engineering districts, three rural districts, and four urban districts. The Pavement Management Division is responsible for the network-level data collection, analysis, and budget optimization through the PMS. The outcome of the budget optimization is typically the selection of sections for M&R. The Pavement and Geotechnical Division is responsible for project-level data collection, pavement design, and analysis after candidate projects are identified for M&R. These projects are assigned to the respective districts, and the districts are responsible for construction bids, quality control, and acceptance.

Flexible pavements correspond to 61 percent of MDSHA’s network, rigid pavements correspond to 2 percent of the network, and the remaining 37 percent are composite pavements.

Overview on MDSHA PMS

The MDSHA PMS is constructed on an Oracle® database platform, and it is supported by the Roadcare™ software. Roadcare™ is responsible for data management, inputs, analysis, and outputs.⁽³¹⁾

The performance of MDSHA's pavement network is monitored annually. Each year, pavement ride quality, rutting, and friction conditions are recorded in the outside lane of both directions of travel for the majority of mainline roadways in Maryland. A video record of the pavement surface and right-of-way is also captured every year. This information (with the exception of friction data) is collected at highway speeds using an Automatic Road Analyzer testing device. Friction condition is tested with the pavement friction tester. MDSHA collects IRI, cracking, and friction data on about 95 percent of the entire pavement network.

Data are collected at 0.1-mi (0.161-km) intervals. After data collection, quality control is performed, and data are processed and entered into the MDSHA's PMS, along with traffic data and structure (mainly changes in structure due to annual M&R). The PMS uses homogenous segments based on region, traffic level, pavement type, M&R treatments, and pavement condition. The identification of homogeneous segments is the first step in the analysis process and precludes all budget optimizations. MDSHA uses the FHWA classification based on IRI to identify the pavement condition qualitatively, as described in table 40.

Table 40. MDSHA pavement classification based on IRI values.

Pavement Classification	IRI Values (inches/mi)
Very good	< 60
Good	60–94
Fair	95–170
Mediocre	171–220
Poor	> 220

1 inch = 25.4 mm

1 mi = 1.61 km

MDSHA uses two preventive and four corrective treatment options for its flexible, concrete, and composite pavements. These treatments are currently assigned based on the age, pavement condition, and history of previously applied treatments. The 2-year maintenance and 4-year preventive maintenance strategies are labeled M2 and M4, respectively. The corrective treatments are classified as T5, T8, T12, and T15 based on the expected service life of the treatment—5, 8, 12, and 15 years, respectively.

Expected service life is assigned for every treatment. This is a crucial step in the development of the treatment decision matrix. It defines the years before any treatment can be applied to a specific road section after the M&R has been carried out. In addition, it also defines the years before the same treatment can be applied on the same section. The last caveat is important to prevent the optimization algorithm to be locked in just one treatment over long analysis periods.

The last step in the development of the decision matrix is the assignment of expected improvement in ride quality (i.e., IRI). MDSHA refers to this as “proposed consequences.” The expected improvement in IRI is considered in the year immediately after the treatment is applied. LTPP's *Results of Long-Term Pavement Performance SPS-3 Analysis: Preventive Maintenance of Flexible Pavements* study, along with the analysis of historical data in the MDSHA PMS, provides guidance for defining the proposed consequences.⁽³²⁾

The complete treatment decision matrix is depicted in table 41. The range for the decrease in IRI after treatment reflects the variation expected in ride quality improvement as a function of pavement surface condition prior to treatment. Pavements in worse condition than others are likely to have a higher percentage improvement in IRI.

Costs are associated with each treatment reported in table 41. These costs are calculated based on road class, pavement type, distress level (IRI), and the region/district the section is located. The budget optimization takes these costs into consideration and uses the expected decrease in IRI values as benefit. The expected span between treatments is used to estimate service life and to program future M&R measures.

Table 41. MDSHA PMS treatment decision matrix.

Treatment Type	Treatment Code	Typical Treatment	Expected Span Between Treatments (years)		Decrease in IRI After Treatment (percent)
			Preventive	Corrective	
Preventive	M2	Fog seal	2	2	2
		Crack sealing			
	M4	Slurry seal	2	4	5
		Microsurfacing			
Preventive/ corrective	T5	In-place recycling	4	5	8–14
		Thin overlay			
Corrective	T8	Thin overlay	5	8	16–23
		Mill/level and recycled			
		Asphalt pavement overlay			
	T12	Thin overlay	6	10	17–27
		Mill/level and recycled			
		Asphalt pavement overlay			
	T15	Mill/level and asphalt overlay	7	12	33–55

Sample of MDSHA Network

The MDHSHA PMS does not currently use deflection data for performance analysis or budget optimization. Network-level deflection surveys were not available. The alternative was to select sections that have been identified as targets for rehabilitation projects but where construction has not begun. In these cases, a complete project-level survey is conducted with FWD deflection testing performed at 0.1-mi (0.161-km) intervals.

In total, 50 sections were selected for this example where sufficient data were available, and the average length was 1.8 mi (2.90 km). The total lane-miles only corresponded to around 1 percent of the entire network. Additionally, 10 different districts were represented, and only flexible

pavements were considered. Detailed descriptions of each site are provided in appendix F, including location, road class, thickness, traffic, and deflections. A summary of the sample statistics is provided in table 42 and table 43.

Table 42. Summary statistics of MDSHA sections used in the example.

Statistics	Average	Standard Deviation	Minimum	Maximum
AC thickness (inches)	7.6	3.96	1.0	18.5
Total thickness (inches)	15.8	3.83	10.0	25.5
AADTT (number of vehicles)	1,322.4	1,562.51	12.5	6,373.5
Volume of class 5 (number of vehicles)	439	423	7	1,748
Volume of class 9 (number of vehicles)	425	700	1	2,520

1 inch = 25.4 mm

Table 43. Summary statistics of MDSHA sections used in the example (percent distribution of sections).

Road Class	Distribution (percent)
Rural interstate	10
Urban interstate	6
Rural principal	8
Urban principal	6
Rural collector	72

Incorporation of Structural Analysis on MDSHA PMS

For this example, a new subset of the PMS database was created containing only sections identified in the sample. Since the sample size was only 1 percent of the total lane-miles in the State, the PMS simulation was carried out on 1 percent of the annual cost allocation for MDSHA pavement M&R program. In 2010, this value was \$177 million. Therefore, the budget scenario for this example was assumed to be \$1.7 million per year.

The analysis period was defined as 25 years, which is a typical period of time for an MDSHA optimization and budget study. 2007 was set as the initial year for this analysis, the earliest in which deflection data were available.

The analysis process consisted of performing the typical functional evaluation and budget optimization process, considering the functional decision matrix already in use and based on IRI performance alone. After the selection of treatments was generated, the structural analysis was incorporated as an extra data element. The following steps were taken as part of the incorporation of structural analysis on MDSHA PMS as an example to this project:

1. Prepare the dataset.
2. Define the analysis period and budget constraints.
3. Perform the functional analysis and budget optimization.
4. Compute the structural condition of each section based on the logistic model.
5. Compare the solutions created from the functional analysis with the structural condition.
6. Adjust the prescribed treatments to reflect the structural needs.
7. Rerun the budget optimization to reflect the changes in the prescribed treatments.
8. Evaluate the impact on expected pavement condition and estimated service life due to structural analysis.

Two logistic models were used; one was based on roughness performance and one was based on rutting. These two models are shown in table 21 and figure 30 for roughness and table 22 and figure 34 for rutting. Table 44 describes the structural decision matrix adopted for this example. Each section was evaluated, and the structural condition was assessed based on the model constants shown in table 45.

Table 44. Structural decision matrix based on roughness and rutting performance.

Structural Condition	Probability of Acceptable Performance	
	Roughness	Rutting
Good	> 0.812	> 0.792
Fair	0.812–0.406	0.792–0.396
Poor	< 0.406	< 0.396

The next step is the comparison between the usual solution generated by the functional analysis only and the need for structural improvement. To simplify this comparison, table 45 was created to help identify where there was disagreement between the solution proposed based on functional analysis and the structural need of the pavement. For purposes of this example, table 45 was created based on engineering best judgment and adaptation to MDSHA current treatment options.

Table 45. Adjustment of MDSHA treatment option based on structural analysis.

Treatment Type	MDSHA Treatment Option	Modified Treatment Option		
		Good	Fair	Poor
Preventive	M2	M2	M4	T5
	M4	M4	T5	T5
Preventive/corrective	T5	M4	T5	T8
Corrective	T8	T5	T8	T8
	T12	T8	T12	T12
	T15	T8	T15	T15

Results of the Analysis Without Structural Component

The results of the analysis without a structural component were provided at the end of step 3 mentioned above. The majority of sections were identified as in need of some type of treatment within the 25-year analysis period. Figure 64 illustrates the distribution of sections by prescribed treatment. Only the first treatment for each section in the analysis period was considered. The average year for the first treatment was 2011 (4 years after the initial year).

In total, 32 percent of the sections were prescribed preventive treatment, 36 percent were prescribed corrective treatment, and 32 percent did not require any treatment. Improvements on the network sample were calculated in terms of improvement in service life and ride quality (i.e., a decrease in IRI). The expected increase in interval between treatments averaged 2.4 years. Additionally, the IRI values were expected to decrease by 6.9 percent between the first and second predicted intervention times.

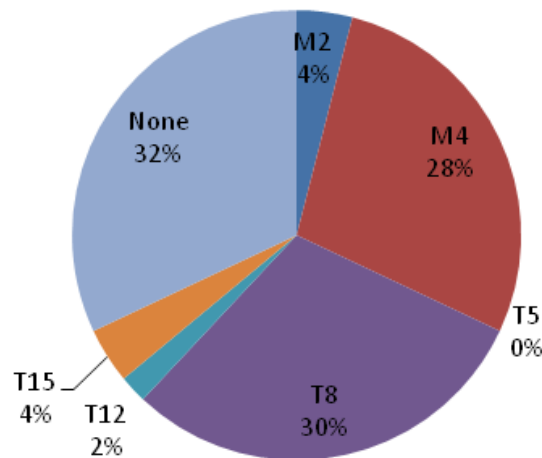


Figure 64. Graph. Distribution of prescribed treatment for the first intervention.

Results of the Simulation With Structural Component

The decision of when to apply a treatment in a pavement section is part of the budget optimization process. In this analysis with a structural component, it was assumed for simplicity that the year the alternative is recommended remained as defined by the previous functional analysis (based on IRI) alone. In other words, the structural analysis did not define or modify

when M&R is planned. Therefore, the new analysis could be carried out without the need to modify the PMS algorithm.

Two logistic structural models were used in this example: roughness and rutting. The models were used to compute the probabilities of acceptable performance based on FWD load deflection parameters. Table 44 was used to qualitatively assess pavement structural condition. Based on this assessment and in conjunction with the prescribed treatment already defined based on the previous functional analysis, table 45 was used to adjust the treatments to incorporate the expected structural needs of each candidate pavement section.

After the conclusion of the analysis, improvements to the network were recomputed to reflect the new selection of treatments. Table 46 combines the results from the optimization with a structural analysis component and the previous results from the optimization without a structural analysis (labeled MDSHA).

The incorporation of the new structural analysis changed the outcome of prescribed treatments in about 60 percent of the sections. The majority of changes happened to sections that initially did not have any prescribed treatment. In these cases, the majority received preventive treatments. The percentage of corrective cases remained the same when the structural analysis was associated with roughness performance. In the cases association with rutting performance, there was a drop in corrective cases. These results agree with the expected outcome. Pavements in MDSHA's network are more likely to fail due to roughness. Rutting is not a major problem in most of the State's highways. The structural analysis reflected this particular characteristic of MDSHA's network.

The new allocation of treatments obtained from the structural analysis provided greater improvement in ride quality. On average, about 10 percent improvement in IRI was expected when the optimization was done with a structural analysis for roughness, compared with 6.9 percent when it was only a functional optimization and 7.4 percent for when it was with structural analysis for rutting.

The interval between treatments also increased. The previous functional analysis had an expected increase of 2.1 years in the period between treatments. The incorporation of a structural analysis in the optimization results expanded this period by some 60 percent to a total of 3.4 years (structural analysis based on roughness) and by 33.7 percent to a total of 2.9 years (structural analysis based on rutting).

Table 46. Results from the PMS optimization considering the structural analysis.

Results	MDSHA	Optimization with Structural Analysis	
		Roughness	Rutting
Preventive cases (percent)	32.0	64.0	78.0
Corrective cases (percent)	36.0	36.0	14.0
Solutions modified by structural analysis (percent)	N/A	60.0	68.0
Improvement in IRI (percent)	6.9	10.0	7.4
Expected average increase in interval between treatments (years)	2.1	3.4	2.9
Improvement in expected average increase in interval between treatments, compared to MDSHA (percent)	N/A	60.6	33.7

N/A = not available.

Cost Implications

The incorporation of structural analysis on the PMS optimization had an impact on the budget. Since the objective was not to perform a comprehensive budget analysis, some assumptions were made to simplify the process shown in this example.

There was no change in year allocated for treatments. Optimization prior to the structural analysis provided the year for any given treatment. In other words, the analysis considering the structural condition did not change the year associated with the first prescribed treatment in the analysis period.

The cost of treating sections without an assigned year was evenly spread across the 25-year analysis period. This reflects directly on sections that did not have any treatment assigned by the functional analysis, most likely due to budget constraints and cost/benefit analysis. However, during the structural analysis, some of these sections needed structural improvement. Without an assigned year, the extra cost of maintaining these sections was evenly distributed over the analysis period.

The cost analysis only reflected the first treatment prescribed to the section during the analysis period. Preventive treatments are common practice at MDSHA. Its PMS reflects this characteristic by incorporating preventive treatments to extend the service life of the pavement. Subsequent maintenance alternatives (M2 and M4 in table 41) were often predicted throughout the analysis period. The costs of subsequent maintenance efforts were not incorporated in this example's cost analysis. The monetary values were not correct by any rate during the analysis period. Figure 65 provides an overview of cost allocation for the first treatment throughout the analysis period.

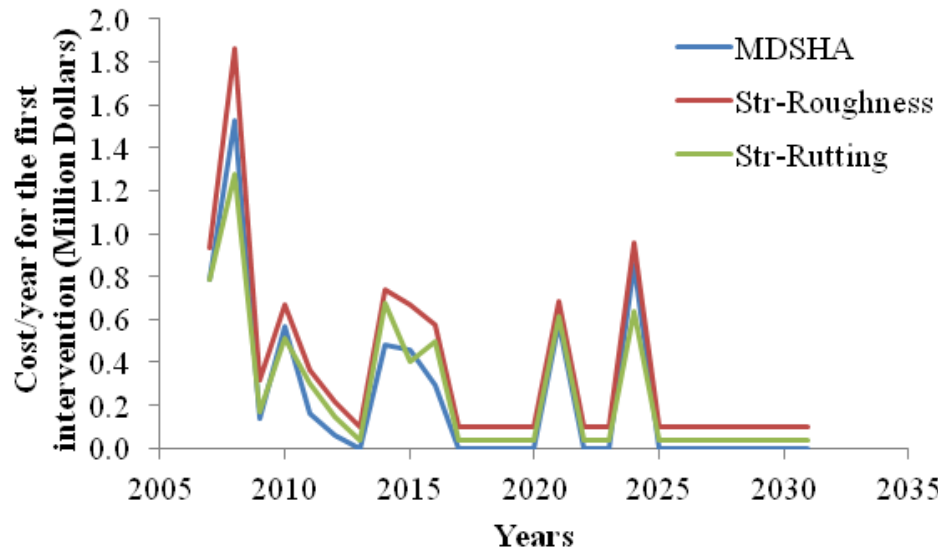


Figure 65. Graph. Cost distribution over the analysis period.

Table 47 provides a summary of differences observed in the budget. The total cost of all first interventions was \$5.9 million for the optimization without structural analysis. The incorporation of structural analysis increased the budget by 59 percent to a total of \$9.4 million (roughness model) and by 10.6 percent to a total of \$6.5 million (rutting model). While these numbers may seem surprising, there is a considerable amount of new mileage being treated. Only 53.6 mi (86.3 kg) from the original 88.7 mi (142.8 kg) in the sample network were prescribed treatment when the current MDSHA PMS was used. Some treatment was prescribed to all sections when the structural model based on roughness was incorporated and to 79.5 mi (127.9 km) if the model was based on rutting.

Table 47. Impact on costs from the PMS optimization considering the structural analysis.

Results	MDSHA	Optimization with Structural Analysis	
		Roughness	Rutting
Total cost (\$ in millions)	5.9	9.4	6.5
Cost difference (percent)	69.5	59.4	10.6
Mileage treated	53.6	88.7	79.5
Cost/mile (\$ in thousands)	110.4	106.3	82.3

The benefit of including the structural component in the PMS can be observed when cost per mile is compared between all three alternatives (see table 47). The cost/mile for the MDSHA PMS was \$110,000/1 mi (1.61 km). After incorporating the structural component, the cost/mile reduced by 4 percent to \$106,000/1 mi (1.61 km) (roughness model) and 25 percent to \$82,000/1 mi (1.61 km) (rutting model). The association of these numbers with the improvements in service life and ride quality and the overall impact of including the structural analysis in the PMS is encouraging.

CONCLUSIONS

The incorporation of structural analysis provided a new dimension in the prediction of performance and prescribed treatments to mitigate ride quality and structural deterioration of the pavement network. The process is simple and can be easily incorporated in existing PMS. An algorithm can be written to include the structural analysis as part of the optimization routine, or it can be done externally, like in the example based on the sample from MDSHA PMS.

Two structural models were tested. In this particular example, the scenario in which the structural model was based on roughness was the critical example. Roughness is the most common performance indicator driving the need for M&R in MDSHA's network.

The incorporation of the new structural analysis changed the outcome of prescribed treatments on about 60 percent of the sections. Sections that initially did not have any prescribed treatment received preventive treatments. Preventive maintenance is key to an effective level of service in any pavement network. The identification of segments where early structural failure is likely to happen helps mitigate them through early preventive maintenance. As a consequence, more M&R can be done with the same budget level and the backlog of pavement repairs can be reduced.

The new allocation of treatments obtained from the structural analysis provided greater improvement in ride quality. On average, about 10 percent improvement in IRI was expected when the optimization was done with a structural analysis for roughness, compared with 6.9 percent when it was only a functional optimization.

The interval between treatments also increased. The previous functional analysis had an expected increase of 2.1 years in the period between treatments. The incorporation of a structural analysis in the optimization results expanded this period by some 60 percent to a total of 3.4 years (structural analysis based on roughness) and by 33.7 percent to a total of 2.9 years (structural analysis based on rutting).

There was a clear impact on budget allocation, which could be better adjusted if the optimization process was repeated with the new treatments. However, even without a new optimization, the benefits outlast the costs. There was a nominal increase in cost of 50 percent, considering the critical scenario. At the same time, there was a significant change in the improvements expected from the new M&R scenario based on the structural analysis. A 44 percent increase in expected ride quality performance and a 60 percent increase are expected in interval between treatments. Overall, the consideration of structural condition in the network-level analysis improved performance, minimized maintenance, and reduced the M&R costs per mile.

CHAPTER 8—CONCLUSIONS AND RECOMMENDATIONS

The primary objectives of this study were to identify/develop, verify, and recommend simplified deflection-based analytical techniques suitable for rapid automated screening of pavement structural capacity for inclusion in a network-level analysis, such as PMS. The LTPP database was the primary source of information for this study.⁽¹⁾ The results can be readily implemented in national, State, and local municipality systems alike.

An additional objective was to provide recommendations for data collection procedures that will maximize testing productivity and minimize risk while still providing adequate information for use in a typical PMS. Test point spacings and frequency of data collection were the two primary parameters of interest.

A handful of successful techniques for use in network-level PMS applications were identified through the literature search. A few highway agencies have been using deflections as part of their network condition assessment. Among these, Texas, Virginia, and South African approaches were selected for further investigation. Several techniques commonly used at the project-level were investigated, as well. Combining all sources available, a list of potential applicable techniques was created. These deflection techniques formed the basis for the analyses carried out in this project.

SIMPLIFIED TECHNIQUES FOR EVALUATION AND INTERPRETATION OF PAVEMENT DEFLECTIONS FOR NETWORK-LEVEL ANALYSIS

Deflection data analysis provides qualitative and quantitative assessment of the structural integrity and bearing capacity of a pavement. Pavements with poor structural quality are more likely to develop distresses prematurely. It is commonly expected that the rate of deterioration increases as the structural condition worsens. Identifying pavements with poor structural condition is important to prevent early and rapid development of load-related distresses.

Based on the above premises, a probabilistic approach was developed to determine the likelihood of premature failure using simplified and easy-to-apply load deflection techniques. Premature failure was defined by the presence of excessive distress occurring prior to the end of the design life of the pavement section (i.e., levels of distress higher than a design threshold). This was achieved by adopting binary logistic models that utilized deflection techniques derived from the FWD deflection basin coupled with various site-specific parameters.

The probability density function was used to determine the threshold levels that define structural condition. This was accomplished by determining the cutoff value in the logistic model, which determines how to convert a continuous probability prediction to a dichotomous outcome (i.e., predicted probabilities above the threshold were defined as acceptable while others were defined as not acceptable). This process was shown to be simple and straightforward. A structural decision matrix can be generated and incorporated as an integral part of an agency's PMS optimization tools.

Several models were created based on pavement type and critical performance measures. For flexible pavements, the models created were based on roughness, rutting, and fatigue cracking. For rigid pavements, the models were based on roughness, faulting, and transverse slab cracking.

The advantages of the stochastic approach to evaluate the structural condition of the pavement for network-level analysis can be summarized as follows:

- It provides a direct link to pavement performance by estimating the likelihood of the development of load-related distresses in the early stages of the pavement's service life. The intent was not to have a regression-based predictive model based on deflection data, but rather a simplified procedure to identify critical sections with a high (stochastic) likelihood of developing structural distresses prematurely.
- The probability density function is based on qualitative performance measures—acceptable and not acceptable.
- Rating criteria can be created in the same a manner equivalent to the functional decision matrix. Different tiers of structural quality can be defined based on deflection thresholds and the likelihood of acceptable performance. The structural decision matrix can then follow rating criteria similar to the functional decision matrix, which facilitates the implementation in existing PMS algorithms.
- The stochastic model is site-specific (i.e., additional variables may be incorporated that reflect site characteristics such as traffic, pavement structure, and climatic conditions).
- Different structural decision matrices can be defined based on different types of distresses. Therefore, the final evaluation can be made based on the most critical or most typical distress(es) observed in the network.
- The calculations are simple and do not require an interactive, labor-intense process. Therefore, it can be automated and incorporated in virtually any PMS in which deflection data are available.
- Deflection data obtained from project-level analyses or quality control after construction can also be used as an agency's initial input data.
- The probabilistic models can be locally calibrated to reflect an agency's own network characteristics (e.g., typical surface distresses observed, the interval between M&R projects, and the threshold of acceptable limits for distresses). In addition, the models can be recalibrated every time a new FWD testing campaign is completed and new load deflection data become available.

The importance of local calibration is underscored. Four examples were provided, which showed the potential improvements in accuracy and predictability that can be obtained if local data are used to calibrate the probabilistic models. The examples were simple exercises retrieved based on subsets of the LTPP database. Nevertheless, it was clear that local calibration could ultimately

enhance the accuracy and quality of predictions, which would significantly benefit analyses at the network level, especially for the creation and allocation of M&R resources.

OPTIMUM DEFLECTION TEST SPACINGS AND FREQUENCY FOR PMS APPLICATIONS

Test Spacing

The approach was based on an evaluation of errors as a function of different test spacings in a variety of section lengths. The error represents the expected difference between the data sample and the idealized true value of the population, which is represented in this case by the average deflection value of a homogeneous road segment. It was assumed that the true value of the population was the average deflection of a homogenous segment where the spacing between deflection points was at the project-level (i.e., 0.1 mi (0.161 km)). Monte Carlo simulations were used to model the error function.

In addition to modeling the predicted (average) error, the results from the Monte Carlo simulation were also used to model a probabilistic component to the calculation of the expected error. This component was easily related to the length of the section and the expected error for a given reliability level. The reliability component is an important characteristic of this approach, as it fits well with current design practices such as the MEPDG.⁽²⁷⁾ Tables were created that relate reliability level and section length with expected error, which can be used to define the optimum test spacings for a given section in a network-level analysis.

Ultimately, it is an agency's budget that controls the quantity of deflection data that can be collected in any given year. Objective recommendations and guidelines were provided in this report to determine optimum test spacings given the level of accuracy and reliability desired.

Frequency

The recommended frequency of FWD data collection on pavements is dependent on the overall "rate of change" of structural conditions over time. The analysis of the deflections available in the LTPP database provided the following conclusions for flexible pavements:

- The annual rate of change of pavement deflections showed little correlation with traffic levels.
- The annual rate of change of pavement deflections showed little correlation to subgrade type.
- The annual rate of change of pavement deflections showed some correlation to AC thickness—lower thicknesses produced higher rates of change, as expected.
- Dry climates seemed to produce larger annual changes in pavement deflections, which is counterintuitive.

- Once temperature influences were removed, the rate of change of deflection measurements was relatively small for most pavement sections contained in the LTPP database.

Based on the analysis of these pavement sections, 5 years between FWD testing is recommended at the network-level for flexible pavements.

A similar analysis was conducted for rigid pavements. As expected, the variations in deflections measured at the center of the slab were significantly smaller than observed for flexible pavements. The recommendation is for a frequency of 10 years maximum between network-level testing.

Time of Day and Season of Year

The vast majority of deflection testing—whether at the network or project level—is carried out during normal daytime (or nighttime in high trafficked areas) work hours. In fact, any agency that may want to limit network-level testing to anything more or less than their normal working hours is unlikely to end up using deflection testing in their PMS at all. Similarly, with seasonal testing, it is generally believed that gathering deflection data should occur when climatic conditions allow it (i.e., pavement temperature is above freezing), except during spring thaw conditions, which are important to avoid since they are not representative of the rest of the year.

It is also important to consider the issue of P&MT. In reality, for most medium to high traffic roads, FWD testing must be carried out to avoid periods of high traffic flow, which often occurs during the morning rush hour (6 to 9 a.m.) and afternoon rush hour (3 to 5 p.m.).

Regarding the adjustment of deflections based on temperature, it is recommended that no adjustment is needed if the deflection data are going to be used at the network level.

Depending on the location and environmental circumstances, the overall recommendations as to when to conduct FWD test surveys at the network level may differ significantly. Obviously, limitations will inhibit any potential network testing program to the degree these limitations impose testing restrictions not generally encountered otherwise by agencies that manage roadway networks.

EXAMPLE OF INCORPORATING STRUCTURAL ANALYSIS ON PMS

The incorporation of structural analysis provided a new dimension in the prediction of pavement performance and prescribed treatments to mitigate ride quality and structural deterioration of the overall pavement network. This process is relatively simple and can be easily incorporated in existing PMS. Algorithms can be written to include the structural analysis as part of the optimization routine. It was also shown that this process can be effectively done externally.

The incorporation of the new structural analysis changed the outcome of prescribed treatments on about 60 percent of the sections. Sections that initially did not have any prescribed treatment received preventive treatments. Preventive maintenance is key to an effective level of service in any pavement network. The identification of segments where early structural failure is likely to happen helps mitigate them through early preventive maintenance. As a consequence, more

M&R can be done with the same budget level, and the backlog of pavement repairs can be reduced.

The new allocation of treatments obtained from the structural analysis provided greater improvement in ride quality. On average, about 10 percent improvement in IRI was expected when the optimization was done with a structural analysis for roughness compared to 6.9 percent when it was only a functional optimization.

The interval between treatments also increased. The previous functional analysis had an expected increase of 2.1 years in the period between treatments. The incorporation of a structural analysis in the optimization results expanded this period by 60 percent to a total of 3.4 years (structural analysis based on roughness) and by 33.7 percent to a total of 2.9 years (structural analysis based on rutting).

The incorporation of structural analysis in the example presented in this report had a clear impact on pavement preventive M&R program budget allocation, with a nominal increase in M&R cost of 50 percent, considering the critical scenario. However, there was a reduction in cost per mile of about 4 percent, indicating that more could be done with the same allocated budget. At the same time, there was a significant change in the improvements expected from the new M&R scenario based on the structural analysis—a 44 percent increase in expected ride quality and a 60 percent increase in the interval between treatments.

Overall, the consideration of structural condition in the network-level analysis improved performance, minimized maintenance, and reduced M&R costs per mile. The pay-off in lowered agency costs of pavement M&R easily surpasses the cost of adding FWD load deflection testing to the agency.

APPENDIX A

Table 48. Useful practices for FWD use in network-level analyses.

Agency and Publication	Use of Deflection Data in PMS	FWD Test Point Spacing	FWD Test Frequency	FWD Sensor Positions	Limiting Specifics on PMS Use	Applicability of Current Analysis Approach in Streamlined and Simple PMS	Would Unmodified Result be Useful Relating Observed Rate of Deterioration to Deflection?	Possibility of this Approach Combined with Others	Summary
Caltrans; <i>Caltrans Test Method No. 356</i> ⁽³⁾	No	N/A	N/A	N/A	N/A	Yes	No	Probably	Uses center deflection only plus existing AC or AC + PCC layer thickness. Since it only applies to the DNF regions of California, the criteria would need shifting, and the time of year or day of testing would have to be better defined. Although it is generally used for rehabilitation design, it could be tiered into three or more categories (e.g., immediate project-level design, cosmetic or pavement preservation improvements, and no rehab or cosmetic improvements at this time).
FHWA; <i>Review of the LTPP Backcalculation Results</i> ⁽⁴⁾	No	N/A	N/A	N/A	N/A	Yes	No	No	If the subgrade modulus or indicator is regressed against various performance indicators, the Hogg model can be regressed at the same time. Furthermore, the entire LTPP database contains all available Hogg model subgrade stiffness values. While it is possible that surface course stiffness can also be derived using a related approach reported to FHWA, this is probably not worth the effort (subject to review by other team members).

NCHRP; “Assessing Pavement Layer Condition Using Deflection Data” ⁽⁵⁾	No; feasibility study only	Probably not studied	Probably not studied	SHRP positions, generally	No limits pavement types were studied using LTPP database	Yes	Yes	Probably	This project used easy-to-obtain deflection basin parameters and related these parameters to observed pavement distresses. As far as performance indicators are concerned, this study fits well into the current study. More information on the specifics should be obtained from the final report.
Swedish Road and Transport; <i>Strategic Highway Research Program and Traffic Safety on Two Continents</i> ⁽³³⁾	No; feasibility study only	N/A	N/A	N/A	N/A	No	No	No	The method uses a kind of forward-calculation using modulus matrices similar to how the MODULUS program works. It was only proposed for a single province in Sweden, and it is not practical or easy to understand for a typical transportation department. Mechanistic concepts are employed, which are unlikely to be met with widespread success in the United States or Canada. AC pavements only.
South Carolina Department of Transportation; <i>Feasibility of Including Structural Adequacy Index as Indicator of Overall Pavement Quality in the SCDOT Pavement Management System</i> ⁽³⁴⁾	No	N/A	N/A	N/A	N/A	No	No	No	Conclusions were that FWD data may be useful for flexible pavements only; recommended pilot study for this purpose. Not useful for the present study.

FHWA; <i>Temperature Predictions and Adjustment Factors for Asphalt Pavement</i> (FHWA-RD-98-085) ⁽⁶⁾	No	N/A	N/A	N/A	N/A	Yes	No	Yes	The adjustment for asphalt pavements for temperature-at-depth and center deflection adjustments for pavement temperature may be used to assist in the present study.
FHWA; <i>Backcalculation of Layer Moduli of LTPP General Pavement Study (GPS) Sites</i> , FHWA-RD-97-086 ⁽³⁵⁾	No	N/A	N/A	N/A	N/A	No	No	No	Not useful for present study (back-calculation only).
Kansas Department of Transportation; “Network-Level Pavement Deflection Testing and Structural Evaluation” ⁽⁷⁾	No; study only based on 3 years of data from one district	Minimum of three tests per mile; five tests is preferred.	One-third of network per year; however, one-fifth of network may be adequate	Unknown; probably unimportant	AC only	Yes	Yes	Probably	Data were used from one Kansas district on AC surfaces only (non-interstate). For the technology and information available at the time, it used a similar approach to the current study. The study was based on the <i>1993 AASHTO Guide for Design of Pavement Structures</i> . FWD, especially center deflection, added considerably to predictive capability of method used. ⁽⁸⁾ Based on the concept of PSE; PSE is twice as important as a pavement performance predictor than any other observable parameter. Bayesian statistical approaches were recommended; however, Kansas did not implement it on a statewide basis thereafter.

Taiwan; “Evaluating the Structural Strength of Flexible Pavements in Taiwan Using the Falling Weight Deflectometer” ⁽²¹⁾	No	N/A	N/A	N/A	N/A	Yes	No	Probably as it uses deflection- based parameters to a structural index	The report elaborates on using a combination of deflection-based parameters into a structural index. The index was empirically developed and relates to poor or good pavement condition assessed by experienced engineers and surveys. The method employed is not clearly described, but it involves binary assessment (0 and 1) of pavement conditions. This assessment is then related to the structural index through a linear equation. The binary analysis is similar in concept to what the research team is proposing using the probabilistic model.
Independent study in the United Kingdom; “Assessing Variability of In Situ Pavement Material Stiffness Moduli” ⁽³⁶⁾	No	N/A	N/A	N/A	N/A	N/A	N/A	N/A	The report discusses variability, and conclusions are made regarding spacing of FWD testing.
Independent study in Minnesota; <i>Spatial Variability of Falling Weight Deflectometer Data: A Geostatistical Analysis</i> ⁽²⁹⁾	No	N/A	N/A	N/A	N/A	Yes	No	Probably	This report discusses variability in FWD measurements using the geostatistical concept. Geostatistics are used when a continuous measure is sampled at discrete points in space, like deflections. They use a variogram to assess the variance of measurements and infer the optimum spacing that will results in maximum coverage of pavement sections with different structural behavior. This approach is similar to what the research team is proposing for phase II.

Netherlands; <i>Application of FWD Measurements at the Network Level</i> ⁽³⁷⁾	No	N/A	N/A	N/A	N/A	Possibly	No	Probably	The report describes development of a structural adequacy indicator based on SCI ₆₀₀ in non-trafficked area, and structural distress indicator based on SCI ₆₀₀ in trafficked and non-trafficked area and cracking.
United Kingdom; <i>Use of Deflections at Network Level in England for Programming and Other Purposes</i> ⁽¹³⁾	Yes	N/A; used deflectograph, complemented by FWD	3–5 years	N/A	Flexible pavements only	No	N/A	N/A	Used TRRL equations to calculate residual life and strengthening requirements based on deflection. The conclusion was that deflection does not increase with time and, in some cases, decreases due to increases in pavement materials stiffness. This approach was used in United Kingdom until 2000.
Department of Main Roads, Queensland, Australia; <i>Reliability of Optimal Intervals for Pavement Strength Data Collection at the Network Level</i> ⁽³⁸⁾	No; feasibility study only	200–1,000 m, 1,000 m selected	N/A	Unknown; probably unimportant	Flexible pavements only, wet and non-reactive soil	No	No	No	Budget estimates were developed for different FWD spacings. SNs were calculated from deflections. The information obtained is not useful in the present project.
Department of Main Roads, Queensland, Australia <i>A Probability-Based Analysis for Identifying Pavement Deflection Test Intervals for Road Data Collection</i> ⁽³⁹⁾	No; feasibility study only	200–1,000 m, 1,000 m selected	N/A	Unknown; probably unimportant	Flexible pavements only, wet and non-reactive soil	Possibly	No	Probably	Kolmogorov-Smirnov probability was used based on goodness-of-fit test to identify optimal interval for pavement deflection data collection. Based on limited amount of data on a specific pavement type (surface treated pavement with granular base) and subgrade. Not applicable to present project.

Hong Kong; “Pavement Management— Development of a Pilot PMS” ⁽⁴⁰⁾	Pilot project	50 m	N/A	N/A	N/A	No	No	No	Only the abstract was available, and it provided little useful information.
Europe; <i>The Way Forward for Pavement Performance Indicators Across Europe, Final Report—COST Action 354 Performance Indicators for Road Pavements</i> ⁽⁴¹⁾	N/A. European project that collected data from different countries/ agencies	N/A	N/A	N/A	N/A	Possibly	No	Yes	The proposed approach uses residual life or SCI_{300} for calculation of bearing capacity performance index. There are no details how remaining life is calculated and that part is probably not useful for current project. The use of parameters of deflection basin (like SCI_{300}) can be considered in present project.
Europe; <i>Use of Falling Weight Deflectometers in Pavement Evaluation</i> ⁽⁴²⁾	Yes	200–500 m	3–5 years	0, 300, 600, 900, 1,200, and 1,500 mm for $d_0 > 1.0$ mm; 0, 300, 600, 900, 1,500, and 2,100 mm for $d_0 < 0.50$ mm	Not specified	Possibly	No	Yes	The proposed approach uses central deflection or SCI (eventually SN calculated from deflections) at the first two levels. At the third level, it proposes the use of back- calculation, which is not feasible for the present project.
Australia; <i>Comparison of Project-Level and Network-Level Pavement Strength Assessment</i> ⁽⁴³⁾	Yes, some members of Austroads	N/A	N/A	0, 900, and 1,500 mm	Flexible and semi-rigid pavements	Possibly	No	Yes	Uses adjusted SN (SNP) as an indicator for pavement bearing capacity. SNP is calculated based on d_0 , d_{900} , and d_{1500} .
United Kingdom; <i>Structural Assessment of the English Strategic Road Network— Latest Developments</i> ⁽¹⁶⁾	Yes, but rolling deflectometer only.	N/A	N/A	N/A	N/A	No	No	No	The report discusses future use of traffic speed deflectometer instead of deflectometer or FWD at the network level. A modified BELLS equation was used for pavement temperature estimate based on air temperatures. Not useful for present project.

AkDOT; <i>Modeling Flexible Pavement Response and Performance</i> ⁽⁹⁾	Yes	0.1 mi	After repaving	SHRP positions	No limits	Possibly, for "standardized" pavement structures	No	Yes	Deflections are converted to layer moduli, which are then used to obtain stress/strain values under a standard ESAL. Transfer functions relate stress/strain to cracking in bound layers and permanent deformation in unbound layers.
TxDOT; <i>Incorporating a Structural Strength Index into the Texas Pavement Evaluation System</i> ⁽¹⁰⁾	Yes, but optional by district	0.5 mi	Recommended one per year	1 ft	Flexible pavements less than 5.5 inches AC thickness	Yes	Yes	Yes	SSI varies from zero (weak) to 100 (strong). Based on normalized basin parameters such as outer deflections, SCI, and center deflection under a 9,000 lb (4,086 kg) load. Can characterize subgrades and pavement structure independently in terms of relative stiffness. The system is based on statistical evaluation of deflections statewide.
TxDOT; "Development of Structural Condition Index to Support Pavement Maintenance and Rehabilitation Decisions at Network Level" ⁽¹⁷⁾	Yes	0.25 mi	N/A	1 ft	Flexible pavements	Yes	Yes	Yes	SN_{eff} and M_r are calculated using deflection parameters and then compared to the structural number required (SN_{req}) using traffic data. Structural condition index (SCI) is the ratio of SN_{eff} and SN_{req} . Novel approach uses simplifications arrive at SN_{eff} directly from deflections.
TxDOT; <i>Development of a New Methodology for Characterizing Pavement Structural Condition for Network-Level Applications</i> ⁽¹⁸⁾	Yes	0.25 mi	N/A	1 ft	Flexible pavements	Yes	Yes	Yes	SN_{eff} and M_r are calculated using deflection parameters, then compared to SN_{req} using traffic data. SCI is the ratio of SN_{eff} and SN_{req} . Novel approach uses simplifications to arrive at SN_{eff} directly from deflections.

TxDOT; <i>Network-Level Deflection Data Collection for Rigid Pavement</i> ⁽¹¹⁾	Yes	0.5 mi	N/A	1 ft	Rigid Pavements	N/A	N/A	N/A	From an analytical standpoint, the report mostly provides recommendations regarding field test procedures. It refers to an earlier document regarding maximum allowable deflections for rigid pavement network testing. ⁽¹¹⁾
VDOT; <i>Network-Level Pavement Evaluation of Virginia's Interstate System Using the Falling Weight Deflectometer</i> ⁽¹²⁾	Yes	0.2 mi	4–5 year cycle	SHRP positions	No	Yes	Yes	Yes	Flexible pavements were analyzed by calculating the subgrade resilient modulus, the effective pavement modulus, and the effective SN. Rigid and composite pavements were analyzed by calculating the area under the deflection basin and the static modulus of subgrade reaction.
United States; <i>Modern Pavement Management</i> ⁽⁴⁴⁾	No; propose method only	Unspecified	Unspecified	Uses center def only	Flexible pavements	Yes	Yes	Yes	Uses traffic loading info to establish a maximum tolerable Benkelman beam deflection. Not useful for purposes at-hand.
South Africa; “Benchmarking the Structural Condition of Flexible Pavements with Deflection Bowl Parameters” ⁽¹⁴⁾	Yes	0.2 km	N/A	300 mm typical	Flexible only	Yes	Yes	Yes	Pavement is divided into three zones based on depth. The report uses basin parameters to characterize base, mid-depth, and subgrade properties as sound, warning, or severe.

N/A = Not available.

1 mi = 1.61 km

1 inch = 25.4 mm

1 ft = 0.305 m

1 lb = 0.454 kg

APPENDIX B

PRE-SCREENING OF DEFLECTION PARAMETERS FOR FLEXIBLE PAVEMENTS

Table 49. Pre-screening of deflection variables for roughness-based logistic model for flexible pavements.

Variable	Pearson R ²	Sig (2-tailed)	Selected Parameter for Further Analysis (Y/N)
CI_6 (μm)	-0.178370162	4.29226E-06	Y
D_4 (μm)	-0.167037282	1.70543E-05	Y
D_3 (μm)	-0.164112365	2.40023E-05	Y
D_5 (μm)	-0.16348482	2.58087E-05	Y
I_3 (1/μm)	0.157423073	5.13086E-05	Y
I_4 (1/μm)	0.156412322	5.73986E-05	Y
CI_5 (μm)	-0.155825464	6.12415E-05	Y
D_2 (μm)	-0.1543182	7.22556E-05	Y
I_2 (1/μm)	0.153150944	8.20426E-05	Y
S_7 adj (μm)	-0.145537369	0.000183728	Y
I_1 (1/μm)	0.145204065	0.000190161	Y
Hogg (MPa)	0.144599721	0.000202367	Y
D_6 (μm)	-0.141494246	0.000277534	Y
I_5 (1/μm)	0.141103268	0.000288662	Y
CI_4 (μm)	-0.140740184	0.000299369	Y
D_1 (μm)	-0.13426463	0.000564927	Y
S_7 (μm)	-0.128831936	0.000942315	Y
CI_3 (μm)	-0.116143945	0.002890483	Y
S_6 (μm)	-0.115692158	0.003002481	Y
TA_7	-0.11326404	0.00367494	Y
F_6	-0.112768646	0.003827883	Y
RA_7	-0.1106046	0.004565907	Y
S_5 (μm)	-0.103761014	0.007821201	Y
CI_2 (μm)	-0.096945272	0.012986893	Y
I_6 (1/μm)	0.095691166	0.014212626	Y
S_4 (μm)	-0.094183161	0.015820468	Y
RA_2	0.091226217	0.0194418	Y
TA_3	0.089415962	0.021998853	Y
RA_3	0.086226561	0.027217802	Y
F_5	-0.082867329	0.033834195	Y
D_7 (μm)	-0.07998036	0.040572597	Y
S_3 (μm)	-0.07923162	0.04249503	Y
TA_6	-0.078396572	0.044729169	Y
TA_2	0.078323562	0.04492912	Y
RA_6	-0.073234091	0.060841102	N

CI_1 (μm)	-0.066884912	0.086944662	N
S_2 (μm)	-0.066884912	0.086944662	N
RoC	0.063457987	0.104406829	N
F_4	-0.056337502	0.149489485	N
ELMOD E_sg (MPa)	0.052969563	0.175402664	N
F_3	-0.046275974	0.236564727	N
F_1 adj	-0.040754908	0.297283156	N
TA_5	-0.040536443	0.299882421	N
RA_5	-0.035445108	0.364728857	N
D_0 adj (μm)	-0.032754064	0.402290133	N
RA_1	0.029409516	0.452064746	N
TA_1	0.025467297	0.514954392	N
S_6 adj (μm)	-0.021204611	0.587730186	N
S_4 adj (μm)	0.019039547	0.626425273	N
D_8 (μm)	0.018874369	0.629421864	N
S_3 adj (μm)	0.018313619	0.639639986	N
D_9 (μm)	0.017910311	0.647031718	N
TA_4	-0.017904864	0.64713179	N
I_7 (1/ μm)	0.015566382	0.690661398	N
TA_1 adj	0.014938567	0.702531384	N
RA_4	-0.01483872	0.704425947	N
F_2	0.014184956	0.716875694	N
S_5 adj (μm)	0.007559144	0.846769384	N
SN_{eff} adj	0.007200049	0.853964888	N
SN_{eff}	0.00667353	0.864536983	N
CI_1 adj (μm)	0.005064275	0.896991944	N
S_2 adj (μm)	0.005064275	0.896991944	N

Note: Variables without units are dimensionless.

1 μm = 0.039 mil

1 MPa = 145.03 psi

1 1/ μm = 25.4 1/mil

Table 50. Pre-screening of deflection variables for rutting-based logistic model for flexible pavements.

Variable	Pearson R²	Sig (2-tailed)	Selected Parameter for Further Analysis (Y/N)
S_7 adj (μm)	-0.167153505	5.79988E-05	Y
S_4 (μm)	-0.159500041	0.000125945	Y
S_5 (μm)	-0.158999373	0.00013234	Y
D_1 (μm)	-0.158966299	0.000132772	Y
S_7 (μm)	-0.157046194	0.000160318	Y
S_6 (μm)	-0.155896287	0.000179293	Y
S_3 (μm)	-0.154475825	0.000205643	Y
CI_2 (μm)	-0.154290947	0.000209328	Y
CI_1 (μm)	-0.152277305	0.000253673	Y
S_2 (μm)	-0.152277305	0.000253673	Y
CI_3 (μm)	-0.151222309	0.000280276	Y
D_2 (μm)	-0.150224418	0.000307818	Y
D_0 adj (μm)	-0.146393262	0.000438791	Y
S_6 adj (μm)	-0.142390152	0.000629805	Y
D_3 (μm)	-0.138246877	0.000906671	Y
I_2 (1/ μm)	0.13559866	0.001138587	Y
I_1 (1/ μm)	0.134151486	0.001287334	Y
Hogg (MPa)	0.134129037	0.001289776	Y
I_3 (1/ μm)	0.131225181	0.001644168	Y
CI_4 (μm)	-0.128016379	0.002138211	Y
S_5 adj (μm)	-0.119820535	0.004075148	Y
I_4 (1/ μm)	0.118144701	0.004628285	Y
CI_1 adj (μm)	-0.114405717	0.006113999	Y
S_2 adj (μm)	-0.114405717	0.006113999	Y
F_1 adj	-0.112114422	0.007223881	Y
TA_5	-0.110044615	0.008378028	Y
RA_5	-0.10896261	0.009044589	Y
D_4 (μm)	-0.108718381	0.009201425	Y
I_5 (1/ μm)	0.107963358	0.009701696	Y
F_4	-0.107833906	0.009789857	Y
TA_4	-0.10680269	0.010517957	Y
F_3	-0.106526151	0.010721206	Y
RA_4	-0.106305726	0.0108857	Y
TA_2	0.102916715	0.013711708	Y
S_4 adj (μm)	-0.102089477	0.014492741	Y
RA_2	0.101108758	0.015469154	Y
S_3 adj (μm)	-0.099499097	0.017197161	Y
RA_6	-0.095460674	0.022294469	Y
RoC	0.094785846	0.023263186	Y

TA_6	-0.093565581	0.025107621	Y
CI_5 (μm)	-0.09292169	0.026130799	Y
I_6 ($1/\mu\text{m}$)	0.091444486	0.028614837	Y
D_5 (μm)	-0.090683049	0.029972663	Y
RA_1	0.08641406	0.038651129	Y
TA_1	0.086062505	0.039452319	Y
I_7 ($1/\mu\text{m}$)	0.078829119	0.059324557	N
F_5	-0.077055931	0.065294931	N
F_2	-0.076739951	0.066409057	N
CI_6 (μm)	-0.075871511	0.069551778	N
D_6 (μm)	-0.073512315	0.078708057	N
SN_{eff}	0.061135443	0.143851844	N
$SN_{eff\ adj}$	0.061050224	0.144412359	N
D_7	-0.058430659	0.162468174	N
TA_3	0.040223503	0.336485173	N
Elmod (MPa)	0.039244059	0.348392765	N
RA_7	-0.037469644	0.370636181	N
TA_7	-0.034111786	0.415071049	N
F_6	-0.029939226	0.474446453	N
$TA_1\ adj$	0.020053403	0.631919684	N
RA_3	0.004643708	0.911682772	N

Note: Variables without units are dimensionless.

1 μm = 0.039 mil

1 MPa = 145.03 psi

1 $1/\mu\text{m}$ = 25.4 1/mil

Table 51. Pre-screening of deflection variables for fatigue cracking-based logistic model for flexible pavements.

Variable	Pearson R²	Sig (2-tailed)	Selected Parameter for Further Analysis (Y/N)
D_5 (μm)	-0.157433136	0.000613975	Y
D_6 (μm)	-0.154864767	0.00075498	Y
D_4 (μm)	-0.154460852	0.000779708	Y
CI_6 (μm)	-0.153654425	0.000831333	Y
I_4 ($1/\mu\text{m}$)	0.151051867	0.001020282	Y
I_2 ($1/\mu\text{m}$)	0.149858715	0.001119523	Y
I_1 ($1/\mu\text{m}$)	0.146532512	0.001445036	Y
Hogg (MPa)	0.145504691	0.001561978	Y
I_3 ($1/\mu\text{m}$)	0.145381074	0.001576613	Y
I_5 ($1/\mu\text{m}$)	0.139867364	0.002372627	Y
D_3 (μm)	-0.129861295	0.004805684	Y
D_7 (μm)	-0.12775584	0.005542626	Y
I_6 ($1/\mu\text{m}$)	0.125224224	0.00656233	Y
CI_5 (μm)	-0.123675232	0.007266266	Y
D_2 (μm)	-0.120957194	0.008666145	Y
I_7 ($1/\mu\text{m}$)	0.11905933	0.009781293	Y
D_{I_adj} (μm)	-0.115409302	0.012289432	Y
CI_4 (μm)	-0.115305763	0.012368194	Y
D_I (μm)	-0.109334164	0.017734818	Y
S_7 (μm)	-0.098533789	0.03270609	Y
S_6 (μm)	-0.087200407	0.058888422	Y
RoC	0.082914884	0.072517007	Y
S_5 (μm)	-0.077466286	0.093448944	Y
CI_2 (μm)	-0.07365144	0.110792825	Y
S_3 (μm)	-0.06978492	0.130861177	Y
S_4 (μm)	-0.068774378	0.13654375	Y
CI_1 (μm)	-0.066345399	0.15097771	Y
S_2 (μm)	-0.066345399	0.15097771	Y
CI_3 (μm)	-0.057965846	0.209704568	Y
F_5	-0.034265062	0.458639839	Y
RA_2	0.033275762	0.471722237	Y
TA_2	0.030577618	0.508422251	N
RA_5	-0.025808734	0.576760343	N
RA_6	-0.025702294	0.578333557	N
TA_5	-0.024710043	0.593095202	N
TA_6	-0.024306983	0.599140244	N
TA_7	0.021979308	0.634581271	N
RA_7	0.020701959	0.654398118	N
Elmod (MPa)	0.020351098	0.659884951	N

F_3	-0.019932256	0.666458795	N
F_2	-0.016123413	0.727360242	N
RA_3	-0.015665734	0.734804513	N
SN_{eff}	0.014228486	0.758340753	N
F_6	-0.01094936	0.812849595	N
TA_3	-0.008833073	0.848533217	N
RA_1	0.008637656	0.85184507	N
TA_1	0.007210874	0.876100985	N
RA_4	-0.006796251	0.88317262	N
TA_4	-0.002443006	0.957873617	N
F_4	-0.002248203	0.961229969	N

Note: Variables without units are dimensionless.

1 μm = 0.039 mil

1 MPa = 145.03 psi

1 $1/\mu\text{m}$ = 25.4 1/mil

PRE-SCREENING OF DEFLECTION PARAMETERS FOR RIGID PAVEMENTS

Table 52. Pre-screening of deflection variables for drop 2 roughness-based logistic model for rigid pavements.

Variable	Pearson R ²	Sig (2-tailed)	Selected Parameter for Further Analysis (Y/N)
CI_6 (μm)	0.290964248	0.00023977	Y
D_3 (μm)	0.248633096	0.00181135	Y
D_2 (μm)	0.246794947	0.001963281	Y
D_4 (μm)	0.245888742	0.002042366	Y
D_5 (μm)	0.2456318	0.00206531	Y
D_6 (μm)	0.240971679	0.002524188	Y
D_1 (μm)	0.229180614	0.004124758	Y
S_7 (μm)	0.226764149	0.004548299	Y
CI_5 (μm)	0.220848663	0.005754184	Y
D_7 (μm)	0.189099045	0.018447614	Y
CI_4 (μm)	0.185710522	0.020693802	Y
I_2 (1/μm)	-0.17606761	0.028420732	Y
I_1 (1/μm)	-0.175443457	0.028996223	Y
I_3 (1/μm)	-0.174607503	0.029782537	Y
I_4 (1/μm)	-0.169595685	0.034887189	Y
I_5 (1/μm)	-0.163303473	0.04232556	Y
I_6 (1/μm)	-0.158141519	0.049380227	Y
CI_3 (μm)	0.150567999	0.061475724	N
S_6 (μm)	0.149266308	0.063781117	N
F_2	-0.133454769	0.097830619	N
RA_4	-0.129301034	0.108825846	N
I_7 (1/μm)	-0.122839154	0.127826608	N
CI_2 (μm)	0.104097936	0.197390008	N
S_5 (μm)	0.101999146	0.206626384	N
TA_4	-0.099066256	0.220047952	N
F_3	-0.095856024	0.235435942	N
TA_1	0.08585525	0.288145047	N
TA_7	0.080398249	0.319999581	N
RA_7	0.076080697	0.34675897	N
F_6	0.073356961	0.364344917	N
RA_1	0.06976884	0.388337761	N
S_4 (μm)	0.065926936	0.415056855	N
RA_5	-0.063757985	0.430604574	N
RA_3	-0.040641468	0.615601402	N
TA_5	-0.039568813	0.624960894	N
TA_2	0.033292173	0.680894243	N
CI_1 (μm)	-0.022171058	0.784217743	N

S_2 (μm)	-0.022171058	0.784217743	N
RA_6	-0.021692424	0.788765571	N
TA_3	-0.013100384	0.871475017	N
TA_6	-0.011709822	0.885018028	N
F_5	0.010944526	0.892485894	N
RA_2	0.008716199	0.914281698	N
F_4	-0.006492686	0.936094241	N
S_3 (μm)	0.005354119	0.947282974	N

Note: Variables without units are dimensionless.

1 μm = 0.039 mil

1 MPa = 145.03 psi

1 $1/\mu\text{m}$ = 25.4 $1/\text{mil}$

Table 53. Pre-screening of deflection variables for drop 2 faulting at joints-based logistic model for rigid pavements.

Variable	Pearson R²	Sig (2-tailed)	Selected Parameter for Further Analysis (Y/N)
RA_4	0.214349291	0.011281936	Y
I_2 (1/ μm)	0.161565404	0.057416035	Y
I_3 (1/ μm)	0.160361554	0.059323912	Y
I_1 (1/ μm)	0.159170852	0.061261829	Y
D_6 (μm)	-0.156200068	0.066323697	Y
I_4 (1/ μm)	0.155593311	0.067398334	Y
D_4 (μm)	-0.153028941	0.072097672	Y
D_7 (μm)	-0.152695779	0.07272723	Y
D_5 (μm)	-0.151896626	0.074255495	Y
D_2 (μm)	-0.147777675	0.0825488	Y
D_3 (μm)	-0.147476565	0.083183089	Y
I_5 (1/ μm)	0.141306072	0.097062111	N
CI_6 (μm)	-0.139053803	0.102562136	N
F_2	0.134250113	0.115110182	N
I_6 (1/ μm)	0.130758489	0.124957373	N
D_1 (μm)	-0.127324496	0.135263402	N
TA_4	0.127273639	0.135420768	N
CI_4 (μm)	-0.126333254	0.138355905	N
TA_5	0.114819951	0.178322227	N
CI_5 (μm)	-0.101339581	0.235209646	N
CI_2 (μm)	-0.093785547	0.27213776	N
I_7 (1/ μm)	0.092003504	0.281392403	N
S_7 (μm)	-0.090384211	0.289982989	N
TA_6	0.086764329	0.309812411	N
RA_3	0.081777812	0.338545115	N
CI_1 (μm)	0.077138643	0.366746497	N
S_2 (μm)	0.077138643	0.366746497	N
F_6	-0.075823917	0.374994804	N
TA_3	0.070939348	0.406620091	N
F_5	-0.059745946	0.484765826	N
TA_2	0.052545667	0.538994225	N
F_3	0.051718498	0.545411074	N
S_3 (μm)	0.048479555	0.5708925	N
RA_7	-0.048003744	0.574682506	N
RA_1	-0.047770038	0.576548354	N
TA_7	-0.044011956	0.606932531	N
S_6 (μm)	-0.042862677	0.616363736	N
RA_2	0.04167614	0.626166819	N
RA_5	0.030637134	0.720321778	N

S_4 (μm)	0.030282662	0.723425468	N
CI_3 (μm)	-0.019433974	0.820364969	N
S_5 (μm)	-0.010779953	0.899771713	N
F_4	0.005368993	0.949982837	N
RA_6	-0.00241349	0.977504457	N
TA_l	-0.000615033	0.994266728	N

Note: Variables without units are dimensionless.

1 μm = 0.039 mil

1 MPa = 145.03 psi

1 $1/\mu\text{m}$ = 25.4 1/mil

Table 54. Pre-screening of deflection variables for drop 2 transverse cracking-based logistic model for rigid pavements.

Variable	Pearson R²	Sig (2-tailed)	Selected Parameter for Further Analysis (Y/N)
<i>TA</i> ₇	-0.319520892	0.000126034	Y
<i>RA</i> ₇	-0.309129475	0.000213244	Y
<i>CI</i> ₄ (μm)	-0.306955021	0.000237474	Y
<i>CI</i> ₆ (μm)	-0.290660239	0.000518252	Y
<i>S</i> ₇ (μm)	-0.274478931	0.00107596	Y
<i>TA</i> ₄	0.256897328	0.002266946	Y
<i>F</i> ₆	-0.247093151	0.003362544	Y
<i>CI</i> ₅ (μm)	-0.238760097	0.004646404	Y
<i>D</i> ₃ (μm)	-0.226070126	0.007450775	Y
<i>D</i> ₂ (μm)	-0.225810314	0.007521264	Y
<i>S</i> ₆ (μm)	-0.223660568	0.00812757	Y
<i>D</i> ₁ (μm)	-0.220186286	0.00919917	Y
<i>TA</i> ₅	0.220101063	0.009226954	Y
<i>D</i> ₄ (μm)	-0.215542071	0.010825472	Y
<i>TA</i> ₃	0.208771514	0.013648107	Y
<i>CI</i> ₃ (μm)	-0.205417654	0.015270576	Y
<i>F</i> ₅	-0.201190574	0.017552769	Y
<i>D</i> ₅ (μm)	-0.200505623	0.017949136	Y
<i>S</i> ₅	-0.199383576	0.018615204	Y
<i>RA</i> ₃	0.194642561	0.021671013	Y
<i>TA</i> ₂	0.185174717	0.029081989	Y
<i>D</i> ₆ (μm)	-0.184261972	0.029898859	Y
<i>TA</i> ₁	0.180364803	0.033609595	Y
<i>RA</i> ₄	0.17853298	0.035484122	Y
<i>RA</i> ₆	-0.166200723	0.050535274	N
<i>F</i> ₄	-0.156545559	0.065718058	N
<i>I</i> ₁ (1/μm)	0.156256774	0.066223983	N
<i>S</i> ₄ (μm)	-0.150107761	0.07777058	N
<i>I</i> ₂ (1/μm)	0.147752122	0.082602476	N
<i>RA</i> ₂	0.146349322	0.085592375	N
<i>I</i> ₃ (1/μm)	0.145766991	0.086858681	N
<i>RA</i> ₁	0.144649399	0.089330809	N
<i>CI</i> ₂ (μm)	-0.135085129	0.112847157	N
<i>I</i> ₄ (1/μm)	0.133642345	0.11677941	N
<i>RA</i> ₅	-0.117173684	0.16952878	N
<i>I</i> ₅ (1/μm)	0.113244047	0.184394515	N
<i>D</i> ₇ (μm)	-0.099745631	0.242693723	N
<i>I</i> ₆ (1/μm)	0.090640262	0.288613104	N
<i>S</i> ₃ (μm)	-0.086547813	0.311025894	N

CI_1 (μm)	-0.059860287	0.483928914	N
S_2	-0.059860287	0.483928914	N
F_2	-0.036991396	0.66550023	N
F_3	-0.031803265	0.710143716	N
I_7 ($1/\mu\text{m}$)	0.020959832	0.806527519	N
TA_6	-0.013199013	0.877439786	N

Note: Variables without units are dimensionless.

1 μm = 0.039 mil

1 MPa = 145.03 psi

1 $1/\mu\text{m}$ = 25.4 1/mil

Table 55. Pre-screening of deflection variables for drop 3 roughness-based logistic model for rigid pavements.

Variable	Pearson R²	Sig (2-tailed)	Selected Parameter for Further Analysis (Y/N)
D_4 (μm)	-0.231018767	0.003712941	Y
D_3 (μm)	-0.229746336	0.003912289	Y
D_6 (μm)	-0.22855743	0.004107194	Y
D_2 (μm)	-0.227149579	0.004349247	Y
D_5 (μm)	-0.226131044	0.004532267	Y
CI_4 (μm)	-0.225944603	0.004566507	Y
D_7 (μm)	-0.220699984	0.005629836	Y
D_1 (μm)	-0.216701832	0.006583631	Y
CI_6 (μm)	-0.206045677	0.00986392	Y
S_7 (μm)	-0.182120356	0.022878806	Y
I_1 ($1/\mu\text{m}$)	0.175994414	0.027972346	Y
CI_5 (μm)	-0.169157994	0.034769885	Y
I_3 ($1/\mu\text{m}$)	0.16634895	0.037942875	Y
I_2 ($1/\mu\text{m}$)	0.165665443	0.038750801	Y
I_4 ($1/\mu\text{m}$)	0.161123224	0.044495586	Y
RA_4	0.1563815	0.051234896	N
I_5 ($1/\mu\text{m}$)	0.147310985	0.066484788	N
S_6 (μm)	-0.139239409	0.082994782	N
I_6 ($1/\mu\text{m}$)	0.135039829	0.092803725	N
S_5 (μm)	-0.112764232	0.161043076	N
CI_3 (μm)	-0.103730919	0.197516944	N
I_7 ($1/\mu\text{m}$)	0.099708982	0.215553836	N
F_2	0.099122913	0.218277178	N
F_3	0.098703882	0.220239284	N
TA_4	0.080175763	0.319763512	N
CI_2 (μm)	-0.078646317	0.329111714	N
RA_7	-0.0674084	0.403092486	N
S_4 (μm)	-0.064462533	0.424004346	N
TA_7	-0.063736586	0.429252484	N
F_5	-0.053849755	0.50435152	N
TA_5	0.05261841	0.514162317	N
RA_3	0.047573575	0.555358928	N
RA_1	-0.04750079	0.555964775	N
F_6	-0.041405776	0.607798199	N
TA_3	0.033801743	0.675283394	N
TA_6	0.028644655	0.722614238	N
S_3 (μm)	-0.027271501	0.735405113	N
F_4	-0.020034283	0.803948281	N
RA_6	-0.019587441	0.808235667	N

TA_1	-0.017775778	0.825675524	N
RA_2	-0.015148917	0.851112643	N
CI_1 (μm)	-0.00682074	0.932653462	N
S_2 (μm)	-0.00682074	0.932653462	N
TA_2	0.006150142	0.939261428	N
RA_5	-0.005108871	0.949530006	N

Note: Variables without units are dimensionless.

1 μm = 0.039 mil

1 MPa = 145.03 psi

1 $1/\mu\text{m}$ = 25.4 1/mil

Table 56. Pre-screening of deflection variables for drop 3 faulting at joints-based logistic model for rigid pavements.

Variable	Pearson R²	Sig (2-tailed)	Selected Parameter for Further Analysis (Y/N)
RA_4	0.188987017	0.023294968	Y
I_1 (1/ μm)	0.161603177	0.052980999	Y
I_2 (1/ μm)	0.152590048	0.067875984	Y
I_3 (1/ μm)	0.152364798	0.068287933	Y
I_4 (1/ μm)	0.146249842	0.080270274	Y
D_4 (μm)	-0.1419625	0.089638018	Y
D_6 (μm)	-0.141573149	0.090530178	Y
D_5 (μm)	-0.140156854	0.093835239	Y
D_2 (μm)	-0.1386745	0.097396262	Y
D_3 (μm)	-0.138555983	0.097685525	Y
D_7 (μm)	-0.135651185	0.104989848	Y
I_5 (1/ μm)	0.132374263	0.113737442	N
TA_4	0.130564787	0.11880547	N
CI_6 (μm)	-0.130322639	0.119496771	N
D_1 (μm)	-0.127358213	0.128214615	N
CI_4 (μm)	-0.124884514	0.135856987	N
TA_5	0.123294493	0.140949989	N
I_6 (1/ μm)	0.116088695	0.165865195	N
CI_5 (μm)	-0.106009787	0.206015806	N
S_7 (μm)	-0.102867226	0.219857942	N
F_6	-0.100247392	0.231892343	N
RA_3	0.093745676	0.263734925	N
TA_3	0.085112094	0.310446542	N
CI_2 (μm)	-0.08460367	0.313356211	N
I_7 (1/ μm)	0.080597394	0.336902843	N
F_5	-0.080316235	0.338596553	N
F_2	0.073339491	0.382346557	N
S_6 (μm)	-0.067625477	0.420614497	N
RA_7	-0.065458196	0.435691782	N
TA_2	0.062337517	0.457934103	N
TA_7	-0.059877081	0.475905951	N
RA_2	0.045153639	0.59099446	N
S_5 (μm)	-0.042101505	0.616344996	N
RA_6	-0.039774591	0.635983013	N
CI_3 (μm)	-0.03486104	0.67827905	N
TA_1	0.033612957	0.689191042	N
TA_6	0.032097654	0.702525638	N
F_3	0.03187355	0.704505571	N
CI_1 (μm)	0.031789962	0.705244568	N

S_2 (μm)	0.031789962	0.705244568	N
F_4	-0.017149361	0.838342746	N
RA_5	0.012474146	0.882034272	N
S_4 (μm)	-0.009344165	0.911493318	N
S_3 (μm)	0.006621708	0.937216504	N
RA_I	0.001026985	0.990252956	N

Note: Variables without units are dimensionless.

1 μm = 0.039 mil

1 MPa = 145.03 psi

1 $1/\mu\text{m}$ = 25.4 1/mil

Table 57. Pre-screening of deflection variables for drop 3 transverse cracking-based logistic model for rigid pavements.

Variable	Pearson R²	Sig (2-tailed)	Selected Parameter for Further Analysis(Y/N)
<i>TA</i> ₇	-0.318133195	0.000127903	Y
<i>CI</i> ₄ (μm)	-0.316043599	0.000142422	Y
<i>RA</i> ₇	-0.309706065	0.000196388	Y
<i>CI</i> ₆ (μm)	-0.282610246	0.0007166	Y
<i>TA</i> ₄	0.277229365	0.00091297	Y
<i>S</i> ₇	-0.274594487	0.001026122	Y
<i>F</i> ₆	-0.254023959	0.002457351	Y
<i>CI</i> ₅ (μm)	-0.230262146	0.006201163	Y
<i>S</i> ₆	-0.228549955	0.006606782	Y
<i>TA</i> ₅	0.225359967	0.00742585	Y
<i>TA</i> ₃	0.218493416	0.009500867	Y
<i>F</i> ₅	-0.217427811	0.009865044	Y
<i>RA</i> ₄	0.216846506	0.010068849	Y
<i>D</i> ₃ (μm)	-0.214288228	0.011010506	Y
<i>D</i> ₂ (μm)	-0.213766402	0.011211815	Y
<i>D</i> ₁ (μm)	-0.213709696	0.011233885	Y
<i>S</i> ₅	-0.210347696	0.012612458	Y
<i>D</i> ₄ (μm)	-0.205333449	0.01494342	Y
<i>RA</i> ₃	0.205106163	0.015057437	Y
<i>CI</i> ₃ (μm)	-0.193490726	0.021987806	Y
<i>TA</i> ₂	0.190745922	0.0239787	Y
<i>D</i> ₅ (μm)	-0.189155654	0.025201446	Y
<i>TA</i> ₁	0.181253285	0.032099053	Y
<i>RA</i> ₆	-0.172706742	0.041297304	Y
<i>D</i> ₆ (μm)	-0.172617805	0.041403564	Y
<i>F</i> ₄	-0.163447125	0.053657567	N
<i>I</i> ₁ (1/μm)	0.162734621	0.054723516	N
<i>S</i> ₄	-0.160655304	0.05793456	N
<i>RA</i> ₂	0.146856149	0.083372035	N
<i>I</i> ₂ (1/μm)	0.143377562	0.091027987	N
<i>I</i> ₃ (1/μm)	0.141640515	0.095055002	N
<i>RA</i> ₁	0.13994456	0.09912168	N
<i>I</i> ₄ (1/μm)	0.13119929	0.122312382	N
<i>CI</i> ₂ (μm)	-0.124717703	0.142053064	N
<i>RA</i> ₅	-0.118078917	0.164690301	N
<i>I</i> ₅ (1/μm)	0.108597401	0.201530737	N
<i>S</i> ₃	-0.105511781	0.21471442	N
<i>D</i> ₇ (μm)	-0.086202733	0.311200346	N
<i>I</i> ₆ (1/μm)	0.084554097	0.320579338	N

CI_1 (μm)	-0.081171507	0.340388524	N
S_2	-0.081171507	0.340388524	N
F_2	-0.043488715	0.60991585	N
TA_6	-0.021620604	0.799839718	N
F_3	-0.02112466	0.804337849	N
I_7 (1/ μm)	0.014311662	0.866718386	N

Note: Variables without units are dimensionless.

1 μm = 0.039 mil

1 MPa = 145.03 psi

1 1/ μm = 25.4 1/mil

FLEXIBLE PAVEMENT STRUCTURAL ANALYSIS

Models Based on Roughness Performance

Table 58. Statistics of calibrated models based on roughness performance of flexible pavements—all models.

Deflection Parameter	Primary Model Evaluation						Final Model
	I_2	CI_4	CI_5	D_2	D_3	Hogg	I_2
Area ROC	0.733	0.720	0.731	0.720	0.727	0.694	0.716
Hosmer-Lemeshow significance test	0.397	0.137	0.339	0.351	0.592	0.198	0.995
Calibration—correct cases (percent)	68.4	62.8	67.9	64.6	67.3	63.9	64.1
Validation—correct cases (percent)	74.2	61.3	69.4	66.1	71.0	74.2	69.4
Error type I (false acceptable) (percent)	6.6	4.7	5.7	5.9	6.5	7.0	6.6
Error type II (false not acceptable) (percent)	25.0	32.5	26.4	29.4	26.2	29.1	29.3
TPR (acceptable) (percent)	69.3	60.0	67.5	63.8	67.8	64.2	64.0
TNR (not acceptable) (percent)	64.4	75.0	69.2	68.3	65.4	62.5	64.4

Models Based on Rutting Performance

Table 59. Statistics of calibrated models based on rutting performance of flexible pavements—all models.

Deflection Parameter	Primary Model Evaluation						Final Model		
	CI_3	CI_2	S_7	D_1	RA_6	Hogg	CI_3	Hogg	D_1
Area ROC	0.669	0.658	0.678	0.710	0.624	0.646	0.659	0.640	0.647
Hosmer-Lemeshow significance test	0.066	0.494	0.398	0.414	0.818	0.115	0.267	0.501	0.137
Calibration—correct cases (percent)	68.8	67.1	64.6	70.1	60.0	60.7	66.5	62.0	61.8
Validation—correct cases (percent)	69.4	67.7	64.5	66.1	59.7	61.3	66.1	61.3	46.8
Error type I (false acceptable) (percent)	9.2	8.8	8.1	9.2	8.1	8.6	8.6	8.8	6.2
Error type II (false not acceptable) (percent)	22.0	24.1	27.3	20.8	31.9	30.6	24.8	29.2	32.0
TPR (acceptable) (percent)	72.0	69.4	65.3	73.6	59.5	61.1	68.5	62.9	59.3
TNR (not acceptable) (percent)	57.0	58.7	62.0	57.0	62.0	59.5	59.5	58.7	71.1

Table 60. Variables in the CI_3 final model (based on rutting).

Variables (b_i)	a_i	p -value
CI_3	-0.01146	0.00001594
Precipitation (mm)	-0.0005259	0.04018
Class 9 volume	-0.0007688	0.00005421
Constant	2.6586	1.0136×10^{-13}
Cutoff		0.792

1 inch = 25.4 mm

Table 61. Variables in the Hogg final model (based on rutting).

Variables (b_i)	a_i	p -value
Hogg	0.008182	0.0008198
Class 9 volume	-0.000633	0.001079
Total pavement thickness (inches)	-0.02071	0.05083
Total HMA thickness (inches)	0.08315	0.01762
Constant	0.552	0.1433
Cutoff		0.777

Table 62. Variables in the D_I final model (based on rutting).

Variables (b_i)	a_i	p -value
D_I	-0.002361	0.00011
Class 9 volume	-0.0006459	0.00034
Constant	2.2818	4.2966×10^{-21}
Cutoff		0.812

Models Based on Fatigue Cracking Performance**Table 63. Statistics of calibrated models based on fatigue cracking performance of flexible pavements.**

Deflection Parameter	Primary Model Evaluation						Final Model	
	I_I	D_I	D_4	CI_6	I_2	Hogg	I_I	Hogg
Area ROC	0.657	0.638	0.625	0.613	0.650	0.620	0.642	0.624
Hosmer-Lemeshow significance test	0.368	0.535	0.533	0.238	0.864	0.284	0.596	0.213
Calibration—correct cases (percent)	63.0	59.0	60.7	59.0	62.5	60.7	59.7	60.4
Validation—correct cases (percent)	65.0	60.0	60.0	55.0	60.0	52.5	70.0	55.0
Error type I (false acceptable) (percent)	15.5	12.6	16.9	15.5	16.4	13.8	12.9	16.9
Error type II (false not acceptable) (percent)	21.5	28.3	22.5	25.5	21.1	25.5	27.4	22.7
TPR (acceptable) (percent)	63.1	51.4	61.4	56.2	63.9	56.2	53.0	61.0
TNR (not acceptable) (percent)	62.9	69.7	59.6	62.9	60.7	66.9	69.1	59.6

Table 64. Variables in the I_I final model (based on fatigue cracking).

Variables (b_i)	a_i	p -value
I_I	154.764	0.0006015
AADTT	-0.0005073	0.0007847
Pavement type	0.3774	0.07598
Constant	-0.2202	0.4422
Cutoff		0.605

Table 65. Variables in the Hogg final model (based on fatigue cracking).

Variables (b_i)	a_i	p -value
Hogg	0.005262	0.006867
AADTT	-0.0004274	0.002824
Constant	0.03849	0.8837
Cutoff		0.581

The Hogg parameter is defined in table 3.

RIGID PAVEMENT STRUCTURAL ANALYSIS FOR 9,000 LB (4,086 KG) FWD LOAD

Models Based on Roughness Performance (9,000 lb (4,086 kg))

Table 66. Statistics of calibrated models based on roughness performance of rigid pavements (9,000 lb (4,086 kg)).

Deflection Parameter	Primary Model Evaluation						Final Model		
	CI_5	I_1	D_5	S_7	D_1	Hogg	CI_5	I_1	LTEA
Area ROC	0.699	0.730	0.692	0.647	0.647	0.625	0.651	0.645	0.620
Hosmer-Lemeshow significance test	0.297	0.181	0.043	0.024	0.024	0.017	0.557	0.007	0.293
Calibration—correct cases (percent)	71.0	73.8	69.0	65.5	65.5	65.7	65.5	65.5	60.1
Validation—correct cases (percent)	42.9	42.9	42.9	42.9	42.9	42.9	28.6	42.9	50.0
Error type I (false acceptable) (percent)	10.3	9.0	11.0	10.3	10.3	14.3	14.5	15.2	13.3
Error type II (false not acceptable) (percent)	18.6	17.2	20.0	24.1	24.1	20.0	20.0	19.3	26.6
TPR (acceptable) (percent)	71.9	74.0	69.8	63.5	63.5	69.6	69.8	70.8	60.0
TNR (not acceptable) (percent)	69.4	73.5	67.3	69.4	69.4	58.3	57.1	55.1	60.4

Note: The deflection parameter is based on a survey at the middle of the slab and LTE calculated at the joint approach.

Table 67. Variables in the CI_5 final model (based on roughness) (9,000 lb (4,086 kg)).

Variables (b_i)	a_i	p -value
CI_5	-0.078	0.00406
Class 9 volume	-0.0003877	0.115
Constant	2.057	0.00002168
Cutoff		0.665

Table 68. Variables in the I_1 final model (based on roughness) (9,000 lb (4,086 kg)).

Variables (b_i)	a_i	p -value
I_1	131.600	0.003928
Class 9 volume	-0.0005649	0.03668
Constant	-0.465	0.375
Cutoff		0.639

Table 69. Variables in the LTEA final model (based on roughness) (9,000 lb (4,086 kg)).

Variables (b_i)	a_i	p -value
LTEA	1.804	0.01261
Constant	-0.429	0.363
Cutoff:		0.69

$$\text{LTEA} = \frac{D_3}{D_1}$$

Figure 66. Equation. Calculation of LTEA.

Table 70. Statistics of calibrated models based on roughness performance of rigid pavements for alternative FWD test locations (9,000 lb (4,086 kg)).

Deflection Parameter	Final Model	
	D_1	D_1
FWD test location	Edge corner slab	Edge midslab
Area ROC	0.641	0.716
Hosmer-Lemeshow significance test	0.446	0.411
Calibration—correct cases (percent)	67.6	75.177
Validation—correct cases (percent)	42.9	57.143
Error type I (false acceptable) (percent)	15.9	12.766
Error type II (false not acceptable) (percent)	16.6	12.057
TPR (acceptable) (percent)	74.7	82.474
TNR (not acceptable) (percent)	54.0	59.091

Table 71. Variables in the D_1 final model for FWD testing at edge corner slab (based on roughness) (9,000 lb (4,086 kg)).

Variables (b_i)	a_i	p -value
D_1	-0.010125	0.01368
Class 9 volume	-0.0004173	0.08322
Constant	1.983	0.0001133
Cutoff		0.652

Table 72. Variables in the D_1 final model for FWD testing at edge midslab (based on roughness) (9,000 lb (4,086 kg)).

Variables (b_i)	a_i	p -value
D_1	-0.01349	0.00003341
Class 9 volume	-0.0007071	0.01186
Constant	3.551	0.0000001944
Cutoff		0.675

Models Based on Faulting at Joints Performance (9,000 lb (4,086 kg))

Table 73. Statistics of calibrated models based on faulting at joints of rigid pavements (9,000 lb (4,086 kg)).

Deflection Parameter	Primary Model Evaluation					Final Model	
	D_6	I_2	I_1	D_7	Hogg	D_6	LTEA
Area ROC	0.624	0.639	0.638	0.603	0.586	0.637	0.590
Hosmer-Lemeshow significance test	0.173	0.009	0.025	0.027	0.078	0.064	0.592
Calibration—correct cases (percent)	60.8	67.7	65.4	42.3	54.3	63.8	57.3
Validation—correct cases (percent)	80.0	100.0	100.0	40.0	50.0	100.0	50.0
Error Type I (False Acceptable) (percent)	10.8	16.2	15.4	0.8	11.0	16.2	9.9
Error Type II (false not acceptable) (percent)	28.5	16.2	19.2	56.9	34.6	20.0	32.8
TPR (acceptable) (percent)	56.0	75.0	70.2	11.9	46.3	69.0	50.0
TNR (not acceptable) (percent)	69.6	54.3	56.5	97.8	68.9	54.3	71.1

Note: The deflection parameter is based on a survey at the middle of the slab and LTE calculated at the joint approach.

Table 74. Variables in the D_6 final model (based on faulting at joints) (9,000 lb (4,086 kg)).

Variables (b_i)	a_i	p -value
D_6	-0.009225	0.138
Subgrade type	-0.495	0.2003
Constant	1.499	0.005818
Cutoff		0.635

Table 75. Variables in the LTEA final model (based on faulting at joints) (9,000 lb (4,086 kg)).

Variables (b_i)	a_i	p -value
LTEA	0.796	0.2804
Subgrade type	-0.5104	0.194
Constant	0.454	0.4401
Cutoff		0.659

Table 76. Statistics of calibrated models based on faulting at joints of rigid pavements (9,000 lb (4,086 kg)).

Deflection Parameter	Final Model	
	D_I	D_I
FWD test location	Edge corner slab	Edge midslab
Area ROC	0.694	0.695
Hosmer-Lemeshow significance test	0.047	0.576
Calibration—correct cases (percent)	64.9	62.6
Validation—correct cases (percent)	40.0	66.7
Error type I (false acceptable) (percent)	10.7	10.7
Error Type II (false not acceptable) (percent)	24.4	26.7
TPR (acceptable) (percent)	63.6	59.3
TNR (not acceptable) (percent)	67.4	68.9

Table 77. Variables in the D_I final model for FWD testing at edge corner slab (based on faulting at joints) (9,000 lb (4,086 kg)).

Variables (b_i)	a_i	p -value
D_I	-0.003976	0.002237
Subgrade type	-0.923	0.03008
Constant	2.315	0.000003115
Cutoff		0.687

Table 78. Variables in the D_I final model for FWD testing at edge midslab (based on faulting at joints) (9,000 lb (4,086 kg)).

Variables (b_i)	a_i	p -value
D_I	-0.00861	0.001208
Subgrade type	-0.836	0.04503
Constant	2.583	0.00001405
Cutoff		0.695

Models Based on Transverse Cracking Performance (9,000 lb (4,086 kg))

Table 79. Statistics of calibrated models based on transverse cracking of rigid pavements (9,000 lb (4,086 kg)).

Deflection Parameter	Primary Model Evaluation				Final Model		
	CI_4	D_I	Hogg	RA_7	CI_4	D_I	LTEA
Area ROC	0.766	0.741	0.703	0.747	0.766	0.726	0.706
Hosmer-Lemeshow significance test	0.363	0.424	0.145	0.136	0.363	0.071	0.948
Calibration—correct cases (percent)	77.5	72.9	76.0	78.3	77.5	72.9	70.1
Validation—correct cases (percent)	100.0	83.3	80.0	83.3	100.0	83.3	40.0
Error Type I (false acceptable) (percent)	10.1	8.5	11.2	11.6	10.1	10.1	8.7
Error Type II (false not acceptable) (percent)	12.4	18.6	12.8	10.1	12.4	17.1	21.3
TPR (acceptable) (percent)	82.8	74.2	82.6	86.0	82.8	76.3	71.9
TNR (not acceptable) (percent)	63.9	69.4	57.6	58.3	63.9	63.9	64.5

Note: The deflection parameter is based on a survey at the middle of the slab and LTE calculated at the joint approach.

Table 80. Variables in the CI_4 final model (based on transverse cracking) (9,000 lb (4,086 kg)).

Variables (b_i)	a_i	p -value
CI_4	-0.254	0.0003759
Class 9 volume	-0.001012	0.001084
Constant	3.630	0.0000003134
Cutoff		0.7

Table 81. Variables in the D_I final model (based on transverse cracking) (9,000 lb (4,086 kg)).

Variables (b_i)	a_i	p -value
D_I	-0.006694	0.168
Class 9 volume	-0.001017	0.001709
Total pavement thickness	0.225	0.0786
Constant	0.209	0.886
Cutoff		0.728

Table 82. Variables in the LTEA final model (based on transverse cracking) (9,000 lb (4,086 kg)).

Variables (b_i)	a_i	p-value
LTEA	3.27	0.0001506
Constant	-0.766	.0135
Cutoff		0.766

Table 83. Statistics of calibrated models based on transverse cracking of rigid pavements (9,000 lb (4,086 kg)).

Deflection Parameter	Final Model	
	D_I	D_I
FWD test location	Edge corner slab	Edge midslab
Area ROC	0.774	0.703
Hosmer-Lemeshow significance test	0.353	0.168
Calibration—correct cases (percent)	79.2	72.2
Validation—correct cases (percent)	100.0	83.3
Error type I (false acceptable) (percent)	9.6	11.1
Error type II (false not acceptable) (percent)	11.2	16.7
TPR (acceptable) (percent)	84.8	77.2
TNR (not acceptable) (percent)	63.6	58.8

Table 84. Variables in the D_I final model for FWD testing at edge corner slab (based on transverse cracking) (9,000 lb (4,086 kg)).

Variables (b_i)	a_i	p-value
D_I	-0.006451	0.0001714
Class 9 volume	-0.0007631	0.006384
Constant	3.328	0.0000000470
Cutoff		0.708

Table 85. Variables in the D_I final model for FWD testing at edge midslab (based on transverse cracking) (9,000 lb (4,086 kg)).

Variables (b_i)	a_i	p-value
D_I	-0.01000	0.0005496
Class 9 volume	-0.0008483	0.004314
Constant	3.347	0.0000005382
Cutoff		0.713

RIGID PAVEMENT STRUCTURAL ANALYSIS FOR 12,000-LB (5,448-KG) FWD LOAD

Models Based on Roughness Performance (12,000 lb (5,448 kg))

Table 86. Statistics of calibrated models based on roughness of rigid pavements (12,000 lb (5,448 kg)).

Deflection Parameter	Primary Model Evaluation				Final Model		
	CI_4	D_6	CI_6	I_1	CI_4	I_1	LTEA
Area ROC	0.663	0.630	0.621	0.638	0.663	0.638	0.620
Hosmer-Lemeshow significance test	0.049	0.626	0.659	0.214	0.049	0.214	0.177
Calibration—correct cases (percent)	64.1	62.1	61.4	69.0	64.1	69.0	60.8
Validation—correct cases (percent)	57.1	57.1	71.4	71.4	57.1	71.4	66.7
Error Type I (false acceptable) (percent)	9.7	13.1	16.6	17.2	9.7	17.2	13.3
Error Type II (false not acceptable) (percent)	26.2	24.8	22.1	13.8	26.2	13.8	25.9
TPR (acceptable) (percent)	60.8	62.9	67.0	79.4	60.8	79.4	61.9
TNR (not acceptable) (percent)	70.8	60.4	50.0	47.9	70.8	47.9	58.7

Note: The deflection parameter is based on a survey at the middle of the slab and LTE calculated at the joint approach.

Table 87. Variables in the CI_4 final model (based on roughness) (12,000 lb (5,448 kg)).

Variables (b_i)	a_i	p -value
CI_4	-0.117	0.007378
Class 9 volume	-0.0004607	0.06459
Constant	2.148	0.0000447
Cutoff		0.695

Table 88. Variables in the I_1 final model (based on roughness) (12,000 lb (5,448 kg)).

Variables (b_i)	a_i	p -value
I_1	160.521	0.008563
Class 9 volume	-0.0005612	0.03519
Constant	-0.293	0.576
Cutoff		0.62

Table 89. Variables in the LTEA final model (based on roughness) (12,000 lb (5,448 kg)).

Variables (b_i)	a_i	p -value
LTEA	1.903	0.01053
Constant	-0.434	0.371
Cutoff		0.697

Table 90. Statistics of calibrated models based on roughness of rigid pavements (12,000 lb (5,448 kg)).

Deflection Parameter	Final Model	
	D_I	D_I
FWD test location	Edge corner slab	Edge midslab
Area ROC	0.654	0.710
Hosmer-Lemeshow significance test	0.479	0.573
Calibration—correct cases (percent)	60.7	70.9
Validation—correct cases (percent)	57.1	71.4
Error Type I (false acceptable) (percent)	12.9	13.5
Error Type II (false not acceptable) (percent)	26.4	15.6
TPR (acceptable) (percent)	61.1	76.8
TNR (not acceptable) (percent)	60.0	58.7

Table 91. Variables in the D_I final model for FWD testing at edge corner slab (based on roughness) (12,000 lb (5,448 kg)).

Variables (b_i)	a_i	p -value
D_I	-0.003005	0.003249
Class 9 volume	-0.0003201	0.185
Constant	1.961	0.000007846
Cutoff		0.707

Table 92. Variables in the D_I final model for FWD testing at edge midslab (based on roughness) (12,000 lb (5,448 kg)).

Variables (b_i)	a_i	p -value
D_I	-0.009806	0.00004818
Class 9 volume	-0.0007354	0.009784
Constant	3.422	0.0000004192
Cutoff		0.664

Models Based on Faulting at Joints Performance (12,000 lb (5,448 kg))

Table 93. Statistics of calibrated models based on faulting at joints of rigid pavements (12,000 lb (5,448 kg)).

Deflection Parameter	Primary Model Evaluation			Final Model	
	D_6	I_1	Hogg	D_6	LTEA
Area ROC	0.644	0.643	0.592	0.634	0.608
Hosmer-Lemeshow significance test	0.131	0.640	0.596	0.222	0.745
Calibration—correct cases (percent)	64.9	61.9	56.6	61.9	58.8
Validation—correct cases (percent)	50.0	66.7	33.3	50.0	50.0
Error type I (false acceptable) (percent)	17.2	9.7	14.0	12.7	13.0
Error type II (false not acceptable) (percent)	17.9	28.4	29.5	25.4	28.2
TPR (acceptable) (percent)	72.4	56.3	53.7	60.9	57.5
TNR (not acceptable) (percent)	51.1	72.3	61.7	63.8	61.4

Note: Deflection parameter based on survey at the middle of the slab and LTE calculated at joint approach.

Table 94. Variables in the D_6 final model (based on faulting at joints) (12,000 lb (5,448 kg)).

Variables (b_i)	a_i	p -value
D_6	-0.008789	0.06896
Subgrade type	-0.579	0.139
Constant	1.734	0.002499
Cutoff		0.651

Table 95. Variables in the LTEA final model (based on faulting at joints) (12,000 lb (5,448 kg)).

Variables (b_i)	a_i	p -value
LTEA	1.106	0.144
Subgrade type	-0.335	0.3899
Constant	0.172	0.773
Cutoff		0.677

Table 96. Statistics of calibrated models based on faulting at joints of rigid pavements (12,000 lb (5,448 kg)).

Deflection Parameter	Final Model	
	D_I	D_I
FWD test location	Edge corner slab	Edge midslab
Area ROC	0.702	0.695
Hosmer-Lemeshow significance test	0.103	0.572
Calibration—correct cases (percent)	64.9	61.832
Validation—correct cases (percent)	60.0	83.333
Error type I (false acceptable) (percent)	9.2	10.687
Error type II (false not acceptable) (percent)	26.0	27.481
TPR (acceptable) (percent)	60.9	58.621
TNR (not acceptable) (percent)	72.7	68.182

Table 97. Variables in the D_I final model for FWD testing at edge corner slab (based on faulting at joints) (12,000 lb (5,448 kg)).

Variables (b_i)	a_i	p -value
D_I	-0.003291	0.002071
Subgrade type	-0.825	0.04834
Constant	2.286	0.000006551
Cutoff		0.691

Table 98. Variables in the D_I final model for FWD testing at edge midslab (based on faulting at joints) (12,000 lb (5,448 kg)).

Variables (b_i)	a_i	p -value
D_I	-0.007078	0.001048
Subgrade type	-0.883	0.03558
Constant	2.764	0.000009804
Cutoff		0.7

Models Based on Transverse Cracking Performance (12,000 lb (5,448 kg))

Table 99. Statistics of calibrated models based on transverse cracking of rigid pavements (12,000 lb (5,448 kg)).

Deflection Parameter	Primary Model Evaluation				Final Model		
	CI_4	D_I	Hogg	TA_7	CI_4	D_I	LTEA
Area ROC	0.778	0.749	0.709	0.739	0.775	0.735	0.683
Hosmer-Lemeshow significance test	0.353	0.396	0.008	0.107	0.200	0.139	0.493
Calibration—correct cases (percent)	74.4	73.6	69.4	77.5	74.4	72.1	66.1
Validation—correct cases (percent)	66.7	50.0	50.0	66.7	83.3	50.0	80.0
Error Type I (false acceptable) (percent)	7.8	8.5	9.7	11.6	9.3	9.3	11.8
Error Type II (false not acceptable) (percent)	17.8	17.8	21.0	10.9	16.3	18.6	22.0
TPR (acceptable) (percent)	75.0	75.0	71.1	84.8	77.2	73.9	69.9
TNR (not acceptable) (percent)	73.0	70.3	64.7	59.5	67.6	67.6	55.9

Note: Deflection parameter based on survey at the middle of the slab and LTE calculated at joint approach.

Table 100. Variables in the CI_4 final model (based on transverse cracking) (12,000 lb (5,448 kg)).

Variables (b_i)	a_i	p -value
CI_4	-0.231	0.00007858
Class 9 volume	-0.001029	0.001282
Constant	3.9796	0.0000001201
Cutoff		0.71

Table 101. Variables in the D_I final model (based on transverse cracking) (12,000 lb (5,448 kg)).

Variables (b_i)	a_i	p -value
D_I	-0.008441	0.07225
Class 9 volume	-0.001027	0.001734
Total pavement thickness	0.1948	0.1398
Constant	0.943	0.5641
Cutoff		0.73

**Table 102. Variables in the LTEA final model (based on transverse cracking)
(12,000 lb (5,448 kg)).**

Variables (b_i)	a_i	p-value
LTEA	2.679	0.001196
Constant	-0.5943	0.2463
Cutoff		0.736

**Table 103. Statistics of calibrated models based on transverse cracking of rigid pavements
(12,000 lb (5,448 kg)).**

Deflection Parameter	Final Model	
	D_I	D_I
FWD test location	Edge corner slab	Edge midslab
Area ROC	0.768	0.694
Hosmer-Lemeshow significance test	0.403	0.131
Calibration—correct cases (percent)	77.6	67.460
Validation—correct cases (percent)	100.0	66.667
Error Type I (false acceptable) (percent)	8.8	7.937
Error Type II (false not acceptable) (percent)	13.6	24.603
TPR (acceptable) (percent)	81.7	66.304
TNR (not acceptable) (percent)	65.6	70.588

**Table 104. Variables in the D_I final model for FWD testing at edge corner slab
(based on transverse cracking) (12,000 lb (5,448 kg)).**

Variables (b_i)	a_i	p-value
D_I	-0.005252	0.0002574
Class 9 volume	-0.0007991	0.005173
Constant	3.409	0.00000009316
Cutoff		0.725

**Table 105. Variables in the D_I final model for FWD testing at edge midslab
(based on transverse cracking) (12,000 lb (5,448 kg)).**

Variables (b_i)	a_i	p-value
D_I	-0.006136	0.01611
Class 9 volume	-0.02948	0.0187
Total PCC thickness	0.1211	0.3503
Constant	2.662	0.1164
Cutoff		0.718

APPENDIX C

FLEXIBLE PAVEMENT STRUCTURAL ANALYSIS

Models Based on Rutting Performance for Flexible Pavements

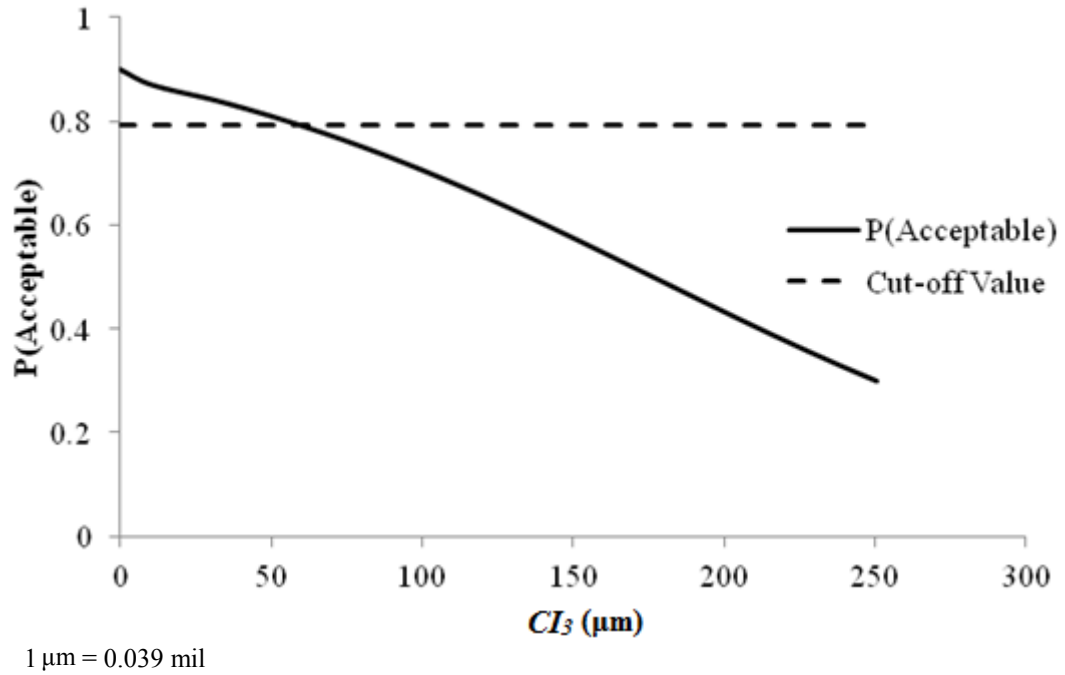


Figure 67. Graph. Sensitivity of rutting acceptable probability to deflection parameter CI_3 for flexible pavements.

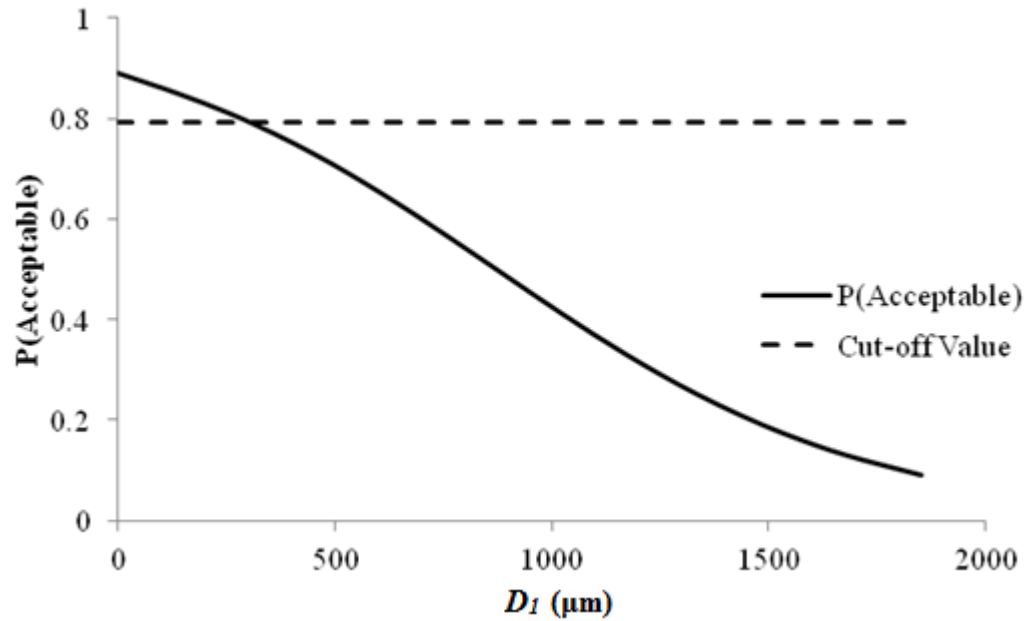


Figure 68. Graph. Sensitivity of rutting acceptable probability to deflection parameter D_1 for flexible pavements.

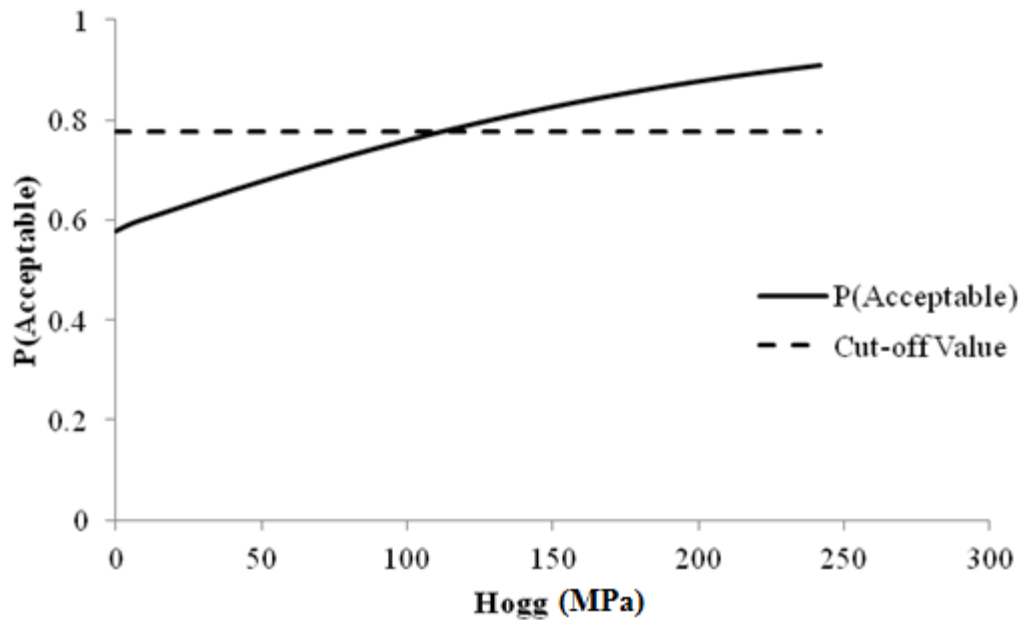
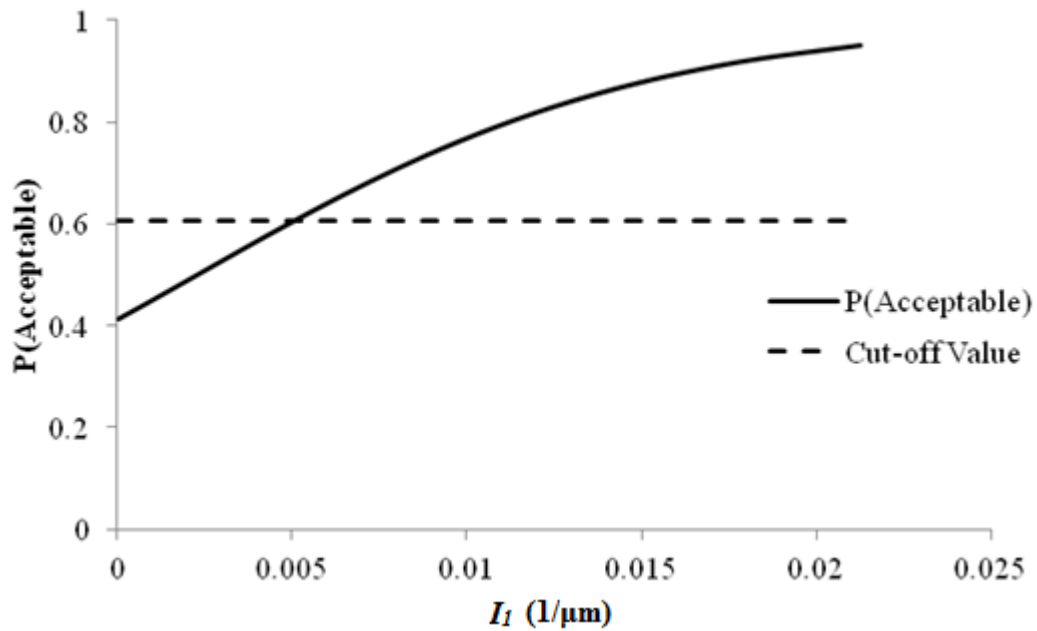


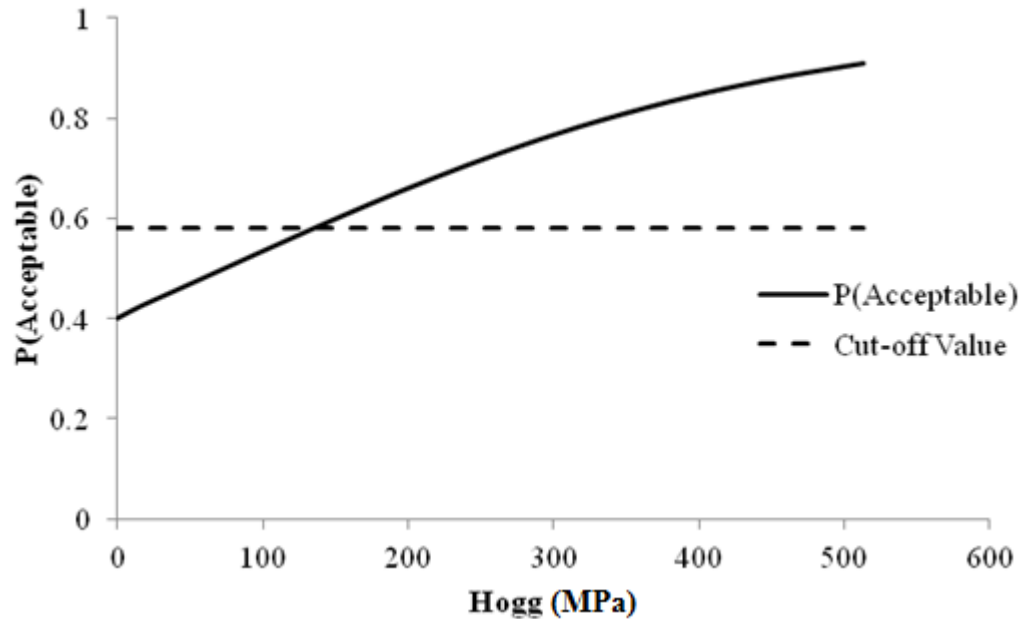
Figure 69. Graph. Sensitivity of rutting acceptable probability to deflection parameter Hogg for flexible pavements.

Models Based on Fatigue Cracking Performance for Flexible Pavements



1 $1/\mu\text{m} = 25.4$ 1/mil

Figure 70. Graph. Sensitivity of fatigue cracking acceptable probability to deflection parameter I_1 for flexible pavements.

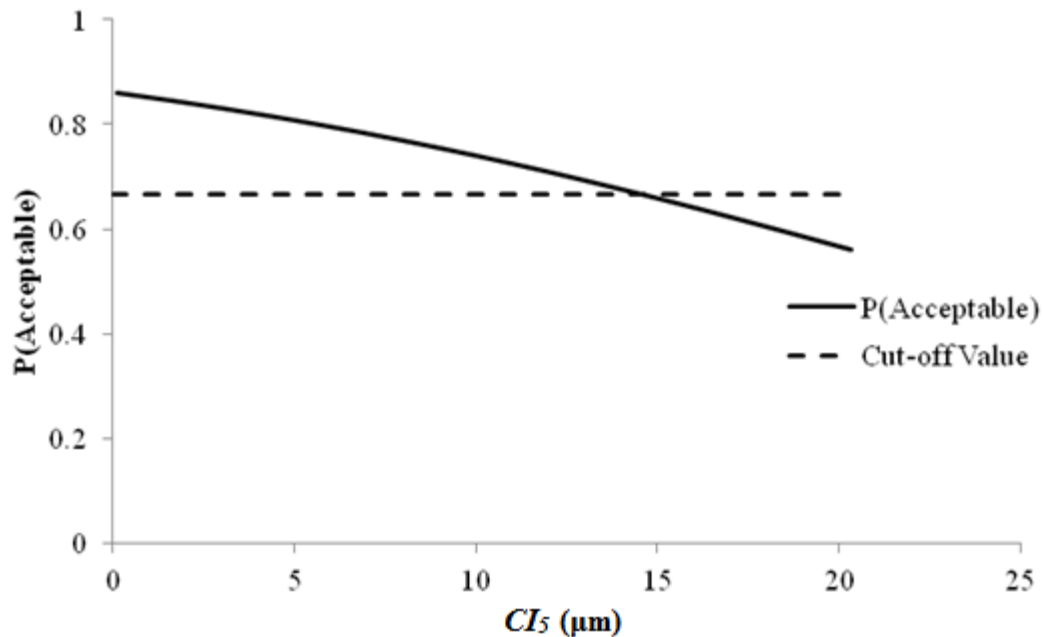


1 MPa = 145.0377 psi

Figure 71. Graph. Sensitivity of fatigue cracking acceptable probability to deflection parameter Hogg for flexible pavements.

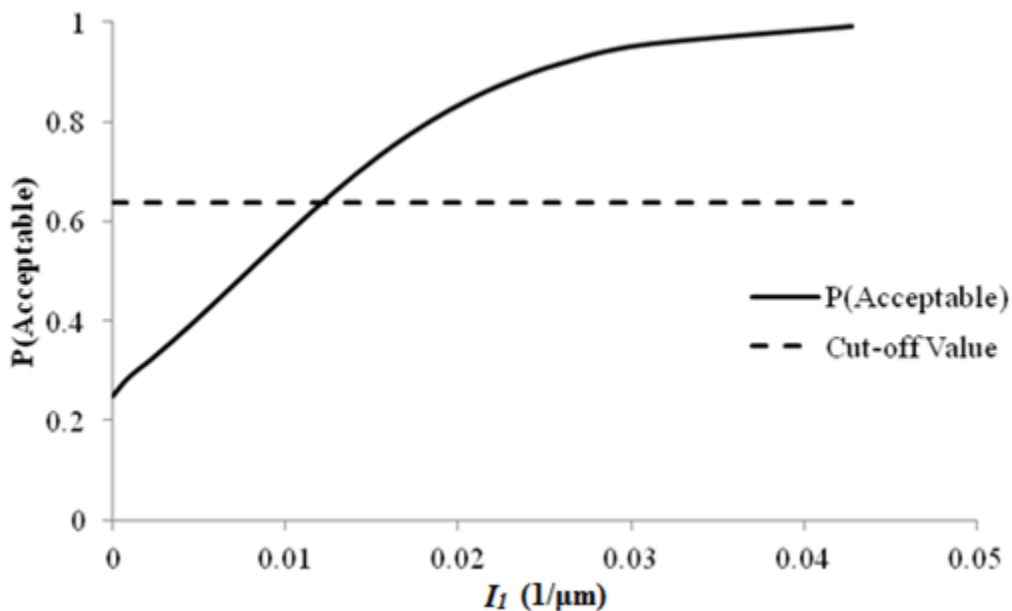
RIGID PAVEMENT STRUCTURAL ANALYSIS FOR 9,000-LB (4,086-KG) FWD LOAD

Models Based on Roughness Performance for Rigid Pavements (9,000 lb (4,086 kg))



1 μm = 0.039 mil

Figure 72. Graph. Sensitivity of roughness acceptable probability to deflection parameter CI_5 for rigid pavements (9,000 lb (4,086 kg)).



1 $1/\mu\text{m}$ = 25.4 1/mil

Figure 73. Graph. Sensitivity of roughness acceptable probability to deflection parameter I_1 for rigid pavements (9,000 lb (4,086 kg)).

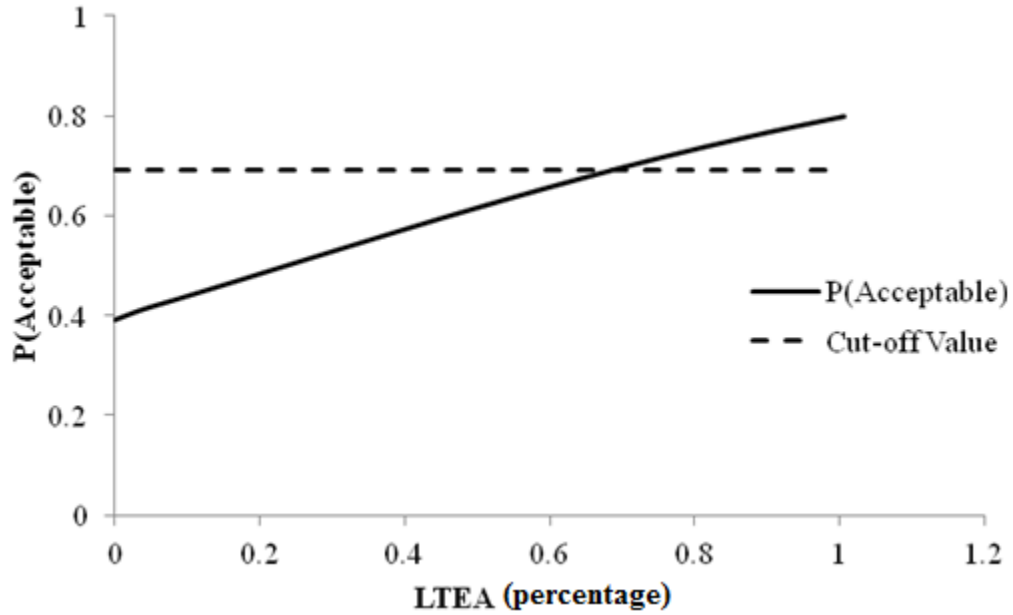
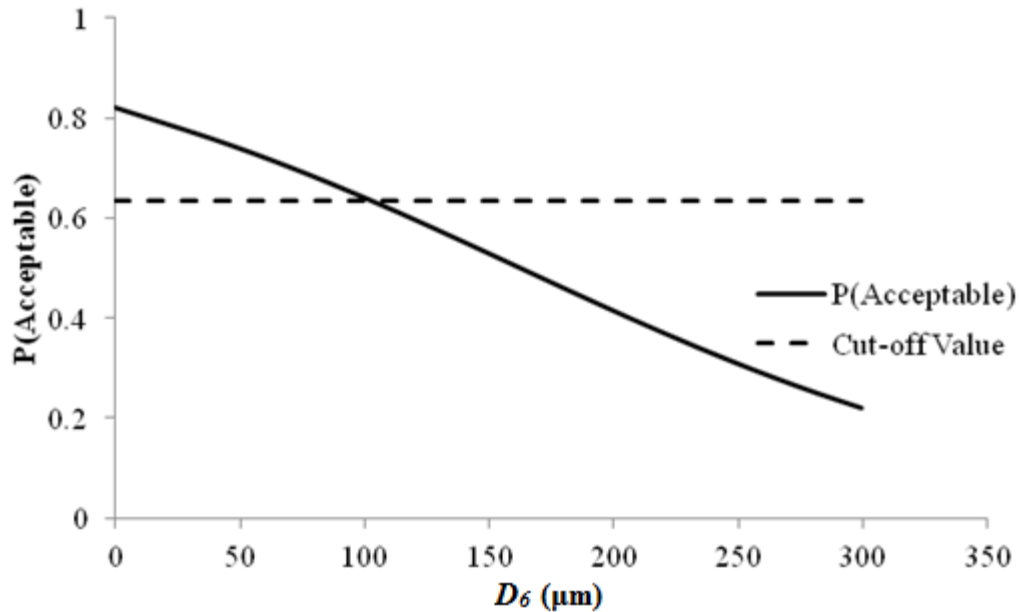


Figure 74. Graph. Sensitivity of roughness acceptable probability to deflection parameter LTEA for rigid pavements (9,000 lb (4,086 kg)).

Models Based on Faulting at Joints Performance for Rigid Pavements (9,000 lb (4,086 kg))



1 μm = 0.039 mil

Figure 75. Graph. Sensitivity of faulting at joints acceptable probability to deflection parameter D_6 for rigid pavements (9,000 lb (4,086 kg)).

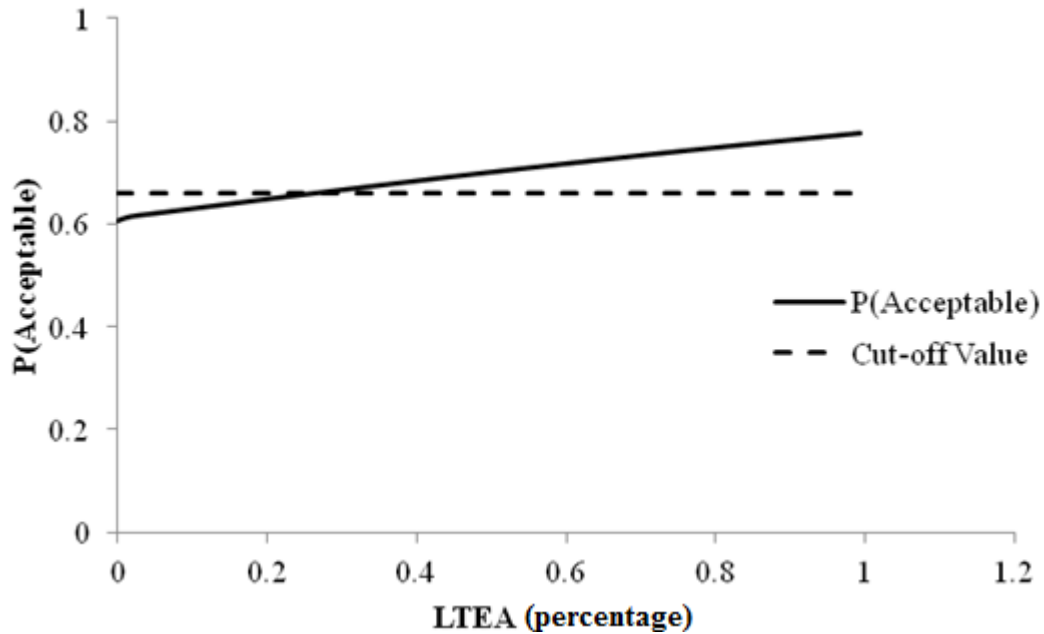
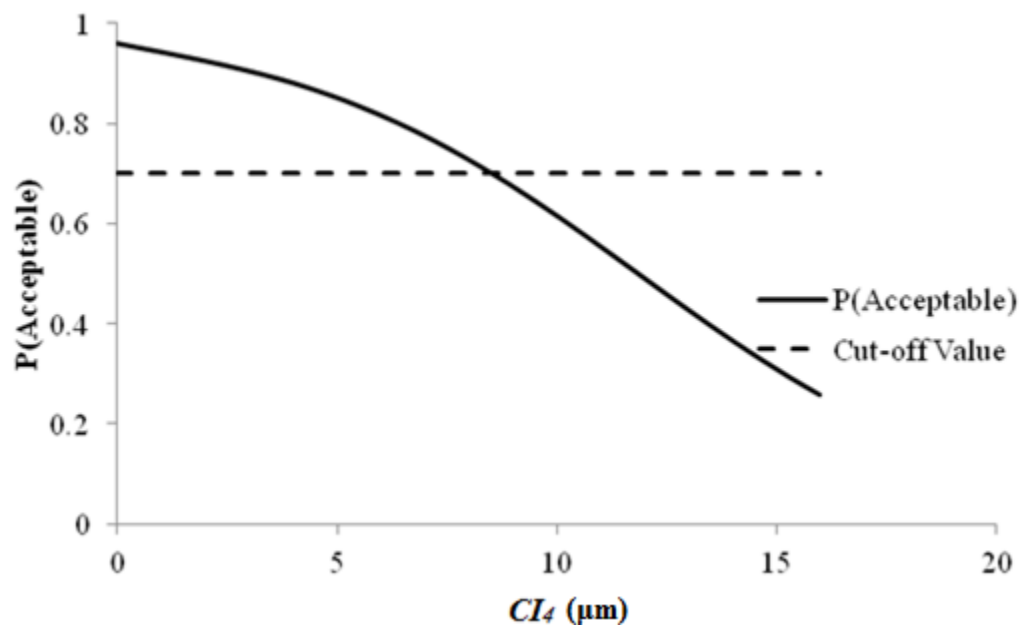


Figure 76. Graph. Sensitivity of faulting at joints acceptable probability to deflection parameter LTEA for rigid pavements (9,000 lb (4,086 kg)).

Models Based on Transverse Cracking Performance for Rigid Pavements (9,000 lb (4,086 kg))



1 μm = 0.039 mil

Figure 77. Graph. Sensitivity of transverse cracking acceptable probability to deflection parameter CI₄ for rigid pavements (9,000 lb (4,086 kg)).

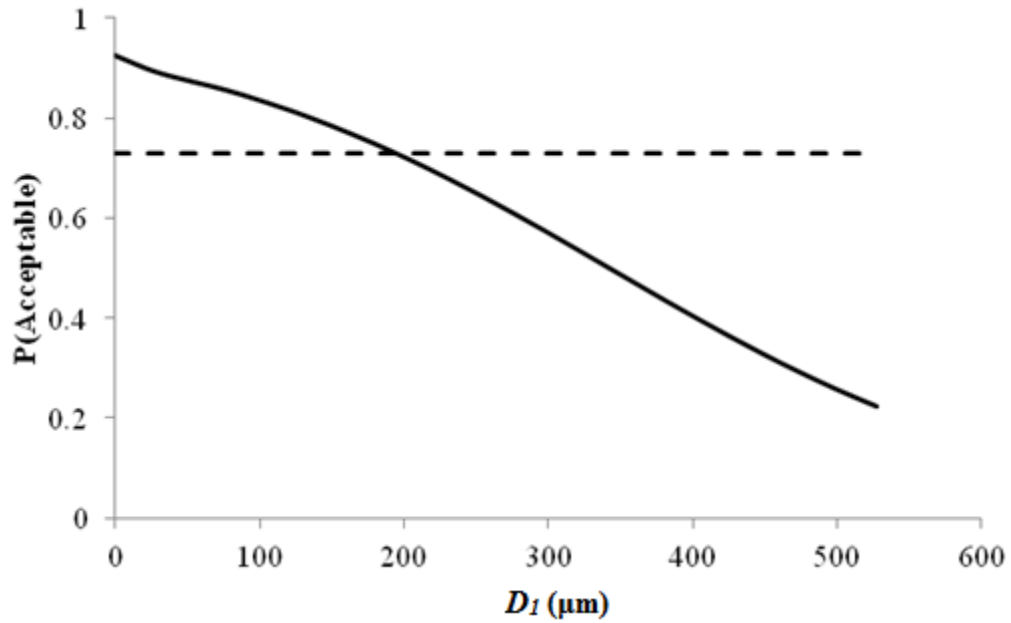


Figure 78. Graph. Sensitivity of transverse cracking acceptable probability to deflection parameter D_I for rigid pavements (9,000 lb (4,086 kg)).

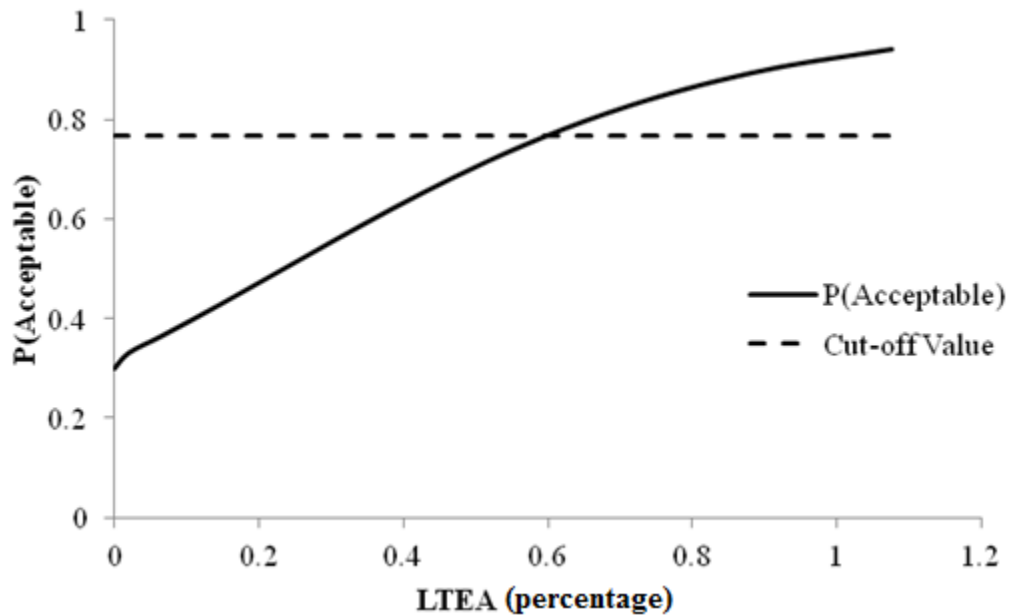


Figure 79. Graph. Sensitivity of transverse cracking acceptable probability to deflection parameter LTEA for rigid pavements (9,000 lb (4,086 kg)).

RIGID PAVEMENT STRUCTURAL ANALYSIS FOR 12,000-LB (5,488-KG) FWD LOAD

Models Based on Roughness Performance for Rigid Pavements (12,000 lb (5,445 kg))

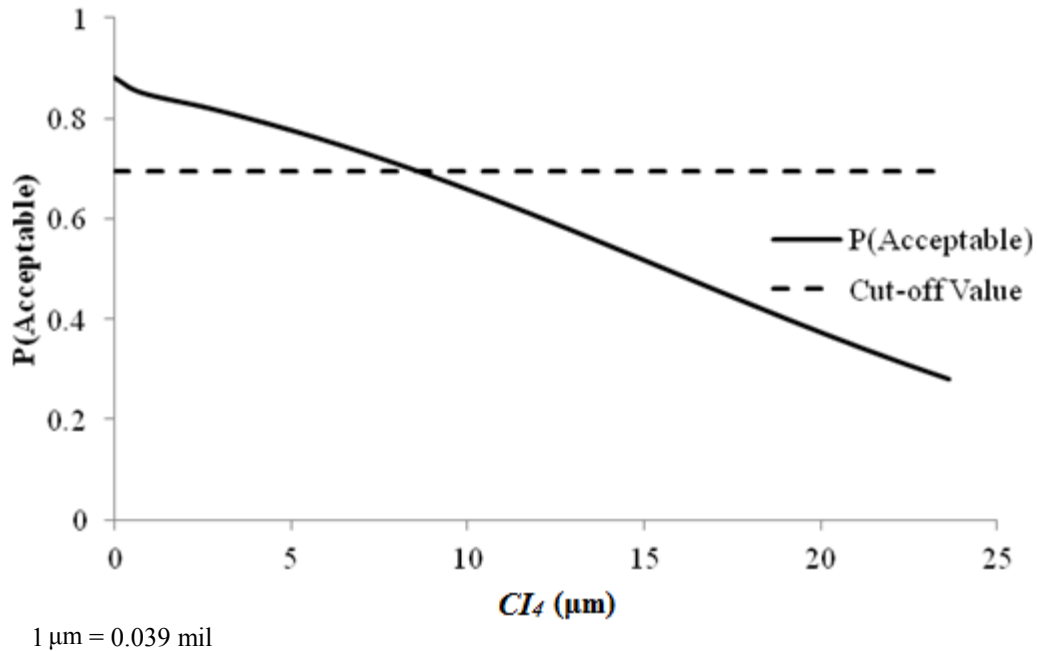


Figure 80. Graph. Sensitivity of roughness acceptable probability to deflection parameter CI_4 for rigid pavements (12,000 lb (5,445 kg)).

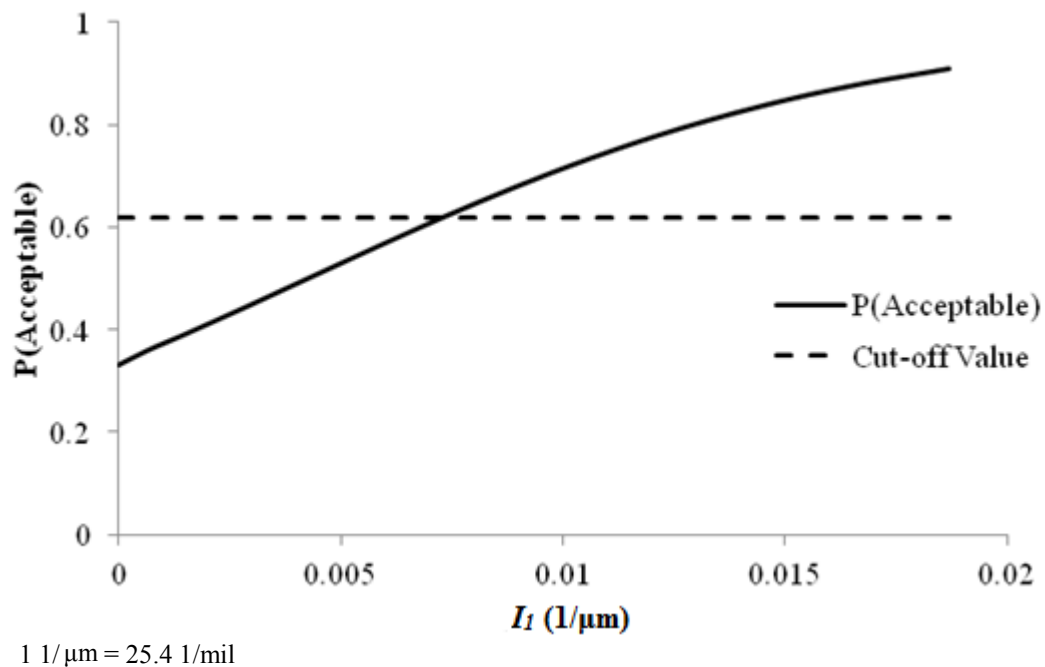


Figure 81. Graph. Sensitivity of roughness acceptable probability to deflection parameter I_1 for rigid pavements (12,000 lb (5,445 kg)).

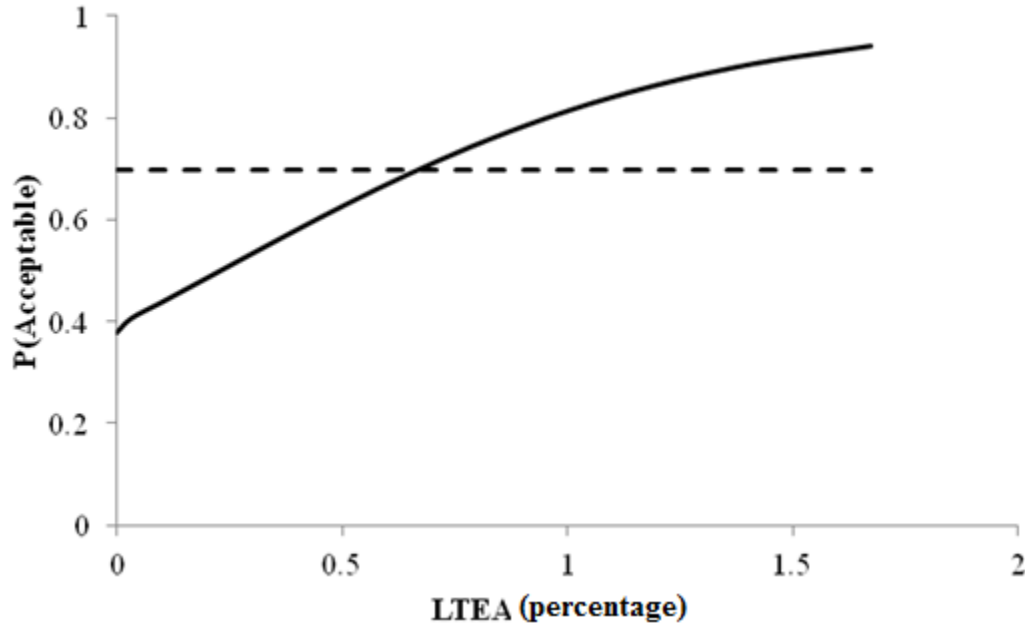
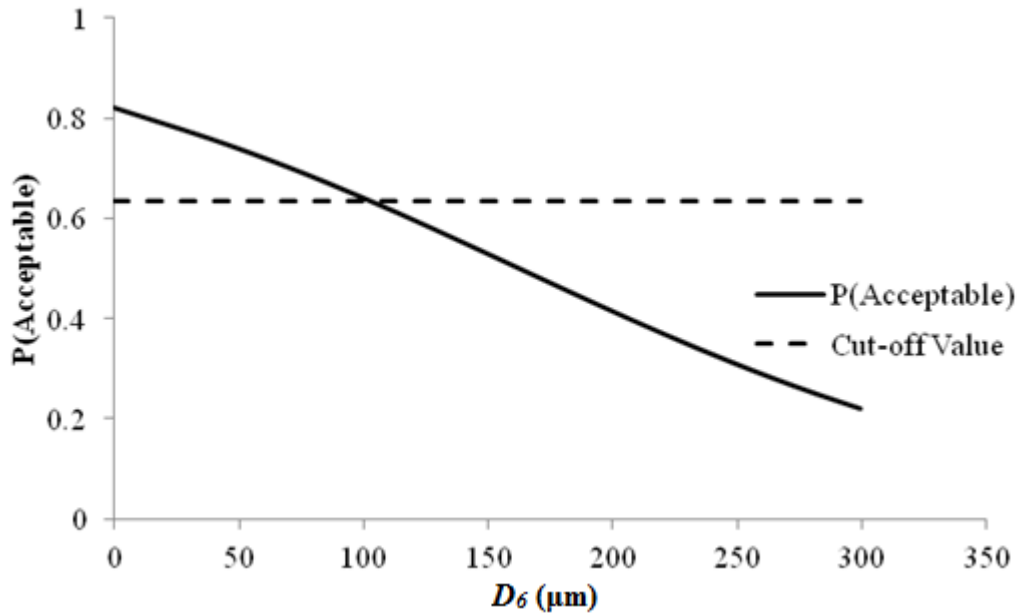


Figure 82. Graph. Sensitivity of roughness acceptable probability to deflection parameter LTEA for rigid pavements (12,000 lb (5,445 kg)).

Models Based on Faulting at Joints Performance for Rigid Pavements (12,000 lb (5,445 kg))



1 μm = 0.039 mil

Figure 83. Graph. Sensitivity of faulting at joints acceptable probability to deflection parameter D_6 for rigid pavements (12,000 lb (5,445 kg)).

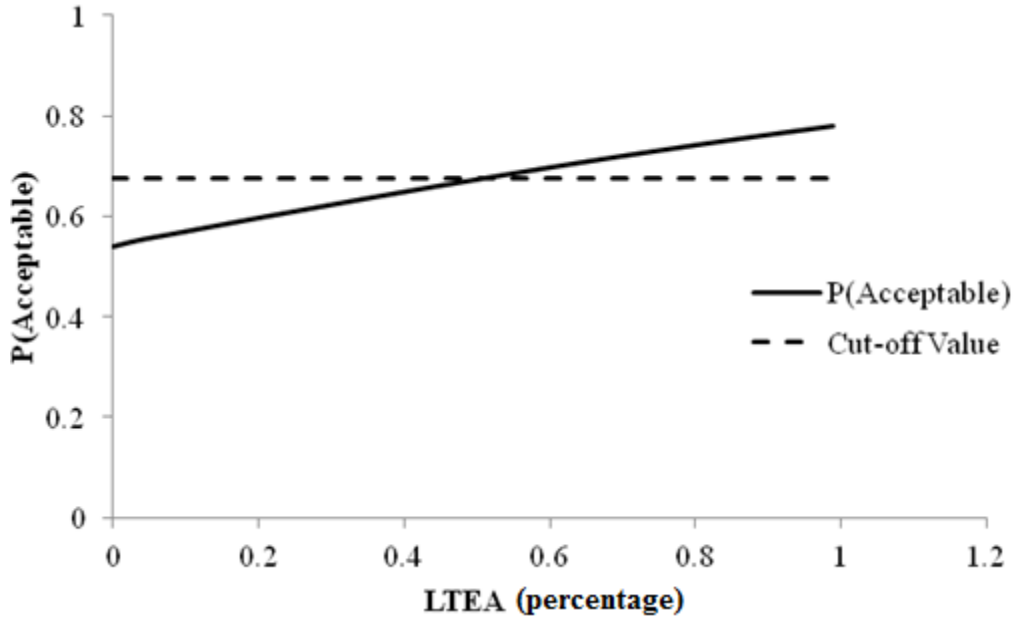
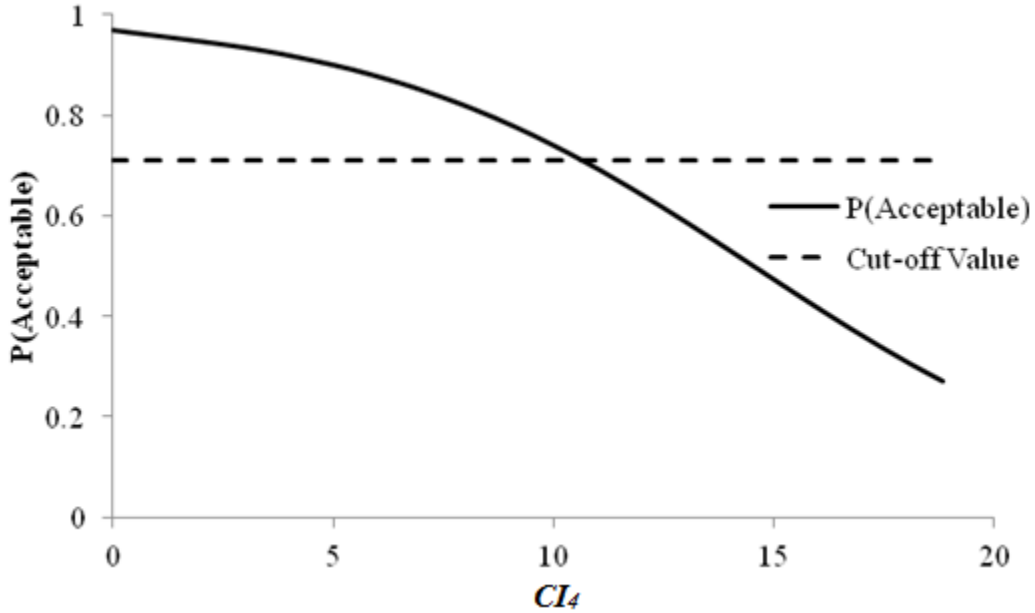


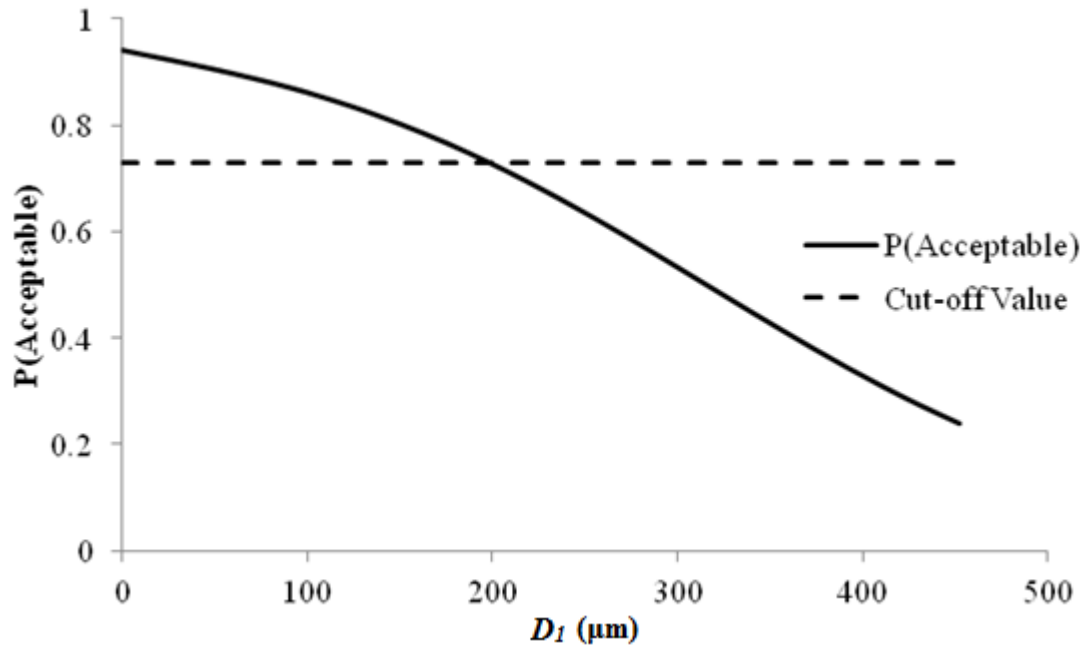
Figure 84. Graph. Sensitivity of faulting at joints acceptable probability to deflection parameter LTEA for rigid pavements (12,000 lb (5,445 kg)).

Models Based on Transverse Cracking Performance for Rigid Pavements (12,000 lb (5,445 kg))



1 μm = 0.039 mil

Figure 85. Graph. Sensitivity of transverse cracking acceptable probability to deflection parameter CI_4 for rigid pavements (12,000 lb (5,445 kg)).



1 μm = 0.039 mil

Figure 86. Graph. Sensitivity of transverse cracking acceptable probability to deflection parameter D_1 for rigid pavements (12,000 lb (5,445 kg)).

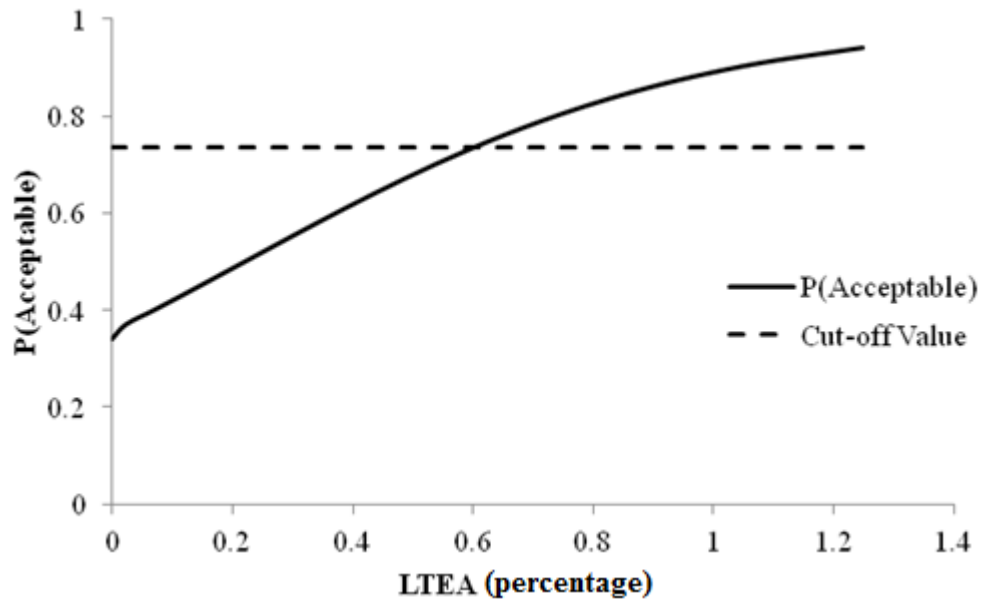


Figure 87. Graph. Sensitivity of transverse cracking acceptable probability to deflection parameter LTEA for rigid pavements (12,000 lb (5,445 kg)).

APPENDIX D

The mechanistic validation was conducted using linear elastic models to predict the responses of the pavement (stresses, strains and deflections) to load. The software KENPAVE, developed by Huang, was used to model typical flexible and rigid pavement structures.⁽²⁸⁾ The mechanistic responses were then used to predict performance using the MEPDG.⁽²⁷⁾

MECHANISTIC-EMPIRICAL ANALYSIS OF FLEXIBLE PAVEMENTS

Several pavement structures were simulated using the KENLAYER computer program, which is part of the KENPAVE software.⁽²⁸⁾ The intention was to evaluate different asphalt concrete and base layer thicknesses at different stiffnesses and different subgrade moduli. A factorial study was designed and is presented in table 18.

The combination of all parameters in the factorial experiment resulted in 1,296 sections. It was necessary to find a common variable for comparing the mechanistic responses among different combinations of the input parameters. The choice was the SN used in the 1993 AASHTO *Guide for Design of Pavement Structures*.⁽⁸⁾

The SN gives a quantitative description of the structural capacity of the different layers in a pavement section. It is a function of layer thicknesses, layer coefficients, and drainage coefficients. The layer coefficients are measures of the relative ability of a unit thickness of a given material to function as a structural component of the pavement. The SN and layer coefficients for a three-layer system can be computed using the following equations:

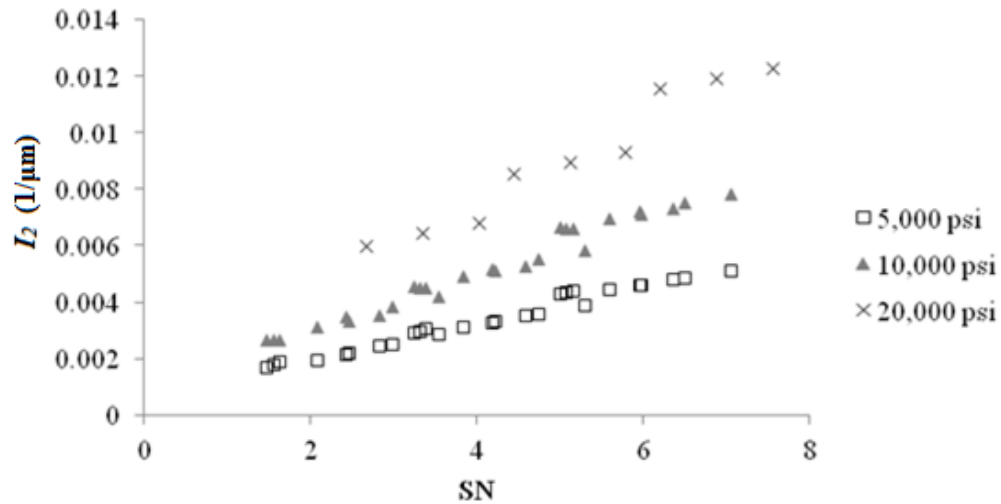
$$SN = a_1 D_1 + a_2 D_2 m_2$$

Figure 88. Equation. Computation of SN.

$$a_2 = 0.249(\log E_2) - 0.977$$

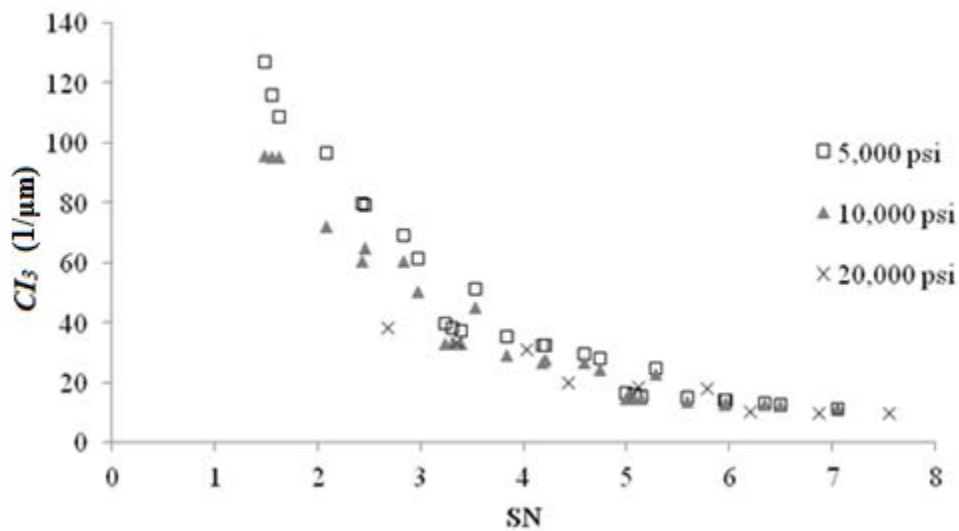
Figure 89. Equation. Computation of the layer coefficient a_2 for base course.

Where a_1 and a_2 are the layer coefficients of the asphalt concrete and base layers, respectively, D_1 and D_2 are the layer thicknesses in inches, and m_2 is the base layer drainage coefficient, assumed as unity for simplicity. SN is a dimensionless variable. In figure 89, E_2 refers to M_r of the base course in pounds per square inch. Figure 90 describes the trends between deflection parameter I_2 and the SN. For simplicity, the data were grouped by subgrade modulus. I_2 is the deflection parameter chosen for the final structural logistic model based on roughness performance. Figure 91 describes the trends between deflection parameter CI_3 and the SN. CI_3 is the deflection parameter chosen for the final structural logistic model based on rutting performance. Figure 92 describes the trends between I_1 and SN. I_1 is the deflection parameter chosen for the final structural logistic model based on fatigue cracking.



$11/\mu\text{m} = 25.4 \text{ 1/mil}$
 $1 \text{ psi} = 6.89 \text{ kPa}$

Figure 90. Graph. Deflection parameter I_2 as a function of SN for a flexible pavement with HMA modulus of 500,000 psi (3,445,000 kPa).



$11/\mu\text{m} = 25.4 \text{ 1/mil}$
 $1 \text{ psi} = 6.89 \text{ kPa}$

Figure 91. Graph. Deflection parameter CI_3 as a function of SN for a flexible pavement with HMA modulus of 500,000 psi (3,445,000 kPa).

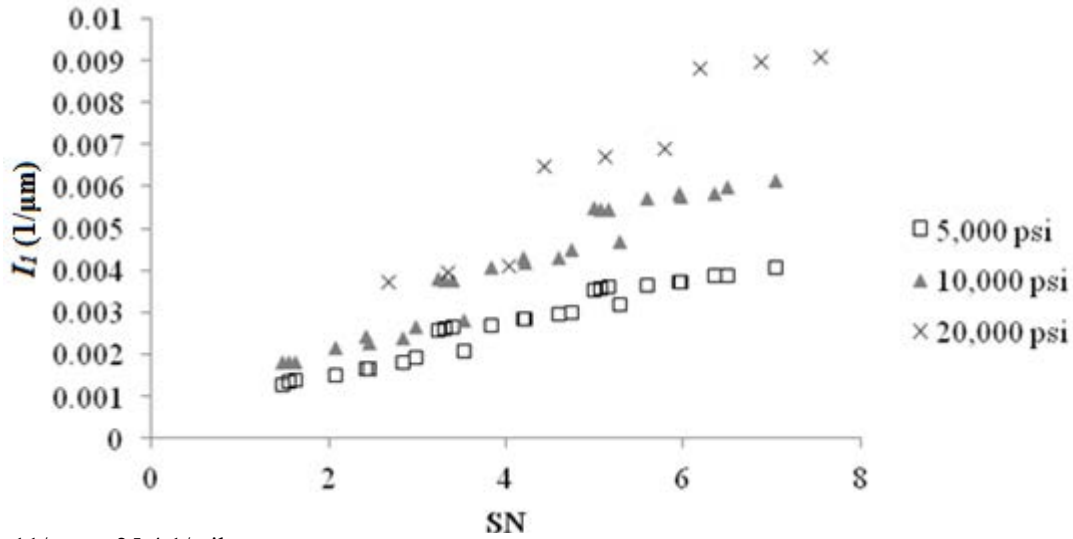


Figure 92. Graph. Deflection parameter I_t as a function of SN for a flexible pavement with HMA modulus of 500,000 psi (3,445,000 kPa).

Comparison with MEPDG Predicted Performance

The MEPDG performance prediction models were used to compare predicted distress performance at the end of the design life with the estimated structural condition obtained from the logistic structural model. This task was accomplished by applying the MEPDG models using the mechanistic responses calculated by KENPAVE.

Two models were considered—rutting and fatigue cracking. At first, the roughness model was also in the scope. However, this particular model requires additional site factors that often dominate the analysis. Therefore, comparison between the outcome of the structural logistic model based on roughness and predicted roughness performance was not included in this exercise. The calculations were performed in Microsoft Excel[®] and not within the MEPDG software due to computational time required to run all scenarios. Since the objective is the comparison and trend evaluation, this assumption had no impact on the outcome or conclusions.

The equation in figure 93 predicts the number of load repetitions to fatigue cracking failure, where ε_t is the tensile strain at the bottom of the asphalt surface layer and E is the elastic modulus of the asphalt layer. k'_1 and C are parameters calculated using equations in figure 94 through figure 96 where V_a is the percentage of air voids and V_b is the percentage of binder content.

$$N_f = 0.00432 k'_1 C \left(\frac{1}{\varepsilon_t} \right)^{3.9492} \left(\frac{1}{E} \right)^{1.281}$$

Figure 93. Equation. Calculation of number of load repetitions to fatigue failure.

$$k_1' = \frac{1}{0.000398 + \frac{0.003602}{1 + e^{11.02 - 3.49h_{ac}}}}$$

Figure 94. Equation. Calculation of correction for different asphalt layer thickness effects.

$$C = 10^M$$

Figure 95. Equation. Calculation of laboratory to field adjustment factor.

$$M = 4.84 \left(\frac{V_b}{V_a + V_b} - 0.69 \right)$$

Figure 96. Equation. Calculation of parameter M .

The damage related to fatigue cracking, D , is computed using the Miner's law and bottom- up cracking in percentage of total lane area is obtained through the equation in figure 97 in which C_1 , C'_1 , C_2 and, C'_2 are constants.

$$FC_{bottom} = \left(\frac{6000}{1 + e^{(C_1 C'_1 + C_2 C'_2 \log_{10}(D * 100))}} \right) \left(\frac{1}{60} \right)$$

Figure 97. Equation. Fatigue cracking prediction.

Figure 32 describes the sensitivity of I_f structural logistic model probability based on fatigue cracking to MEPDG predicted fatigue cracking performance for flexible pavements. The trends agree with expectations; high probabilities of good structural condition are associated with low levels of fatigue cracking. As the probability decreases, the predicted area of fatigue cracking increases.

The analysis using the rutting model was simplified, and only rutting at the asphalt concrete surface layer was used. The current MEPDG model for asphalt concrete rutting is provided in figure 98 where ε_p is the plastic strain, ε_r is the elastic strain, T is temperature (Fahrenheit), N is the number of load applications, and k_1 is a constant that depends on depth at which the elastic strain is calculated and is given by equations in figure 99 and figure 100. The total rutting in the asphalt layer is calculated by integrating the calculated plastic strain over the thickness of the layer.

$$\frac{\varepsilon_p}{\varepsilon_r} = k_1 * 10^{-3.35412} T^{1.5606} N^{0.4791}$$

Figure 98. Equation. Calculation of permanent deformation.

$$k_1 = (C_1 + C_2 * depth) * 0.328196^{depth}$$

Figure 99. Equation. Calculation of k_1 .

$$C_1 = -0.1039 * h_{ac}^2 + 2.4868 * h_{ac} - 17.342$$

$$C_2 = 0.0172 * h_{ac}^2 - 1.7331 * h_{ac} + 27.428$$

Figure 100. Equation. Calculation of C_1 and C_2 .

Figure 101 describes the sensitivity of CI_3 structural logistic model probability based on rutting to MEPDG predicted AC rutting performance for flexible pavements. In this plot, the trends agree with expectations; high probabilities of good structural condition are associated with small permanent deformation. As the probability decreases, predicted AC rutting increases.

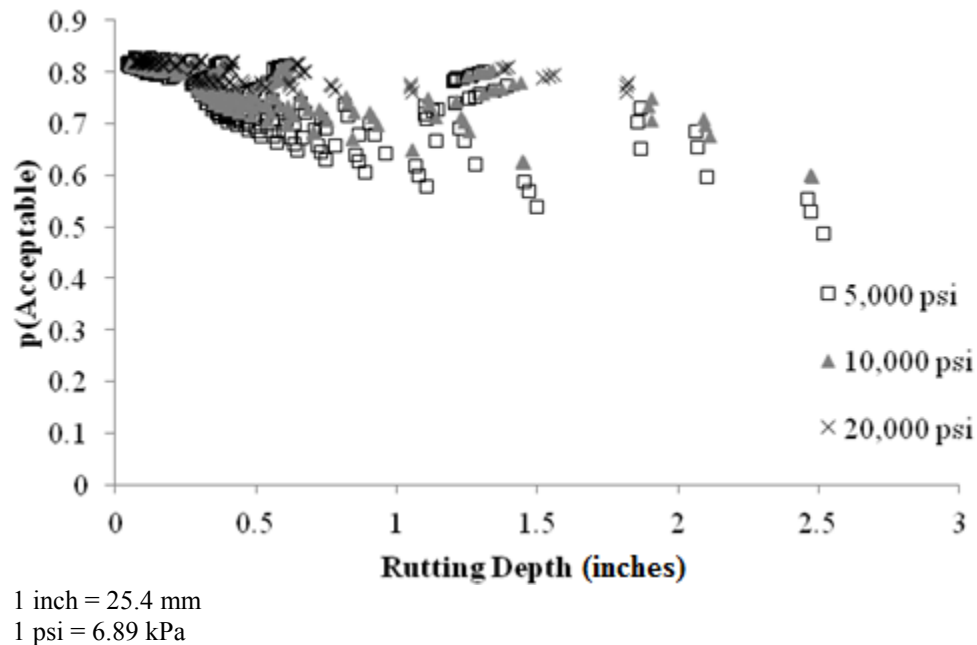


Figure 101. Graph. Sensitivity of CI_3 structural logistic model probability based on rutting performance to MEPDG predicted rutting for flexible pavements.

MECHANISTIC-EMPIRICAL ANALYSIS OF RIGID PAVEMENTS

Several pavement structures were simulated using the KENSLAB computer program, which is part of the KENPAVE software. The intention was to evaluate different JPCP slab thicknesses and subgrade moduli and the consequences to the outcome of the structural logistic models. A factorial study was designed and is presented in table 19.

The deflection parameters of the best logistic models developed were computed for the structures simulated in the factorial experiment. Only the FWD test at the center of the slab was evaluated. The objective was to verify if trends would agree with expected outcomes from the models. At first, the deflection parameters were plotted against the slab thickness (i.e., considered as reference for the strength of the pavement section). Figure 31 shows the trends between deflection parameter I_1 and slab thickness for three subgrade moduli. I_1 was chosen for the final structural logistic model based on roughness performance. The results indicate that I_1 increased as slab thickness increased, as expected.

Figure 102 shows the trends between deflection parameter D_6 and slab thickness. D_6 was chosen for the final structural logistic model based on faulting performance. D_6 is decreased as slab thickness increased, as expected. However, the sensitivity reduced when the subgrade modulus was stiffer.

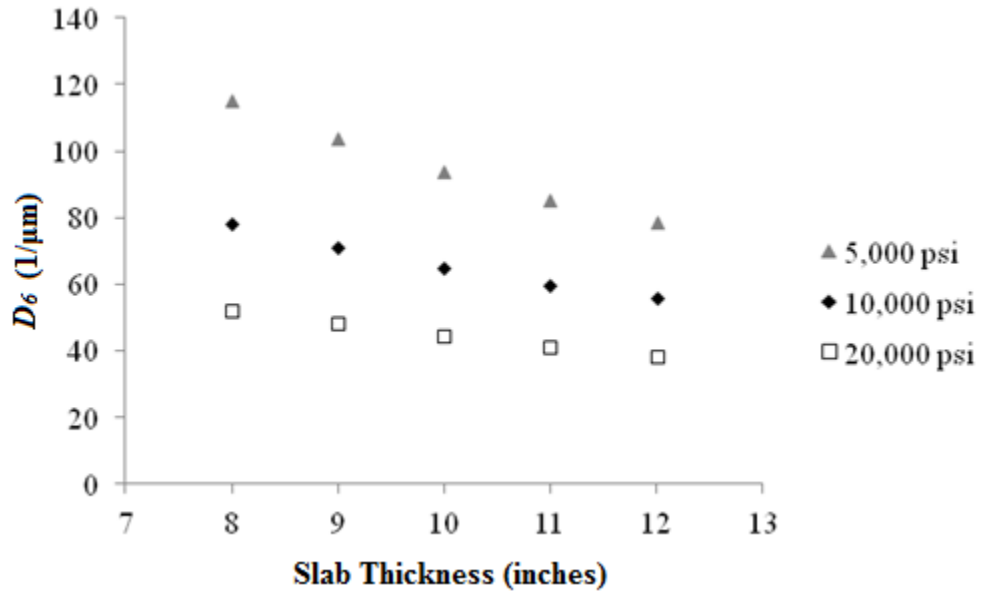


Figure 102. Graph. Sensitivity of deflection parameter D_6 to slab thickness.

Figure 103 shows the trends between CI_4 and slab thickness. CI_4 was chosen for the final structural logistic model based on transverse slab cracking. CI_4 is sensitive to slab thickness, and the trend indicates that the value decreased as slab thickness increased, as expected.

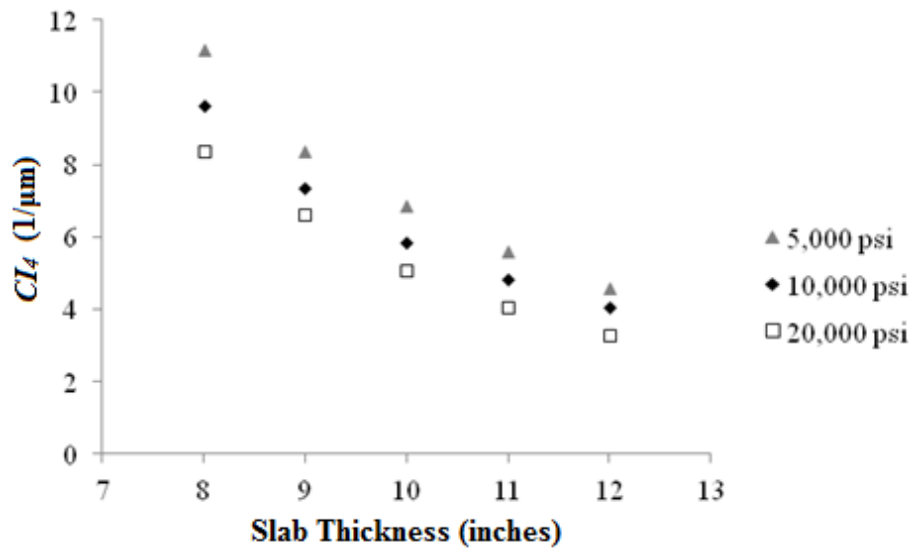


Figure 103. Graph. Sensitivity of deflection parameter CI_4 to slab thickness.

Comparison with MEPDG Predicted Performance

In the case of rigid pavements, the MEPDG was used to generate the performance predictions. There were only 15 scenarios to run, and the rigid pavement analysis was performed much faster than the flexible pavement analysis.

Figure 33 shows the sensitivity of I_1 structural logistic model probability based on roughness to the MEPDG predicted roughness performance for rigid pavements. It can be seen that the trends agree with expectations; high probabilities of good structural condition are associated with low values of IRI. As the probability decreased, the predicted IRI increased. This plot confirms that the structural logistic model is capable of providing an assessment of structural condition that is tied to an expectation of performance.

Figure 104 shows the sensitivity of D_6 structural logistic model probability based on faulting to MEPDG predicted faulting performance for rigid pavements. Again in this plot, the trends agree with expectations; high probabilities of good structural condition are associated with low faulting values. As the probability decreases, predicted joint faulting increases. It is important to note that in this particular model, although the trends agree with expectation, the variation in probability of acceptable structural condition is small when compared to previous models.

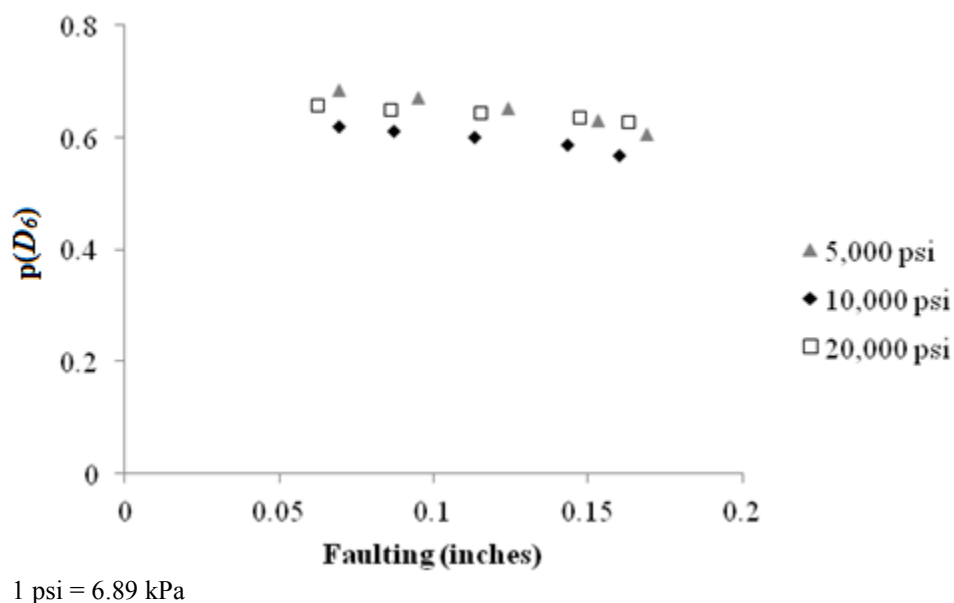


Figure 104. Graph. Sensitivity of D_6 structural logistic model probability based on faulting performance to MEPDG predicted faulting for rigid pavements.

Figure 105 shows the sensitivity of CI_4 structural logistic model probability based on slab cracking to MEPDG predicted slab cracking performance for rigid pavements. The x-axis is presented in log scale to improve the visualization. The trends agree with expectations; high probabilities of good structural condition are associated with low to no slab cracking. As the probability decreases, predicted percentage of cracked slab increases.

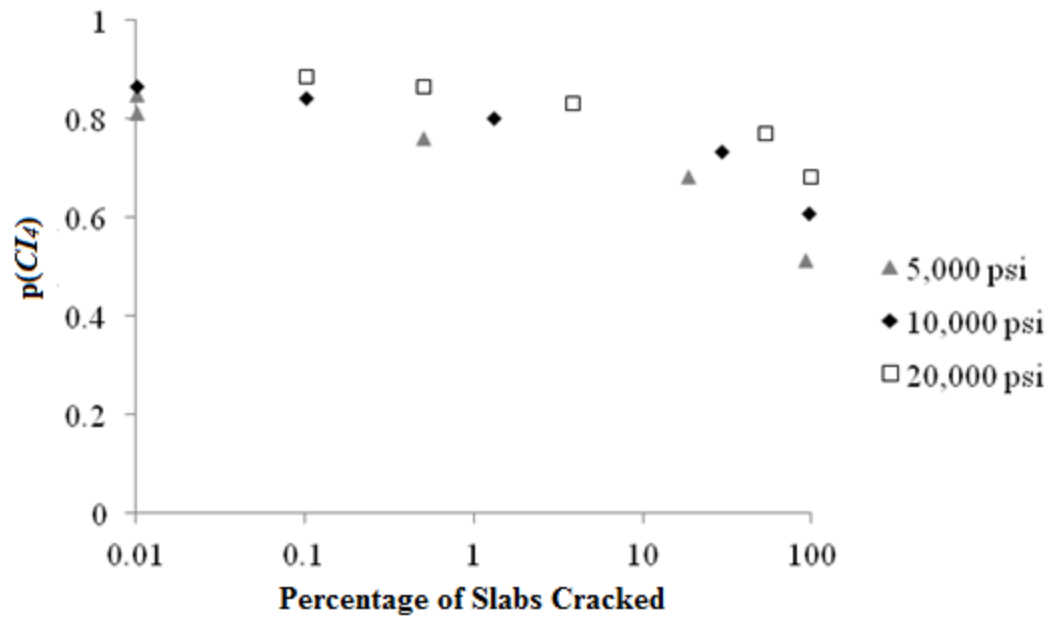


Figure 105. Graph. Sensitivity of CI_4 structural logistic model probability based on slab cracking performance to MEPDG predicted slab cracking for rigid pavements.

APPENDIX E

Table 106. Information about the different States used in the analysis.

State	Section ID	AC Thickness (inches)	Mean Deflection (mils)	Standard Deviation	Length (mi)	Test Spacing (mi)
New Mexico	US70 EB	6	7.54	1.89	2.3	0.1
		6.8	7.06	2.17	37.6	0.1
		7	6.3	2.117	19.8	0.1
	US70 WB	5.5	8.26	1.952	3.1	0.1
		9.2	9.72	2.435	16.5	0.1
		5	7.36	2.214	37.7	0.1
		5.5	7.08	2.811	4.3	0.1
		5.5	7.22	2.289	15.3	0.1
	US550 NB	9.71	7.87	1.268	6.8	0.1
		9.94	7.64	3.449	15.8	0.1
		9.43	5.5	1.835	10.3	0.1
		9.95	4.68	1.047	6.3	0.1
		9.15	7.2	2.657	21.4	0.1
		9.46	11.34	4.379	14	0.1
		9.35	4.33	1.381	9.7	0.1
		9.77	4.49	1.294	16.1	0.1
		9.49	5.75	0.76	16.4	0.1
	US550 SB	13.4	10.7	3.775	19.8	0.1
		9.6	7.2	2.748	8.5	0.1
		9.61	7	3.566	29.3	0.1
		9.4	10.9	5.232	5.6	0.1
		9.6	5.8	3.347	37.7	0.1
		9.7	5.7	0.857	15.7	0.1
Oregon	I-5		7.151	2.421	0.9	0.1
	OR38		10.442	3.728	8.65	0.1
	US101		13.794	4.466	3.35	0.1
			16.869	6.663	8.65	0.1
	OR18		7.386	2.713	37	0.1
	OR221		22.482	6.691	16.7	0.1
	OR99E		6.948	2.272	2.2	0.1
			7.192	2.553	2.2	0.1
			9.402	4.075	9.85	0.1
	US26		6.675	1.88	1.5	0.1
			4.308	2.263	1.6	0.1
			8.907	3.391	4.95	0.1
			9.376	2.272	5.35	0.1
	US97		8.9	2.945	4.25	0.1

Kansas	4	8	13.87	4.114	6.3	0.1
		8	14.06	3.837	5.2	0.1
		8.7	10.6	2.336	3.9	0.1
		7.3	12.93	3.305	2.9	0.1
		5.7	11.14	3.447	2.1	0.1
	56	13	8.37	3.212	5.9	0.1
		14.5	5.17	1.254	8.4	0.1
		11.5	9.76	2.591	12.9	0.1
	99	10.2	11.85	2.539	8.1	0.1
		7.7	15.26	4.628	5.1	0.1
		7.1	14.42	3.886	2.8	0.1
		7	16.98	3.669	7.3	0.1
		7.8	15.86	3.523	7.6	0.1
		9.2	10.88	3.387	2.3	0.1
	170	13.1	6.24	2.879	1.9	0.1
		7.1	15.2	4.851	10.5	0.1
		8.2	15.9	3.338	7.2	0.1
	56	9	9.06	2.257	5.7	0.1
	31	6.4	13.97	3.135	9.7	0.1
		7.7	14.91	5.287	4.3	0.1
	56	7.5	11.43	3.539	3.7	0.1
		8.8	8.26	2.3	8.8	0.1
	59	7.4	9.66	3.702	7.3	0.1
		12	5.32	1.642	6.2	0.1
		12.1	9.28	4.273	2.9	0.1
		12.9	7	2.59	3.9	0.1
		13.8	5.36	2.473	7.9	0.1
		10.5	6.54	1.886	6.1	0.1
	39	4.9	16.78	4.818	6.7	0.1
		5	18.2	3.728	1.8	0.1
		6.3	14.97	7.157	4.7	0.1
	75	5	14.07	3.855	2.9	0.1
		8.9	10.4	2.338	7.5	0.1
	54	9.2	7.34	2.399	5.3	0.1
	58	8	10.65	3.659	9.4	0.1
		6.9	11.64	3.354	11.6	0.1

	75	7.2	4.27	0.782	3.9	0.1
		17.5	8.35	2.14	4.2	0.1
		15.7	7.3	1.732	3.9	0.1
		10.8	5.51	1.754	4.1	0.1
		11.2	7.32	2.975	11.9	0.1
		11.2	5.18	1.377	2.2	0.1
		14.4	6.16	1.423	1.9	0.1
		10.8	6.29	1.589	4.9	0.1

Note: Blank cells indicate that no thickness was available.

1 inch = 25.4 mm

1 μm = 0.039 mil

1 mile = 1.61 km

Table 107. Errors in percentage for 50, 70, and 80 percent reliability for section lengths up to 10 mi (16.1 km).

Probability	Length (mi)	Spacing (mi)								
		0.2	0.3	0.4	0.5	0.6	0.7	0.8	0.9	1
50 percent	1	8.98	11.77	14.27	16.57	18.72	20.75	22.69	24.55	26.34
	2	6.39	8.34	10.06	11.64	13.12	14.51	15.84	17.11	18.33
	3	5.24	6.81	8.20	9.47	10.66	11.77	12.84	13.85	14.83
	4	4.55	5.90	7.09	8.18	9.20	10.15	11.06	11.92	12.76
	5	4.08	5.28	6.34	7.30	8.20	9.05	9.85	10.61	11.35
	6	3.73	4.82	5.78	6.66	7.47	8.23	8.96	9.65	10.32
	7	3.46	4.46	5.35	6.15	6.90	7.60	8.27	8.91	9.52
	8	3.24	4.17	5.00	5.75	6.44	7.10	7.72	8.31	8.88
	9	3.05	3.93	4.71	5.41	6.07	6.68	7.26	7.81	8.35
	10	2.90	3.73	4.46	5.13	5.75	6.33	6.87	7.40	7.90
70 percent	1	11.11	14.30	17.12	19.70	22.10	24.36	26.50	28.56	30.53
	2	7.91	10.12	12.07	13.85	15.50	17.04	18.51	19.91	21.26
	3	6.48	8.27	9.84	11.27	12.59	13.83	15.00	16.12	17.20
	4	5.63	7.17	8.51	9.73	10.86	11.92	12.93	13.88	14.80
	5	5.04	6.41	7.61	8.69	9.69	10.63	11.52	12.36	13.17
	6	4.61	5.85	6.94	7.92	8.83	9.67	10.48	11.24	11.97
	7	4.28	5.42	6.42	7.32	8.15	8.94	9.67	10.37	11.05
	8	4.00	5.07	6.00	6.84	7.62	8.34	9.03	9.68	10.30
	9	3.78	4.78	5.65	6.44	7.17	7.85	8.49	9.10	9.69
	10	3.59	4.54	5.36	6.11	6.79	7.43	8.04	8.62	9.17
80 percent	1	12.39	15.83	18.85	21.59	24.14	26.54	28.81	30.99	33.07
	2	8.82	11.21	13.29	15.18	16.93	18.57	20.13	21.61	23.03
	3	7.23	9.16	10.83	12.35	13.76	15.07	16.32	17.50	18.63
	4	6.28	7.93	9.37	10.67	11.87	13.00	14.06	15.07	16.03
	5	5.63	7.10	8.37	9.53	10.59	11.58	12.52	13.42	14.27
	6	5.15	6.48	7.64	8.68	9.65	10.55	11.40	12.20	12.97
	7	4.77	6.00	7.07	8.03	8.91	9.74	10.52	11.26	11.97
	8	4.47	5.61	6.61	7.50	8.32	9.09	9.82	10.51	11.16
	9	4.22	5.29	6.22	7.06	7.84	8.56	9.24	9.88	10.50
	10	4.00	5.02	5.90	6.70	7.42	8.10	8.75	9.36	9.94

1 mi = 1.61 km

Table 108. Errors in percentage for 90, 95, and 99.5 percent reliability for section lengths up to 10 mi (16.1 km).

Probability	Length (mi)	Spacing (mi)								
		0.2	0.3	0.4	0.5	0.6	0.7	0.8	0.9	1
90 percent	1	14.18	17.94	21.24	24.22	26.98	29.57	32.02	34.35	36.59
	2	10.10	12.71	14.98	17.03	18.93	20.70	22.37	23.96	25.48
	3	8.28	10.38	12.21	13.86	15.38	16.80	18.13	19.41	20.62
	4	7.19	9.00	10.56	11.97	13.27	14.48	15.63	16.71	17.75
	5	6.44	8.05	9.44	10.69	11.84	12.91	13.92	14.88	15.80
	6	5.89	7.35	8.61	9.74	10.78	11.75	12.67	13.54	14.36
	7	5.46	6.80	7.97	9.01	9.97	10.86	11.70	12.49	13.25
	8	5.11	6.36	7.45	8.42	9.31	10.14	10.92	11.66	12.36
	9	4.82	6.00	7.02	7.93	8.76	9.54	10.27	10.96	11.62
	10	4.58	5.69	6.65	7.51	8.30	9.03	9.72	10.38	11.00
95 percent	1	15.65	19.69	23.21	26.39	29.32	32.07	34.66	37.13	39.50
	2	11.15	13.95	16.37	18.56	20.57	22.45	24.22	25.90	27.51
	3	9.14	11.40	13.35	15.10	16.72	18.22	19.64	20.98	22.27
	4	7.93	9.87	11.55	13.05	14.43	15.71	16.92	18.07	19.16
	5	7.11	8.83	10.32	11.65	12.87	14.01	15.08	16.09	17.06
	6	6.50	8.07	9.41	10.62	11.72	12.75	13.72	14.64	15.51
	7	6.03	7.47	8.71	9.82	10.83	11.78	12.67	13.51	14.31
	8	5.64	6.99	8.14	9.17	10.12	11.00	11.82	12.60	13.35
	9	5.33	6.59	7.67	8.64	9.53	10.35	11.12	11.86	12.55
	10	5.06	6.25	7.27	8.19	9.03	9.80	10.53	11.22	11.88
99.5 percent	1	19.43	24.17	28.27	31.95	35.33	38.48	41.44	44.26	46.94
	2	13.84	17.12	19.95	22.47	24.79	26.94	28.96	30.88	32.71
	3	11.34	13.99	16.26	18.29	20.15	21.87	23.49	25.02	26.48
	4	9.85	12.12	14.07	15.80	17.39	18.86	20.24	21.55	22.79
	5	8.83	10.85	12.57	14.11	15.51	16.82	18.04	19.19	20.29
	6	8.07	9.90	11.47	12.86	14.13	15.31	16.41	17.46	18.45
	7	7.48	9.17	10.61	11.89	13.06	14.14	15.16	16.11	17.02
	8	7.01	8.58	9.92	11.11	12.20	13.20	14.14	15.03	15.88
	9	6.61	8.09	9.35	10.47	11.48	12.43	13.31	14.14	14.93
	10	6.28	7.67	8.86	9.92	10.88	11.77	12.60	13.39	14.14

1 mi = 1.61 km

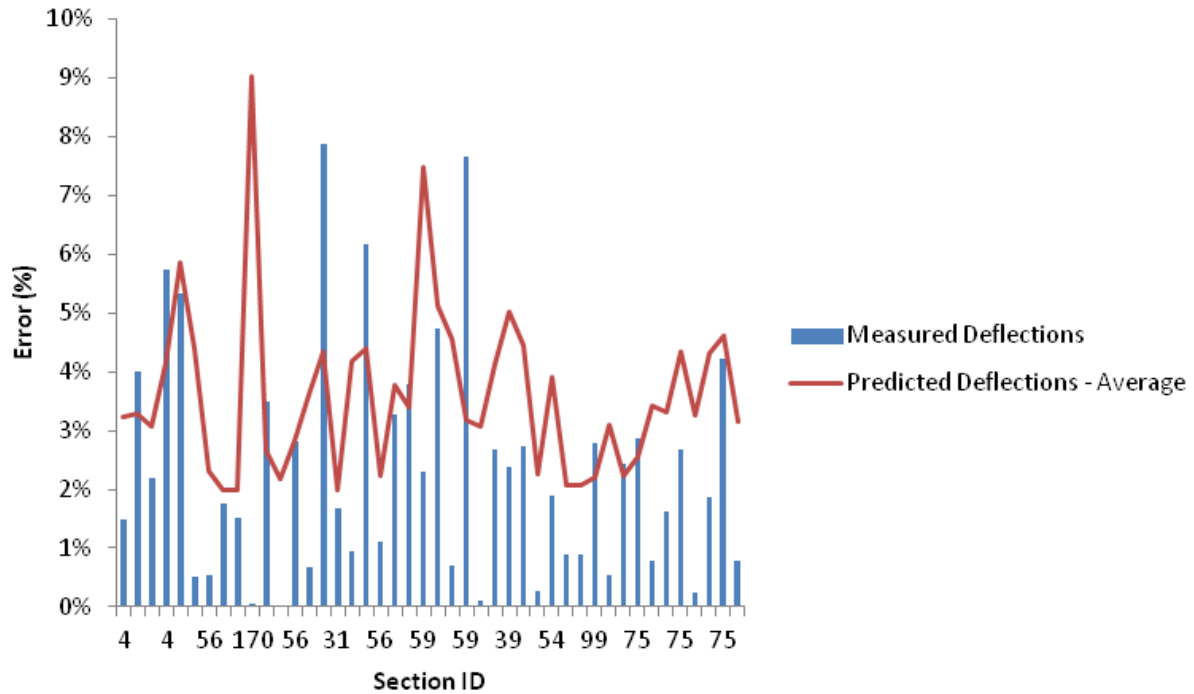


Figure 106. Graph. Comparison between measured error and predicted error for all Kansas sections at 0.2-mi (0.322-km) spacing.

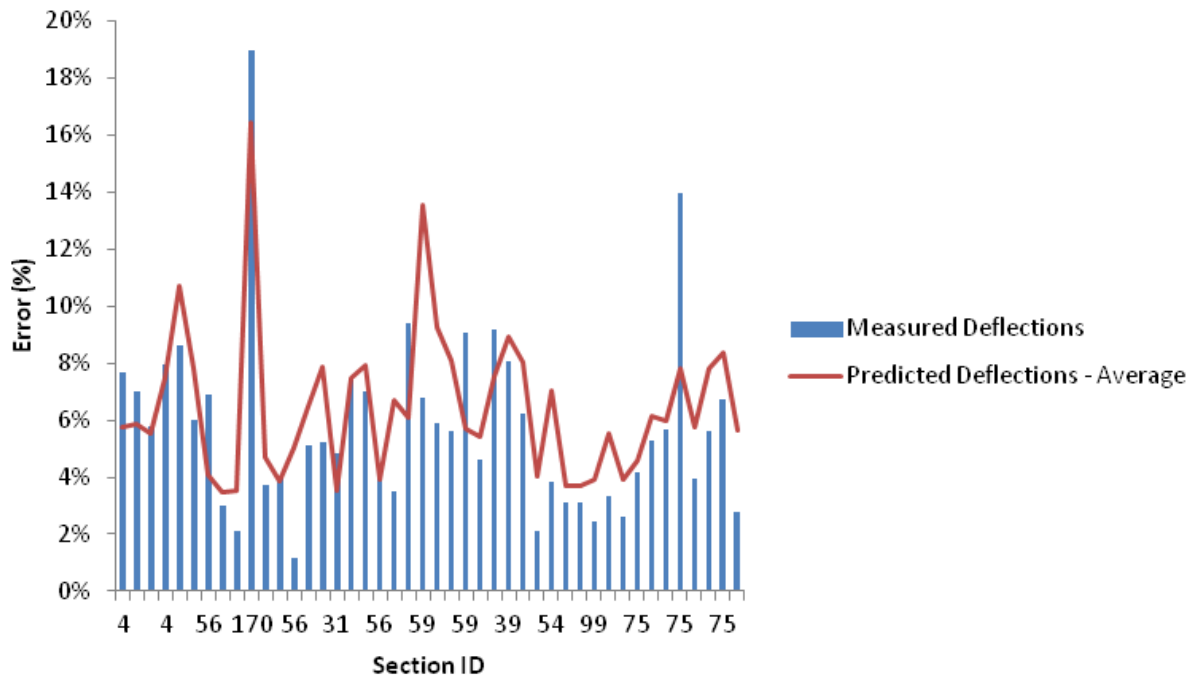


Figure 107. Graph. Comparison between measured error and predicted error for all Kansas sections at 0.5-mi (0.805-km) spacing.

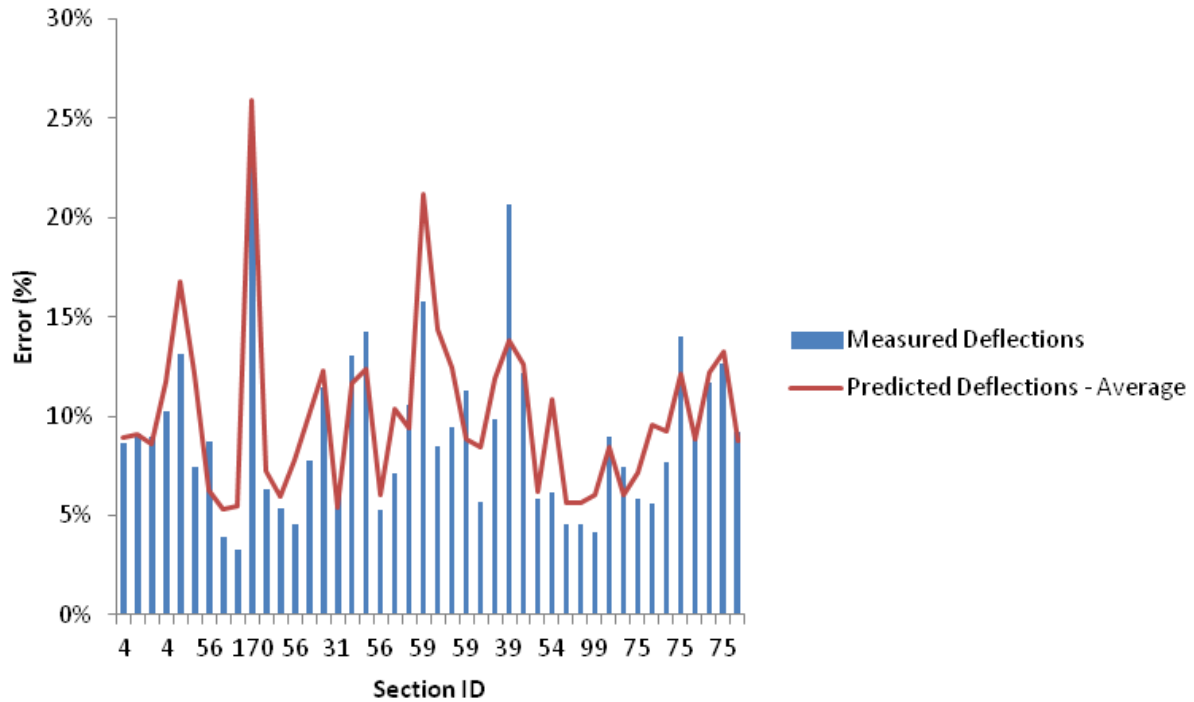


Figure 108. Graph. Comparison between measured error and predicted error for all Kansas sections at 1-mi (1.61-km) spacing.

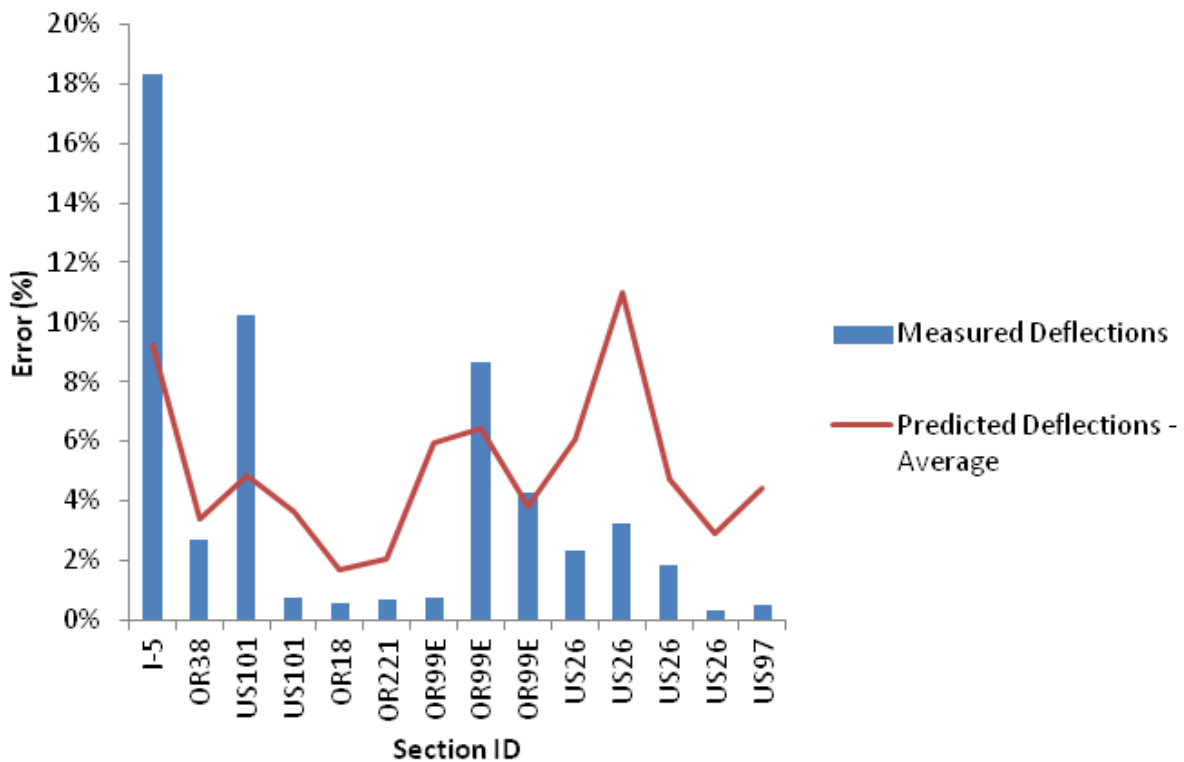


Figure 109. Graph. Comparison between measured error and predicted error for all Oregon sections at 0.2-mi (0.322-km) spacing.

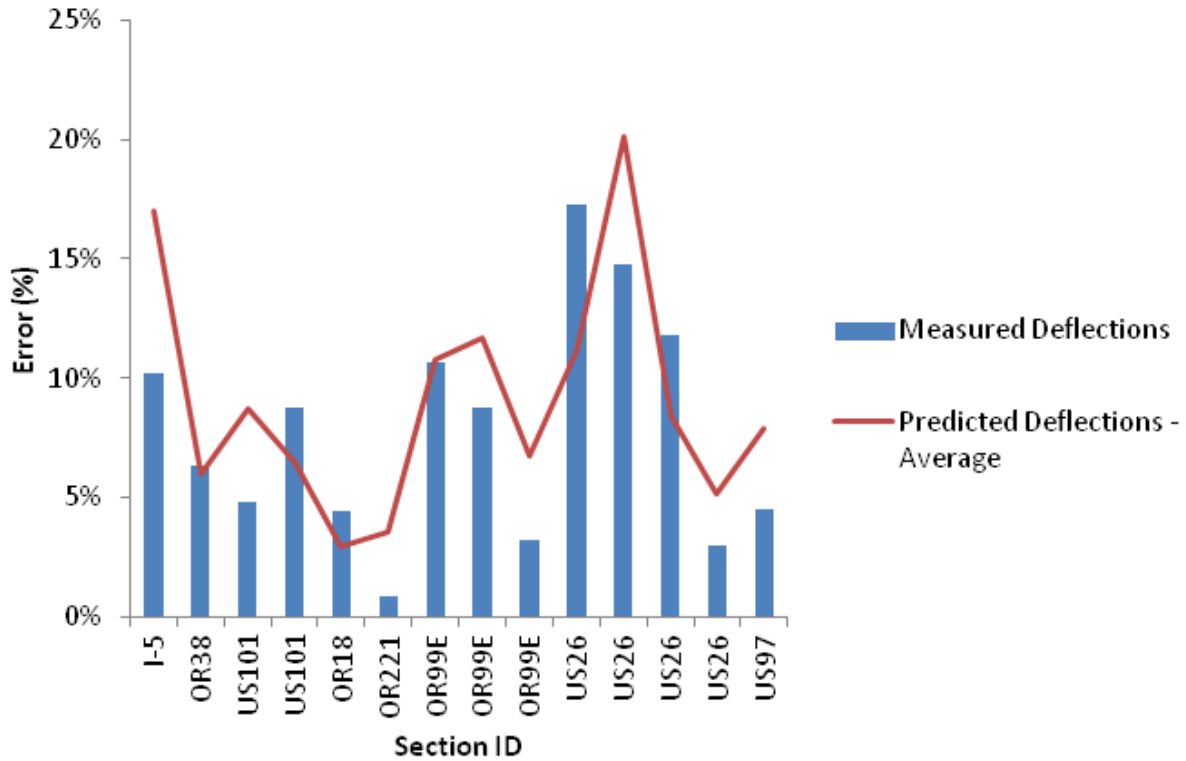


Figure 110. Graph. Comparison between measured error and predicted error for all Oregon sections at 0.5-mi (0.805-km) spacing.

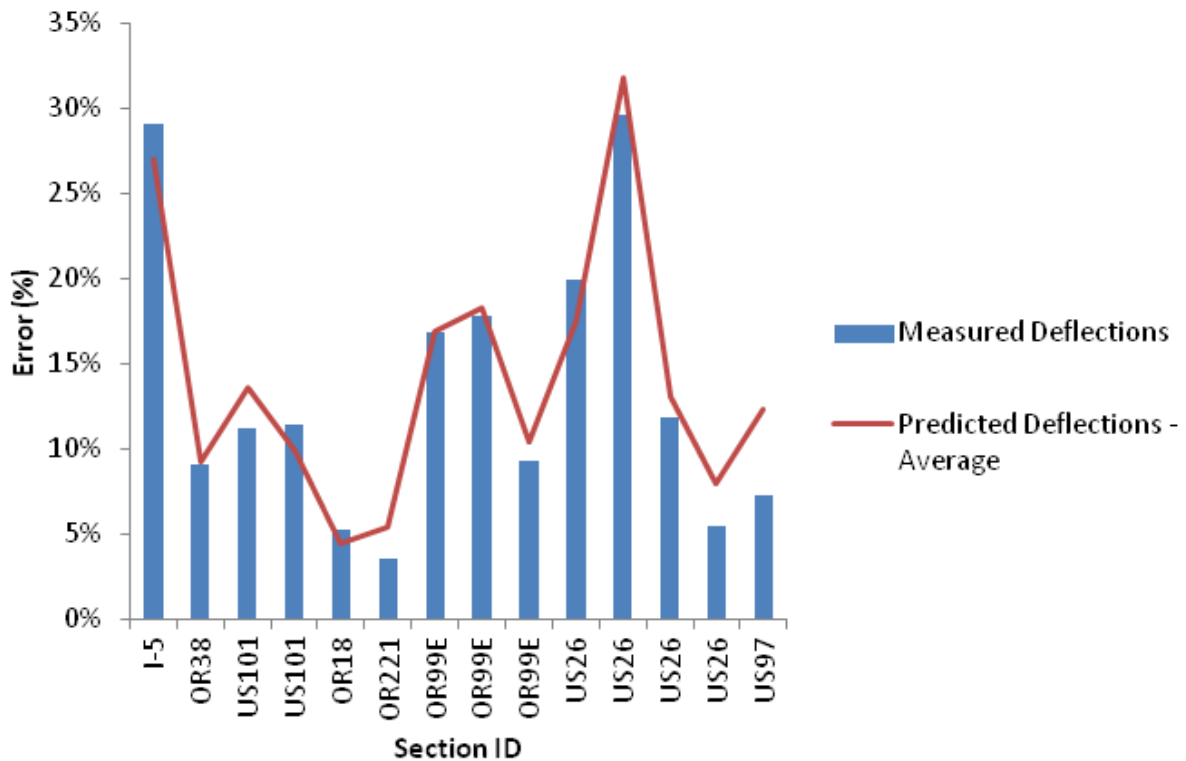


Figure 111. Graph. Comparison between measured error and predicted error for all Oregon sections at 1-mi (1.61-km) spacing

APPENDIX F

Table 109. Description of the Maryland sections used in the example.

ID	Road Name	Mile Post Initial	Mile Post End	HMA Thickness (inches)	Total Thickness (inches)	Bound Layer	AADTT	Class 5 (percent)	Class 9 (percent)	Road Classification	Pavement Age at the Time of FWD Testing	FWD Test Date
1	IS 68 E	37.25	40.27	11.96	23.96	No	4186	20.85	47.43	Rural interstate	9	5/23/2007
2	IS 68 W	37.25	38.2	9	23	No	4186	20.85	47.43	Rural interstate	9	5/23/2007
3	IS 68 W	38.2	40.27	11.38	23.38	No	4186	20.85	47.43	Rural interstate	9	5/23/2007
4	I 68 E	4.76	7.6	15	19	No	3926	27.43	39.54	Urban interstate	11	6/10/2008
5	I 68 E	7.6	8.05	16.5	20.5	No	3926	27.43	39.54	Urban interstate	11	6/10/2008
6	US 40 W	0.37	1.78	7.5	15.5	No	12.5	52.01	8.25	Rural minor collector	15	9/24/2008
7	US 40 W	1.78	4.3	7	15	No	12.5	52.01	8.25	Rural minor collector	18	9/24/2008
8	US 40 W	4.3	5.77	6.5	14.5	No	12.5	52.01	8.25	Rural minor collector	16	9/24/2008
9	US 40 E	0.37	1.78	7.5	15.5	No	12.5	52.01	8.25	Rural minor collector	15	9/24/2008
10	US 40 E	1.78	4.3	7	15	No	12.5	52.01	8.25	Rural minor collector	18	9/24/2008
11	US 40 E	4.3	5.77	6.5	14.5	No	12.5	52.01	8.25	Rural minor collector	16	9/24/2008
12	MD 2 S	8.06	9.9	6	15	No	1944	47.74	15.3	Rural minor arterial	9	7/23/2007
13	MD 2 S	9.9	11.8	6.5	15.5	No	1944	47.74	15.3	Rural minor arterial	10	7/23/2007
14	MD 2 S	11.8	12.04	5.5	17.5	No	1944	47.74	15.3	Rural minor arterial	10	7/23/2007
15	MD 2 N	8.06	9.9	6	15	No	1944	47.74	15.3	Rural minor arterial	9	7/10/2007
16	MD 2 N	9.9	11.8	6.5	15.5	No	1944	47.74	15.3	Rural minor arterial	11	7/23/2007
17	MD 2 N	11.8	12.04	5.5	17.5	No	1944	47.74	15.3	Rural minor arterial	10	7/23/2007

22	MD 45 N	4.4	5.05	9.5	13.5	No	1390	42.44	11.94	Urban other principal arterial	23	6/26/2009
23	MD 45 N	5.05	5.15	9.5	13.5	No	1390	42.44	11.94	Urban other principal arterial	2	6/26/2009
24	MD 45 S	4.4	5.05	9.5	13.5	No	1390	42.44	11.94	Urban other principal arterial	23	6/26/2009
42	MD 265 N	0	1.75	5	14	No	204.75	52.01	8.25	Rural minor collector	16	6/15/2010
43	MD 265 S	0	1.75	5	14	No	204.75	52.01	8.25	Rural minor collector	16	6/15/2010
44	MD 5 N	3.688	5.274	10.5	22.5	No	2090	33.67	34	Rural other principal arterial	15	6/18/2010
45	MD 225 E	1.56	3.51	9	13	No	1442.5	49.19	11.49	Rural major collector	16	5/25/2010
46	MD 225 W	1.56	3.51	9	13	No	1442.5	49.19	11.49	Rural major collector	16	5/25/2010
47	MD 335 N	6.56	11.41	5	13	No	275.5	47.74	15.3	Rural minor arterial	11	7/22/2008
48	MD 335 S	6.56	11.41	5	13	No	275.5	47.74	15.3	Rural minor arterial	11	7/21/2008
49	US 50 E	4.65	4.85	11	19	No	2085	33.67	34	Rural other principal arterial	11	6/17/2009
50	US 50 E	4.85	6.06	9.75	15.75	Yes	2085	33.67	34	Rural other principal arterial	11	6/17/2009
51	US 50 W	4.65	4.8	10	18	No	2085	33.67	34	Rural other principal arterial	6	6/17/2009
56	I 70 E	8.82	13.63	10.5	25.5	Yes	6373.5	27.43	39.54	Urban interstate	14	—
57	I 68 E	18	22.26	18.5	22.5	No	4224	20.85	47.43	Rural interstate	10	—
58	I 68 W	18	22.26	18.5	22.5	No	4224	20.85	47.43	Rural interstate	10	—
82	MD 235 N	7.67	8.9	6.5	15.5	No	440	47.74	15.3	Rural minor arterial	29	—
83	MD 235 N	8.9	9.27	8.5	17.5	No	440	47.74	15.3	Rural minor arterial	6	—
84	MD 235 S	7.67	8.9	6.5	15.5	No	440	47.74	15.3	Rural minor arterial	29	—
85	MD 235 S	8.9	9.27	8.5	17.5	No	440	47.74	15.3	Rural minor Arterial	6	—

86	MD 238 N	4.09	7.16	3	12	No	260	52.01	8.25	Rural minor collector	31	5/25/2010
87	MD 238 S	4.09	7.16	3	12	No	260	52.01	8.25	Rural minor collector	31	5/25/2010
88	MD 470 S	0	1.35	1	10	No	91	52.01	8.25	Rural minor collector	24	8/22/2006
89	MD 470 S	1.35	2.35	2.5	11.5	No	91	52.01	8.25	Rural minor collector	15	8/22/2006
90	MD 470 S	2.35	3.75	1	10	No	91	52.01	8.25	Rural minor collector	24	8/22/2006
91	MD 470 N	0	1.35	1	10	No	91	52.01	8.25	Rural minor collector	24	8/22/2006
92	MD 470 N	1.35	2.35	2.5	11.5	No	91	52.01	8.25	Rural minor collector	15	8/22/2006
93	MD 470 N	2.35	3.75	1	10	No	91	52.01	8.25	Rural minor collector	24	8/22/2006
101	MD 63 N	0	3.88	6.5	14.5	No	98	52.01	8.25	Rural minor collector	23	6/30/2010
102	MD 63 S	0	3.88	6.5	14.5	No	98	52.01	8.25	Rural minor collector	23	6/30/2010
108	MD 367 E	1.75	2.15	8	14.5	No	272	49.19	11.49	Rural major collector	9	10/2/2008
109	MD 367 E	2.15	2.6	8	16.5	Yes	272	49.19	11.49	Rural major collector	9	10/2/2008
113	MD 367 W	1.75	2.15	8	14.5	No	272	49.19	11.49	Rural major collector	9	10/2/2008
114	MD 367 W	2.15	2.6	8	16.5	Yes	272	49.19	11.49	Rural major collector	9	10/2/2008

— Indicates that information was not available.

1 inch = 25.4 mm

Table 110. FWD test data for all of the Maryland sites.

ID	Load (kPa)	D_1 (μm)	D_2 (μm)	D_3 (μm)	D_4 (μm)	D_5 (μm)	D_6 (μm)	D_7 (μm)	D_8 (μm)	D_9 (μm)
1	697.98	152.95	110.48	91.02	73.89	58.37	37.29	24.29	16.59	11.97
2	685.36	280.26	223.65	193.91	158.89	124.49	77.71	48.47	31.42	20.97
3	696.36	156.42	103.64	84.88	66.74	50.77	29.90	18.57	12.61	9.55
4	651.62	193.35	146.56	121.75	96.39	73.73	42.09	23.39	13.82	8.79
5	645.99	187.96	120.23	91.86	70.53	53.17	31.67	19.81	14.05	10.50
6	651.71	196.43	150.28	119.85	90.17	71.50	45.85	29.00	19.69	14.48
7	642.96	319.15	252.87	204.29	157.68	121.82	71.05	44.03	29.28	19.78
8	646.07	348.02	252.84	192.86	138.52	100.55	57.44	35.54	23.44	15.55
9	666.16	256.38	194.73	153.52	111.60	80.06	43.49	24.95	16.13	11.18
10	650.25	307.22	247.16	202.77	156.12	119.60	70.95	42.59	27.98	20.10
11	637.96	427.17	345.69	286.39	220.61	168.56	100.82	64.03	42.52	29.95
12	652.76	349.17	270.40	216.23	165.89	130.19	89.24	66.27	53.55	44.28
13	665.03	308.16	253.90	217.53	178.17	145.12	101.36	73.60	56.96	45.75
14	670.64	276.61	222.38	183.90	143.89	113.03	75.18	54.36	42.93	35.56
15	657.40	326.83	257.17	209.99	165.15	131.14	90.46	66.79	53.39	43.93
16	660.28	347.26	275.62	230.87	182.19	143.33	95.05	67.55	53.20	43.79
17	659.63	378.33	294.77	237.93	183.52	142.05	91.44	63.63	48.45	38.67
22	646.80	370.69	271.62	210.35	154.82	113.20	66.54	42.95	31.44	25.15
23	654.74	354.69	241.76	180.80	134.11	97.28	55.42	34.49	25.70	19.96
24	649.22	326.06	242.79	190.16	142.39	105.39	62.85	41.33	30.58	24.14
42	647.67	488.30	393.12	319.89	248.67	192.00	121.67	83.83	62.07	48.11
43	652.37	486.40	401.50	333.08	258.36	197.46	123.58	83.46	61.96	48.24
44	663.07	346.53	272.43	216.75	161.84	120.89	73.11	47.91	35.90	27.98
45	655.55	267.17	208.77	171.20	136.86	108.56	71.09	48.53	35.49	27.97
46	660.32	272.34	205.92	167.05	132.43	103.28	66.39	44.72	32.77	25.94
47	636.96	526.30	389.25	303.91	229.15	174.37	108.82	74.84	57.47	46.23
48	635.08	506.31	369.30	287.20	214.94	162.87	102.00	70.65	54.74	44.04
49	668.93	183.68	141.65	119.59	104.56	91.65	71.54	55.46	44.58	36.79
50	661.45	276.42	209.93	168.29	140.80	120.72	88.40	64.80	49.52	38.57

51	674.00	145.54	95.15	73.96	67.92	63.91	55.37	47.09	39.73	32.82
56	676.85	86.08	77.00	71.25	64.81	58.48	47.53	38.34	31.16	24.47
57	683.34	89.72	72.55	64.76	58.33	52.04	41.04	31.77	24.68	65.16
58	687.30	91.63	78.28	70.30	62.40	54.98	42.53	32.64	24.49	70.31
82	680.88	180.01	153.57	135.39	113.14	89.60	58.42	39.77	29.56	23.51
83	685.72	188.76	161.65	142.09	120.25	98.30	65.93	44.56	31.21	24.38
84	685.95	171.67	148.69	131.27	110.68	91.85	61.81	43.54	31.90	25.01
85	686.95	286.16	245.47	210.67	156.01	125.07	79.71	51.36	36.02	27.18
86	637.34	681.44	533.49	411.59	295.53	212.38	122.38	80.32	61.65	48.93
87	643.13	541.75	430.59	344.85	262.69	199.39	125.30	85.90	64.65	49.00
88	636.46	775.11	620.40	490.11	349.81	241.91	123.61	73.31	54.79	44.56
89	629.90	863.83	690.09	543.28	382.99	262.89	140.09	89.87	68.12	54.43
90	637.88	699.13	548.46	424.64	293.76	199.88	104.05	66.58	51.85	41.87
91	632.25	856.79	677.76	528.26	371.96	254.37	126.84	75.86	55.89	47.20
92	629.75	834.83	664.03	528.14	379.22	268.20	143.79	89.92	66.83	53.02
93	625.65	866.70	658.32	487.73	325.88	216.68	109.35	69.71	53.90	43.94
101	670.32	397.30	306.75	241.88	177.22	129.20	72.97	45.44	33.09	25.86
102	660.16	436.23	338.29	264.54	193.49	140.30	79.78	51.36	38.33	30.34
108	654.17	274.04	230.29	199.87	166.29	136.51	93.05	63.67	45.16	34.01
109	645.53	292.99	229.98	182.90	136.88	102.64	63.84	43.88	33.34	27.16
113	649.83	297.21	245.17	210.41	173.99	142.37	97.60	69.18	51.85	41.02
114	642.40	294.13	224.84	174.29	125.89	93.17	57.82	40.94	32.40	26.35

1 psi = 6.89 kPa

1 μm = 0.039 mil

REFERENCES

1. Federal Highway Administration. *How to Get LTPP Data*, U.S. Department of Transportation, Washington, DC. Obtained from: <http://www.fhwa.dot.gov/research/tfhrc/programs/infrastructure/pavements/ltp/getdata.cfm>.
2. Strategic Highway Research Program. (1993). *Manual for FWD Testing in the Long-Term Pavement Performance Program*, 9, Report No. SHRP-P-661, Version 2.0, National Research Council, Washington, DC.
3. California Department of Transportation. (1979). "Test to Determine Overlay and Maintenance Requirements by Pavement Deflection Measurements," *Caltrans Test Method No. 356*, Sacramento, CA.
4. Stubstad, R., Jiang, Y.J., Clevenston, M.L., and Lukanen, E.O. (2006). *Review of the LTPP Backcalculation Results*, Report No. FHWA-HRT-05-150, Federal Highway Administration, Washington, DC.
5. Kim, Y.R. (2000). "Assessing Pavement Layer Condition Using Deflection Data," *National Cooperative Highway Research Program Project 10-48*, Final Report, Transportation Research Board, Washington, DC.
6. Lukanen, E.O., Stubstad, R., and Briggs, R. (2000). *Temperature Predictions and Adjustment Factors for Asphalt Pavement*, Report No. FHWA-RD-98-085, Federal Highway Administration, Washington, DC.
7. Hossain, M., Chowdhury, T., Chitrapu, S., and Gisi, A.J. (2000). "Network-Level Pavement Deflection Testing and Structural Evaluation," *Journal of Testing and Evaluation*, 28(3), 199–206.
8. AASHTO. (1993). *Guide for Design of Pavement Structures*, American Association of State Highway and Transportation Officials, Washington, DC.
9. Ullidtz, P. (1998). *Modeling Flexible Pavement Response and Performance*, Polyteknisk Forlag, Lyngby, Denmark.
10. Scullion, T. (1988). *Incorporating a Structural Strength Index into the Texas Pavement Evaluation System*, Report No. FHWA/TX-88/409-3F, Federal Highway Administration, Washington, DC.
11. Perrone, E., Dossey, T., and Hudson, W.R. (1994). *Network-Level Deflection Data Collection for Rigid Pavement*, Interim Report, Texas Department of Transportation, Austin, TX.
12. Diefenderfer, B.K. (2008). *Network-Level Pavement Evaluation of Virginia's Interstate System Using the Falling Weight Deflectometer*, Report VTRC 08-R18, Virginia Transportation Research Council, Charlottesville, VA.

13. Ferne, B.W. (1997). *Use of Deflections at Network Level in England for Programming and Other Purposes*, Cost 336 Workshop at National Laboratory for Civil Engineering, Lisbon, Portugal.
14. Horak, E. (2008). "Benchmarking the Structural Condition of Flexible Pavements with Deflection Bowl Parameters," *Journal of the South African Institution of Civil Engineering*, 50(2), 2–9.
15. Sapkota, B. (2003). *Use of FWD in the Network Level Pavement Condition Survey*, Presented at the 12th Annual FWD Users Group Meeting, Wichita, KS.
16. Ferne, B., Sinhal, R., and Fairclough, R. (2009). *Structural Assessment of the English Strategic Road Network— Latest Developments*, Proceedings from the Eighth International Conference on Bearing Capacity of Roads, Railways, and Airfields, Champaign, IL.
17. Zhang, Z., Claros, G., Manuel, L., and Damnjanovic, I. (2003). "Development of Structural Condition Index to Support Pavement Maintenance and Rehabilitation Decisions at Network Level," *Transportation Research Record 1827*, 10–17, Transportation Research Board, Washington, DC.
18. Zhang, Z., Manuel, L., Damnjanovic, I., and Li, Z. (2003). *Development of a New Methodology for Characterizing Pavement Structural Condition for Network-Level Applications*, Report No. FHWA/TX-04/0-4322-1, Federal Highway Administration, Washington, DC.
19. AASHTO. (1998). *AASHTO Guide for Design of Pavement Structures: Part II—Rigid Pavement Design and Rigid Pavement Joint Design*, 4th Edition, Supplement, American Association of State Highway and Transportation Officials, Washington, DC.
20. Virginia Department of Transportation. (1992). *The Pavement Subsystem User Manual for the Highway and Traffic Records Information System (HTRIS)*, Richmond, VA.
21. Chang, J-R., Lin, J-D., Chung, W-C., and Chen, D-H. (2002). "Evaluating the Structural Strength of Flexible Pavements in Taiwan Using the Falling Weight Deflectometer," *International Journal of Pavement Engineering*, 3(3), 131–141.
22. Ullidtz, P. and Stubstad, R. (1996–1997). *ELMOD Users Guide*, Dynatest International A/S, Copenhagen, Denmark.
23. Carvalho, R.L., Ayres, M., Shirazi, H., Selezneva, O., and Darter, M. (2011). *Impact of Design Features on Pavement Response and Performance in Rehabilitated Flexible and Rigid Pavements*, Report No. FHWA-HRT-10-066, Federal Highway Administration, Washington, DC.
24. Airport Cooperative Research Program. (2008). *ACRP Report 3—Analysis of Aircraft Overruns and Undershoots for Runway Safety Areas*, Transportation Research Board, Washington, DC.

25. Hosmer, D. and Lemeshow, S. (2000). *Applied Logistic Regression*, John Wiley & Sons, Hoboken, NJ.
26. Fawcett, T. (2006). "An Introduction to ROC Analysis," *Pattern Recognition Letters*, 27, 861–874.
27. National Cooperative Highway Research Program. (2004). *Mechanistic-Empirical Pavement Design Guide*, NCHRP Project 1-37A, Transportation Research Board, Washington, DC.
28. Huang, Y.H. (2004). *Pavement Analysis and Design*, 2nd Edition, Prentice Hall, Inc., Upper Saddle River, NJ.
29. Kestler, M., Harr, M.E., Berg, R.L., and Johnson, D.M. (1994). *Spacial Variability of Falling Weight Deflectometer Data: A Geostatistical Analysis*, 318–330, Fourth International Conference on Bearing Capacity of Roads, Railways, and Airfields, Minneapolis, MN.
30. Baladi, G., Dawson, T., and Sessions, C. (2009). *Pavement Subgrade MR Design Values for Michigan's Seasonal Changes*, Report No. RC-1531, Michigan Department of Transportation, Lansing, MI.
31. Arambula, E., George, R., Xiong, W., and Hall, G. (2011). *Development and Validation of Pavement Performance Models for the State of Maryland*, Transportation Research Board 2011 Annual Meeting, Washington, DC.
32. FHWA. (2011). *Results of Long-Term Pavement Performance SPS-3 Analysis: Preventive Maintenance of Flexible Pavements*, TechBrief No. FHWA-HRT-11-049, Federal Highway Administration, Washington, DC.
33. Strategic Highway Research Program. (1993). *Strategic Highway Research Program and Traffic Safety on Two Continents*, Conference Proceedings, Gothenburg, Sweden.
34. Baus, R.L., Pierce, C., and Hong, W. (2001). *Feasibility of Including Structural Adequacy Index as an Indicator of Overall Pavement Quality in the SCDOT Pavement Management System*, Summary Report, Report No. FHWA-SC-01-03, Federal Highway Administration, Washington, DC.
35. Killingsworth, B. and Von Quintus, H. (1997). *Backcalculation of Layer Moduli of LTPP General Pavement Study (GPS) Sites*, Report No. FHWA-RD-97-086, Federal Highway Administration, Washington, DC.
36. Collop, A.C., Armitage, R.J., and Thom, N.H. (2001). "Assessing Variability of In Situ Pavement Material Stiffness Moduli," *Journal of Transportation Engineering*, 127(1), 74–81, American Society of Civil Engineers, Reston, VA.
37. Eijbersen M.J. and Van Zwieten J. (1998). *Application of FWD Measurements at the Network Level, I*, 438–450, 4th International Conference on Managing Pavements, Pretoria, South Africa.

38. Piyatrapoomi, N., Kumar, A., Robertson, N., and Weligamage, J. (2004). *Reliability of Optimal Intervals for Pavement Strength Data Collection at the Network Level*, Proceedings of the 6th International Conference on Managing Pavements, Brisbane, Australia.
39. Piyatrapoomi, N., Kumar, A., Robertson, N., and Weligamage, J. (2003). *A Probability-Based Analysis for Identifying Pavement Deflection Test Intervals for Road Data Collection*, 291–302, Proceedings of the International Conference on Highway Pavement Data Analysis and Mechanistic Design Application, Columbus, OH.
40. Howard, K.R. and Tongue, F.T. (1995). “Pavement Management—Development of a Pilot PMS,” *Highways and Transportation*, 25–27, London, UK.
41. Litzka, J., Leben, B., La Torre, F., Weninger-Vycudil, A., Antunes, M.L., Kokot, D., Mladenovic, G., Brittain, S., and Viner, H. (2008). *The Way Forward for Pavement Performance Indicators Across Europe, Final Report, COST Action 354: Performance Indicators for Road Pavements*, COST, Brussels, Belgium.
42. COST. (1998). *COST 336: Use of Falling Weight Deflectometers in Pavement Evaluation*, COST, Brussels, Belgium. Obtained from: <http://cordis.europa.eu/cost-transport/src/cost-336.htm>.
43. Austroads. (2003). *Comparison of Project-Level and Network-Level Pavement Strength Assessment*, Publication No. AP-T21/03, Sydney, Australia.
44. Haas, R., Hudson, W.R., and Zaniewski, J. (1994), *Modern Pavement Management*, Krieger Publishing Company, Malabar, FL.

